Multi-omics Characterization of the Breast Cancer Radiation Response Identifies Apoptosis and Cell Cycle Proteins as Mediators of Radiation Resistance

by

Benjamin Charles Chandler

A dissertation submitted in partial fulfillment
of the requirements for the degree of
Doctor of Philosophy
(Cancer Biology)
in the University of Michigan
2020

Doctoral Committee:

Professor Arul Chinnaiyan, Co-Chair
Assistant Professor Corey W. Speers, Co-Chair
Professor Sofia Merajver
Associate Professor Meredith Morgan
Associate Professor Arvind Rao

Benjamin Chandler

chandleb@umich.edu

ORCID ID: 0000-0001-6963-9468

Dedication

This dissertation is dedicated to Nan Gilbreath Chandler (1926-1981) and Lois Jane Gipper (1933-1985), two grandmothers whom I never got the chance to meet due to breast cancer.

Acknowledgements

To Dr. Corey Speers, thank you for your time and mentorship over the past 4 years that helped me to become a successful scientist. Your patience and insight made for great experience. Additionally, thank you for many lab outings including curling, footgolf, lab cornhole, water skiing, and many ice creams walks. Furthermore, thank you for wise input on non-scientific issues including real BBQ and proper cowboy boots. Together your mentorship and easy going demeanor allowed me to a have fulfilling graduate school experience.

To Dr. Arul Chinnaiyan, thank you for allowing me to begin my research career as an undergraduate student and technician in your lab as well as a co-mentor for graduate school. I appreciate you taking the time to meet with me throughout the years to discuss my dissertation work and future career objectives. Your mentorship has helped drive my passion for science and fulfill my career goals thus far.

To my thesis committee, Dr. Meredith Morgan, Dr. Sofia Merajver, and Dr. Arvind Rao thank you for taking the time to mentor me over the years in both one-on-one meetings and during my thesis committee meetings. Your guidance and expertise allowed me to learn multiple research disciplines and become a successful graduate student.

To the current and past members of the Speers Lab, thank you for your help and mentorship over the years. To Dr. Shyam Nyati, thank you for taking the time to explain and teach laboratory techniques. To Dr. Meilan Liu, for helping me learn and perform experiments throughout my years as a student. To Kari, thank you for teaching me and performing *in vivo* studies for multiple projects. Additionally, thank you for updating the Premier League standings board so everyone in lab knew Tottenham was better than Arsenal. To Cassie Ritter, thank you for working with me for 4 years, for your hard work help related to my thesis, and for dealing with my shenanigans over the years. To fellow graduate students Andrea Pesch and Anna Michmerhuizen, thank you for your help performing experiments, editing my paper, abstracts and thesis, as well as making lab a fun environment to work in. To the many undergraduate students – Eric Olsen, Meleah Cameron, Nicole Hirsch, Amanda Zhang, Marlie Androsiglio, and Rachel Schwartz– thank you for performing experiments that contributed to this thesis and for being dedicated and teachable students.

To the Cancer Biology Program and Department of Computational Medicine and Bioinformatics, thank you for the providing the educational framework that allowed me to learn and explore cancer biology and bioinformatics.

To my family and friends, who have supported me throughout my time in graduate school, thank you for the many fun times traveling, snowboarding, golfing, tubing, etc that made graduate school such a wonderful time of my life. To my family, thank you for the many dinners, excursions, and fun times over the past 5 years. I look forward to many more over the years!

Finally, to my fiancé, Allie Bouza, for her love and support throughout graduate school and for pushing me to be the best scientist possible. Graduate school would not have been as great of an experience had I not met you here on day one!

Table of Contents

List of Tables

List of Figures

Abstract

Breast cancer (BC) is the most commonly diagnosed cancer in women and the second most deadly. Trimodality therapy consisting of surgery, chemotherapy, and radiation therapy is used to treat the majority of BC patients. However, despite the use of RT, a significant portion of patients, specifically those with basal-like BC, develop recurrences within 5-years of treatment completion. In an effort to understand why patients with basal-like BC are more likely to recur than patients with luminal or Her2-enriched BC we undertook a series of studies to understand the biology underlying radioresistance in basal-like BC. We first performed transcriptomic and proteomic analysis in cell lines representing the spectrum of BC subtypes treated with radiation (RT). RT induced RNA and protein expression changes in cell cycle, DNA damage, and p53 signaling pathways, which may act as modulators of the RT response in basal-like BC and lead to resistance. RT was unable to induce genes and proteins related to apoptosis after RT in radioresistant, p53-mutant BC cell lines, indicating that an inability to activate this pathway may contribute to radioresistance.

Activation of the apoptosis pathway, through inhibition of Bcl-2 family anti-apoptotic proteins, radiosensitized p53-mutant, PIK3CA/PTEN wild-type basal-like BC. Specific inhibition of Bcl-xL, but not Bcl-2, lead to radiosensitization of p53-mutant PIKCA/PTEN wild-type basal-like BC. Radiosensitization was mediated through RT induced Mcl-1 degradation, that in combination with Bcl-xL specific inhibition, increased the percentage of apoptotic cells. Overexpression of Mcl-1 in p53-mutant, PIK3CA/PTEN wild-type basal-like BC rescued this radioresistance. *In vivo*, pan inhibition of Bcl-2 family proteins or specific inhibition of Bcl-xL in

combination with RT delayed tumor growth and increase time to tumor doubling and tripling. These data provide a rationale for using Bcl-xL inhibitors for the radiosensitization of p53-mutant, PIK3CA/PTEN wild-type basal-like BC.

To expand upon these studies and further identify proteins related to recurrence we correlated gene expression to early recurrence (<3 years) in four independent datasets with patient outcomes and found TTK, a cell cycle kinase, was most differentially expressed. Inhibition of TTK (both genetic and pharmacologic) radiosensitized basal-like BC. Reintroduction of wild-type TTK, after endogenous TTK knockdown, rescued radiosensitization, however reintroduction of kinase-dead TTK was unable to do so. TTK inhibition (both genetic and pharmacologic) led to unresolved double stranded DNA (dsDNA) damage over time after RT, indicating that TTK inhibition may compromise dsDNA repair efficiency. Using a homologous recombination (HR) specific reporter system, we found that TTK inhibition (both genetic and pharmacologic) decreased HR efficiency. Furthermore, TTK knockdown decreased Rad51 foci formation, a marker for active HR, after RT. Reintroduction of wild-type TTK, after endogenous TTK knockdown, rescued HR repair efficiency and Rad51 foci formation, however reintroduction of kinase-dead TTK was unable to do so. Using a specific non-homologous end joining (NHEJ) reporter system, we found that TTK inhibition (both genetic and pharmacologic) had no effect on NHEJ repair efficiency. *In vivo*, TTK inhibition (both genetic and pharmacologic) in combination with RT reduced tumor growth and increase time to tumor tripling in subcutaneous basal-like BC cell line models. In an orthotopic patient derived xenograft model, pharmacologic inhibition of TTK in combination with RT synergistically reduced tumor growth and increased time to tumor tripling. Together our results

show that a multi-omics characterization of the RT response led to successful nomination of radiosensitization targets that may be clinically tractable.

Chapter 1

Introduction

Breast cancer, diagnosis, and treatment

Breast cancer is the most commonly diagnosed cancer in women and second most deadly behind only lung cancer (1). Approximately one in eight women will be diagnosed with breast cancer within their lifetime, however the lifetime risk from dying of breast cancer is only approximately one in forty (1-3). Early diagnosis is common, with 70% of cases diagnosed at an early stage (stage I and II). While Stage III and IV are less commonly diagnosed, they have the worst outcomes among breast cancer patients and are responsible for most of the mortality associated with breast cancer (3). This underscores the importance of early detection in breast cancer.

More effective screening strategies have played a major role in improving survival for breast cancer patients. Historically breast cancer diagnoses were made based on physical exam findings, most commonly a palpable breast mass or enlarged lymph nodes (4). With these less sensitive techniques women were more commonly diagnosed with advanced stage disease, including breast cancers that had already spread to the lymph nodes. With the advent of mammography, detection of breast cancers are more commonly diagnosed at an earlier stage,

which has led to an improvement in survival (5, 6). Monitoring for disease progression or recurrence has also improved, due to more sensitive imaging and blood-based (circulating tumor DNA or circulating tumor cells) testing allowing for the earlier detection of disease recurrence and/or progression (7-10).

Once diagnosed with breast cancer treatment decisions are predicated on several factors including tumor stage, tumor grade, as well as hormone-receptor status. Patients are typically treated using a trimodality therapy consisting of surgery, chemotherapy, and radiation therapy (3). This trimodality therapy, while very effective, does not result in a cure for all patients. Nuclear hormone receptor and *HER2* amplification status are important markers for the effectiveness of therapy, with ER expression a predictive biomarker of response to endocrine therapy and *HER2* amplification being a predictive biomarker of response to anti-HER2 therapies including trastuzumab (11, 12). Hormone-receptor status and HER2 expression have also been used as a prognostic marker for patient outcomes (13, 14). Furthermore, patients often receive additional treatments that target these nuclear hormone receptors or *HER2* amplification, in addition to the trimodality treatment discussed previously (15-17).

Nuclear Hormone receptors and HER2 amplification in breast cancer

Nuclear hormone receptors, estrogen receptor (ER) and progesterone receptor (PR), as well as human epidermal growth factor receptor 2 (Her2) have been well documented for their prognostic role in breast cancer (13, 14). ER and PR classically group together into ER/PR-positive (ER/PR+) subtype, while Her2-positive (Her2+) breast cancers represent an independent subtype

(18-20). Breast cancers that do not express ER, PR, or Her2 are defined as triple-negative breast cancers (TNBC) (21). The majority of breast cancer patients are diagnosed with ER+ breast cancer, while HER+ and TNBC are much less commonly diagnosed (3, 20, 21). ER, which is expressed in ~70% of breast cancers, is a hormone receptor that, when activated by its ligand estradiol, homodimerizes and translocates to the nucleus where it acts as a transcription factor that can activate expression of genes that govern growth and proliferation (22, 23). PR, a hormone receptor similar to ER, is often co-expressed with ER. However, PR's role in breast cancer development and prognosis is still not well understood (24, 25). ER+ breast cancers have the best outcomes, in part, due to more indolent disease as well as targeted therapies aimed at inhibition of ER signaling, the driver of this subtype of breast cancer (26, 27). Amplification of the *HER2* gene and subsequent overexpression of Her2 protein occurs in ~25% of breast cancers (28, 29). Her2 is part of the epidermal growth factor receptor (EGFR) family, and thus is involved in signaling processes related to cell growth (30, 31). While patients with Her2+ cancer historically had the worst outcomes, the discovery and clinical development of targeted therapies aimed at Her2 has led to increased patient survival, with survival rates for patients with Her2+ breast cancer rivaling survival rates in women with ER+ breast cancer (28, 32, 33). TNBC, which does not express any of the previously mentioned receptors, represent ~10-20% of breast cancer diagnoses. These cancer have the worst outcomes due to the inherent aggressiveness of the disease as well as a lack of targeted therapies available for treatment. Studies are underway to identify what pathways drive TNBC and how these pathways could be targeted for treatment (34-38).

Breast cancer subtypes

Despite the utility of ER, PR, and *HER2* expression as prognostic biomarkers and predictors of treatment response, it is clear that the expression of these three genes does not completely explain the heterogeneity of breast cancer. Seminal work by several investigators, including Dr. Chuck Perou at UNC, more fully characterized breast cancers using transcriptional profiling of breast cancer patient tumors (39, 40). This profiling has revealed a number of clinically and biologically relevant subtypes – Luminal A, Luminal B, Her2-enriched, and basal-like breast cancer, known as intrinsic subtypes of breast cancer (39). Importantly, these intrinsic subtypes are prognostic of patient outcomes as well as predictive of response to therapy, including chemotherapy (40-45). Additional studies have attempted to further stratify these breast cancer subtypes based on their gene expression profiles to aid in guiding therapeutic decisions and better stratify patient outcomes (36, 46-48).

Luminal breast cancers

The luminal A and luminal B breast cancer subtypes include the majority of ER/PR+, Her2-negative (Her2-) breast cancers and are the most commonly diagnosed subtypes of breast cancer, comprising over approximately 40-60% and 10-20% of breast cancer diagnoses, respectively (3, 39, 40, 49). Luminal A cancers have the best prognosis of all breast cancers, comprising less than 2% of all breast cancer related deaths, while Luminal B breast have worse outcomes (50-52). While the underlying drivers of these differences in outcomes in not entirely clear, the drivers are at least multifactorial. Luminal A breast cancers are enriched for ER related genes but exhibit low

expression of proliferation markers, such as Ki67. Luminal B breast cancers are also enriched for ER related genes, however, they exhibit high expression of proliferation markers (*CCNB1*, *CCNE1*, *MYBL2*, *MELK*, etc) and are generally higher grade tumors compared to luminal A tumors (39, 40).

In addition to treatment with surgery, radiation, and often chemotherapy, by virtue of their expression of ER, luminal breast cancers are treated with hormonal therapy targeting the ER. The addition of tamoxifen, a competitive antagonist of the ER, significantly increases survival for pre-menopausal ER+ patients (11, 53). More recently, studies have shown that 3rd generation nonsteroidal inhibitors letrozole and anastrozole are more effective than tamoxifen as first line therapies for post-menopausal women with ER+ breast cancer (54-56). Despite the efficacy of these therapies, they are not universally effective, especially in women with metastatic breast cancer. In this setting, patients often develop resistance to hormone therapies creating a need for additional therapies to combat recurrences and further metastases (57, 58). CDK4/6 inhibitors, which target the cell cycle proteins to reduce proliferation and arrest cells, have been found to increase survival in metastatic breast cancer patients and represent the new standard of care, in combination with anti-estrogens, in the first line treatment of women with ER+ metastatic breast cancer (59, 60).

Her2-enriched breast cancers

The Her2-enriched (Her2+) subtype consists of the majority of breast cancers with an amplification of the *HER2* gene and overexpression of HER2 protein and comprise ~20-25% of

breast cancer patients (39, 40, 61). Her2+ breast cancers are enriched for Her2 and Her2 related genes GRB7 and MMP11. Additionally, Her2+ cancers have high expression of proliferation related genes, which is thought to be driven by Her2 itself. Prior to the introduction of anti-Her2 therapy, Her2+ patients had poor outcomes, similar to that of Luminal B breast cancers; however, the development of therapies specifically targeting Her2, the first targeted molecular therapy to be used for breast cancer treatment after hormone therapy, has increased survival for these patients (15, 32, 33, 62, 63). Trastuzumab (Herceptin), a monoclonal antibody and the first approved therapy targeting HER2, improved patient survival through binding to the extracellular domain (ECD) to inhibit dimerization (64-66). More recently, pertuzumab, a monoclonal antibody that interacts with a different ECD of HER2, prevents heterodimerization of HER2 and HER3 (67, 68). Although modest efficacy has been seen with the use of pertuzumab alone, studies are underway examining the combination therapy of pertuzumab with trastuzumab (68, 69). Furthermore, the development of ado-trastuzumab emtansine (T-DMI), a conjugation of trastuzumab and microtubule inhibitor, is currently under clinical trial and has been shown to improved survival as a second-line treatment strategy for Her2+ patients (65, 70-72).

Basal-like breast cancers

The basal-like subtype contains the majority of breast cancers with low expression of ER, PR, and Her2 (TNBC), as well as their related genes, with high expression of proliferation related genes (73). Basal-like breast cancers account for ~10-20% of breast cancers (74, 75). P53, PIK3CA, and BRCA1 mutations are commonly found in basal-like breast cancer, as is loss of the

Rb pathway (36, 37, 76). Patients with basal-like breast cancer have the worst survival outcomes across subtypes due to, at least in part, the high proliferative potential of the cancer as well as the lack of targeted therapies (77-79). Additionally, basal-like breast cancers are more resistant to conventional therapies, including radiation therapy (80, 81). While aromatase inhibitors and Herceptin are available for the treatment of luminal and Her2+ breast cancers, few treatments are available for the treatment of basal-like breast cancer. Inhibition of poly ADP-ribose polymerase (PARP), an enzyme family that plays a role in single strand DNA break repair mechanism, base excision repair, has recently been approved for treatment of BRCA1/2 mutant breast cancers, however this represents only a small subset of basal-like breast cancers (82-84). Currently, many therapeutic targets are under investigation for treatment of basal-like breast cancers.

Difference in response to radiation between the subtypes

Despite the use of radiation, basal-like breast cancers continue to have highest rates of local recurrence across breast cancer subtypes. Radiation therapy and surgery are least effective in treating and curing basal-like breast cancers compared luminal and Her2+ breast cancer subtypes (49, 80, 85-88). This difference in clinical response to radiation therapy underscores the importance of understanding how different subtypes respond to radiation therapy and demonstrates the need for radiosensitization efforts for cancers resistant to radiation therapy. Several groups have sought to examine and predict radiosensitivity across cancers, however the factors underlying radioresistance remain unknown (89-91).

Radiosensitization mechanisms

In trying to understand the radiation response across breast cancer subtypes and what might drive the differences in response to therapy, studies have also aimed to identify and characterize novel targets for the treatment of basal-like breast cancer (92). The majority of the radiosensitization targets identified to date can be grouped into four different categories of cellular pathways, each related to the response to radiation – DNA damage, cell cycle, cell death, and oxygen deprivation.

DNA Damage

Radiation therapy causes DNA damage through either direct or indirect effects (93). Direct effects occur when ionizing radiation generates free electrons from orbital electron shells displaced by the energy of photons that then directly break covalent bonds either in the ribose phosphate backbone of the double helix or between the paired base pairs in the DNA. Indirect damage occurs as radical oxygen species (ROS) are generated due to displaced electrons that then react with the negatively charged DNA strand or oxidize lipids and proteins within the cell (93-95). The majority of DNA damage (~2/3 of the damage) is caused by these indirect effects, mediated by ROS, that interact with DNA to cause single and double strand DNA breaks (93). Although, single strand lesions make up ~60-70% of the damage cause by radiation therapy, double strand DNA (dsDNA) breaks are more lethal to cells, as the single strand repair mechanisms base excision repair and nucleotide excision repair more faithfully correct single stranded DNA breaks (96, 97). dsDNA damage is primarily repaired by two mechanism, homologous recombination (HR) and non-

homologous end joining (NHEJ) (98-101). The fidelity of these repair pathways are critical for the repair of not only radiation induced damage but also natural damage occurring from other genotoxic factors (102).

HR repair uses the sister chromatid as a template to accurately repair dsDNA damage, thus repair by HR can only occur in late S phase or G2 of the cell cycle, when sister chromatids are available as a template for HR (103, 104). NHEJ repairs dsDNA breaks by blindly ligating two blunt ends of a dsDNA break in a non-templated fashion (105). This can lead to the introduction of insertions and deletions of base pairs (indels) or chromosomal rearrangements due to ligating of unpaired DNA breaks, making NHEJ the less accurate form of repair (105, 106). However, because NHEJ does not rely on sister chromatids for repair, cells are able to use NHEJ repair throughout the cell cycle to repair dsDNA damage and is more often utilized after ionizing radiation due to its cell cycle independent availability (105).

The accumulation of DNA damage has been shown to be lethal to cells. To this end, studies have shown that inhibition of DNA damage repair pathways can increase DNA damage to the point of cell death (107). Furthermore, inhibition of DNA damage repair proteins in combination with radiation therapy has proven to be a successful mechanism for increasing the efficiency of radiation therapy, by increasing DNA damage to the point of cell death (108).

Preclinical studies have shown inhibition of either ataxia telangiectasia mutated (ATM) or ataxia telangiectasia and Rad3-related (ATR), apex protein kinases in both the DNA damage and cell cycle checkpoint, leads to radiosensitization of cancer through decreased DNA damage repair after radiation (109-112). Inhibition of Rad51, a recombinase critical for successful HR, also

sensitizes cancers, including basal-like breast cancer cell lines, to DNA damaging agents through impaired DNA repair (113-115). Inhibition of NHEJ specific proteins, such as DNA-dependent protein kinase (DNAPK), can also radiosensitize cancer cells (116, 117).Additionally, inhibition of Poly ADP-ribose (PARP), an enzyme involved in the regulation of the multiple DNA repair mechanisms, radiosensitizes multiple cancer models, including TNBCs (118-125). Despite the efficacy of radiosensitization by inhibiting these proteins, the critical reliance of normal cells to these same proteins limits their clinical utility given the off target effects.

Cell Cycle

Radiation therapy is most effective in the S and G2 phases of the cell cycle, when DNA is replicated for division and before/during mitosis, when mitotic errors can be propagated to daughter cells. After radiation therapy and in response to appropriately sensed DNA damage, cycling cells often arrest at G1 or G2 checkpoints (126, 127). These checkpoints, as well as others, ensure that damaged does not occur during synthesis of DNA and that cells do not continue through mitosis, thus propagating damaged DNA into daughter cells. This prevents damaged cells from propagating mutations and breaks caused by radiation therapy (128). To increase DNA damage and mitotic errors after DNA damage, researchers have used inhibitors targeted towards critical members of cell cycle checkpoints to increase cell cycling and DNA damage (129, 130). Additionally, many cell cycle targets that have been targeted for radiosensitization have also been found to play a role in DNA damage response, as the two are closely related (129-132). Inhibition of Wee1, a cell cycle kinase responsible for phosphorylating cdc2, which in part controls entry

into mitosis, has been shown to increase radiosensitivity by removing the G2 checkpoint thus pushing cells into mitosis (132-134). Inhibition of maternal embryonic leucine zipper kinase (MELK), a known cell cycle protein, has been shown to specifically radiosensitize TNBCs (131). Inhibition of Checkpoint kinase 1 (Chk1), a protein known to regulate both cell cycle and DNA damage pathways, has been shown to radiosensitize multiple cancer models, including TNBC, through changes to the cell cycle, DNA damage repair, and cell death (129, 135-138). Finally, CDK4/6 inhibition, which leads to G1/S transition blockade, is merging as a potential radiosensitizing strategy in breast, head and neck, and glioblastoma cancer treatment (139-141).

Cell Death

Radiation therapy causes DNA damage that can lead to the induction of programmed cell death, including apoptosis, ferroptosis, autophagy, mitotic catastrophe, and necrosis (142-146). Each cell death pathway operates independent of one another and are thus targeted separately for radiosensitization. Radiation therapy has been thought to primarily induce apoptosis, a programmed cell death mechanism, through unrecoverable DNA damage (146). However, studies detailing the effect of radiation on the induction of ferroptosis and autophagy underscore the fact that different cancers likely induce programmed cell death via different mechanisms (147-150). Previously, groups have sought to radiosensitizes multiple cancer models though inhibition of anti-apoptotic proteins (Bcl-2 family proteins Bcl-2, Bcl-w, Bcl-xL, and Mcl-1), to increase cell death after radiation therapy (151-155). Other studies have sought to increase radiosensitivity through modulating p53 phosphorylation to increase apoptosis (156). Inhibition of MDM2, an E3 ubiquitin

ligase for p53, has been shown to increase both apoptosis and autophagy (157, 158). Interesting, both inhibition and activation of autophagy have been shown to enhance radiation effectiveness, detailing the complication nature of autophagy in cancer treatment (149, 150, 159, 160). Inhibition of autophagy has been shown to increase apoptosis related cell death, while decreasing nutrients available for cancer cells (159-161). While other studies have demonstrated that increased autophagy leads to greater cell death and regression of tumors (150, 162). Multiple studies have detailed how inhibition of cell cycle targets in combination with radiation therapy can lead to an increase in mitotic catastrophe related cell death, through deregulation of cell cycle checkpoints necessary to maintain the integrity of DNA (130, 163).

Oxygen Deprivation

As noted previously, the majority of DNA damage induced by radiation therapy is mediated through indirect effects and reliant on oxygen for the production radical oxygen species (ROS) that subsequently cause DNA damage (164, 165). It has been well characterized that tumors with low oxygen supply are more resistant to radiation therapy, and normalization of oxygen tension in tumors (either through normalization of the tumor vasculature or through oxygen mimentics) has improved the efficacy of radiation in multiple preclinical and clinical studies (165, 166). TNBC are noted to be more hypoxic than other subtypes of breast cancers, likely contributing to their resistance to radiation therapy (167-169). Radiation therapy is often give in a fractionated manner to patients, in part, because poorly vascularized tumors have lower oxygen content and are therefore more resistant to radiation (165, 170). With daily fractionated, the more normoxic

"outer" cells of the tumor are preferentially killed and removed, allowing for diffusion of oxygen into the previously hypoxic core. Thus, these previously hypoxic centers are exposed to oxygen and increase their likelihood of cell kill with each successive fraction of radiation. When sequenced over weeks to months (often 30-40 fractions of treatment for patients with cancer), radiation can effectively kill all clonogens in a tumor, including those that were previously at the hypoxic center of the tumor (171, 172). As hypoxic tumors are more resistant to radiation therapy, efforts have been made to radiosensitize hypoxic cancers (173, 174). Studies have shown that re-oxygenation of hypoxic *in vivo* TNBC models leads to radiosensitization (175).

Novel radiosensitizers

While the majority of radiosensitization agents and experimental radiosensitization targets are directed toward the previously mentioned cellular pathways, more recently studies have shown that inhibition of receptors and signaling networks can radiosensitize cancers. Inhibition of androgen receptor (AR), a hormone receptor expressed in prostate and a subset of breast cancers, has been shown to radiosensitize both prostate and TNBCs through regulation of DNA damage repair genes (176-178). Inhibition of PIK3CA and related pathway members, have also been shown to increase radiosensitization across numerous cancer models. Studies have detailed how inhibition of the PIK3CA pathway leads to cell cycle arrest, decrease DNA damage repair efficiency, and increased apoptosis (179-182).

Our Studies

In an effort to further understand how breast cancer subtypes respond to radiation therapy, we describe transcriptomic and proteomic changes that occur in breast cancer in response to radiation therapy. Using this data we compared the radiation response across breast cancer subtypes to describe differences that may dictate the effectiveness of radiation therapy. This allows for the nomination of potentially key regulators of the radiation response that be targeted for radiosensitization of basal-like breast cancers. We show that p53, in part, mediates the radiation response and also demonstrate how radioresistance in p53 mutant breast cancers might be overcome. Finally we demonstrate that inhibition of a cell cycle protein, TTK (Mps1), canonically involved in the regulation of the spindle assembly checkpoint (SAC) complex, radiosensitizes aggressive breast cancers through a non-canonical role in the DNA damage response. Together our studies provide a more complete view of the radiation response across breast cancer subtypes and nominate radiosensitization targets to aid in the treatment of the most aggressive breast cancer subtype, basal-like breast cancer.

References

1. Siegel RL, Miller KD, and Jemal A. Cancer statistics, 2020. *CA: A Cancer Journal for Clinicians.* 2020;70(1):7-30.
2. Ferlay J, Soerjomataram I, Dikshit R, Eser S, Mathers C, Rebelo M, Parkin DM, Forman D, and Bray F. Cancer incidence and mortality worldwide: Sources, methods and major patterns in GLOBOCAN 2012. *International Journal of Cancer.* 2015;136(5):E359-E86.
3. DeSantis CE, Ma J, Gaudet MM, Newman LA, Miller KD, Goding Sauer A, Jemal A, and Siegel RL. Breast cancer statistics, 2019. *CA: A Cancer Journal for Clinicians.* 2019;69(6):438-51.

4. McDonald ES, Clark AS, Tchou J, Zhang P, and Freedman GM. Clinical Diagnosis and Management of Breast Cancer. *Journal of Nuclear Medicine.* 2016;57(Supplement 1):9S-16S.
5. Berry DA, Cronin KA, Plevritis SK, Fryback DG, Clarke L, Zelen M, Mandelblatt JS, Yakovlev AY, Habbema JDF, and Feuer EJ. Effect of Screening and Adjuvant Therapy on Mortality from Breast Cancer. *New England Journal of Medicine.* 2005;353(17):1784-92.
6. Pace LE, and Keating NL. A Systematic Assessment of Benefits and Risks to Guide Breast Cancer Screening Decisions. *JAMA.* 2014;311(13):1327-35.
7. Cristofanilli M, Budd GT, Ellis MJ, Stopeck A, Matera J, Miller MC, Reuben JM, Doyle GV, Allard WJ, Terstappen LWMM, et al. Circulating Tumor Cells, Disease Progression, and Survival in Metastatic Breast Cancer. *New England Journal of Medicine.* 2004;351(8):781-91.
8. Cristofanilli M, Hayes DF, Budd GT, Ellis MJ, Stopeck A, Reuben JM, Doyle GV, Matera J, Allard WJ, Miller MC, et al. Circulating Tumor Cells: A Novel Prognostic Factor for Newly Diagnosed Metastatic Breast Cancer. *Journal of Clinical Oncology.* 2005;23(7):1420-30.
9. Ignatiadis M, Rothé F, Chaboteaux C, Durbecq V, Rouas G, Criscitiello C, Metallo J, Kheddoumi N, Singhal SK, Michiels S, et al. HER2-positive circulating tumor cells in breast cancer. *PLoS One.* 2011;6(1):e15624-e.
10. Giuliano M, Giordano A, Jackson S, Hess KR, De Giorgi U, Mego M, Handy BC, Ueno NT, Alvarez RH, De Laurentiis M, et al. Circulating tumor cells as prognostic and predictive markers in metastatic breast cancer patients receiving first-line systemic treatment. *Breast Cancer Research.* 2011;13(3):R67.
11. Effects of chemotherapy and hormonal therapy for early breast cancer on recurrence and 15-year survival: an overview of the randomised trials. *The Lancet.* 2005;365(9472):1687-717.
12. Baselga J. Clinical trials of Herceptin® (trastuzumab). *European Journal of Cancer.* 2001;37(18-24.
13. Wolff AC, Hammond M, Schwartz JN, Hagerty KL, Allred DC, Cote RJ, Dowsett M, Fitzgibbons PL, Hanna WM, and Langer A. College of American Pathologists guideline recommendations for human epidermal growth factor receptor 2 testing in breast cancer. *J Clin Oncol.* 2007;25(1):118-45.
14. Fisher B, Redmond C, Fisher ER, and Caplan R. Relative worth of estrogen or progesterone receptor and pathologic characteristics of differentiation as indicators of prognosis in node negative breast cancer patients: findings from National Surgical Adjuvant Breast and Bowel Project Protocol B-06. *Journal of Clinical Oncology.* 1988;6(7):1076-87.
15. Slamon DJ, Leyland-Jones B, Shak S, Fuchs H, Paton V, Bajamonde A, Fleming T, Eiermann W, Wolter J, Pegram M, et al. Use of Chemotherapy plus a Monoclonal Antibody against HER2 for Metastatic Breast Cancer That Overexpresses HER2. *New England Journal of Medicine.* 2001;344(11):783-92.
16. Jordan VC. Tamoxifen: a most unlikely pioneering medicine. *Nature Reviews Drug Discovery.* 2003;2(3):205-13.
17. Dhingra K. Antiestrogens – Tamoxifen, SERMs and Beyond. *Investigational New Drugs.* 1999;17(3):285-311.
18. Zahnow CA. ErbB receptors and their ligands in the breast. *Expert Reviews in Molecular Medicine.* 2006;8(23):1-21.
19. Zhang H, Berezov A, Wang Q, Zhang G, Drebin J, Murali R, and Greene MI. ErbB receptors: from oncogenes to targeted cancer therapies. *J Clin Invest.* 2007;117(8):2051-8.

20. Nadji M, Gomez-Fernandez C, Ganjei-Azar P, and Morales AR. Immunohistochemistry of estrogen and progesterone receptors reconsidered: experience with 5,993 breast cancers. *Am J Clin Pathol.* 2005;123(1):21-7.
21. Sporikova Z, Koudelakova V, Trojanec R, and Hajduch M. Genetic Markers in Triple-Negative Breast Cancer. *Clinical Breast Cancer.* 2018;18(5):e841-e50.
22. Heldring N, Pike A, Andersson S, Matthews J, Cheng G, Hartman J, Tujague M, Ström A, Treuter E, Warner M, et al. Estrogen Receptors: How Do They Signal and What Are Their Targets. *Physiological Reviews.* 2007;87(3):905-31.
23. Waks AG, and Winer EP. Breast Cancer Treatment: A Review. *JAMA.* 2019;321(3):288-300.
24. Purdie CA, Quinlan P, Jordan LB, Ashfield A, Ogston S, Dewar JA, and Thompson AM. Progesterone receptor expression is an independent prognostic variable in early breast cancer: a population-based study. *British Journal of Cancer.* 2014;110(3):565-72.
25. Dunnwald LK, Rossing MA, and Li CI. Hormone receptor status, tumor characteristics, and prognosis: a prospective cohort of breast cancer patients. *Breast Cancer Research.* 2007;9(1):R6.
26. Bentzon N, During M, Rasmussen BB, Mouridsen H, and Kroman N. Prognostic effect of estrogen receptor status across age in primary breast cancer. *Int J Cancer.* 2008;122(5):1089-94.
27. Yu KD, Wu J, Shen ZZ, and Shao ZM. Hazard of breast cancer-specific mortality among women with estrogen receptor-positive breast cancer after five years from diagnosis: implication for extended endocrine therapy. *The Journal of clinical endocrinology and metabolism.* 2012;97(12):E2201-9.
28. Slamon DJ, Clark GM, Wong SG, Levin WJ, Ullrich A, and McGuire WL. Human breast cancer: correlation of relapse and survival with amplification of the HER-2/neu oncogene. *Science.* 1987;235(4785):177.
29. Slamon DJ, Godolphin W, Jones LA, Holt JA, Wong SG, Keith DE, Levin WJ, Stuart SG, Udove J, Ullrich A, et al. Studies of the HER-2/neu proto-oncogene in human breast and ovarian cancer. *Science.* 1989;244(4905):707.
30. Yarden Y, and Sliwkowski MX. Untangling the ErbB signalling network. *Nature Reviews Molecular Cell Biology.* 2001;2(2):127-37.
31. Arteaga CL, and Engelman JA. ERBB receptors: from oncogene discovery to basic science to mechanism-based cancer therapeutics. *Cancer Cell.* 2014;25(3):282-303.
32. Perez EA, Romond EH, Suman VJ, Jeong J-H, Davidson NE, Geyer CE, Jr., Martino S, Mamounas EP, Kaufman PA, and Wolmark N. Four-year follow-up of trastuzumab plus adjuvant chemotherapy for operable human epidermal growth factor receptor 2-positive breast cancer: joint analysis of data from NCCTG N9831 and NSABP B-31. *J Clin Oncol.* 2011;29(25):3366-73.
33. Perez EA, Romond EH, Suman VJ, Jeong J-H, Sledge G, Geyer CE, Jr., Martino S, Rastogi P, Gralow J, Swain SM, et al. Trastuzumab plus adjuvant chemotherapy for human epidermal growth factor receptor 2-positive breast cancer: planned joint analysis of overall survival from NSABP B-31 and NCCTG N9831. *J Clin Oncol.* 2014;32(33):3744-52.
34. Hashmi AA, Naz S, Hashmi SK, Irfan M, Hussain ZF, Khan EY, Asif H, and Faridi N. Epidermal growth factor receptor (EGFR) overexpression in triple-negative breast cancer: association with clinicopathologic features and prognostic parameters. *Surgical and Experimental Pathology.* 2019;2(1):6.
35. Barton VN, D'Amato NC, Gordon MA, Lind HT, Spoelstra NS, Babbs BL, Heinz RE, Elias A, Jedlicka P, Jacobsen BM, et al. Multiple molecular subtypes of triple-negative breast cancer

critically rely on androgen receptor and respond to enzalutamide in vivo. *Mol Cancer Ther.* 2015;14(3):769-78.
36. Lehmann BD, Bauer JA, Chen X, Sanders ME, Chakravarthy AB, Shyr Y, and Pietenpol JA. Identification of human triple-negative breast cancer subtypes and preclinical models for selection of targeted therapies. *The Journal of Clinical Investigation.* 2011;121(7):2750-67.
37. Sharma P, Klemp JR, Kimler BF, Mahnken JD, Geier LJ, Khan QJ, Elia M, Connor CS, McGinness MK, Mammen JMW, et al. Germline BRCA mutation evaluation in a prospective triple-negative breast cancer registry: implications for hereditary breast and/or ovarian cancer syndrome testing. *Breast cancer research and treatment.* 2014;145(3):707-14.
38. Traina TA, Miller K, Yardley DA, Eakle J, Schwartzberg LS, O'Shaughnessy J, Gradishar W, Schmid P, Winer E, Kelly C, et al. Enzalutamide for the Treatment of Androgen Receptor–Expressing Triple-Negative Breast Cancer. *Journal of Clinical Oncology.* 2018;36(9):884-90.
39. Perou CM, Sørlie T, Eisen MB, van de Rijn M, Jeffrey SS, Rees CA, Pollack JR, Ross DT, Johnsen H, Akslen LA, et al. Molecular portraits of human breast tumours. *Nature.* 2000;406(6797):747-52.
40. Sørlie T, Perou CM, Tibshirani R, Aas T, Geisler S, Johnsen H, Hastie T, Eisen MB, van de Rijn M, Jeffrey SS, et al. Gene expression patterns of breast carcinomas distinguish tumor subclasses with clinical implications. *Proc Natl Acad Sci U S A.* 2001;98(19):10869-74.
41. Prat A, Parker JS, Karginova O, Fan C, Livasy C, Herschkowitz JI, He X, and Perou CM. Phenotypic and molecular characterization of the claudin-low intrinsic subtype of breast cancer. *Breast Cancer Res.* 2010;12(5):R68-R.
42. Hu Z, Fan C, Oh DS, Marron JS, He X, Qaqish BF, Livasy C, Carey LA, Reynolds E, Dressler L, et al. The molecular portraits of breast tumors are conserved across microarray platforms. *BMC Genomics.* 2006;7(96-.
43. Hugh J, Hanson J, Cheang MCU, Nielsen TO, Perou CM, Dumontet C, Reed J, Krajewska M, Treilleux I, Rupin M, et al. Breast cancer subtypes and response to docetaxel in node-positive breast cancer: use of an immunohistochemical definition in the BCIRG 001 trial. *J Clin Oncol.* 2009;27(8):1168-76.
44. Rouzier R, Perou CM, Symmans WF, Ibrahim N, Cristofanilli M, Anderson K, Hess KR, Stec J, Ayers M, Wagner P, et al. Breast Cancer Molecular Subtypes Respond Differently to Preoperative Chemotherapy. *Clinical Cancer Research.* 2005;11(16):5678.
45. Rouzier R, Pusztai L, Delaloge S, Gonzalez-Angulo AM, Andre F, Hess KR, Buzdar AU, Garbay J-R, Spielmann M, Mathieu M-C, et al. Nomograms to Predict Pathologic Complete Response and Metastasis-Free Survival After Preoperative Chemotherapy for Breast Cancer. *Journal of Clinical Oncology.* 2005;23(33):8331-9.
46. Tishchenko I, Milioli HH, Riveros C, and Moscato P. Extensive Transcriptomic and Genomic Analysis Provides New Insights about Luminal Breast Cancers. *PLoS One.* 2016;11(6):e0158259-e.
47. Kumar N, Zhao D, Bhaumik D, Sethi A, and Gann PH. Quantification of intrinsic subtype ambiguity in Luminal A breast cancer and its relationship to clinical outcomes. *BMC Cancer.* 2019;19(1):215-.
48. Raj-Kumar P-K, Liu J, Hooke JA, Kovatich AJ, Kvecher L, Shriver CD, and Hu H. PCA-PAM50 improves consistency between breast cancer intrinsic and clinical subtyping reclassifying a subset of luminal A tumors as luminal B. *Scientific reports.* 2019;9(1):7956-.

49. Voduc KD, Cheang MCU, Tyldesley S, Gelmon K, Nielsen TO, and Kennecke H. Breast Cancer Subtypes and the Risk of Local and Regional Relapse. *Journal of Clinical Oncology.* 2010;28(10):1684-91.
50. Fallahpour S, Navaneelan T, De P, and Borgo A. Breast cancer survival by molecular subtype: a population-based analysis of cancer registry data. *CMAJ Open.* 2017;5(3):E734-E9.
51. Martín M, Prat A, Rodríguez-Lescure Á, Caballero R, Ebbert MTW, Munárriz B, Ruiz-Borrego M, Bastien RRL, Crespo C, Davis C, et al. PAM50 proliferation score as a predictor of weekly paclitaxel benefit in breast cancer. *Breast Cancer Research and Treatment.* 2013;138(2):457-66.
52. Dunbier AK, Anderson H, Ghazoui Z, Salter J, Parker JS, Perou CM, Smith IE, and Dowsett M. Association between breast cancer subtypes and response to neoadjuvant anastrozole. *Steroids.* 2011;76(8):736-40.
53. Tamoxifen for early breast cancer: an overview of the randomised trials. *The Lancet.* 1998;351(9114):1451-67.
54. Mouridsen H, Gershanovich M, Sun Y, Pérez-Carrión R, Boni C, Monnier A, Apffelstaedt J, Smith R, Sleeboom HP, Jänicke F, et al. Superior Efficacy of Letrozole Versus Tamoxifen as First-Line Therapy for Postmenopausal Women With Advanced Breast Cancer: Results of a Phase III Study of the International Letrozole Breast Cancer Group. *Journal of Clinical Oncology.* 2001;19(10):2596-606.
55. Nabholtz JM, Buzdar A, Pollak M, Harwin W, Burton G, Mangalik A, Steinberg M, Webster A, and von Euler M. Anastrozole Is Superior to Tamoxifen as First-Line Therapy for Advanced Breast Cancer in Postmenopausal Women: Results of a North American Multicenter Randomized Trial. *Journal of Clinical Oncology.* 2000;18(22):3758-67.
56. Bonneterre J, Thürlimann B, Robertson JFR, Krzakowski M, Mauriac L, Koralewski P, Vergote I, Webster A, Steinberg M, and von Euler M. Anastrozole Versus Tamoxifen as First-Line Therapy for Advanced Breast Cancer in 668 Postmenopausal Women: Results of the Tamoxifen or Arimidex Randomized Group Efficacy and Tolerability Study. *Journal of Clinical Oncology.* 2000;18(22):3748-57.
57. Rani A, Stebbing J, Giamas G, and Murphy J. Endocrine Resistance in Hormone Receptor Positive Breast Cancer–From Mechanism to Therapy. *Frontiers in Endocrinology.* 2019;10(245).
58. Razavi P, Chang MT, Xu G, Bandlamudi C, Ross DS, Vasan N, Cai Y, Bielski CM, Donoghue MTA, Jonsson P, et al. The Genomic Landscape of Endocrine-Resistant Advanced Breast Cancers. *Cancer Cell.* 2018;34(3):427-38.e6.
59. Finn RS, Crown JP, Lang I, Boer K, Bondarenko IM, Kulyk SO, Ettl J, Patel R, Pinter T, Schmidt M, et al. The cyclin-dependent kinase 4/6 inhibitor palbociclib in combination with letrozole versus letrozole alone as first-line treatment of oestrogen receptor-positive, HER2-negative, advanced breast cancer (PALOMA-1/TRIO-18): a randomised phase 2 study. *The Lancet Oncology.* 2015;16(1):25-35.
60. Finn RS, Martin M, Rugo HS, Jones S, Im S-A, Gelmon K, Harbeck N, Lipatov ON, Walshe JM, Moulder S, et al. Palbociclib and Letrozole in Advanced Breast Cancer. *New England Journal of Medicine.* 2016;375(20):1925-36.
61. Arteaga CL, Sliwkowski MX, Osborne CK, Perez EA, Puglisi F, and Gianni L. Treatment of HER2-positive breast cancer: current status and future perspectives. *Nature Reviews Clinical Oncology.* 2012;9(1):16-32.

62. Pinto AC, Ades F, de Azambuja E, and Piccart-Gebhart M. Trastuzumab for patients with HER2 positive breast cancer: Delivery, duration and combination therapies. *The Breast.* 2013;22(S152-S5.
63. Molina MA, Codony-Servat J, Albanell J, Rojo F, Arribas J, and Baselga J. Trastuzumab (Herceptin), a Humanized Anti-HER2 Receptor Monoclonal Antibody, Inhibits Basal and Activated HER2 Ectodomain Cleavage in Breast Cancer Cells. *Cancer Res.* 2001;61(12):4744.
64. Shak S. Overview of the trastuzumab (Herceptin) anti-HER2 monoclonal antibody clinical program in HER2-overexpressing metastatic breast cancer. Herceptin Multinational Investigator Study Group. *Semin Oncol.* 1999;26(4 Suppl 12):71-7.
65. Wang J, and Xu B. Targeted therapeutic options and future perspectives for HER2-positive breast cancer. *Signal Transduction and Targeted Therapy.* 2019;4(1):34.
66. Spector NL, and Blackwell KL. Understanding the Mechanisms Behind Trastuzumab Therapy for Human Epidermal Growth Factor Receptor 2–Positive Breast Cancer. *Journal of Clinical Oncology.* 2009;27(34):5838-47.
67. Agus DB, Gordon MS, Taylor C, Natale RB, Karlan B, Mendelson DS, Press MF, Allison DE, Sliwkowski MX, Lieberman G, et al. Phase I clinical study of pertuzumab, a novel HER dimerization inhibitor, in patients with advanced cancer. *J Clin Oncol.* 2005;23(11):2534-43.
68. von Minckwitz G, Procter M, de Azambuja E, Zardavas D, Benyunes M, Viale G, Suter T, Arahmani A, Rouchet N, Clark E, et al. Adjuvant Pertuzumab and Trastuzumab in Early HER2-Positive Breast Cancer. *New England Journal of Medicine.* 2017;377(2):122-31.
69. Bachelot T, Ciruelos E, Schneeweiss A, Puglisi F, Peretz-Yablonski T, Bondarenko I, Paluch-Shimon S, Wardley A, Merot JL, du Toit Y, et al. Preliminary safety and efficacy of first-line pertuzumab combined with trastuzumab and taxane therapy for HER2-positive locally recurrent or metastatic breast cancer (PERUSE). *Annals of Oncology.* 2019;30(5):766-73.
70. Kiewe P, and Thiel E. Ertumaxomab: a trifunctional antibody for breast cancer treatment. *Expert opinion on investigational drugs.* 2008;17(10):1553-8.
71. Boyraz B, Sendur MA, Aksoy S, Babacan T, Roach EC, Kizilarslanoglu MC, Petekkaya I, and Altundag K. Trastuzumab emtansine (T-DM1) for HER2-positive breast cancer. *Current medical research and opinion.* 2013;29(4):405-14.
72. Baron JM, Boster BL, and Barnett CM. Ado-trastuzumab emtansine (T-DM1): a novel antibody-drug conjugate for the treatment of HER2-positive metastatic breast cancer. *Journal of Oncology Pharmacy Practice.* 2014;21(2):132-42.
73. Prat A, Adamo B, Cheang MCU, Anders CK, Carey LA, and Perou CM. Molecular characterization of basal-like and non-basal-like triple-negative breast cancer. *Oncologist.* 2013;18(2):123-33.
74. Millikan RC, Newman B, Tse C-K, Moorman PG, Conway K, Dressler LG, Smith LV, Labbok MH, Geradts J, Bensen JT, et al. Epidemiology of basal-like breast cancer. *Breast cancer research and treatment.* 2008;109(1):123-39.
75. Cleator S, Heller W, and Coombes RC. Triple-negative breast cancer: therapeutic options. *The Lancet Oncology.* 2007;8(3):235-44.
76. Atchley DP, Albarracin CT, Lopez A, Valero V, Amos CI, Gonzalez-Angulo AM, Hortobagyi GN, and Arun BK. Clinical and pathologic characteristics of patients with BRCA-positive and BRCA-negative breast cancer. *J Clin Oncol.* 2008;26(26):4282-8.

77. Cheang MCU, Voduc D, Bajdik C, Leung S, McKinney S, Chia SK, Perou CM, and Nielsen TO. Basal-Like Breast Cancer Defined by Five Biomarkers Has Superior Prognostic Value than Triple-Negative Phenotype. *Clinical Cancer Research.* 2008;14(5):1368.
78. Rakha EA, and Ellis IO. Triple-negative/basal-like breast cancer: review. *Pathology.* 2009;41(1):40-7.
79. Sotiriou C, Neo S-Y, McShane LM, Korn EL, Long PM, Jazaeri A, Martiat P, Fox SB, Harris AL, and Liu ET. Breast cancer classification and prognosis based on gene expression profiles from a population-based study. *Proceedings of the National Academy of Sciences.* 2003;100(18):10393.
80. Kyndi M, Sørensen FB, Knudsen H, Overgaard M, Nielsen HM, and Overgaard J. Estrogen Receptor, Progesterone Receptor, HER-2, and Response to Postmastectomy Radiotherapy in High-Risk Breast Cancer: The Danish Breast Cancer Cooperative Group. *Journal of Clinical Oncology.* 2008;26(9):1419-26.
81. Rody A, Karn T, Solbach C, Gaetje R, Munnes M, Kissler S, Ruckhäberle E, Minckwitz Gv, Loibl S, Holtrich U, et al. The erbB2+ cluster of the intrinsic gene set predicts tumor response of breast cancer patients receiving neoadjuvant chemotherapy with docetaxel, doxorubicin and cyclophosphamide within the GEPARTRIO trial. *The Breast.* 2007;16(3):235-40.
82. Chambon P, Weill JD, and Mandel P. Nicotinamide mononucleotide activation of new DNA-dependent polyadenylic acid synthesizing nuclear enzyme. *Biochem Biophys Res Commun.* 1963;11(39-43.
83. Fong PC, Boss DS, Yap TA, Tutt A, Wu P, Mergui-Roelvink M, Mortimer P, Swaisland H, Lau A, O'Connor MJ, et al. Inhibition of Poly(ADP-Ribose) Polymerase in Tumors from BRCA Mutation Carriers. *New England Journal of Medicine.* 2009;361(2):123-34.
84. Curtin NJ. PARP inhibitors for cancer therapy. *Expert Reviews in Molecular Medicine.* 2005;7(4):1-20.
85. Sjöström M, Lundstedt D, Hartman L, Holmberg E, Killander F, Kovács A, Malmström P, Niméus E, Werner Rönnerman E, Fernö M, et al. Response to Radiotherapy After Breast-Conserving Surgery in Different Breast Cancer Subtypes in the Swedish Breast Cancer Group 91 Radiotherapy Randomized Clinical Trial. *Journal of Clinical Oncology.* 2017;35(28):3222-9.
86. Arvold ND, Taghian AG, Niemierko A, Abi Raad RF, Sreedhara M, Nguyen PL, Bellon JR, Wong JS, Smith BL, and Harris JR. Age, breast cancer subtype approximation, and local recurrence after breast-conserving therapy. *J Clin Oncol.* 2011;29(29):3885-91.
87. Gabos Z, Thoms J, Ghosh S, Hanson J, Deschênes J, Sabri S, and Abdulkarim B. The association between biological subtype and locoregional recurrence in newly diagnosed breast cancer. *Breast Cancer Research and Treatment.* 2010;124(1):187-94.
88. Nguyen PL, Taghian AG, Katz MS, Niemierko A, Abi Raad RF, Boon WL, Bellon JR, Wong JS, Smith BL, and Harris JR. Breast Cancer Subtype Approximated by Estrogen Receptor, Progesterone Receptor, and HER-2 Is Associated With Local and Distant Recurrence After Breast-Conserving Therapy. *Journal of Clinical Oncology.* 2008;26(14):2373-8.
89. Speers C, Zhao SG, Liu M, Bartelink H, Pierce LJ, and Feng FY. Development and validation of a novel radiosensitivity signature in human breast cancer. *Clinical Cancer Research.* 2015:clincanres.2898.014.
90. Yard BD, Adams DJ, Chie EK, Tamayo P, Battaglia JS, Gopal P, Rogacki K, Pearson BE, Phillips J, Raymond DP, et al. A genetic basis for the variation in the vulnerability of cancer to DNA damage. *Nat Commun.* 2016;7(11428-.

91. Abazeed ME, Adams DJ, Hurov KE, Tamayo P, Creighton CJ, Sonkin D, Giacomelli AO, Du C, Fries DF, Wong K-K, et al. Integrative radiogenomic profiling of squamous cell lung cancer. *Cancer Res.* 2013;73(20):6289-98.
92. Speers C, Tsimelzon A, Sexton K, Herrick AM, Gutierrez C, Culhane A, Quackenbush J, Hilsenbeck S, Chang J, and Brown P. Identification of novel kinase targets for the treatment of estrogen receptor-negative breast cancer. *Clin Cancer Res.* 2009;15(20):6327-40.
93. Griffin RJ. *International Journal of Radiation Oncology • Biology • Physics.* 2006;66(2):627.
94. Herskind C, and Westergaard O. Inactivation of a Single Eucaryotic Gene Irradiated in Vitro in Transcriptionally Active Chromatin Form. *Radiation Research.* 1986;106(3):331-44.
95. Stewart RD, Yu VK, Georgakilas AG, Koumenis C, Park JH, and Carlson DJ. Effects of radiation quality and oxygen on clustered DNA lesions and cell death. *Radiat Res.* 2011;176(5):587-602.
96. Prasad R, Beard WA, Batra VK, Liu Y, Shock DD, and Wilson SH. A review of recent experiments on step-to-step "hand-off" of the DNA intermediates in mammalian base excision repair pathways. *Mol Biol (Mosk).* 2011;45(4):586-600.
97. Iliakis G, Wang H, Perrault AR, Boecker W, Rosidi B, Windhofer F, Wu W, Guan J, Terzoudi G, and Pantelias G. Mechanisms of DNA double strand break repair and chromosome aberration formation. *Cytogenetic and genome research.* 2004;104(1-4):14-20.
98. Moynahan ME, and Jasin M. Mitotic homologous recombination maintains genomic stability and suppresses tumorigenesis. *Nat Rev Mol Cell Biol.* 2010;11(3):196-207.
99. Liang F, Han M, Romanienko PJ, and Jasin M. Homology-directed repair is a major double-strand break repair pathway in mammalian cells. *Proc Natl Acad Sci U S A.* 1998;95(9):5172-7.
100. Pellicioli A, Lee SE, Lucca C, Foiani M, and Haber JE. Regulation of Saccharomyces Rad53 Checkpoint Kinase during Adaptation from DNA Damage–Induced G2/M Arrest. *Molecular Cell.* 2001;7(2):293-300.
101. Jeggo PA, Geuting V, and Löbrich M. The role of homologous recombination in radiation-induced double-strand break repair. *Radiotherapy and Oncology.* 2011;101(1):7-12.
102. Chapman JR, Taylor Martin RG, and Boulton Simon J. Playing the End Game: DNA Double-Strand Break Repair Pathway Choice. *Molecular Cell.* 2012;47(4):497-510.
103. Chapman JR, Sossick AJ, Boulton SJ, and Jackson SP. BRCA1-associated exclusion of 53BP1 from DNA damage sites underlies temporal control of DNA repair. *Journal of Cell Science.* 2012;125(15):3529.
104. Ira G, Pellicioli A, Balijja A, Wang X, Fiorani S, Carotenuto W, Liberi G, Bressan D, Wan L, Hollingsworth NM, et al. DNA end resection, homologous recombination and DNA damage checkpoint activation require CDK1. *Nature.* 2004;431(7011):1011-7.
105. Lieber MR. The mechanism of double-strand DNA break repair by the nonhomologous DNA end-joining pathway. *Annu Rev Biochem.* 2010;79(181-211.
106. Rodgers K, and McVey M. Error-Prone Repair of DNA Double-Strand Breaks. *J Cell Physiol.* 2016;231(1):15-24.
107. Mladenov E, Magin S, Soni A, and Iliakis G. DNA double-strand break repair as determinant of cellular radiosensitivity to killing and target in radiation therapy. *Front Oncol.* 2013;3(113-.
108. Morgan MA, and Lawrence TS. Molecular Pathways: Overcoming Radiation Resistance by Targeting DNA Damage Response Pathways. *Clin Cancer Res.* 2015;21(13):2898-904.
109. Karlin JD, Tokarz M, Beckta J, Farhan A, Pike K, Barlaam B, MacFaul P, Patel B, Thomason A, Tudge E, et al. A Novel ATM Kinase Inhibitor Effectively Radiosensitizes Glioblastoma in Mice. *International Journal of Radiation Oncology • Biology • Physics.* 2014;90(1):S35.

110. Fokas E, Prevo R, Pollard JR, Reaper PM, Charlton PA, Cornelissen B, Vallis KA, Hammond EM, Olcina MM, Gillies McKenna W, et al. Targeting ATR in vivo using the novel inhibitor VE-822 results in selective sensitization of pancreatic tumors to radiation. *Cell Death Dis.* 2012;3(12):e441-e.
111. Shiloh Y. ATM and ATR: networking cellular responses to DNA damage. *Current Opinion in Genetics & Development.* 2001;11(1):71-7.
112. Collis SJ, Swartz MJ, Nelson WG, and DeWeese TL. Enhanced Radiation and Chemotherapy-mediated Cell Killing of Human Cancer Cells by Small Inhibitory RNA Silencing of DNA Repair Factors. *Cancer Res.* 2003;63(7):1550.
113. Budke B, Logan HL, Kalin JH, Zelivianskaia AS, Cameron McGuire W, Miller LL, Stark JM, Kozikowski AP, Bishop DK, and Connell PP. RI-1: a chemical inhibitor of RAD51 that disrupts homologous recombination in human cells. *Nucleic Acids Res.* 2012;40(15):7347-57.
114. Huang F, and Mazin AV. A small molecule inhibitor of human RAD51 potentiates breast cancer cell killing by therapeutic agents in mouse xenografts. *PLoS One.* 2014;9(6):e100993-e.
115. Krejci L, Altmannova V, Spirek M, and Zhao X. Homologous recombination and its regulation. *Nucleic Acids Res.* 2012;40(13):5795-818.
116. Dolman MEM, van der Ploeg I, Koster J, Bate-Eya LT, Versteeg R, Caron HN, and Molenaar JJ. DNA-Dependent Protein Kinase As Molecular Target for Radiosensitization of Neuroblastoma Cells. *PLoS One.* 2015;10(12):e0145744-e.
117. Lee TW, Wong WW, Dickson BD, Lipert B, Cheng GJ, Hunter FW, Hay MP, and Wilson WR. Radiosensitization of head and neck squamous cell carcinoma lines by DNA-PK inhibitors is more effective than PARP-1 inhibition and is enhanced by SLFN11 and hypoxia. *International Journal of Radiation Biology.* 2019;95(12):1597-612.
118. Michmerhuizen AR, Pesch AM, Moubadder L, Chandler BC, Wilder-Romans K, Cameron M, Olsen E, Thomas DG, Zhang A, Hirsh N, et al. PARP1 Inhibition Radiosensitizes Models of Inflammatory Breast Cancer to Ionizing Radiation. *Mol Cancer Ther.* 2019;18(11):2063.
119. Jagsi R, Griffith KA, Bellon JR, Woodward WA, Horton JK, Ho AY, Schott A, and Pierce LJ. TBCRC 024 Initial Results: A Multicenter Phase 1 Study of Veliparib Administered Concurrently With Chest Wall and Nodal Radiation Therapy in Patients With Inflammatory or Locoregionally Recurrent Breast Cancer. *International Journal of Radiation Oncology • Biology • Physics.* 2015;93(3):S137.
120. Mangoni M, Sottili M, Salvatore G, Meattini I, Desideri I, Greto D, Loi M, Becherini C, Garlatti P, Paoli CD, et al. Enhancement of Soft Tissue Sarcoma Cell Radiosensitivity by Poly(ADP-ribose) Polymerase-1 Inhibitors. *Radiation Research.* 2018;190(5):464-72.
121. Han S, Brenner JC, Sabolch A, Jackson W, Speers C, Wilder-Romans K, Knudsen KE, Lawrence TS, Chinnaiyan AM, and Feng FY. Targeted radiosensitization of ETS fusion-positive prostate cancer through PARP1 inhibition. *Neoplasia.* 2013;15(10):1207-17.
122. Amé J-C, Rolli V, Schreiber V, Niedergang C, Apiou F, Decker P, Muller S, Höger T, Murcia JM-d, and de Murcia G. PARP-2, A Novel Mammalian DNA Damage-dependent Poly(ADP-ribose) Polymerase. *Journal of Biological Chemistry.* 1999;274(25):17860-8.
123. Gradwohl G, Ménissier de Murcia JM, Molinete M, Simonin F, Koken M, Hoeijmakers JH, and de Murcia G. The second zinc-finger domain of poly(ADP-ribose) polymerase determines specificity for single-stranded breaks in DNA. *Proc Natl Acad Sci U S A.* 1990;87(8):2990-4.

124. Masson M, Niedergang C, Schreiber V, Muller S, Menissier-de Murcia J, and de Murcia G. XRCC1 is specifically associated with poly(ADP-ribose) polymerase and negatively regulates its activity following DNA damage. *Mol Cell Biol.* 1998;18(6):3563-71.
125. Haince J-F, McDonald D, Rodrigue A, Déry U, Masson J-Y, Hendzel MJ, and Poirier GG. PARP1-dependent Kinetics of Recruitment of MRE11 and NBS1 Proteins to Multiple DNA Damage Sites. *Journal of Biological Chemistry.* 2008;283(2):1197-208.
126. Pawlik TM, and Keyomarsi K. Role of cell cycle in mediating sensitivity to radiotherapy. *International Journal of Radiation Oncology*Biology*Physics.* 2004;59(4):928-42.
127. Hartwell LH, and Kastan MB. Cell cycle control and cancer. *Science.* 1994;266(5192):1821.
128. Cuddihy AR, and O'Connell MJ. *International Review of Cytology*. Academic Press; 2003:99-140.
129. Morgan MA, Parsels LA, Zhao L, Parsels JD, Davis MA, Hassan MC, Arumugarajah S, Hylander-Gans L, Morosini D, Simeone DM, et al. Mechanism of radiosensitization by the Chk1/2 inhibitor AZD7762 involves abrogation of the G2 checkpoint and inhibition of homologous recombinational DNA repair. *Cancer Res.* 2010;70(12):4972-81.
130. Maachani UB, Kramp T, Hanson R, Zhao S, Celiku O, Shankavaram U, Colombo R, Caplen NJ, Camphausen K, and Tandle A. Targeting MPS1 Enhances Radiosensitization of Human Glioblastoma by Modulating DNA Repair Proteins. *Mol Cancer Res.* 2015;13(5):852-62.
131. Speers C, Zhao SG, Kothari V, Santola A, Liu M, Wilder-Romans K, Evans J, Batra N, Bartelink H, Hayes DF, et al. Maternal Embryonic Leucine Zipper Kinase (MELK) as a Novel Mediator and Biomarker of Radioresistance in Human Breast Cancer. *Clinical Cancer Research.* 2016;22(23):5864.
132. Bridges KA, Hirai H, Buser CA, Brooks C, Liu H, Buchholz TA, Molkentine JM, Mason KA, and Meyn RE. MK-1775, a novel Wee1 kinase inhibitor, radiosensitizes p53-defective human tumor cells. *Clin Cancer Res.* 2011;17(17):5638-48.
133. Nurse P. Universal control mechanism regulating onset of M-phase. *Nature.* 1990;344(6266):503-8.
134. O'Connell MJ, Raleigh JM, Verkade HM, and Nurse P. Chk1 is a wee1 kinase in the G2 DNA damage checkpoint inhibiting cdc2 by Y15 phosphorylation. *EMBO J.* 1997;16(3):545-54.
135. Engelke CG, Parsels LA, Qian Y, Zhang Q, Karnak D, Robertson JR, Tanska DM, Wei D, Davis MA, Parsels JD, et al. Sensitization of pancreatic cancer to chemoradiation by the Chk1 inhibitor MK8776. *Clin Cancer Res.* 2013;19(16):4412-21.
136. Zhou Z-r, Yang Z-z, Wang S-j, Zhang L, Luo J-r, Feng Y, Yu X-l, Chen X-x, and Guo X-m. The Chk1 inhibitor MK-8776 increases the radiosensitivity of human triple-negative breast cancer by inhibiting autophagy. *Acta Pharmacologica Sinica.* 2017;38(4):513-23.
137. Alsubhi N, Middleton F, Abdel-Fatah TMA, Stephens P, Doherty R, Arora A, Moseley PM, Chan SYT, Aleskandarany MA, Green AR, et al. Chk1 phosphorylated at serine345 is a predictor of early local recurrence and radio-resistance in breast cancer. *Mol Oncol.* 2016;10(2):213-23.
138. Dinkelborg PH, Wang M, Gheorghiu L, Gurski JM, Hong TS, Benes CH, Juric D, Jimenez RB, Borgmann K, and Willers H. A common Chk1-dependent phenotype of DNA double-strand break suppression in two distinct radioresistant cancer types. *Breast Cancer Research and Treatment.* 2019;174(3):605-13.
139. Dean JL, McClendon AK, and Knudsen ES. Modification of the DNA damage response by therapeutic CDK4/6 inhibition. *J Biol Chem.* 2012;287(34):29075-87.

140. Hashizume R, Zhang A, Mueller S, Prados MD, Lulla RR, Goldman S, Saratsis AM, Mazar AP, Stegh AH, Cheng S-Y, et al. Inhibition of DNA damage repair by the CDK4/6 inhibitor palbociclib delays irradiated intracranial atypical teratoid rhabdoid tumor and glioblastoma xenograft regrowth. *Neuro Oncol.* 2016;18(11):1519-28.
141. Toogood PL, Harvey PJ, Repine JT, Sheehan DJ, VanderWel SN, Zhou H, Keller PR, McNamara DJ, Sherry D, Zhu T, et al. Discovery of a Potent and Selective Inhibitor of Cyclin-Dependent Kinase 4/6. *Journal of Medicinal Chemistry.* 2005;48(7):2388-406.
142. Denton D, and Kumar S. Autophagy-dependent cell death. *Cell Death & Differentiation.* 2019;26(4):605-16.
143. Xie Y, Hou W, Song X, Yu Y, Huang J, Sun X, Kang R, and Tang D. Ferroptosis: process and function. *Cell Death & Differentiation.* 2016;23(3):369-79.
144. Elmore S. Apoptosis: a review of programmed cell death. *Toxicol Pathol.* 2007;35(4):495-516.
145. Berghe TV, Linkermann A, Jouan-Lanhouet S, Walczak H, and Vandenabeele P. Regulated necrosis: the expanding network of non-apoptotic cell death pathways. *Nature Reviews Molecular Cell Biology.* 2014;15(2):135-47.
146. Eriksson D, and Stigbrand T. Radiation-induced cell death mechanisms. *Tumor Biology.* 2010;31(4):363-72.
147. Lang X, Green MD, Wang W, Yu J, Choi JE, Jiang L, Liao P, Zhou J, Zhang Q, Dow A, et al. Radiotherapy and immunotherapy promote tumoral lipid oxidation and ferroptosis via synergistic repression of SLC7A11. *Cancer Discovery.* 2019:CD-19-0338.
148. Lei G, Zhang Y, Koppula P, Liu X, Zhang J, Lin SH, Ajani JA, Xiao Q, Liao Z, Wang H, et al. The role of ferroptosis in ionizing radiation-induced cell death and tumor suppression. *Cell Research.* 2020;30(2):146-62.
149. Tam SY, Wu VWC, and Law HKW. Influence of autophagy on the efficacy of radiotherapy. *Radiat Oncol.* 2017;12(1):57-.
150. Galluzzi L, Bravo-San Pedro JM, Demaria S, Formenti SC, and Kroemer G. Activating autophagy to potentiate immunogenic chemotherapy and radiation therapy. *Nature Reviews Clinical Oncology.* 2017;14(4):247-58.
151. Zerp SF, Stoter TR, Hoebers FJP, van den Brekel MWM, Dubbelman R, Kuipers GK, Lafleur MVM, Slotman BJ, and Verheij M. Targeting anti-apoptotic Bcl-2 by AT-101 to increase radiation efficacy: data from in vitro and clinical pharmacokinetic studies in head and neck cancer. *Radiation Oncology.* 2015;10(1):158.
152. Li J-Y, Li Y-Y, Jin W, Yang Q, Shao Z-M, and Tian X-S. ABT-737 reverses the acquired radioresistance of breast cancer cells by targeting Bcl-2 and Bcl-xL. *Journal of Experimental & Clinical Cancer Research.* 2012;31(1):102.
153. Wu H, Schiff DS, Lin Y, Neboori HJR, Goyal S, Feng Z, and Haffty BG. Ionizing radiation sensitizes breast cancer cells to Bcl-2 inhibitor, ABT-737, through regulating Mcl-1. *Radiation research.* 2014;182(6):618-25.
154. Yip KW, Mocanu JD, Au PYB, Sleep GT, Huang D, Busson P, Yeh W-C, Gilbert R, Sullivan B, Gullane P, et al. Combination Bcl-2 Antisense and Radiation Therapy for Nasopharyngeal Cancer. *Clinical Cancer Research.* 2005;11(22):8131.
155. Moretti L, Li B, Kim KW, Chen H, and Lu B. AT-101, a Pan-Bcl-2 Inhibitor, Leads to Radiosensitization of Non-small Cell Lung Cancer. *Journal of Thoracic Oncology.* 2010;5(5):680-7.

156. Mi J, Bolesta E, Brautigan DL, and Larner JM. PP2A regulates ionizing radiation–induced apoptosis through Ser46 phosphorylation of p53. *Mol Cancer Ther.* 2009;8(1):135.
157. Werner LR, Huang S, Francis DM, Armstrong EA, Ma F, Li C, Iyer G, Canon J, and Harari PM. Small Molecule Inhibition of MDM2–p53 Interaction Augments Radiation Response in Human Tumors. *Mol Cancer Ther.* 2015;14(9):1994.
158. Iwakuma T, and Lozano G. MDM2, An Introduction. *Molecular Cancer Research.* 2003;1(14):993.
159. Chen Y, Li X, Guo L, Wu X, He C, Zhang S, Xiao Y, Yang Y, and Hao D. Combining radiation with autophagy inhibition enhances suppression of tumor growth and angiogenesis in esophageal cancer. *Mol Med Rep.* 2015;12(2):1645-52.
160. Liang DH, El-Zein R, and Dave B. Autophagy Inhibition to Increase Radiosensitization in Breast Cancer. *J Nucl Med Radiat Ther.* 2015;6(5):254.
161. Han MW, Lee JC, Choi J-Y, Kim GC, Chang HW, Nam HY, Kim SW, and Kim SY. Autophagy Inhibition Can Overcome Radioresistance in Breast Cancer Cells Through Suppression of TAK1 Activation. *Anticancer Research.* 2014;34(3):1449-55.
162. Yoshifumi T, Masanori K, Shoichi N, Yumiko H, Hironaga K, Nakamasa H, Isao K, and Shunro E. Induction of autophagic cell death and radiosensitization by the pharmacological inhibition of nuclear factor–kappa B activation in human glioma cell lines. *Journal of Neurosurgery JNS.* 2009;110(3):594-604.
163. Yoon YN, Choe MH, Jung K-Y, Hwang S-G, Oh JS, and Kim J-S. MASTL inhibition promotes mitotic catastrophe through PP2A activation to inhibit cancer growth and radioresistance in breast cancer cells. *BMC Cancer.* 2018;18(1):716-.
164. Quintiliani M. The Oxygen Effect in Radiation Inactivation of DNA and Enzymes. *International Journal of Radiation Biology and Related Studies in Physics, Chemistry and Medicine.* 1986;50(4):573-94.
165. Overgaard J. Hypoxic Radiosensitization: Adored and Ignored. *Journal of Clinical Oncology.* 2007;25(26):4066-74.
166. Nordsmark M, Overgaard M, and Overgaard J. Pretreatment oxygenation predicts radiation response in advanced squamous cell carcinoma of the head and neck. *Radiotherapy and Oncology.* 1996;41(1):31-9.
167. Semenza GL. The hypoxic tumor microenvironment: A driving force for breast cancer progression. *Biochim Biophys Acta.* 2016;1863(3):382-91.
168. Chen X, Iliopoulos D, Zhang Q, Tang Q, Greenblatt MB, Hatziapostolou M, Lim E, Tam WL, Ni M, Chen Y, et al. XBP1 promotes triple-negative breast cancer by controlling the HIF1α pathway. *Nature.* 2014;508(7494):103-7.
169. Bernardi R, and Gianni L. Hallmarks of triple negative breast cancer emerging at last? *Cell research.* 2014;24(8):904-5.
170. Overgaard J. Sensitization of Hypoxic Tumour Cells—Clinical Experience. *International Journal of Radiation Biology.* 1989;56(5):801-11.
171. Kallman RF. The phenomenon of reoxygenation and its implications for fractionated radiotherapy. *Radiology.* 1972;105(1):135-42.
172. Hu F, Vishwanath K, Salama JK, Erkanli A, Peterson B, Oleson JR, Lee WT, Brizel DM, Ramanujam N, and Dewhirst MW. Oxygen and Perfusion Kinetics in Response to Fractionated Radiation Therapy in FaDu Head and Neck Cancer Xenografts Are Related to Treatment Outcome. *Int J Radiat Oncol Biol Phys.* 2016;96(2):462-9.

173. Zeman EM, Brown JM, Lemmon MJ, Hirst VK, and Lee WW. SR-4233: A new bioreductive agent with high selective toxicity for hypoxic mammalian cells. *International Journal of Radiation Oncology*Biology*Physics.* 1986;12(7, Part 1):1239-42.
174. Rockwell S. Use of hypoxia-directed drugs in the therapy of solid tumors. *Semin Oncol.* 1992;19(4 Suppl 11):29-40.
175. Mast JM, and Kuppusamy P. Hyperoxygenation as a Therapeutic Supplement for Treatment of Triple Negative Breast Cancer. *Front Oncol.* 2018;8(527-.
176. Speers C, Zhao SG, Chandler B, Liu M, Wilder-Romans K, Olsen E, Nyati S, Ritter C, Alluri PG, Kothari V, et al. Androgen receptor as a mediator and biomarker of radioresistance in triple-negative breast cancer. *NPJ Breast Cancer.* 2017;3(29-.
177. Polkinghorn WR, Parker JS, Lee MX, Kass EM, Spratt DE, Iaquinta PJ, Arora VK, Yen W-F, Cai L, Zheng D, et al. Androgen receptor signaling regulates DNA repair in prostate cancers. *Cancer discovery.* 2013;3(11):1245-53.
178. Goodwin JF, Schiewer MJ, Dean JL, Schrecengost RS, de Leeuw R, Han S, Ma T, Den RB, Dicker AP, Feng FY, et al. A hormone-DNA repair circuit governs the response to genotoxic insult. *Cancer discovery.* 2013;3(11):1254-71.
179. Park JH, Jung KH, Kim SJ, Fang Z, Yan HH, Son MK, Kim J, Kang YW, Lee JE, Han B, et al. Radiosensitization of the PI3K inhibitor HS-173 through reduction of DNA damage repair in pancreatic cancer. *Oncotarget.* 2017;8(68):112893-906.
180. Shi F, Guo H, Zhang R, Liu H, Wu L, Wu Q, Liu J, Liu T, and Zhang Q. The PI3K inhibitor GDC-0941 enhances radiosensitization and reduces chemoresistance to temozolomide in GBM cell lines. *Neuroscience.* 2017;346(298-308.
181. Chang L, Graham PH, Hao J, Ni J, Bucci J, Cozzi PJ, Kearsley JH, and Li Y. PI3K/Akt/mTOR pathway inhibitors enhance radiosensitivity in radioresistant prostate cancer cells through inducing apoptosis, reducing autophagy, suppressing NHEJ and HR repair pathways. *Cell Death Dis.* 2014;5(10):e1437-e.
182. Tonlaar N, Galoforo S, Thibodeau BJ, Ahmed S, Wilson TG, Yumpo Cardenas P, Marples B, and Wilson GD. Antitumor activity of the dual PI3K/MTOR inhibitor, PF-04691502, in combination with radiation in head and neck cancer. *Radiotherapy and Oncology.* 2017;124(3):504-12.

Chapter 2

Multi-omics Characterization of the Breast Cancer Radiation Response

Summary

Radiation therapy is a mainstay of treatment of breast cancer and delivered to the majority of breast cancer patients after surgery; however, relatively little is known about the breast cancer radiation response. The effectiveness of radiation differs across breast cancer subtypes and mutational profiles, indicating that these cancers likely have different transcriptomic and proteomic responses to radiation. Understanding how different breast cancer subtypes and mutations respond to radiation will allow for a further understanding of why breast cancers exhibit a heterogeneous response to radiation. Using microarray and reverse phase protein array (RPPA) we characterize the transcriptomic and proteomic response to radiation across a panel of breast cancer cell lines. Transcriptional changes occur as early as 12- and 24- hours after radiation across cell lines, though earlier responses were not detected. Radiation induces DNA replication, cell cycle, and p53 responses across all cell lines; however, differential expression of cell cycle related genes changes in a breast cancer subtype-dependent manner. Transcriptionally, apoptosis pathway related genes are induced in p53 wild-type cell lines but not in p53 mutant cell lines. RPPA protein analysis demonstrates differential protein and phosphor-protein expression changes in apoptosis and cell cycle pathways across breast cancer subtypes and p53 mutation status. Together, our data provides the most comprehensive description of the radiation response to date.

Introduction

Breast cancer is the most commonly diagnosed cancer among women and the second most deadly (1). Breast cancer subtyping is based on the expression of three receptors estrogen receptor (ER), progesterone receptor (PR), and the human epidermal growth factor receptor 2 (HER2), and this expression also dictates prognosis in this disease (2-4). More recently, advances in transcriptomic sequencing technology have allowed for subtyping of breast cancer based on the expression of genes in each tumor. For example, a panel of fifty genes has been used to classify breast cancers into four different subtypes, Luminal A, Luminal B, Her2-enriched (Her2+), and basal-like breast cancer. Luminal A breast cancers are typically ER-positive (ER+)/PR-positive (PR+) with low expression of the proliferation marker Ki67. Luminal B breast cancers are also typically ER/PR+ but with high Ki67 expression (5, 6). *HER2* enriched breast cancers typically have high expression of the Her2 receptor, due to amplification of the *HER2* gene, though this is not required for a tumor to be classified as Her2-enriched (5-7). Finally, basal-like breast cancers typically have low expression of all nuclear hormone receptors, lack Her2 amplification, and have high expression of proliferation and cell cycle markers (5, 6). Importantly, subtyping of tumors has allowed for the discrimination of patient outcomes based on standard treatment modalities and can be used to guide treatment decisions as well as help to predict their response to treatments (8-13).

Radiation therapy (RT) is given to the majority of breast cancer patients regardless of their subtype; however, patients with basal-like breast cancer are more likely to have locoregional recurrences than patients with luminal or Her2+ breast cancer, even when treated with RT (14,

15). Unfortunately, the reason for the increased rates in locoregional recurrence within the basal-like breast cancer subtype has yet to be elucidated despite the numerous studies describing this phenomenon (14, 16, 17).

Previous studies aimed at characterizing the RT response have focused solely on the transcriptional response (18). However, as many changes after RT are acute changes, interrogating the protein and phosphoprotein changes elicited by radiation treatment remains a critical gap in our understanding of the breast cancer response to ionizing radiation. Reverse phase protein array (RPPA) is a miniaturized dot-blot array capable of measuring hundreds of protein/phosphoprotein changes simultaneously (19). Recently, RPPA has been used to measure and identify complex signaling changes in response to various treatments (20-23). Using this approach, proteins and their corresponding phosphoproteins can be quantitatively assessed, thus providing a snapshot of the activation state of assayed proteins, pathways, and networks in a given tumor (24-27). To identify proteins and pathways that may be mediators of radiation response, one could use RPPA to identify proteins and phosphoproteins whose expression changes acutely after radiation treatment in multiple models of breast cancer, representing various subtypes of this heterogeneous disease. To date, however, no studies have examined the radiation response using RPPA or using a multi-omics approach.

In an effort to more fully characterized the RT response we used publicly available microarray data in which breast cancer cell lines were harvested 24 hours after 5 Gy RT to examine differential expression across all breast cancer subtypes (18). We also used microarray data generated within our lab to pair with the open source data. These data, in combination with RPPA,

allowed us to more fully characterize the RT response in various subtypes of breast cancer. Furthermore, these data allowed us to nominate multiple targets that may be regulating the radiation response in breast cancer and thus serve as targets for the radiosensitization of breast cancer.

Results

High variance in public dataset leads to low differential gene expression

To begin to characterize the transcriptomic changes after RT, we used publically available data from Gene Expression Omnibus (GEO) (GSE59732) in which breast cancer cell lines, across all subtypes, were given 5 Gy RT (a clinically relevant dose of radiation) and harvested for RNA 24 hours after RT (18). Previously published differential expression analysis showed only 4 of the 16 cell lines had robust different gene expression 24 hours after RT, and these changes were only seen in the luminal-subtype of cancers. This led the authors to claim that only the luminal subtype of breast cancer cell lines exhibit differential expression after radiation while the basal-like or *HER2* enriched subtype do not. Clinical response data, including data already discussed in this thesis, contradicted this claim and we sought to independently verify this claim. To do this we accessed the primary source data from the authors available from GEO and performed our own differential expression analysis. Our analysis also showed that only the 4 luminal-like breast cancer cell lines had any appreciable differentially gene expression after radiation (data not shown). To investigate further, we performed principal component analysis (PCA) to determine how similar the technical replicates within the experiment behaved. PCA analysis is a statistical method used

to measure the similarity between samples by combining multiple unrelated variables into singular linear values referred to as principle components (PC). These PCs are then plotted together to visually depict the similarity of samples to one another (28).

In the estrogen receptor-positive (ER+), luminal breast cancer cell lines, MCF-7, T47D, and ZR-75-1 had tight clustering of triplicate treatment samples together **(Figure 2.1A-C)**. However, PCA of the CAMA-1 samples showed inconsistent clustering of triplicate samples **(Figure 2.1D)**. When we performed PCA for Her2+ **(Figure 2.2A-D)**, triple-negative breast cancer (TNBC) **(Figure 2.3A-E)**, and normal cell lines **(Figure 2.4A-C)**, we saw inconsistent clustering across all cell lines except for HBL-100 using PCA. Unsurprisingly the only cell lines with robust differential gene expression reported by the authors were the four cell lines in which PCA produced the expected pattern of technical replicate clustering. We therefore concluded that a lack of differential gene expression in non-luminal cell lines was not due to radiation only eliciting a response in luminal-type tumors, rather due to high variance from inconsistent clustering of their non-luminal subtype samples.

Radiation induces cell cycle changes and p53 pathway response

While we were unable to use the publically available datasets to characterize the transcriptomic changes after radiation, we performed our own transcriptomic analysis to determine gene expression changes induced after radiation treatment in three breast cancer cell lines (MDA-MB-231 [TNBC], BT-549 [TNBC], and MCF-7 [luminal]) across multiple time points to begin to understand the timing of transcriptomic changes after RT. Here, we harvested RNA from the three cell lines 3-, 12-, and 24-hours after 4 Gy RT and performed microarray analysis. Although robust

differential gene expression was found at the 12- and 24-hour time points across all three cell lines **(Figure 2.5A)**, little differential gene expression was seen at the 3-hour time points in MDA-MB-231 (1 gene with Log(FC) > 0.4, FDR < 0.05) and BT-549 (10 gene with Log(FC) > 0.4, FDR < 0.05) cell lines, and more modest differential expression was seen at 3-hours in MCF-7 cell line (135 gene with Log(FC) > 0.4, FDR < 0.05). Volcano plots at 12- and 24-hours in all three cell lines show the distribution of differential expression across cell lines **(Figure 2.5B-G)**. These data suggest that the transcriptional level changes induced by radiation are not immediate, and that the signaling cascade that induces radiation-induced gene expression changes is a delayed event that takes hours to be detected.

PCA analysis was perform to ensure appropriate clustering was seen across time points within each cell line. Unlike with the publically available datasets, both MDA-MB-231 and BT-549 cells had consistent technical replicate clustering at the 12- and 24-hour time points as well as robust differential expression, as would be expected **(Figure 2.6A-B & D-E)**. In contrast, the 3-hour time point had inconsistent clustering, potentially owing to the lack of differential expression noted in these samples **(Figure 2.6C&F)**. The MCF-7 cell line had replicate clustering at the 24-hour time point, while the 12- and 3-hour time points had more loose clustering **(Figure 2.6G-I)**. Interestingly, MCF-7 cells had high levels of differential gene expression across all time points despite the lack of clear triplicate clustering at early time points.

While differential gene expression analysis allows one to understand expression changes on a gene-by-gene basis, it does not allow for a more global assessment of pathways or cellular processes that may be changing. To address this limitation, we performed KEGG (Kyoto

Encyclopedia of Genes and Genomes) analysis to identify pathways enriched after radiation, using differentially expressed genes as the input (29). Across all three cell lines numerous pathways were significantly altered, including cell cycle and p53 signaling, which were enriched 24-hours after RT **(Figure 2.7A-C)**. Pathways enriched 12-hours after RT included DNA damage repair pathways such as homologous recombination and Fanconi anemia as well as cell cycle and p53 signaling, as seen with the 24-hour time point **(Figure 2.7B&C)**. MDA-MB-231 cells 12-hours after RT did not have enough differentially expressed genes for accurate KEGG analysis and was therefore the results were excluded.

Radiation induces different changes to cell cycle related genes between luminal and basal-like breast cancers

To further investigate pathways that may be related to RT across cell lines, we specifically looked at differentially expressed genes within the cell-cycle pathway. In both MDA-MB-231 and BT-549 cell lines we saw similar patterns of downregulated genes in G1 and S phase of the cell cycle and upregulated genes in the G2 and mitosis phases of the cell cycle. Downregulated genes included E2F1-5, Cyclin D, E, and A, as well as CDK2. Upregulated genes included CDK1, Plk1, Rb, and several genes associated with the spindle assembly checkpoint (SAC) complex (Mps1, Mad1, Mad2, Bub1, etc) **(Figure 2.8A&B)**. However, in the MCF-7 cell line, which is p53 wild-type and ER+, we see downregulation of G2 and mitosis related genes, such as CDK1, cyclin A and B, as well as many members of SAC complex (Mps1, Mad1, Mad2, Bub1, etc) **(Figure 2.9)**. In addition, few changes were identified in genes related to G1 and S phase in these luminal-like MCF-7 cells compared to MDA-MB-231 and BT-549 cell lines. Together these results indicate

that different subtypes of breast cancer likely respond differently to RT as evidenced by the differential effects of RT on cell-cycle effects, DNA damage response, and other pathways in these models. These data also suggest that these differences in gene expression may be dependent on p53 functional status, as it is a major checkpoint protein after DNA damage and is induced by ionizing radiation.

p53 mutation status may dictate apoptotic response to radiation therapy

One noticeably absent pathway from all cell lines and across all time points was the apoptotic pathway. As RT is known to induce single- and double strand DNA breaks that, when unrepaired, lead to a subsequent induction of apoptosis, the lack of differentially expressed genes within the apoptosis signaling pathway was surprising (30, 31). To investigate this further we interrogated the gene expression changes of over 40 genes known to be related to apoptosis. Gene expression changes were then visualized by generation of a heat map and gene expression changes after RT were assessed. Across all three time points the MCF-7 cell line has a consistent group of apoptosis-related genes whose expression was significantly altered, including genes whose expression went both up- and down- after RT, particularly at the 3- and 24-hour time points. However, in both basal-like cell lines, MDA-MB-231 and BT-549, we see general downregulation of transcripts associated with apoptosis and a lack of induction of the pathway globally **(Figure 2.10A-C)**. While the differences seen between basal-like and luminal breast cancer cell lines could be due to estrogen receptor status, p53 mutation status, or other factors, we hypothesized that p53 mutations may be causing differential regulation between cell lines.

To test this hypothesis we used the open source data from GEO previous described. Using the four cell lines for which there was appropriate clustering on PCA and for which we had robust differential gene expression data, three of these cell lines were known to be wild-type for the p53 gene while one had a mutation in p53. When we visualized gene expression in the apoptotic pathway, a similar trend as noted in our initial analysis emerged. The p53 wild-type cell lines (MCF-7, ZR-75-1, and HBL-100) had upregulation and differential expression of many genes in the apoptosis pathway, while the p53 mutant cell line (T47D) had very little upregulation of apoptosis related genes **(Figure 2.10D)**. Using this second dataset we were able to show that within the same subtype of breast cancer, p53 mutation status could predict differential expression of apoptosis related genes suggesting alterations in pathway activity between p53 wild type and mutant models of breast cancer.

Microarray data from an additional eight cell lines is inconclusive

In an effort to make more definitive conclusions about the transcriptional consequences of RT, we treated eight additional cell lines with 4 Gy RT and harvest RNA 24-hours after RT. Five basal-like breast cancer cell lines, SUM-159, MDA-MB-453, MDA-MB-468, CAL-120, and HCC-38 and 3 luminal cell lines, T47D, CAMA-1, and BT-474 were included in our second analysis that again utilized a Affymetrix microarray platform. Unfortunately, after differential expression analysis none of the additional eight cell lines had more than 50 differentially expressed genes **(Figure 2.11A)**.

We performed PCA across all samples to determine if the new samples clustered by cell line or RT treatment. Each cell line clustered together separately from RT treatment **(Figure**

2.11B). When we performed PCA within each cell line we found inconsistent clustering across all cell lines **(Figure 2.12A-H)**. This again indicates that high levels of variance caused low differential expression, which was seen previously in the samples downloaded from GEO, making it impossible to draw conclusions about radiation-induced gene changes in these cell lines.

Reverse phase protein array shows changes in protein expression after radiation therapy

Thus far all of our analyses related to gene expression changes that occur after radiation were limited to transciptomic analysis of differentially expressed RNA transcripts. This ignores protein and phosphoprotein changes that may be induced by radiation in breast cancer models that may influence sensitivity to this treatment. To aid in our characterization of changes that occur in response to RT, we performed reverse phase protein arrays (RPPA) with protein harvested 1-, 6-, and 24-hours after 4 Gy RT.

RPPA is a novel quantitative protein detection system that relies on validated, high-quality antibodies to measure protein expression levels and function states of many signaling pathways. RPPA is also able to quantitate very small amounts of protein expression (femtograms of target in nanograms of starting material), and in particular the activation state of cellular signaling pathways and networks using phospho-specific antibodies. Thus, RPPA may be useful for target discovery, in addition to being a means of measuring the global activation status of multiple signaling pathways at one time in individual samples after treatment, including radiation (32, 33).

We compared changes in protein expression at 1-, 6-, and 24-hours after RT to an untreated control group for each cell line. To examine proteomic changes after RT we used multiple basal-like (MDA-MB-231 and BT-549) and luminal (MCF-7 and T47D) breast cancer cell lines. We

expected to see significant overlap between basal-like cell lines and luminal cell lines separately; however, no clear proteomic changes were seen within breast cancer subtypes at either 1- or 24-hours **(Figure 2.13A&B)**. In the basal-like cell lines only Her3, p53, p-FAK (Y925), caveolin, and p-EGFR (Y1068) increased in both cell lines and only XRCC1, p-Cdc2 (Y15), and AURKB decreased. In the luminal cell lines only p-AKT (T308), p-ERK1 (S217), Bcl-xL, and CCND3 increased and RSK, CASP9 Cleaved-5330, and CAS7 Cleaved-D198 decreased in both cell lines. At the 24-hour time point Her3, p-FAK (Y925), caveolin, and p-EGFR (Y1068) increased in both basal-like cell lines, while multiple genes related cell cycle (p-Wee1 [S625], p-Cdc2 [Y15], p-CDK1 [S296]), AKT signaling (p-AKT [S473 and T308], and MAPK signaling (p-AMPK [T172], p-MAPK [T202]) decrease. In the luminal cell lines multiple genes related to MAPK and MEK signaling increase (MEK1, pMEK1 [S217], p-ERK1 [S217], and MAPK [T202]) while cell cycle (p-p27 [T157] and p27) and Src (Src and p-Src [Y416]) related genes decreased. This small number of commonly differentially expressed genes within breast cancer subtypes was unexpected and indicates that the RT response may not be dictated by breast cancer subtype but by other factors, as has been suggested before (34).

While proteomic changes across all genes show little overlap between breast cancer subtypes, we next focused on genes related to the apoptotic response to identify if various breast cancer cell lines had a similar proteomic response to RT that was identified in our transcriptomic analysis. Interesting the T47D cell line, a luminal cell line with mutant p53 had increased expression of several apoptotic proteins **(Figure 2.14A&B)**. Additionally, all p53 mutant cell lines had a large increase in p53 protein expression 1-hour after RT, indicating that those cell lines may

have been attempting to elicit a p53 response but were unable to due to mutations in the p53 gene (35). Also, of note, Bcl-2 family proteins (Bcl-xL and Mcl-1), which are clinically targetable, had robust changes in expression 1-hour after RT, indicating that these may be viable targets for radiosensitization in specific breast cancers worthy of additional interrogation.

We also examined changes in cell cycle proteins after RT and found that there is a general decrease in cell cycle proteins across all cell lines after RT **(Figure 2.14C&D)**. Although few genes decreased across all cell lines (p27 and p-p27 [T157]) many cell cycle related protein were downregulated in 3 of the 4 of the breast cancer cell lines including p-CDK1 (S296), pCdc2 (Y15), p-Wee1 (S462), AURKB, Wee1, and Chk1. Many of these genes were downregulated both 1- and 24-hours after RT, which is an expected result, as RT is used to decrease tumor growth (36-38).

Finally, as ionizing radiation elicits its effect by inducing DNA damage, we evaluated DNA damage response genes separately to examine how each cell line respond to DNA damage over time. Three cell lines (MDA-MB-231, MCF-7, and T47D) exhibited a 2-fold increase in phospho-ATM (Ser 1981) (p-ATM), an indicator of DNA damage, 1-hour after RT **(Figure 2.15A, C, & D)**. Across all cell lines, proteins that increase in response to RT decrease to normal levels by 24-hours **(Figure 2.15A-D)**. This is likely because the DNA breaks have been successfully repaired by this time, which aligns with other studies showing that double strand DNA damage is repaired by approximately 24-hours across cancer cell line models (39, 40). Taken together, these RPPA results provide a more complete view of how breast cancers respond to RT and show that breast cancer cell lines respond differently independent of subtype.

Discussion

In our studies we show, using a multi-omics approach (RNA and protein quantification), that there is a heterogeneous response to radiation therapy in breast cancer cell lines, independent of subtypes both transcriptomically and proteomically. We go on to highlight differences in gene expression across multiple cell lines and subtypes of breast cancer. We use this data to perform pathway analysis and show that RT induces changes in DNA replication, cell cycle, and p53 related genes across all three cell lines at the transcriptomic level. Furthermore, we show that genes within the cell cycle pathway are upregulated in G1 and S phase in the luminal call line, MCF-7, while genes in G2 and mitosis are downregulated. However, in the basal-like cell lines, MDA-MB-231 and BT-549, we see downregulation of cell cycle genes within G1 and S phase and upregulation of genes in the G2 and M phases of the cell cycle. Finally, we note the lack of programmed cell death, in multiple breast cancer cell lines model, through apoptosis identified using pathway analysis and hypothesize that re-activation of the apoptosis pathway may be an effective strategy to radiosensitize radioresistant breast cancer cell lines by inducing cell death after RT. Using reverse phase protein array (RPPA) we also show specific changes in protein expression across multiple pathways including cell cycle, DNA damage, and apoptosis pathways. Together, our results provide a more comprehensive and accurate description of changes, both transcriptomic and proteomic, after RT in breast cancer cell lines. These data provide additional insights into targetable genes and pathways that can be followed up with *in vitro* and *in vivo* studies.

We began our studies by attempting to use open source microarray data, in which breast cancer cell lines were treated with radiation and compared to untreated samples. Unfortunately,

these data were unusable due to high variance between technical replicates. Previously, this data was used in a study where the authors concluded that only luminal subtype breast cancer cell lines have differential expression after RT, while Her2+ and basal-like cell lines do not have differential expression after RT (18). Based on our re-analysis of that data, we draw a different conclusion and as noted above, the lack of differential expression in Her2+ and basal-like subtypes was likely due to high variance in the data and not biological difference in the RT response. Additionally, we attempted to replicate their study to provide data with lower variance that may be useable for differential gene expression and pathway analysis. However, as seen in the previously published study, our data too had high variance and low differential expression across several cell lines. This highlights the importance of quality assurance in large datasets, including transcriptomic data, and that without proper quality checks, inappropriate conclusions can be drawn using flawed data. While the cause of the variance is unknown, we analyzed RNA quality before microarray analysis and all samples had an RNA integrity number (RIN) of 9 or greater, indicating RNA quality was not a reason for high variance. Furthermore, all samples with a cell line were processed and run on a single microarray chip, thereby eliminating any batch effects in each sample. This makes it difficult to define what caused the high variance and low number of differentially expressed genes among many cell lines. Interestingly, there was overlap between breast cancer cell lines on the open source dataset and what was run by our group. Within the overlap only one cell line, MCF-7, showed consistent differential expression after RT. 161 genes were differentially expressed in both datasets, about 33% of the total genes in the Duke dataset (which had less total differentially expressed genes) **(Figure 2.16A)**. However, when we performed KEGG pathway analysis six of

the top 10 pathways were common across both datasets, indicating that genes in similar pathways were differentially expressed **(Figure 2.16B)**. Furthermore, of the four pathways not in common in the top ten, three were still significantly enriched in the opposing dataset (data not shown). Together, these results indicate that RT induces similar pathway responses in the MCF-7 cell lines across multiple groups.

While we were unable to generate usable data in eight cell lines, we did generate usable microarray data in three cell lines, at three time points, after RT. In this study we were able to accurately cluster triplicates together and perform differential expression analysis and pathway analysis. Here, we were able to show that unlike in other studies, basal-like breast cancer cell lines did in fact have transcriptional changes after RT (18). Additionally, we identified that basal-like breast cancer cell lines had different transcriptional cell cycle changes as compared to a luminal breast cancer cell line. This difference in cell cycle gene expression may contribute to basal-like breast cancers to be more radioresistant than luminal cell lines. Additionally, differences in expression of DNA damage linked genes, p53 pathway genes, and apoptosis related genes likely contribute to radioresistance in basal-like breast cancer compared to luminal breast cancer. Theses pathways have all previous been targeted for radiosensitization but no studies to date have shown transcriptional differences across all pathways after RT between basal-like and luminal breast cancer subtypes (41-45).

Alternatively, differences in gene expression across these pathways could also be linked to p53 mutation status, as both MDA-MB-231 and BT-549 cell lines have mutations in p53, while MCF-7 cells have wild-type p53 (46, 47). P53 is a master regulator of genomic integrity and DNA

integrity and has been well characterized in the regulation of cell cycle, DNA damage response, and apoptosis. Thus, functional p53 may be regulating gene expression changes between breast cancer subtypes in a p53-dependent manner, and this regulation is lost in the p53 mutant models (48-52). The use additional cell lines, with different p53 mutational status, would help to further characterize the role of p53 in mediating these gene expression changes and whether gene expression differences are due to differences in p53 mutational status or breast cancer subtypes.

Our RPPA data show consistent changes in protein expression after RT in genes that are known to change after (i.e. controls). For example, phospho-ATM, a canonical marker for DNA damage significantly changed 1-hour after RT in three of the four cell lines (53, 54). In BT-549 cells, which did not have an increase in p-ATM, a large increase in phospho-CHK2, a phosphorylation target of ATM, was seen (55). Although no increase in p-ATM was seen in this cell line, the increase in p-CHK2 acts a strong positive control that the RT did induce DNA damage. Furthermore, all four cell lines had a decrease in multiple members of the cell cycle pathway, which also acts as an experimental positive control for RT. However, we were limited in the number of proteins and phosphor-proteins that we could assess (only ~100 in the current study) and future studies utilizing additional validated antibodies will allow for a more complete picture of the protein and phosphoprotein changes occurring after radiation.

Using a multi-omics approach we provide the most comprehensive characterization of how breast cancer cell lines respond to radiation therapy. Understanding transcriptomic and proteomic changes in response to radiation allows for the nomination of potential radiosensitization targets for radioresistant breast cancers. Our data show that activation of the apoptosis pathway in basal-

like breast cancer cell lines may be a promising strategy for radiosensitization. Furthermore, G2 and mitosis related cell cycle proteins (CDK1, Plk1, TTK/Mps1, Bub1, and Wee1) that are overexpressed in basal-like breast cancers after radiation therapy may also represent promising targets for radiosensitization. We hypothesize that inhibition of these proteins will increase the effectiveness of radiation therapy in aggressive basal-like breast cancers, that are typically resistant to radiation therapy. These hypotheses will be explored in the following 2 chapters

Methods

Irradiation

Irradiations were performed using a Kimtron IC 225 (Kimtron Medical) at a dose rate of approximately 2 Gy/min in the University of Michigan Comprehensive Cancer Center Experimental Irradiation Core (Ann Arbor, MI). Dosimetry is performed semiannually using an ionization chamber connected to an electrometer system that is directly traceable to a National Institute of Standards and Technology calibration. The beam was collimated with a 0.1 mm Cu inherent filter and a 0.2 mm Cu filter was used for cell line irradiation. A 2 mm Cu filter was used for in vivo xenograft experiments.

RNA isolations

Cells were treated with 4 Gy RT or no treatment and harvested either 1-, 6-, or 24-hours after radiation. After the indicated treatment RNA was isolated from cells by the manufacturer's

instructions on the miRNeasy kit (Qiagen). The optional DNase treatment was performed on each sample.

Microarray platform

RNA integrity number (RIN) of 9 or higher was measured for each sample using an Agilent 2100 Bioanalyzer. The Human Gene ST 2.1 plate was used for microarray analysis and processed by the University of Michigan microarray facility using the Affy Plus kit.

Microarray analysis

Microarray analysis was performed in R version 3.6.1. Gene values were assigned using robust multi-array average (RMA), which is able to normalize values to the background of each chip and output the data in log-transformed values (56). A weight linear model specifically designed for microarray analysis was fit to the data to perform differential expression analyses of interest (57). We then used a gene-by-gene algorithm to assigned weights to each and thus increasing the power of downstream differential gene expression (58). Upon calculation of differential expression the data were analyzed (significantly impacted pathways, biological processes, molecular interactions, miRNAs, SNPs, etc.) using Advaita Bio's iPathwayGuide (https://www.advaitabio.com/ipathwayguide). This software analysis tool implements the 'Impact Analysis' approach that takes into consideration the direction and type of all signals on a pathway, the position, role and type of every gene, etc., as described in (59-62). Threshold for differential expression was log2 fold change (FC) greater than or equal to 0.4 and a Bonferroni corrected p-value of less than or equal to 0.05. R version 3.4 was used for principal

component analysis (PCA) and programs used include, limma, oligo, ggplot2, pd.hugene.2.1.st, and dplyr (63, 64).

Protein isolation

Breast cancer cells were grown in 6-well plates, treated with 4 Gy RT, and harvest either 3, 12, or 24 hours after RT. Cells were then washed twice with PBS (Invitrogen) and harvested with RIPA lysis buffer (Thermo Fischer) supplemented with cOmplete Mini protease (Sigma-Aldrich) and phosSTOP (Roche) inhibitors. BCA assay was used to quantify protein concentration and the concentration was adjusted to 1.5µg/µl as necessary. Bond-Breaker TCEP solution (Pierce Biotechnology) was added at $1/10^{th}$ volume and samples were boiled at 95˚.

Reverse phase protein array (RPPA)

After protein lysates were prepared as described above, the lysates were serially diluted (1:2, 1:4, 1:8, and 1:16). An Aushon 2470 arrayer (Quanterix) was used to create a spot array containing all samples for each antibody measured (>100 antibodies in total) on Oncyte Avid nitrocellulose-coated slides (Grace Bio-Labs) according to the manufacturer's instructions. Slides were stored at -80˚C until immunostaining using an automated slide stainer (Dako Link 48), Dako). All antibodies were validated at MD Anderson as well as Royal College of Surgeons, Dublin, Ireland. Scanned slides were analyzed using MicroVigene software V.5.1 (VigeneTech). Spot intensities were generated using MicroVigene software where a four-parameter logistic-log model, 'SuperCurve' algorithm, was used to fit a curve to each sample (65). Global sample median

normalization was used to normalize all samples with one antibody. Differential expression was measured by comparing RT samples at each time point to the untreated cells within each cell line.

Figures

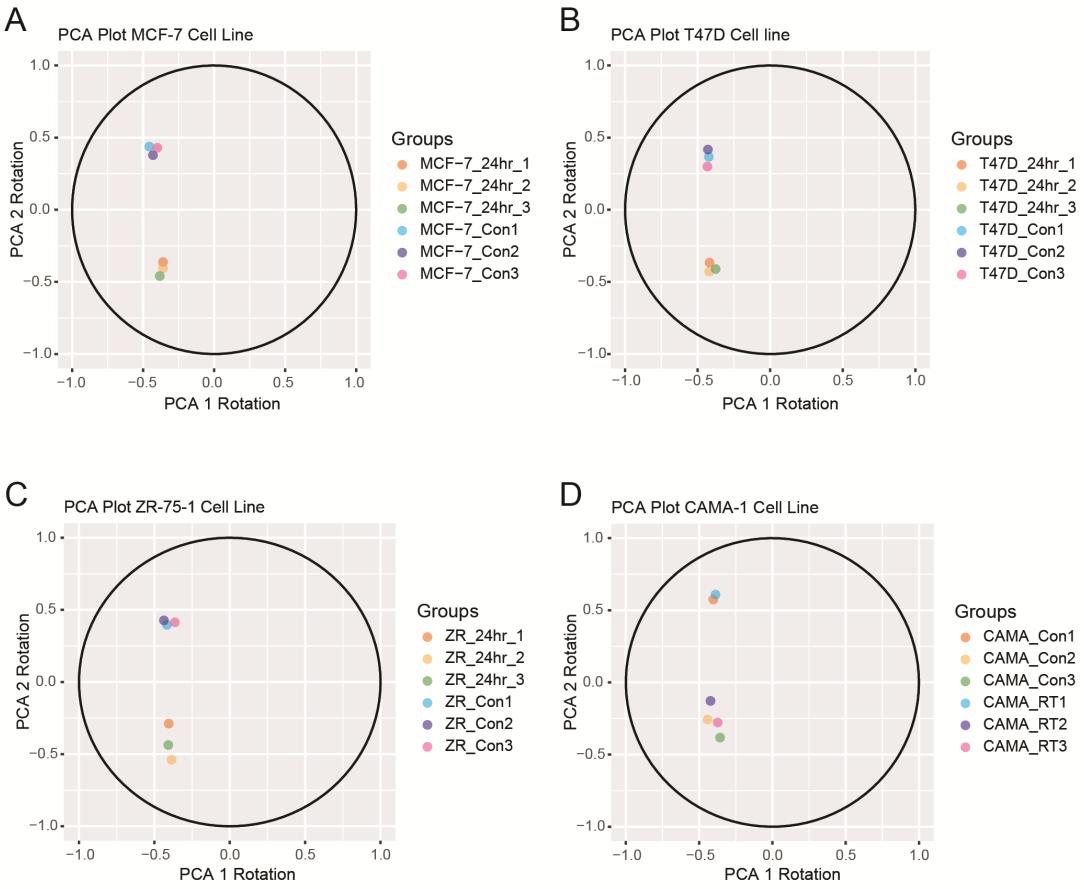

Figure 2.1: Principal component plots (PCA) from the Duke dataset for luminal breast cancer cell lines. A-C) PCA plots for MCF-7 (A), T47D (B), and ZR-75-1 (C) cell lines show clustering between triplicate for each treatment (control v. radiation). D) PCA plot for the CAMA-1 cell line does not show clustering between treatment groups. Control (Con) vs. radiation at 24 hours (RT) in triplicate.

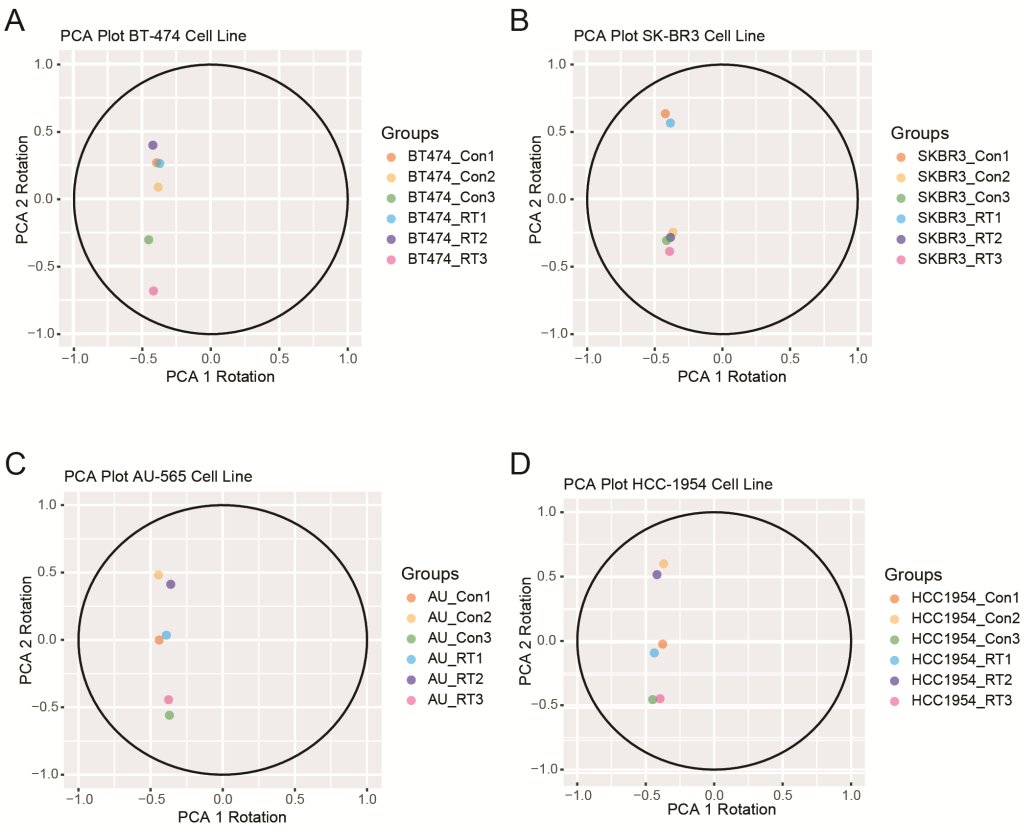

Figure 2.2: Principal component plots (PCA) from the Duke dataset for Her2 positive breast cancer cell lines. A-D) PCA plots for BT-474 (A), SK-BR3 (B), AU-565 (C), and HCC-1954 (D) cell lines do not show clustering between triplicates for each treatment. Control (Con) vs. radiation at 24 hours (RT) in triplicate.

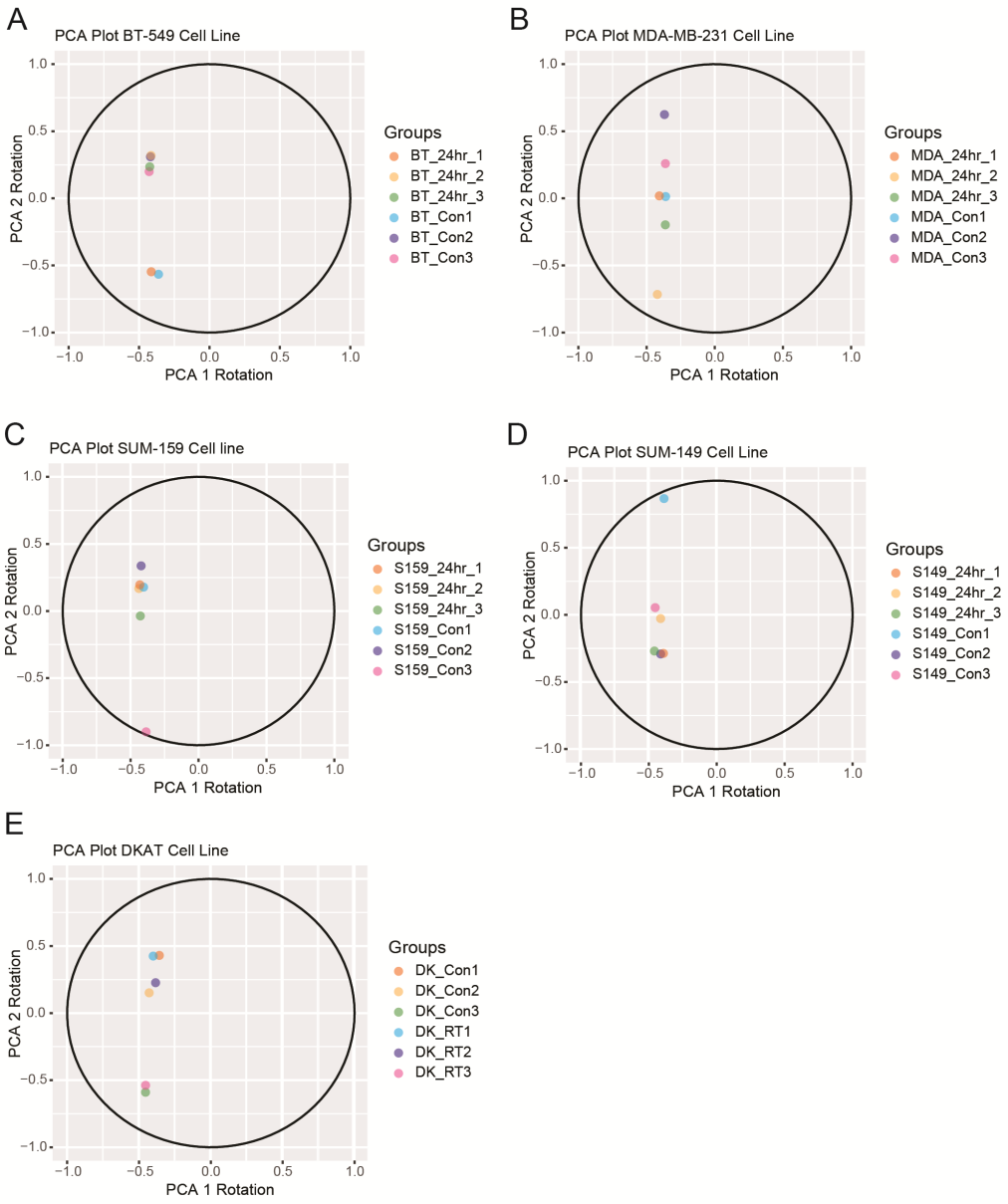

Figure 2.3: Principal component plots (PCA) from the Duke dataset for basal-like breast cancer cell lines. A-E) PCA plots for BT-549 (A), MDA-MB-231 (B), SUM-159 (C), SUM-149 (D), and DKAT (E) cell lines do not show clustering between triplicates for each treatment. Control (Con) vs. radiation at 24 hours (RT) in triplicate.

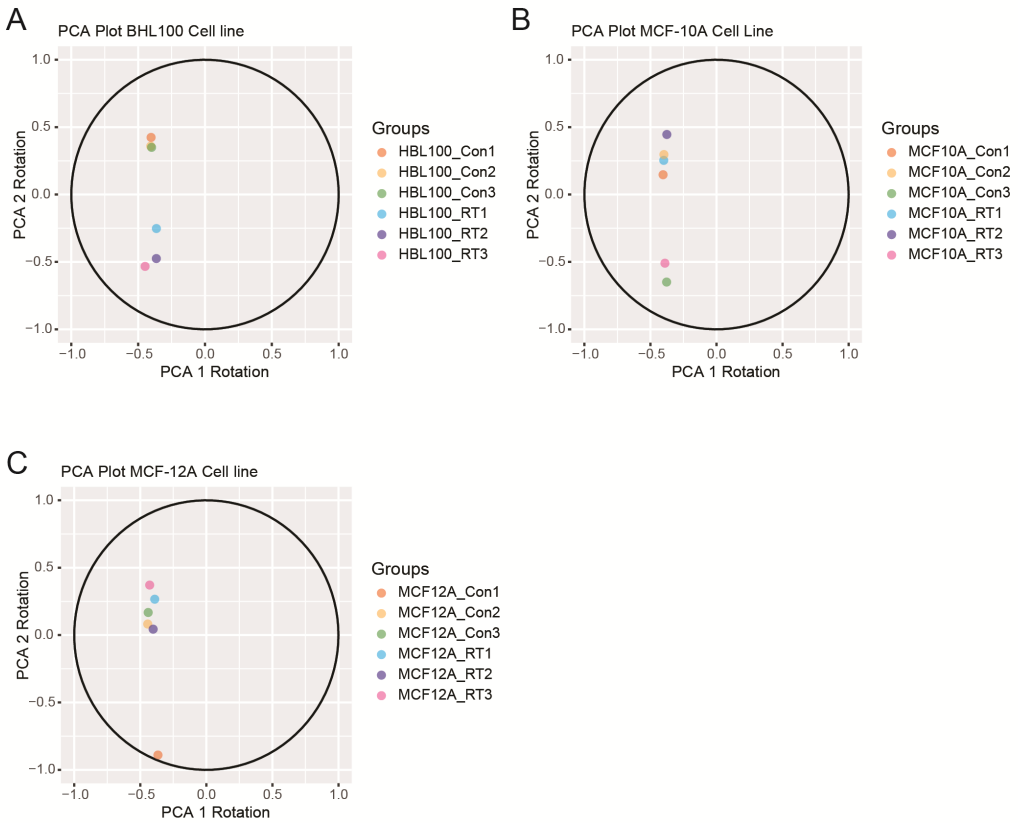

Figure 2.4: Principal component plots (PCA) from the Duke dataset for normal breast cell lines. A) PCA plot for the HBL100 cell line shows clustering between triplicates for each treatment. B&C) PCA plots for MCF-10A (B) MCF-12A (C) cell lines do not show clustering between triplicates for each treatment. Control (Con) vs. radiation at 24 hours (RT) in triplicate.

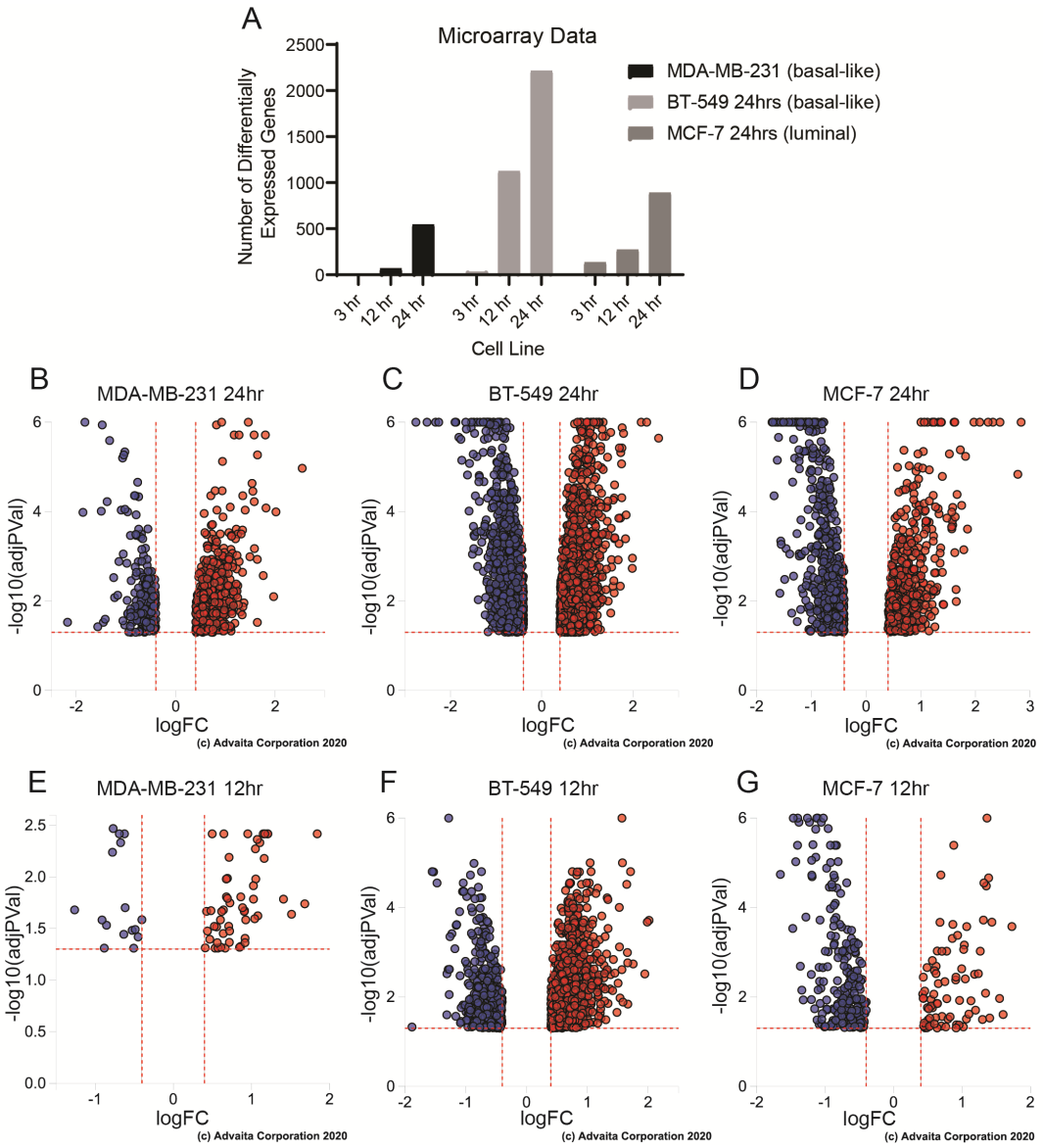

Figure 2.5: Gene expression changes after radiation (RT) are greatest after 24 hours. A) The number of differential expressed genes after RT (4 Gy) increase with time up to 24 hours. B-D) Volcano plots showing the number of differentially expressed genes 24 hours after RT in MDA-MB-231 (B), BT-540 (C), and MCF-7 (D) cell lines. E-G) Volcano plots showing the number of differentially expressed genes 12hours after RT in MDA-MB-231 (E), BT-540 (F), and MCF-7 (G) cell lines. Log2FC > 0.4, AdjPVal<0.05

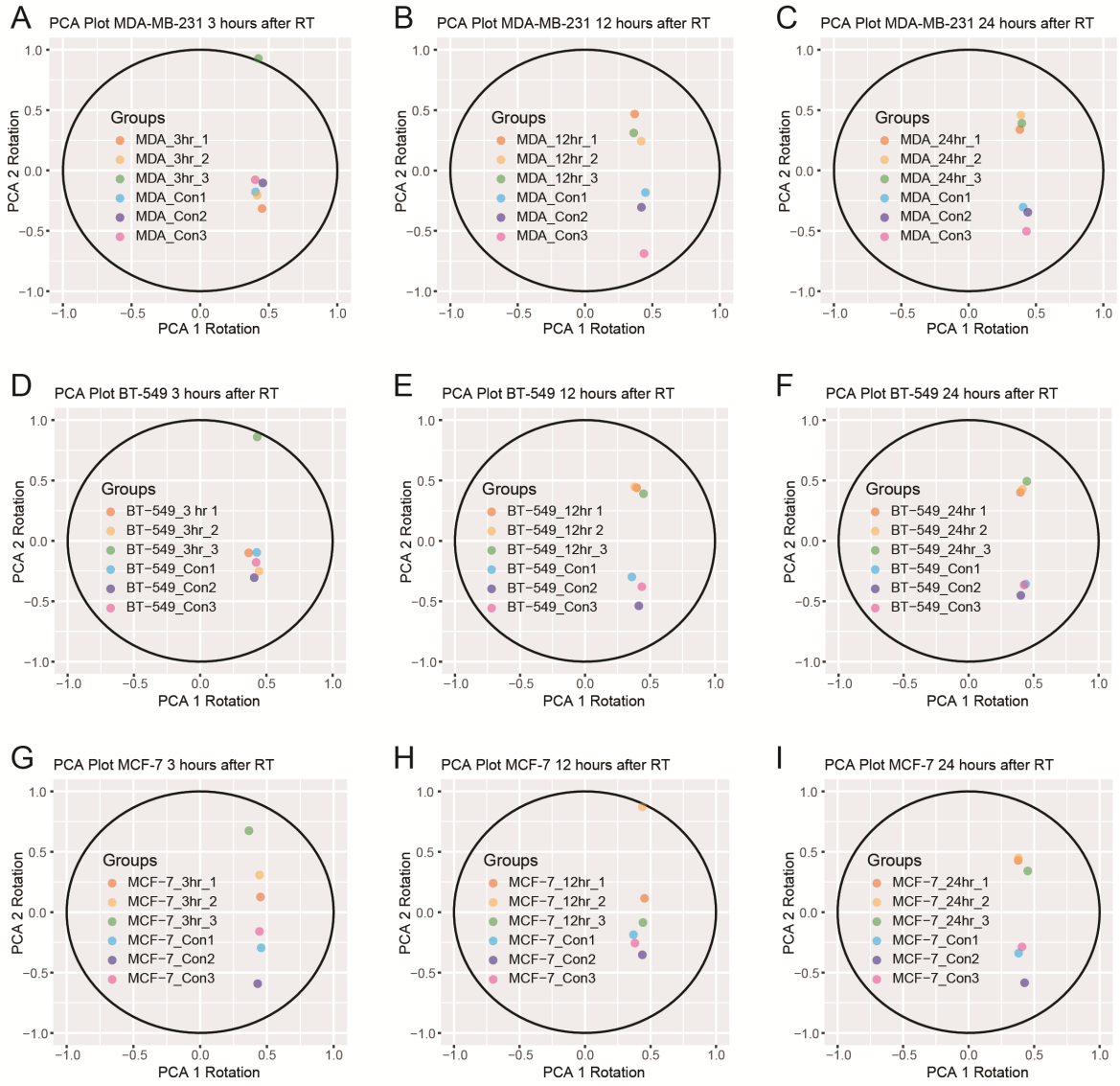

Figure 2.6: Principal component plots (PCA) for MDA-MB-231, BT-549, and MCF-7 cell lines after radiation (RT) over multiple time points. A-C) PCA plots for MDA-MB-231 cell line over multiple time points 3 hours (A), 12 hours (B), and 24 hours (C). The PCA plots for 12 and 24 hours after radiation show good clustering between control and RT groups. D-F) PCA plots for BT-549 cell line over multiple time points 3 hours (D), 12 hours (E), and 24 hours (F). The PCA plots for 12 and 24 hours after radiation show good clustering between control and RT groups. G-I) PCA plots for MCF-7 cell line over multiple time points 3 hours (G), 12 hours (H), and 24 hours (I). All PCA plots show good clustering between control and RT groups.

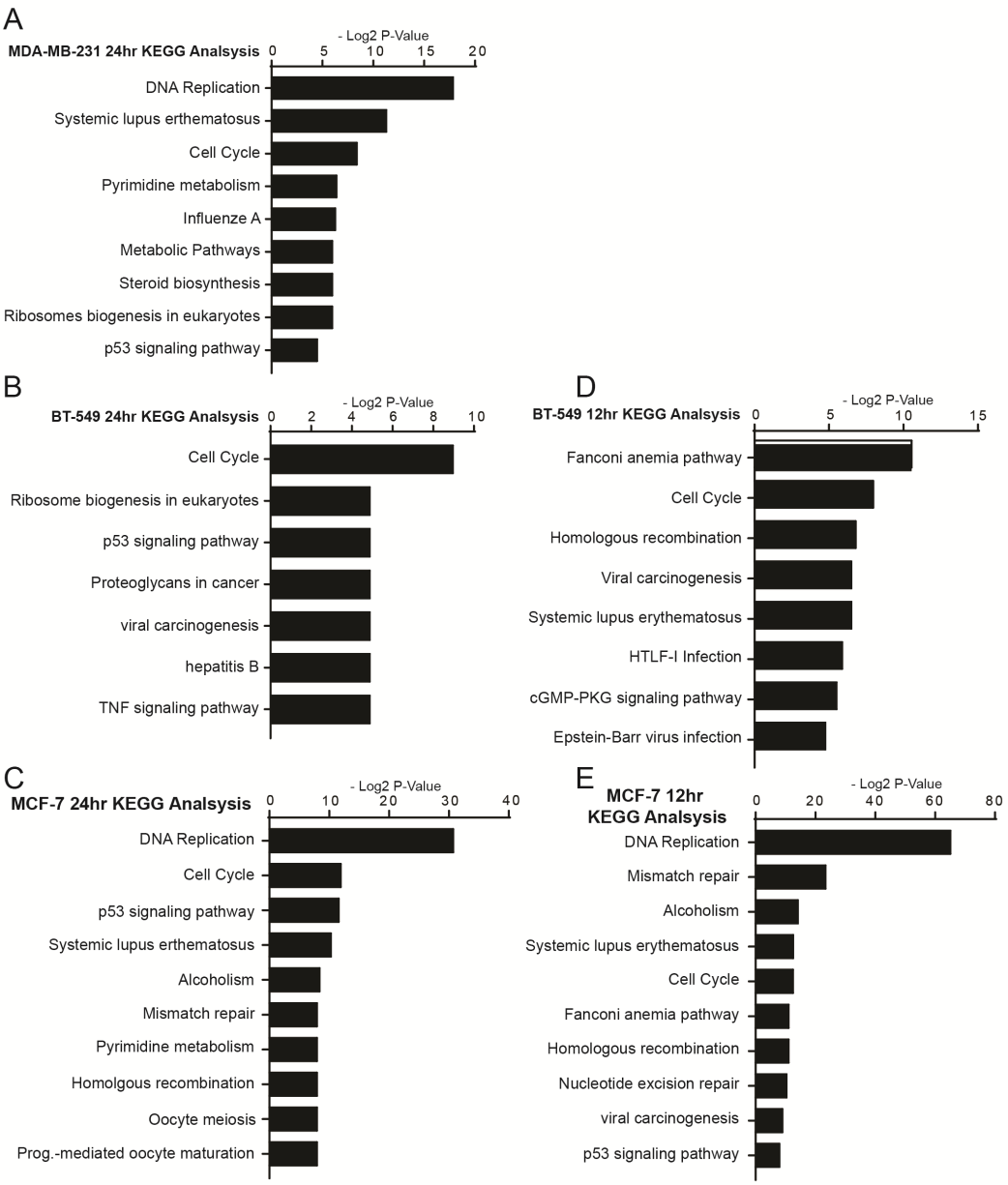

Figure 2.7: Kyoto Encyclopedia of Genes and Genomes (KEGG) analysis. A) KEGG analysis for MDA-MB-231 cell line at the 24 hour time point. B&D) KEGG analysis for BT-549 cell line 24 (B) and 12 (D) hours after RT. C&E) KEGG analysis for MCF-7 cell line 24 (C) and 12 (E) hours after RT.

A

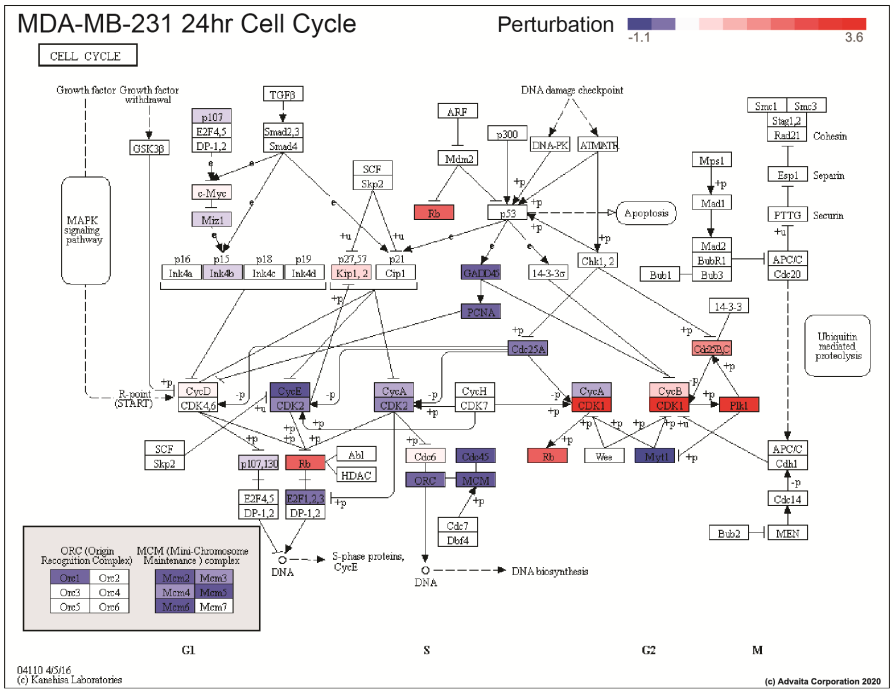
MDA-MB-231 24hr Cell Cycle
Perturbation
-1.1
3.6
CELL CYCLE
Growth factor
Growth factor withdrawal
TGFβ
p107
E2F4,5
DP-1,2
Smad2,3
Smad4
GSK3β
MAPK signaling pathway
c-Myc
Miz1
SCF
Skp2
ARF
Mdm2
p300
DNA-PK
ATM/ATR
DNA damage checkpoint
Rb
p53
Apoptosis
Mps1
Mad1
Mad2
BubR1
Bub3
Bub1
Smc1
Smc3
Stag1,2
Rad21
Cohesin
Esp1
Separin
PTTG
Securin
APC/C
Cdc20
p16
p15
p18
p19
p27,57
p21
Ink4a
Ink4b
Ink4c
Ink4d
Kip1, 2
Cip1
GADD45
14-3-3σ
Chk1, 2
PCNA
14-3-3
Cdc25A
Cdc25B,C
Ubiquitin mediated proteolysis
R-point (START)
CycD
CDK4,6
CycE
CDK2
CycA
CycH
CDK7
CycB
CDK1
Plk1
Abl
HDAC
p107,130
E2F4,5
DP-1,2
E2F1,2,3
Cdc6
Cdc45
ORC
MCM
Cdc7
Dbf4
Wee
Myt1
Cdc14
Cdh1
Bub2
MEN
ORC (Origin Recognition Complex)
Orc1
Orc2
Orc3
Orc4
Orc5
Orc6
MCM (Mini-Chromosome Maintenance) complex
Mcm2
Mcm3
Mcm4
Mcm5
Mcm6
Mcm7
DNA
S-phase proteins, CycE
DNA biosynthesis
G1
S
G2
M
04110 4/5/16
(c) Kanehisa Laboratories
(c) Advaita Corporation 2020

B

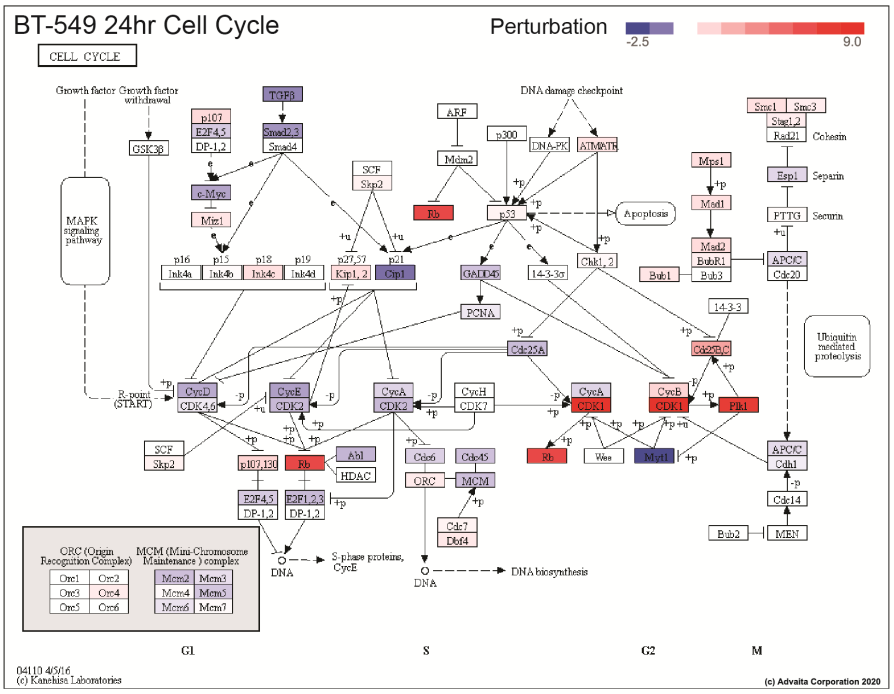
BT-549 24hr Cell Cycle
Perturbation
-2.5
9.0
CELL CYCLE
Growth factor
Growth factor withdrawal
TGFβ
p107
E2F4,5
DP-1,2
Smad2,3
Smad4
GSK3β
MAPK signaling pathway
c-Myc
Miz1
SCF
Skp2
ARF
Mdm2
p300
DNA-PK
ATM/ATR
DNA damage checkpoint
Rb
p53
Apoptosis
Mps1
Mad1
Mad2
BubR1
Bub3
Bub1
Smc1
Smc3
Stag1,2
Rad21
Cohesin
Esp1
Separin
PTTG
Securin
APC/C
Cdc20
p16
p15
p18
p19
p27,57
p21
Ink4a
Ink4b
Ink4c
Ink4d
Kip1, 2
Cip1
GADD45
14-3-3σ
Chk1, 2
PCNA
14-3-3
Cdc25A
Cdc25B,C
Ubiquitin mediated proteolysis
R-point (START)
CycD
CDK4,6
CycE
CDK2
CycA
CycH
CDK7
CycB
CDK1
Plk1
Abl
HDAC
p107,130
E2F4,5
DP-1,2
E2F1,2,3
Cdc6
Cdc45
ORC
MCM
Cdc7
Dbf4
Wee
Myt1
Cdc14
Cdh1
Bub2
MEN
ORC (Origin Recognition Complex)
Orc1
Orc2
Orc3
Orc4
Orc5
Orc6
MCM (Mini-Chromosome Maintenance) complex
Mcm2
Mcm3
Mcm4
Mcm5
Mcm6
Mcm7
DNA
S-phase proteins, CycE
DNA biosynthesis
G1
S
G2
M
04110 4/5/16
(c) Kanehisa Laboratories
(c) Advaita Corporation 2020

Figure 2.8: Basal-like breast cancer cell lines have increased expression of G2 and M genes 24 hours after radiation (RT). A&B) Differentially expressed genes in the cell cycle pathway of MDA-MB-231 (A) and BT-549 (B) cell lines 24 hours after RT.

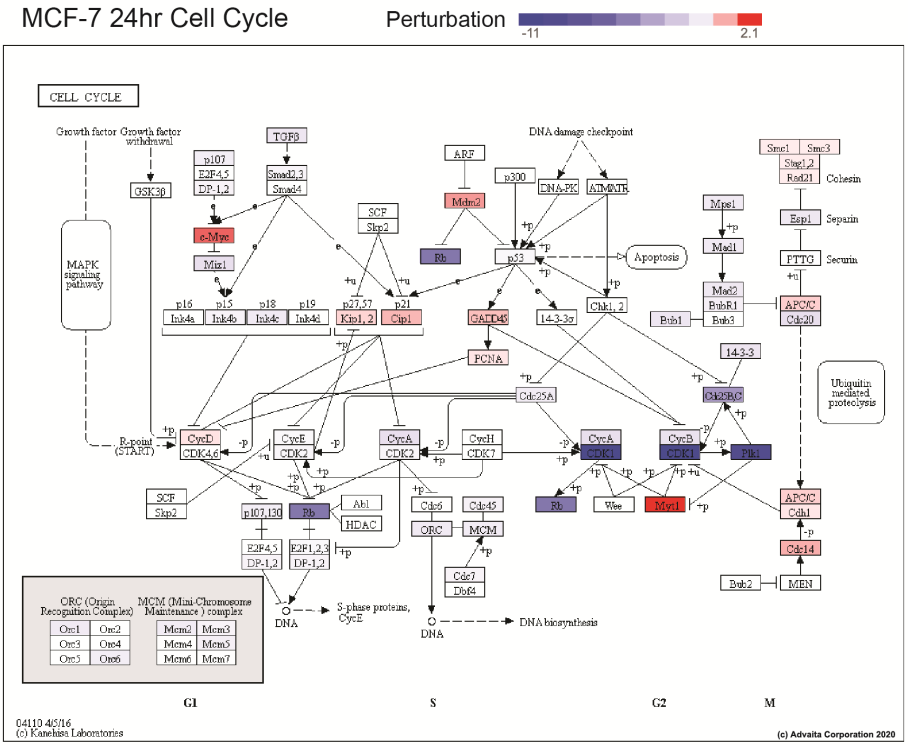

Figure 2.9: The luminal cell line, MCF-7, has decreased expression of genes in G2 and M 24 hours after radiation.

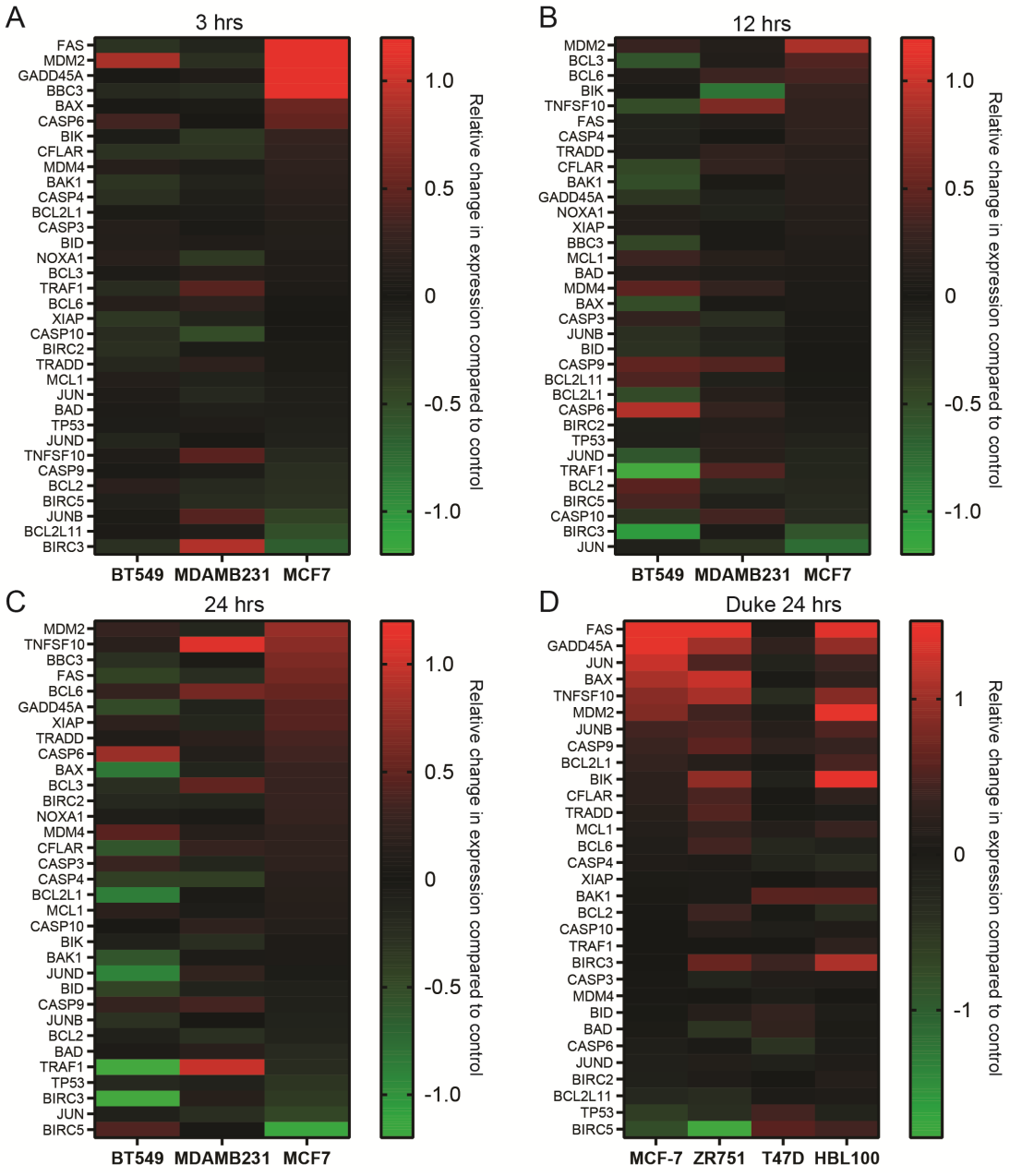

Figure 2.10: p53 mutant cell lines have no induction of apoptosis related genes. A-C) Heatmap shows no change in apoptosis related genes in p53 mutant cell lines (MDA-MB-231 and BT-549) across 3 (A), 12 (B), and 24 (C) hour time points compared to a p53 wild-type cell line (MCF-7). D) In cell lines with robust differential gene expression within the Duke dataset p53 wild-type cell lines have robust induction of apoptosis related genes compared to the p53-mutant cell line T47D.

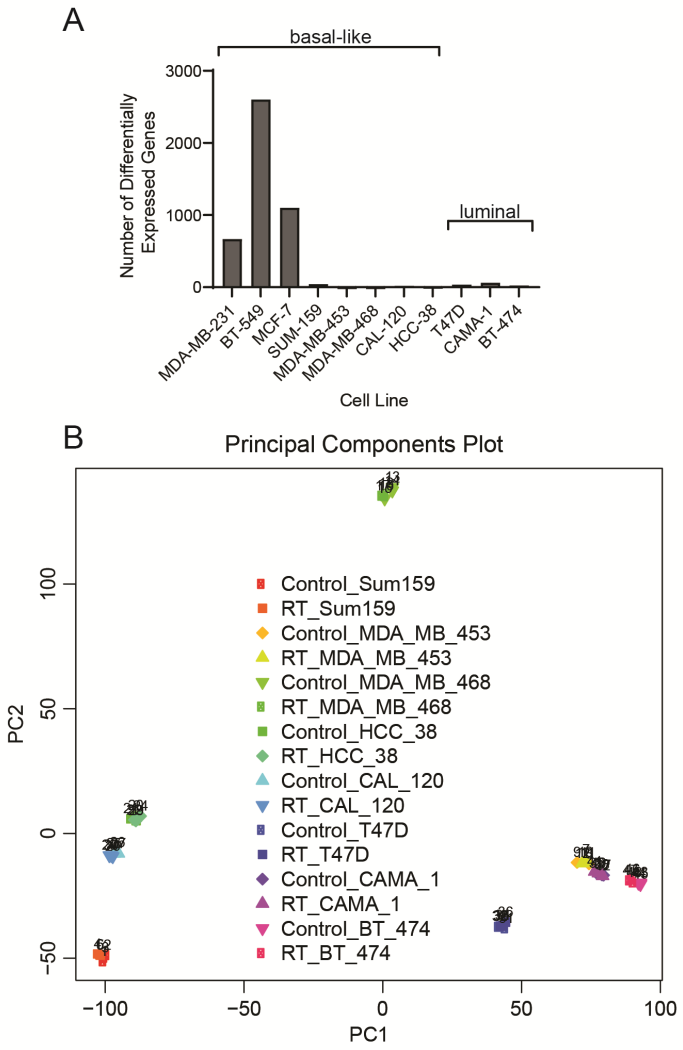

Figure 2.11: Microarray analysis on 8 additional cell lines demonstrate little differential expression after radiation (RT). A) Number of differentially expressed genes 24 hours after RT in 8 additional cell lines. B) Principal component analysis (PCA) of all eight cell lines together. After RT control and RT cluster together within each cell line.

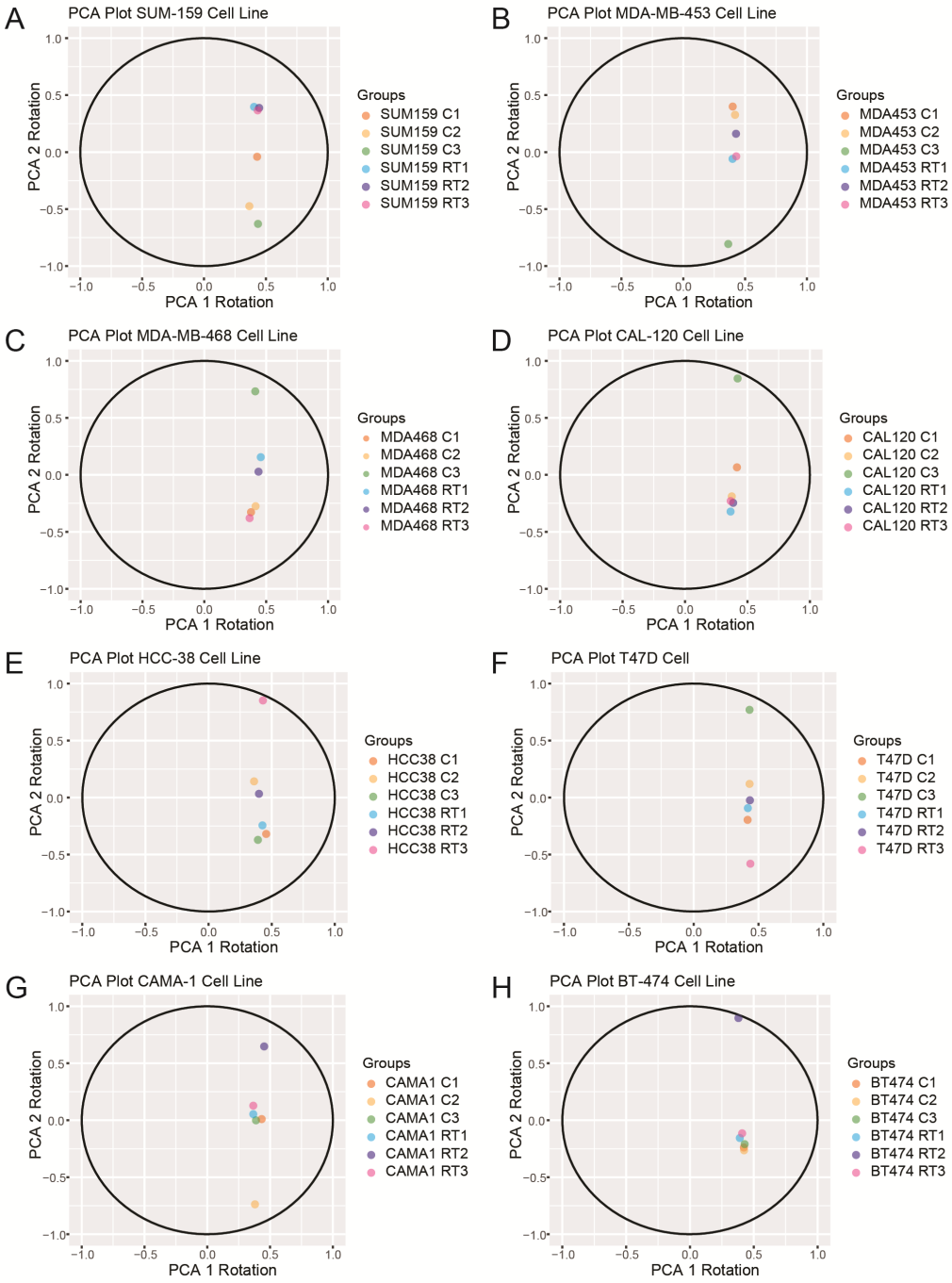

Figure 2.12: Principal component analysis (PCA) for individual cell lines 24 hours after radiation (RT). A-H) PCA analysis shows no clustering within treatment groups in SUM-159 (A), MDA-MB-453

(B), MDA-MB-468 (C), CAL-120 (D), HCC-38 (E), T47D (F), CAMA-1 (G), and BT-474 (H) cell lines. Control (Con) vs. radiation at 24 hours (RT) in triplicate.

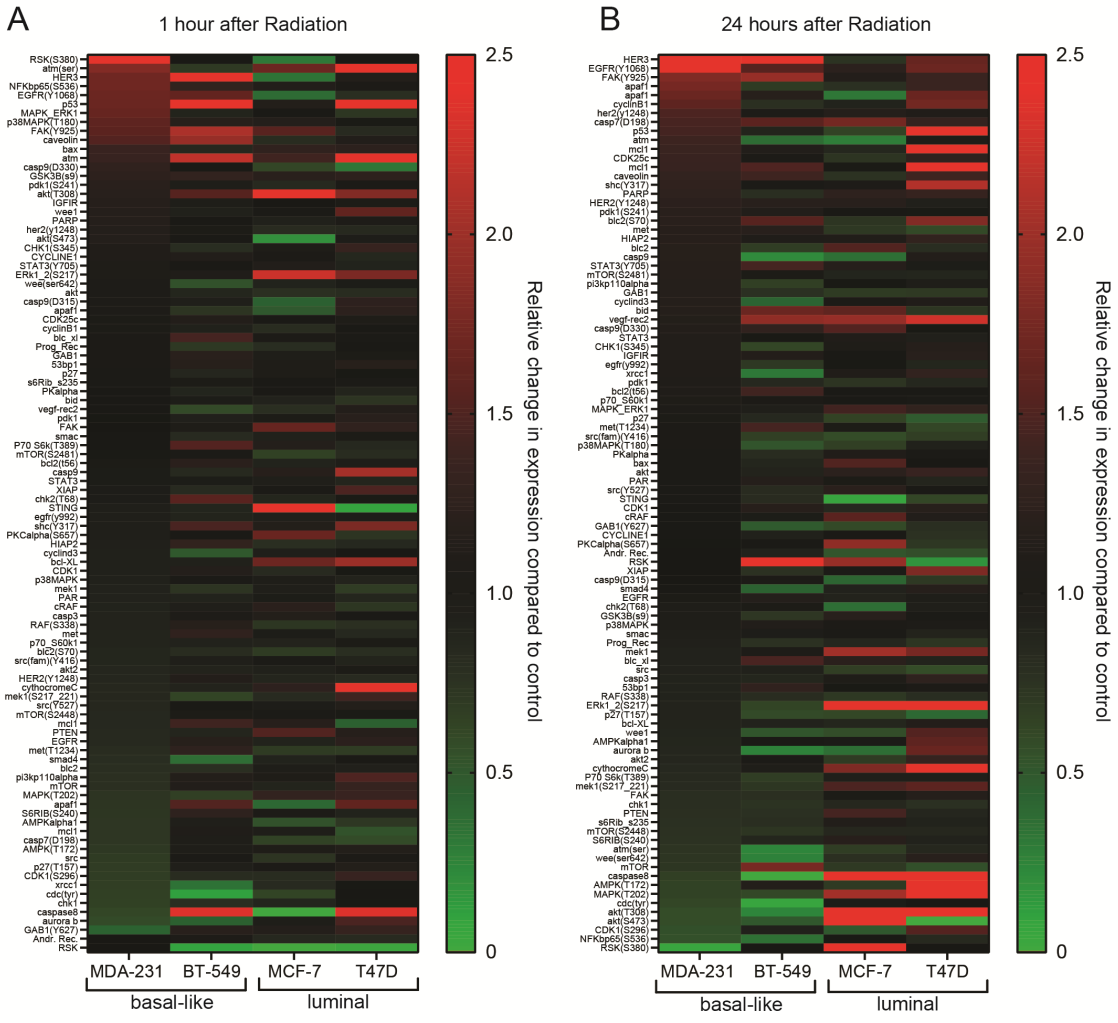

Figure 2.13: Reverse phase protein array (RPPA) highlights differences in protein expression after radiation (RT) across cell lines. A) Relative change in protein expression compared to untreated cells 1-hour after RT across four cell lines. B) Relative change in protein expression compared to untreated cells 24-hours after RT across four cell lines.

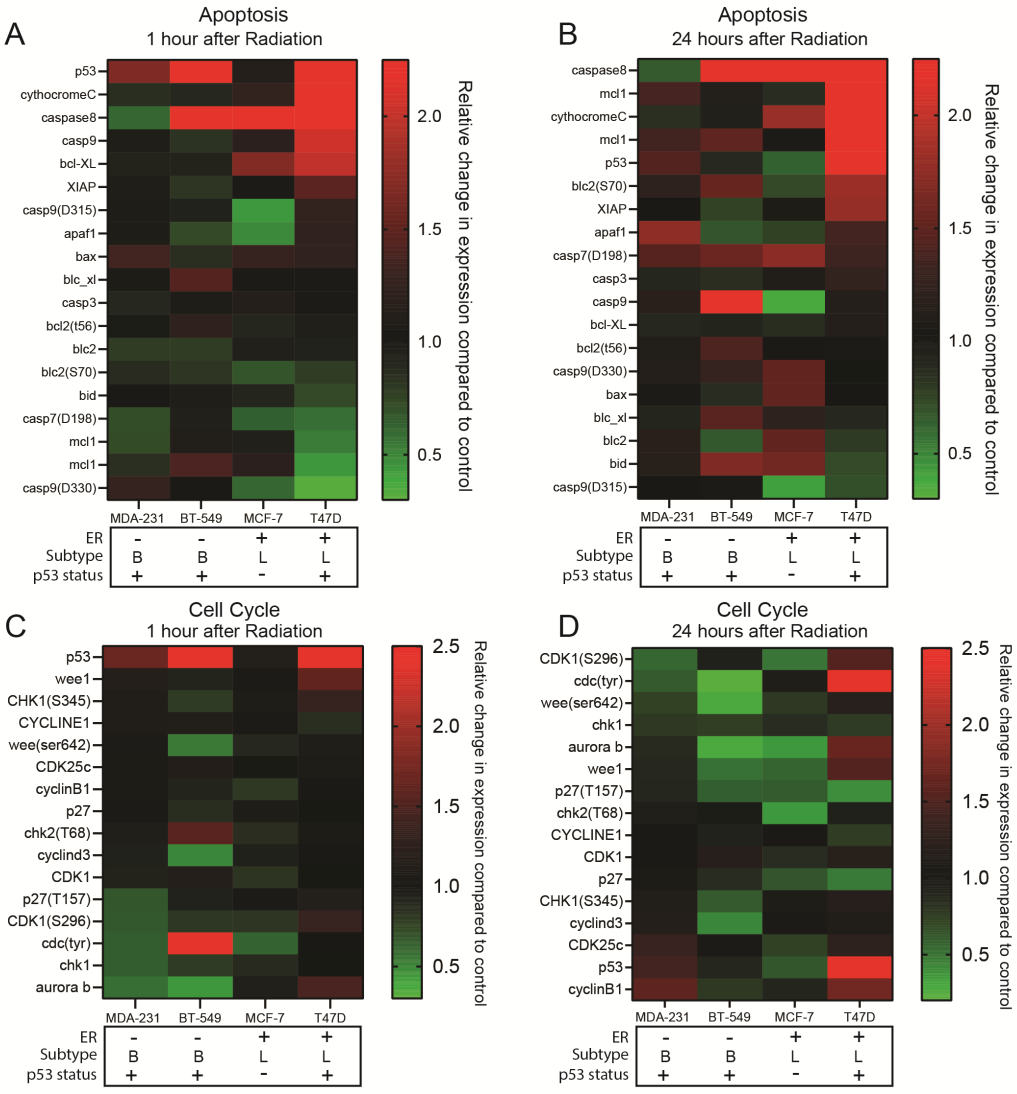

Figure 2.14: Protein changes in the apoptosis and cell cycle pathways 1- and 24-hours after radiation. A&B) Relative changes in protein expression of genes within the apoptotic response 1- (A) and 24- (B) hours after RT. C&D) Relative changes in protein expression of genes in the cell cycle pathway 1- (C) and 24- (D) hours after RT.

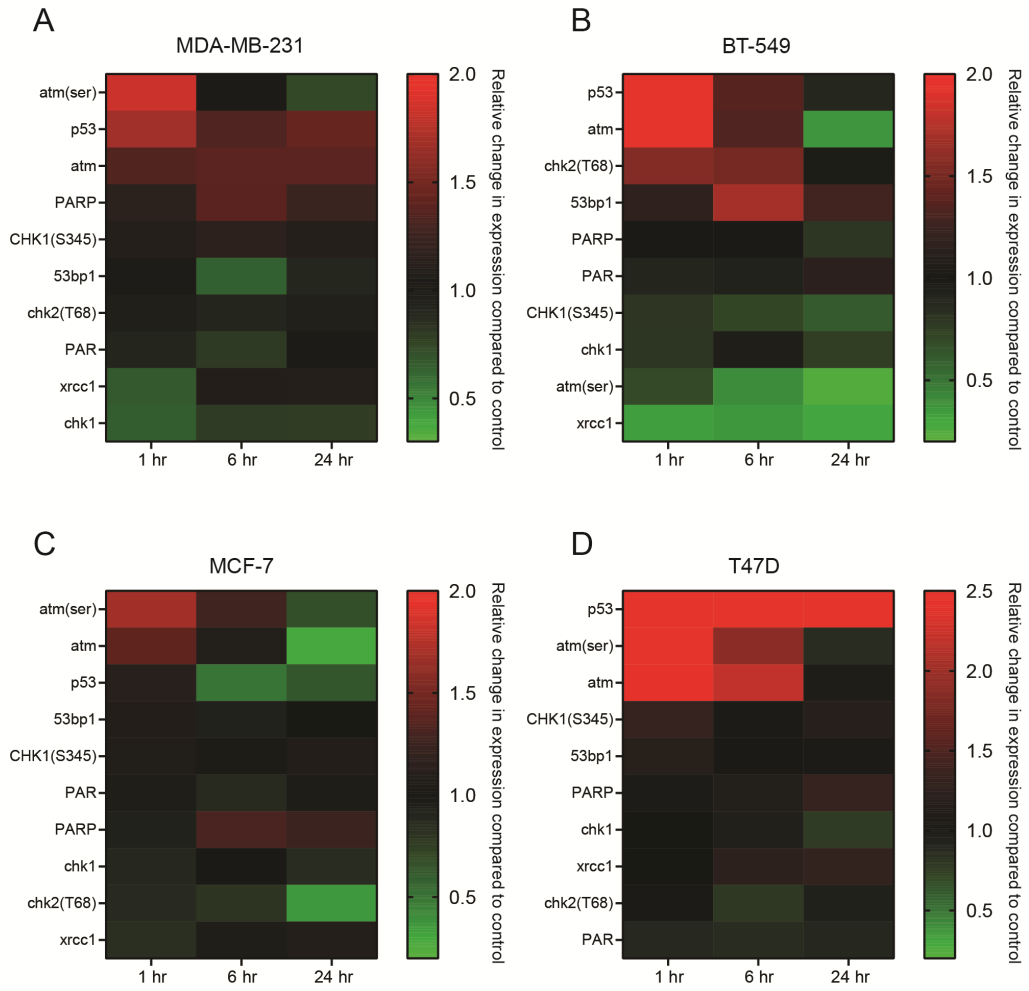

Figure 2.15: Changes in the DNA damage response proteins after radiation across multiple time points. A-D) Relative change in protein expression compared to untreated cells across three time points, 1-, 6-, and 24- hours after RT in MDA-MB-231 (A), BT-549 (B), MCF-7 (C), and T47D (D) cell lines.

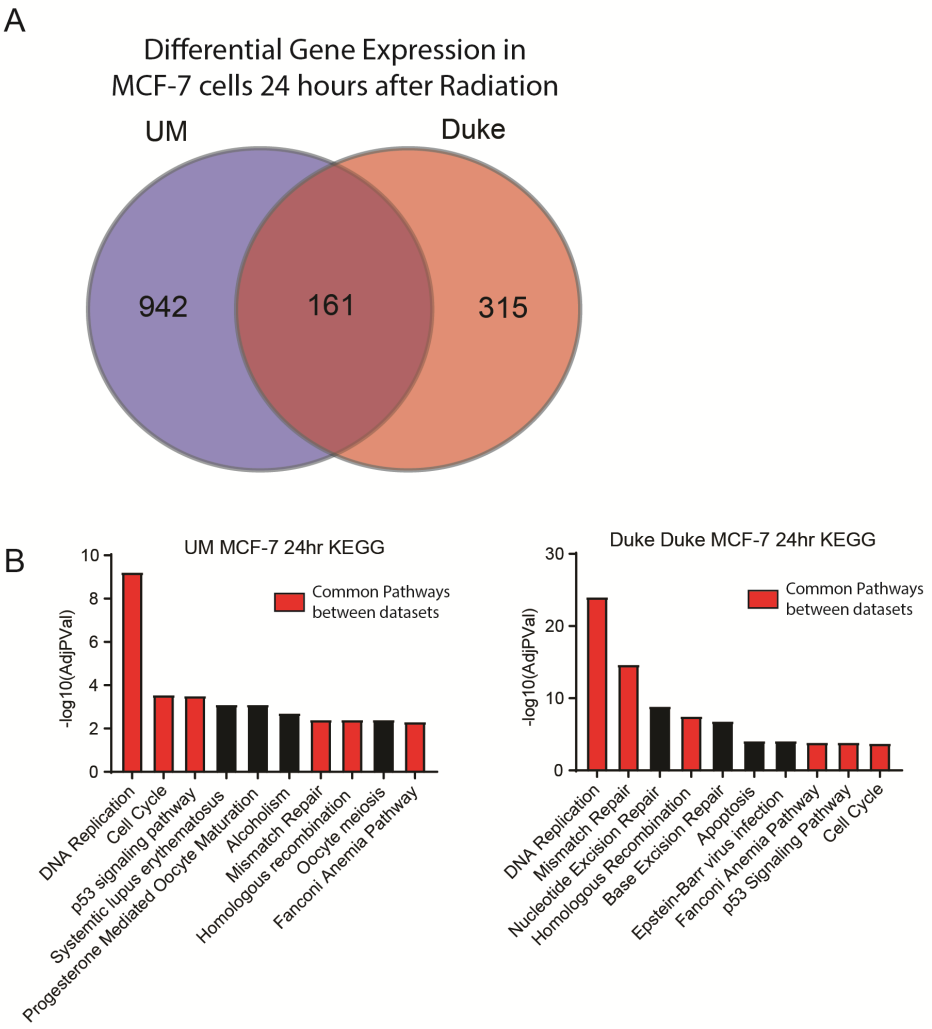

Figure 2.16: The MCF-7 cell line has similar differential expression after radiation (RT) in both the University of Michigan dataset and the Duke dataset. A) Venn diagram depicting differentially expressed genes shared in common between the two datasets (FC > 0.4, AdjPval < 0.05) after RT. B) Kyoto encyclopedia of genes and genomes (KEGG) analysis of MCF-7 cells show 6 of the top 10 pathways are common across both datasets.

References

1. Siegel RL, Miller KD, and Jemal A. Cancer statistics, 2018. *CA: A Cancer Journal for Clinicians.* 2018;68(1):7-30.
2. Dunnwald LK, Rossing MA, and Li CI. Hormone receptor status, tumor characteristics, and prognosis: a prospective cohort of breast cancer patients. *Breast Cancer Res.* 2007;9(1):R6-R.
3. Fisher B, Redmond C, Fisher ER, and Caplan R. Relative worth of estrogen or progesterone receptor and pathologic characteristics of differentiation as indicators of prognosis in node negative breast cancer patients: findings from National Surgical Adjuvant Breast and Bowel Project Protocol B-06. *Journal of Clinical Oncology.* 1988;6(7):1076-87.
4. Aaltomaa S, Lipponen P, Eskelinen M, Kosma V-M, Marin S, Alhava E, and Syrjänen K. Hormone Receptors as Prognostic Factors in Female: Breast Cancer. *Annals of Medicine.* 1991;23(6):643-8.
5. Perou CM, Sørlie T, Eisen MB, van de Rijn M, Jeffrey SS, Rees CA, Pollack JR, Ross DT, Johnsen H, Akslen LA, et al. Molecular portraits of human breast tumours. *Nature.* 2000;406(6797):747-52.
6. Sørlie T, Perou CM, Tibshirani R, Aas T, Geisler S, Johnsen H, Hastie T, Eisen MB, van de Rijn M, Jeffrey SS, et al. Gene expression patterns of breast carcinomas distinguish tumor subclasses with clinical implications. *Proc Natl Acad Sci U S A.* 2001;98(19):10869-74.
7. Slamon DJ, Godolphin W, Jones LA, Holt JA, Wong SG, Keith DE, Levin WJ, Stuart SG, Udove J, Ullrich A, et al. Studies of the HER-2/neu proto-oncogene in human breast and ovarian cancer. *Science.* 1989;244(4905):707.
8. Hugh J, Hanson J, Cheang MCU, Nielsen TO, Perou CM, Dumontet C, Reed J, Krajewska M, Treilleux I, Rupin M, et al. Breast cancer subtypes and response to docetaxel in node-positive breast cancer: use of an immunohistochemical definition in the BCIRG 001 trial. *J Clin Oncol.* 2009;27(8):1168-76.
9. Nielsen TO, Parker JS, Leung S, Voduc D, Ebbert M, Vickery T, Davies SR, Snider J, Stijleman IJ, Reed J, et al. A comparison of PAM50 intrinsic subtyping with immunohistochemistry and clinical prognostic factors in tamoxifen-treated estrogen receptor-positive breast cancer. *Clin Cancer Res.* 2010;16(21):5222-32.
10. Rouzier R, Perou CM, Symmans WF, Ibrahim N, Cristofanilli M, Anderson K, Hess KR, Stec J, Ayers M, Wagner P, et al. Breast Cancer Molecular Subtypes Respond Differently to Preoperative Chemotherapy. *Clinical Cancer Research.* 2005;11(16):5678.

11. Carey LA, Dees EC, Sawyer L, Gatti L, Moore DT, Collichio F, Ollila DW, Sartor CI, Graham ML, and Perou CM. The Triple Negative Paradox: Primary Tumor Chemosensitivity of Breast Cancer Subtypes. *Clinical Cancer Research.* 2007;13(8):2329.
12. Pritchard KI, Shepherd LE, O'Malley FP, Andrulis IL, Tu D, Bramwell VH, and Levine MN. HER2 and Responsiveness of Breast Cancer to Adjuvant Chemotherapy. *New England Journal of Medicine.* 2006;354(20):2103-11.
13. Cobleigh MA, Vogel CL, Tripathy D, Robert NJ, Scholl S, Fehrenbacher L, Wolter JM, Paton V, Shak S, Lieberman G, et al. Multinational Study of the Efficacy and Safety of Humanized Anti-HER2 Monoclonal Antibody in Women Who Have HER2-Overexpressing Metastatic Breast Cancer That Has Progressed After Chemotherapy for Metastatic Disease. *Journal of Clinical Oncology.* 1999;17(9):2639-.
14. Sjöström M, Lundstedt D, Hartman L, Holmberg E, Killander F, Kovács A, Malmström P, Niméus E, Werner Rönnerman E, Fernö M, et al. Response to Radiotherapy After Breast-Conserving Surgery in Different Breast Cancer Subtypes in the Swedish Breast Cancer Group 91 Radiotherapy Randomized Clinical Trial. *Journal of Clinical Oncology.* 2017;35(28):3222-9.
15. Horton JK, Jagsi R, Woodward WA, and Ho A. Breast Cancer Biology: Clinical Implications for Breast Radiation Therapy. *International Journal of Radiation Oncology*Biology*Physics.* 2018;100(1):23-37.
16. Kyndi M, Sørensen FB, Knudsen H, Overgaard M, Nielsen HM, and Overgaard J. Estrogen Receptor, Progesterone Receptor, HER-2, and Response to Postmastectomy Radiotherapy in High-Risk Breast Cancer: The Danish Breast Cancer Cooperative Group. *Journal of Clinical Oncology.* 2008;26(9):1419-26.
17. Arvold ND, Taghian AG, Niemierko A, Abi Raad RF, Sreedhara M, Nguyen PL, Bellon JR, Wong JS, Smith BL, and Harris JR. Age, breast cancer subtype approximation, and local recurrence after breast-conserving therapy. *J Clin Oncol.* 2011;29(29):3885-91.
18. Horton JK, Siamakpour-Reihani S, Lee C-T, Zhou Y, Chen W, Geradts J, Fels DR, Hoang P, Ashcraft KA, Groth J, et al. FAS Death Receptor: A Breast Cancer Subtype-Specific Radiation Response Biomarker and Potential Therapeutic Target. *Radiat Res.* 2015;184(5):456-69.
19. Paweletz CP, Charboneau L, Bichsel VE, Simone NL, Chen T, Gillespie JW, Emmert-Buck MR, Roth MJ, Petricoin Iii EF, and Liotta LA. Reverse phase protein microarrays which capture disease progression show activation of pro-survival pathways at the cancer invasion front. *Oncogene.* 2001;20(16):1981-9.
20. Gulmann C, Sheehan KM, Conroy RM, Wulfkuhle JD, Espina V, Mullarkey MJ, Kay EW, Liotta LA, and Petricoin Iii EF. Quantitative cell signalling analysis reveals down-regulation of MAPK pathway activation in colorectal cancer. *The Journal of Pathology.* 2009;218(4):514-9.
21. Spurrier B, Ramalingam S, and Nishizuka S. Reverse-phase protein lysate microarrays for cell signaling analysis. *Nature Protocols.* 2008;3(11):1796-808.
22. Sonntag J, Bender C, Soons Z, der Heyde Sv, König R, Wiemann S, Sinn H-P, Schneeweiss A, Beißbarth T, and Korf U. Reverse phase protein array based tumor profiling identifies a biomarker signature for risk classification of hormone receptor-positive breast cancer. *Translational Proteomics.* 2014;2(52-9.
23. Masuda M, Chen W-Y, Miyanaga A, Nakamura Y, Kawasaki K, Sakuma T, Ono M, Chen C-L, Honda K, and Yamada T. Alternative mammalian target of rapamycin (mTOR) signal activation in sorafenib-resistant hepatocellular carcinoma cells revealed by array-based pathway profiling. *Mol Cell Proteomics.* 2014;13(6):1429-38.

24. Cheng KW, Lu Y, and Mills GB. Assay of Rab25 function in ovarian and breast cancers. *Methods Enzymol.* 2005;403(202-15.
25. Tibes R, Qiu Y, Lu Y, Hennessy B, Andreeff M, Mills GB, and Kornblau SM. Reverse phase protein array: validation of a novel proteomic technology and utility for analysis of primary leukemia specimens and hematopoietic stem cells. *Mol Cancer Ther.* 2006;5(10):2512-21.
26. Sheehan KM, Calvert VS, Kay EW, Lu Y, Fishman D, Espina V, Aquino J, Speer R, Araujo R, Mills GB, et al. Use of reverse phase protein microarrays and reference standard development for molecular network analysis of metastatic ovarian carcinoma. *Mol Cell Proteomics.* 2005;4(4):346-55.
27. Grubb RL, Calvert VS, Wulkuhle JD, Paweletz CP, Linehan WM, Phillips JL, Chuaqui R, Valasco A, Gillespie J, Emmert-Buck M, et al. Signal pathway profiling of prostate cancer using reverse phase protein arrays. *Proteomics.* 2003;3(11):2142-6.
28. Jolliffe IT, and Cadima J. Principal component analysis: a review and recent developments. *Philos Trans A Math Phys Eng Sci.* 2016;374(2065):20150202-.
29. Kanehisa M, and Goto S. KEGG: kyoto encyclopedia of genes and genomes. *Nucleic Acids Res.* 2000;28(1):27-30.
30. Cadet J, Douki T, and Ravanat J-L. Oxidatively Generated Damage to the Guanine Moiety of DNA: Mechanistic Aspects and Formation in Cells. *Accounts of Chemical Research.* 2008;41(8):1075-83.
31. Sutherland BM, Bennett PV, Sidorkina O, and Laval J. Clustered DNA damages induced in isolated DNA and in human cells by low doses of ionizing radiation. *Proceedings of the National Academy of Sciences.* 2000;97(1):103.
32. Boellner S, and Becker K-F. Reverse Phase Protein Arrays-Quantitative Assessment of Multiple Biomarkers in Biopsies for Clinical Use. *Microarrays (Basel).* 2015;4(2):98-114.
33. Creighton CJ, and Huang S. Reverse phase protein arrays in signaling pathways: a data integration perspective. *Drug Des Devel Ther.* 2015;9(3519-27.
34. Speers C, Zhao SG, Liu M, Bartelink H, Pierce LJ, and Feng FY. Development and validation of a novel radiosensitivity signature in human breast cancer. *Clinical Cancer Research.* 2015:clincanres.2898.014.
35. Mantovani F, Collavin L, and Del Sal G. Mutant p53 as a guardian of the cancer cell. *Cell Death & Differentiation.* 2019;26(2):199-212.
36. Wang J-S, Wang H-J, and Qian H-L. Biological effects of radiation on cancer cells. *Mil Med Res.* 2018;5(1):20-.
37. Luzhna L, Lykkesfeldt AE, and Kovalchuk O. Altered radiation responses of breast cancer cells resistant to hormonal therapy. *Oncotarget.* 2015;6(3):1678-94.
38. Anastasov N, Höfig I, Vasconcellos IG, Rappl K, Braselmann H, Ludyga N, Auer G, Aubele M, and Atkinson MJ. Radiation resistance due to high expression of miR-21 and G2/M checkpoint arrest in breast cancer cells. *Radiat Oncol.* 2012;7(206-.
39. Chandler BC, Moubadder L, Ritter CL, Liu M, Cameron M, Wilder-Romans K, Zhang A, Pesch AM, Michmerhuizen AR, Hirsh N, et al. TTK inhibition radiosensitizes basal-like breast cancer through impaired homologous recombination. *The Journal of Clinical Investigation.* 2020;130(2):958-73.
40. Kim KH, Yoo HY, Joo KM, Jung Y, Jin J, Kim Y, Yoon SJ, Choi SH, Seol HJ, Park WY, et al. Time-course analysis of DNA damage response-related genes after in vitro radiation in H460 and H1229 lung cancer cell lines. *Exp Mol Med.* 2011;43(7):419-26.

41. Chandler BC, Moubadder L, Ritter CL, Liu M, Cameron M, Wilder-Romans K, Zhang A, Pesch AM, Michmerhuizen AR, Hirsh N, et al. TTK inhibition radiosensitizes basal-like breast cancer through impaired homologous recombination. *The Journal of Clinical Investigation.* 2020;130(2).
42. Wu H, Schiff DS, Lin Y, Neboori HJR, Goyal S, Feng Z, and Haffty BG. Ionizing radiation sensitizes breast cancer cells to Bcl-2 inhibitor, ABT-737, through regulating Mcl-1. *Radiat Res.* 2014;182(6):618-25.
43. Michmerhuizen AR, Pesch AM, Moubadder L, Chandler BC, Wilder-Romans K, Cameron M, Olsen E, Thomas DG, Zhang A, Hirsh N, et al. PARP1 Inhibition Radiosensitizes Models of Inflammatory Breast Cancer to Ionizing Radiation. *Molecular Cancer Therapeutics.* 2019;18(11):2063.
44. Wei D, Parsels LA, Karnak D, Davis MA, Parsels JD, Marsh AC, Zhao L, Maybaum J, Lawrence TS, Sun Y, et al. Inhibition of protein phosphatase 2A radiosensitizes pancreatic cancers by modulating CDC25C/CDK1 and homologous recombination repair. *Clin Cancer Res.* 2013;19(16):4422-32.
45. Werner LR, Huang S, Francis DM, Armstrong EA, Ma F, Li C, Iyer G, Canon J, and Harari PM. Small Molecule Inhibition of MDM2–p53 Interaction Augments Radiation Response in Human Tumors. *Molecular Cancer Therapeutics.* 2015;14(9):1994.
46. Lehmann BD, Bauer JA, Chen X, Sanders ME, Chakravarthy AB, Shyr Y, and Pietenpol JA. Identification of human triple-negative breast cancer subtypes and preclinical models for selection of targeted therapies. *The Journal of Clinical Investigation.* 2011;121(7):2750-67.
47. Smith SE, Mellor P, Ward AK, Kendall S, McDonald M, Vizeacoumar FS, Vizeacoumar FJ, Napper S, and Anderson DH. Molecular characterization of breast cancer cell lines through multiple omic approaches. *Breast Cancer Res.* 2017;19(1):65-.
48. Kastan MB, Onyekwere O, Sidransky D, Vogelstein B, and Craig RW. Participation of p53 Protein in the Cellular Response to DNA Damage. *Cancer Research.* 1991;51(23 Part 1):6304.
49. Clarke AR, Purdie CA, Harrison DJ, Morris RG, Bird CC, Hooper ML, and Wyllie AH. Thymocyte apoptosis induced by p53-dependent and independent pathways. *Nature.* 1993;362(6423):849-52.
50. Lowe SW, Schmitt EM, Smith SW, Osborne BA, and Jacks T. p53 is required for radiation-induced apoptosis in mouse thymocytes. *Nature.* 1993;362(6423):847-9.
51. Shay JW, Pereira-Smith OM, and Wright WE. A role for both RB and p53 in the regulation of human cellular senescence. *Experimental Cell Research.* 1991;196(1):33-9.
52. Serrano M, Lin AW, McCurrach ME, Beach D, and Lowe SW. Oncogenic ras Provokes Premature Cell Senescence Associated with Accumulation of p53 and p16INK4a. *Cell.* 1997;88(5):593-602.
53. Biddlestone-Thorpe L, Sajjad M, Rosenberg E, Beckta JM, Valerie NCK, Tokarz M, Adams BR, Wagner AF, Khalil A, Gilfor D, et al. ATM kinase inhibition preferentially sensitizes p53-mutant glioma to ionizing radiation. *Clin Cancer Res.* 2013;19(12):3189-200.
54. Bakkenist CJ, Beumer JH, and Schmitz JC. ATM serine-1981 phosphorylation is a plausible biomarker. *Cell Cycle.* 2015;14(20):3207-8.
55. Matsuoka S, Rotman G, Ogawa A, Shiloh Y, Tamai K, and Elledge SJ. Ataxia telangiectasia-mutated phosphorylates Chk2 in vivo and in vitro. *Proc Natl Acad Sci U S A.* 2000;97(19):10389-94.

56. Irizarry RA, Hobbs B, Collin F, Beazer-Barclay YD, Antonellis KJ, Scherf U, and Speed TP. Exploration, normalization, and summaries of high density oligonucleotide array probe level data. *Biostatistics.* 2003;4(2):249-64.
57. Smyth G. Linear Models and Empirical Bayes Methods for Assessing Differential Expression in Microarray Experiments. *Statistical applications in genetics and molecular biology.* 2004;3(Article3.
58. Ritchie ME, Diyagama D, Neilson J, van Laar R, Dobrovic A, Holloway A, and Smyth GK. Empirical array quality weights in the analysis of microarray data. *BMC Bioinformatics.* 2006;7(261-.
59. Draghici S, Khatri P, Tarca AL, Amin K, Done A, Voichita C, Georgescu C, and Romero R. A systems biology approach for pathway level analysis. *Genome Res.* 2007;17(10):1537-45.
60. Donato M, Xu Z, Tomoiaga A, Granneman JG, Mackenzie RG, Bao R, Than NG, Westfall PH, Romero R, and Draghici S. Analysis and correction of crosstalk effects in pathway analysis. *Genome Res.* 2013;23(11):1885-93.
61. Tarca AL, Draghici S, Khatri P, Hassan SS, Mittal P, Kim J-S, Kim CJ, Kusanovic JP, and Romero R. A novel signaling pathway impact analysis. *Bioinformatics (Oxford, England).* 2009;25(1):75-82.
62. Ahsan S, and Drăghici S. Identifying Significantly Impacted Pathways and Putative Mechanisms with iPathwayGuide. *Current Protocols in Bioinformatics.* 2017;57(1):7.15.1-7..30.
63. Carvalho BS, and Irizarry RA. A framework for oligonucleotide microarray preprocessing. *Bioinformatics (Oxford, England).* 2010;26(19):2363-7.
64. Wickham H. *ggplot2: Elegant Graphics for Data Analysis.* Springer Publishing Company, Incorporated; 2009.
65. Hu J, He X, Baggerly KA, Coombes KR, Hennessy BTJ, and Mills GB. Non-parametric quantification of protein lysate arrays. *Bioinformatics.* 2007;23(15):1986-94.

Chapter 3

Bcl-xL Inhibition Radiosensitizes p53 mutant, PIK3CA/PTEN wild-type Basal-like Breast Cancer

Summary

Apoptosis related gene expression is induced after radiation therapy (RT) in p53 wild-type breast cancer cells, while p53 mutant breast cancers have little induction of p53 related genes. Mutations in p53 are correlated with radioresistance in breast cancer cell line models. Inhibition of Bcl-2 family proteins radiosensitizes p53 mutant, PIK3CA/PTEN wild-type basal-like breast cancer cell lines, but has no effect on p53 mutant, PIK3CA/PTEN mutant basal-like breast cancer. Combination treatment of Bcl-2 family inhibition and RT significantly increases the percent of apoptotic cells. Bcl-xL specific, but not Bcl-2 specific, inhibition leads to radiosensitization of p53 mutant, PIK3CA/PTEN wild-type cell lines. Furthermore, Bcl-xL inhibition in combination with RT increases the percent of apoptotic cells while Bcl-2 inhibition does not. Radiosensitization is mediated by a decrease in Mcl-1 protein expression induced by RT in combination with Bcl-xL inhibition and overexpression of Mcl-1 rescues radioresistance. *In vivo*, Bcl-2 family inhibition or specific Bcl-xL inhibition in combination with RT decreases tumor growth and increases time to tumor doubling and tripling. Additionally, specific inhibition of Bcl-xL in combination with radiation leads to ~80% stable tumors in an *in vivo* orthotopic basal-like breast cancer cell line model. Together these results indicate that Bcl-xL inhibition may be a feasible clinical strategy for the radiosensitization of p53 mutant, PIK3CA/PTEN wild-type basal-like breast cancers.

Introduction

While most breast cancer patients are effectively cured with the addition of radiation therapy (RT) to their surgical management, a significant number develop locoregional recurrence despite RT and might be aided by the addition of radiosensitization agents to decrease their chance of local recurrence after RT (1). While previous efforts aimed at identifying particular patient populations at risk for local recurrences after RT, it is still unclear what the molecular drivers of these recurrences are (2-4). One approach to understand these drivers has been to characterize the transcriptomic response after RT with the rationale that gene expression changes between tumors that respond to RT may be different than non-responding tumors. Thus far, however, these studies have focused on the most radioresponsive luminal subtypes, without assessing other breast cancer subtypes and ignoring the most radioresistant subtype of breast cancer, basal-like tumors that lack estrogen and progesterone receptor expression (5).

To date, radiosensitization efforts have primarily focused on DNA synthesis and DNA damage related targets as possible radiosensitization agents, including cisplatin gemcitabine and PARP inhibitors (6, 7). Unfortunately despite their efficacy, these treatments are often associated with extensive normal tissue toxicities that has limited their clinical translatability (8). An alternative method for radiosensitization is to directly increase the percent of apoptotic cells after RT by targeting anti-apoptotic proteins. Apoptosis, a closely regulated pathway of programmed cell death, is controlled by activator (BH3 only proteins – BID, BIM, PUMA, and NOXA), sensitizer (BH3 only proteins – BAD, BIK, NOXA, HRK, PUMA, and BML), effector (BAX, BAK, and BOK), and anti-apoptotic proteins (Bcl-2 family proteins – BCL2, BCLXL, MCL1,

BCLW, and BFL1) (9-15). Under normal physiological conditions anti-apoptotic proteins are bound to effector proteins to inhibit apoptosis (10). Under cellular stress conditions, a signaling cascade, that is often, but not exclusively, mediated by p53, allows BH3 only sensitizer proteins to bind to anti-apoptotic proteins, releasing effector proteins (often Bax/Bak) from anti-apoptotic proteins (16-19). Upon release effector proteins form both hetereo and homo-dimers that allow for the release of cytochrome c from the mitochondria, thus irreversibly committing a cell to death through apoptosis (20, 21).

Inhibition of anti-apoptotic proteins, specifically, Bcl-2, Bcl-xL, and Mcl-1, has been to shown to be a successful cancer treatment strategy for acute myeloid leukemia (AML), chronic lymphocutic leukemia (CLL), and small lymphocytic lymphoma (22-25). As a result efforts are underway to inhibit anti-apoptotic proteins in other cancers, particularly in combination with treatments, such as DNA damaging agents or targeting of PIK3CA/PTEN pathway members (26-30). To date, few studies have focused on inhibition of anti-apoptotic proteins in combination with RT and none have specifically examined Bcl-xL inhibition in combination with RT (31).

In this study we aimed to identify an at risk population of breast cancer patients that could benefit from the addition of radiosensitization. We found that sensitivity to RT was correlated with p53 mutational status, and that p53 mutant tumors were significantly more resistant to ionizing radiation than p53 wild-type models. To explore this association, we performed microarray analysis to assess transcript expression from cell lines treated with or without RT. This analysis identified that p53 mutant breast cancer cell lines have a limited apoptotic transcriptional response to RT compared to p53 wild-type cell lines. We hypothesized that “re-activation” of the apoptotic

pathway, through inhibition of anti-apoptotic proteins, could lead to radiosensitization of these non-responsive p53 mutant breast cancers. Inhibition of Bcl-2 family proteins led to radiosensitization of p53 mutant breast cancers in a PIK3CA/PTEN pathway dependent manner. This radiosensitization was dependent on Bcl-xL, but not Bcl-2 or Bcl-w, inhibition. Mechanistically, we found that Bcl-xL inhibition induced radiosensitivity was mediated by RT-induced Mcl-1 protein loss and that overexpression of Mcl-1 rescued radioresistance. *In vivo*, using an orthotopic xenograft model, combination treatment of pan Bcl-2 family, or specific Bcl-xL, inhibition in combination with RT led to a significant delay in tumor growth and increased time to tumor doubling and tripling. In addition, the combination of Bcl-xL inhibition and RT led to tumor stasis or regression in 9 out of 11 tumors. Together, our results provide preclinical data in support of Bcl-xL inhibition as a potential clinical strategy for radiosensitization of p53 mutant, PIK3CA/PTEN wild-type breast cancers.

Results

Breast cancers with p53 mutations are more radioresistant and have a decreased apoptotic response

To asses factors that may correlate with radiosensitivity we determined the intrinsic radiosensitivity 21 breast cancer cells with known hormone receptor and p53 mutation status **(Figure 3.1A)**. Correlation analysis revealed that radiosensitivity was significantly correlated with p53 mutation status; p53 mutant breast cancer cell lines were significantly more radioresistant than p53 wild-type cell lines **(Figure 3.1B)**. Evaluation of the transcriptional response using gene

expression microarray data 24 hours after RT demonstrated that the p53 wild-type cell line, MCF-7, had robust transcriptional induction of genes associated with the apoptotic pathway; however, in p53 mutant cell lines, MDA-MB-231 and BT-549, few of these apoptosis-associated genes were overexpressed after RT **(Figure 3.1C)**. Using open source data (GSE59732) we compared gene expression after RT within only luminal breast cancer cell lines with varying p53 mutation status. This comparison allowed us to eliminate confounding results due to high variances in estrogen receptor, progesterone receptor, and HER2 expression differences in these models. Here, we found that p53 wild-type cell lines, MCF-7 and ZR-75-1, had a large number of apoptosis related genes with increased expression after RT. As previously seen, the p53 mutant cell line, T47D, had few apoptosis related genes overexpressed after RT. Additionally, the normal breast cell line, HBL-100, which is p53 wild-type, also had significant overexpression of apoptosis related genes **(Figure 3.1D)**. Together these results suggest that mutations in p53 may blunt a transcriptional apoptotic response which contributes to their radioresistant phenotype. We therefore hypothesized that inhibition of anti-apoptotic proteins may "reactivate" this death pathway and render p53 mutant breast cancer cell lines more sensitive to RT.

Pan Bcl-2 family inhibition radiosensitizes p53 mutant, PIK3CA/PTEN wild-type basal-like breast cancer

To assess the impact of Bcl-2 family inhibition on breast cancer cell lines we identified the IC50 of proliferation of ABT-263, an inhibitor of Bcl-2, Bcl-xL, and Bcl-w, on multiple radioresistant basal-like breast cancer cell lines, all with mutant p53 (32). We found a range of IC50s from ~40nM to greater than 10μM. However, basal-like breast cancer cell lines with

mutations in the PIK3CA/PTEN pathway had significantly higher IC50s than those cell lines with no mutations in the PIK3CA/PTEN pathway **(Figure 3.2A&B)**. Thus, we hypothesized that cell lines with an intact PIK3CA/PTEN pathway would be radiosensitized by ABT-263 while those with mutations in the PIK3CA/PTEN pathway would not. To asses this, we performed clonogenic survival assays in multiple cell lines either wild-type or mutant for the genes in the PIK3CA/PTEN pathway. MDA-MB-231, CAL-120, and HCC-38 cell lines, which all have an intact PIK3CA/PTEN pathway, were significantly radiosensitized by sub IC50 concentrations of ABT-263 (MDA-MB-231 radiation enhancement ratio (rER) 100nM: 109-1.21, 500nM: 1.22-1.37, 1μM: 1.40-1.66; CAL-120 rER 100nM: 1.10-1.33, 250nM: 1.15-1.63, 500nM: 1.36-1.74; HCC-38 rER 10nM: 1.06-1.11, 25nM: 1.12-1.27, 50nM: 1.37-1.40). Additionally, there was a significant decrease in surviving fraction of cells after 2 Gy RT (SF 2-Gy) in cells treated with ABT-263 compared to DMSO control **(Figure 3.2C-E)**. Combination treatment of ABT-263 and RT (4 Gy) significantly increased the percent of apoptotic cells compared to RT alone in both MDA-MB-231 and CAL-120 cell lines **(Figure 3.3A&B)**. Finally, a combination of ABT-263 and RT (4 Gy) increased in cleaved-PARP, a marker for apoptosis, compared to either RT or drug alone in MDA-MB-231 and CAL-120 cells **(Figure 3.3C&D)** (33).

Conversely, in p53 mutant cell line models with mutations in the PIK3CA/PTEN pathway, SUM-159 and MDA-MB-453 cell lines, ABT-263 did not lead to radiosensitization (SUM-159 rER 100nM: 0.93-1.17, 500nM: 0.87-1.00, 1μM: 0.94-1.03; MDA-MB-453 rER 100nM: 1.10-1.15, 500nM: 1.02-1.14, 1μM: 1.00-1.30) and no decrease in SF-2 Gy was seen **(Figure 3.4A&B)**. Additionally, combination treatment of ABT-263 and RT (4 Gy) did not lead to a significant

increase in apoptotic cells compared to RT **(Figure 3.4C&D)**. Thus, inhibition of Bcl-2, Bcl-xL, and Bcl-w, with ABT-263, radiosensitized p53 mutant basal-like breast cancers in a PIK3CA/PTEN pathway dependent manner, and that this radiosensitization was mediated through increased apoptosis.

Specific inhibition of Bcl-xL radiosensitizes p53 mutant, PIK3CA/PTEN wild-type basal-like breast cancers

We next sought to identify which protein of the three targeted by ABT-263 (Bcl-2. Bcl-xL, or Bcl-w) was responsible for the radiosensitization of PIK3CA/PTEN wild-type basal-like breast cancer. To do this, we first determined the IC50 of proliferation of WEHI-539, a Bcl-xL specific inhibitor **(Figure 3.5A)** (34). MDA-MB-231, CAL-120, and HCC-38 all had similar WEHI-539 IC50s compared to ABT-263, indicating that Bcl-xL may be the protein responsible for inhibiting apoptosis in these cell lines **(Figure 3.5B)**. Using clonogenic survival assays we found that specific inhibition of Bcl-xL, using WEHI-539, radiosensitized the p53 mutant, PIK3CA/PTEN intact breast cancer cell lines MDA-MB-231, CAL-120, and HCC-38 **(Figure 3.5C-E)** and significantly decreased SF-2 Gy across all three cell lines (MDA-MB-231 rER 100nM: 0.90-1.13, 500nM: 1.18-1.25, 1μM: 1.27-1.38; CAL-120 rER 50nM: 1.13-1.21, 100nM: 1.31-1.35, 250nM: 1.60-2.14; HCC-38 rER 25nM: 1.24-.150, 50nM: 1.30-1.93, 100nM: 1.45-1.99). As with the pan-Bcl-2 family inhibitor ABT-263, combination of WEHI-539 and RT (4 Gy) significantly increased the percent of apoptotic cells compared to RT alone in MDA-MB-231 and CAL-120 cells **(Figure 3.6A&B)**. Furthermore, combination treatment of WEHI-539 and RT (4 Gy) increased cleaved PARP compared to RT or drug alone **(Figure 3.6C&D)**.

To further confirm that Bcl-xL inhibition is indeed responsible for radiosensitization of PIK3CA/PTEN wild-type basal-like breast cancer cell lines we performed clonogenic survival assays using a different Bcl-xL inhibitor, A-1331852, which was developed for *in vivo* use (35). As with the WEHI-539 compound, treatment with A-1331825 radiosensitized MDA-MB-231 cells (rER 250nM: 1.12-1.19, 500nM: 1.18-1.28, 1μM: 1.26-1.40) and significantly decrease SF-2 Gy **(Figure 3.5F)**. Thus, we concluded Bcl-xL inhibition is sufficient to radiosensitize p53 mutant, PIK3CA/PTEN wild-type basal-like breast cancers.

Inhibition of Bcl-2 does not radiosensitization p53 mutant, PIK3CA/PTEN basal-like breast cancer

Having established that Bcl-xL inhibition was sufficient to confer radiosensitivity in p53 mutant, PIK3CA/PTEN wild-type basal-like breast cancer, we next sought to determine if Bcl-2 also played a role in this radiosensitization. Using ABT-199, a Bcl-2 specific inhibitor, we first determined the IC50 of proliferation of ABT-199 in our model systems of p53 mutant breast cancers **(Figure 3.7A)** (22). p53 mutant, PIK3CA/PTEN wild-type basal-like breast cancer cell lines MDA-MB-231, CAL-120, and HCC-38 all had much higher ABT-199 IC50s compared to both ABT-263 (pan Bcl-2 family inhibitor) and WEHI-539 (Bcl-xL specific inhibitor), initially indicating that Bcl-2 inhibition may not be as effective in the radiosensitization of PIK3CA/PTEN wild-type basal-like breast cancers **(Figure 3.7B)**.

Clonogenic survival assays using the Bcl-2 inhibitor, ABT-199, showed that Bcl-2 inhibition did not radiosensitize MDA-MB-231 or CAL-120 cell lines (MDA-MB-231 rER 100nM: 0.97-1.21, 500nM: 0.96-1.12, 1μM: 0.97-1.10; CAL-120 rER 100nM: 1.02-1.05, 500nM:

0.94-1.12, 1μM: 0.97-1.10) and did not decrease the SF-2 Gy **(Figure 3.7C&D)**. Similarly, combination of ABT-199 and RT (4 Gy) did not increase the percent of apoptotic cells compared to RT in either cell line **(Figure 3.7E&F)**. Finally, the combination of ABT-199 and RT (4 Gy) did not increase cleaved PARP compared to either RT or drug alone **(Figure 3.7G&H)**. Thus we concluded that inhibition of Bcl-2 does not contribute to radiosensitization of PIK3CA/PTEN wild-type basal-like breast cancer.

Radiation leads to decreased Mcl-1 expression, allowing for radiosensitization by Bcl-xL inhibition

In an effort to identify why p53 mutant, PIK3CA/PTEN mutant basal-like breast cancers did not respond to Bcl-xL inhibition mediated radiosensitization, we sought to identify the mechanism for radiosensitization in PIK3CA/PTEN wild-type cell lines. Previous studies demonstrated that dual inhibition of Bcl-xL and Mcl-1 in cancer cell lines led to decreased growth both *in vitro* and *in vivo* (28, 36, 37). Furthermore, previous studies have demonstrated Bcl-2 family inhibition increases Mcl-1 expression in the MDA-MB-231 basal-like breast cancer cell line and that RT reduces Mcl-1 expression after Bcl-2 family inhibition (31). Therefore we hypothesize that RT may be impacting Mcl-1 protein expression, in a PIK3CA/PTEN dependent manner, thus allowing for increased radiosensitivity after Bcl-xL inhibition. To address this we assessed Mcl-1 protein levels after combination treatment of ABT-263 and RT (6 Gy). After a 24-hour pretreatment with ABT-263, Mcl-1 protein levels increased, however, 30 minutes after RT (6 Gy) Mcl-1 levels returned to baseline in the CAL-120 cell line **(Figure 3.8A)**.

To further confirm that decreased Mcl-1 expression is necessary for Bcl-2 family inhibition dependent radiosensitization of PIK3CA/PTEN wild-type basal-like breast cancer, we sought to rescue radioresistance by overexpressing Mcl-1 protein. While Bcl-xL inhibition significantly radiosensitized p53 mutant, PIK3CA/PTEN wild-type cell lines MDA-MB-231 and CAL-120 treated with lipofectamine alone (MDA-MB-231 rER WEHI-539: 1.19-1.32; CAL-120 rER WEHI-539: 1.34-1.35), the overexpression of Mcl-1 in these cells reversed the radiosensitization phenotype of Bcl-xL inhibition (MDA-MB-231 rER Mcl-1 & WEHI-539: 1.03-1.06; CAL-120 rER Mcl-1 & WEHI-539: 0.99-1.09) and rescued SF-2 Gy **(Figure 3.8B&D)**. Overexpression of exogenous FLAG-tag Mcl-1 was confirmed through western blot **(Figure 3.8C&E)** These results demonstrate that Bcl-xL inhibition in combination with RT leads to radiosensitization of PIK3CA/PTEN wild-type basal-like breast cancer in a manner that is dependent on decreased Mcl-1 expression.

Bcl-xL inhibition radiosensitizes p53 mutant, PIK3CA/PTEN wild-type basal-like breast cancer *in vivo*

To examine the effect of Bcl-2 family member inhibition, and specifically Bcl-xL inhibition, *in vivo*, we orthotopically injected SCID CB-17 female mice with MDA-MB-231 cells and allowed them to grow to approximately 80mm^3. Once the tumors had established (~80mm^3), mice were given either 25 mg/kg of ABT-263 (pan Bcl-2 family inhibitor) once a day for 10 days, 25 mg/kg of A-1331852 (Bcl-xL inhibitor) once a day for 10 days, 9 fractions of 2 Gy RT, or a combination of either ABT-263 or A-1331852 and RT, which started 24 hours after the first treatment with drug **(Figure 3.9A)**. A combination of pan Bcl-2 family inhibition with ABT-263

and RT significantly decreased tumor growth compared to drug or RT alone with the time to tumor doubling extended from 12 days in the control arm to 31 days in the combination treated arm. Furthermore, the combination of Bcl-xL inhibition with A-1331852 and RT more effectively delayed tumor growth with time to tumor doubling extended from 12 days in the control arm to an undefined number of days in the combination treated arm **(Figure 3.9B)**. Both combination treatments significantly decreased tumor volume compared to drug alone (**Figure 3.9C**). Furthermore, combination treatment of either ABT-263 or A-1331852 with RT significantly delayed time to tumor doubling (Control – 12 days, RT – 14 days, ABT-263 – 16 days, ABT + RT – 31 days, A-1331852 – 15 days, and A-1331 + RT – Undefined) and tripling (Control – 15.5 days, RT – 28 days, ABT-263 – 29 days, ABT + RT – Undefined days, A-1331852 – 24 days, and A-1331 + RT – Undefined) **(Figure 3.9D&E)**. The combination of A-1331852 and RT led to the tripling of no tumors after 31 days and doubling of only 2 tumors in that same time. This established that inhibition of Bcl-xL, with either the pan Bcl-2 family inhibitor, ABT-263, or with the specific Bcl-xL inhibitor, A-1331852, in combination with RT not only radiosensitized MDA-MB-231 cells *in vitro* but also *in vivo* and led to stability or regression of 9 out of 11 tumors in the combination treatment arm, even after one month.

Discussion

In an effort to identify mediators of radiation resistance in breast cancer, we profiled the intrinsic sensitivity of a panel of over 20 breast cancer cell lines. Such profiling identified p53 mutation status as being significantly correlated with radiation sensitivity. We show p53 mutant

breast cancers are more resistant to ionizing radiation than p53 wild-type breast cancers and p53 mutant breast cancers are unable to induce a transcriptional apoptotic response after radiation treatment compared to p53 wild-type breast cancers **(Figure 3.1)**. Although more resistant to ionizing radiation, we hypothesized that inhibiting anti-apoptotic proteins in p53 mutant breast cancers may allow for the re-introduction of apoptosis after RT and thus radiosensitize these cancers. Treatment of p53 mutant breast cancer cell lines with the Bcl-2 family inhibitor ABT-263 significantly radiosensitized these cells in a PIK3CA/PTEN dependent manner. Mechanistically, this radiosensitization of p53 mutant, PIK3CA/PTEN wild-type cell lines was caused by an increase in the percent of apoptotic cells after a combination of ABT-263 and RT **(Figure 3.2, 3.3, and 3.4)**. In an effort to identify which Bcl-2 family protein was responsible for radiosensitization we performed clonogenic survival assays with the Bcl-xL specific inhibitor, WEHI-539. Specific inhibition of Bcl-xL significantly radiosensitized p53 mutant, PIK3CA/PTEN wild-type basal-like breast cancer cell lines and significantly increased the percent of apoptotic cells in combination with RT **(Figure 3.5 and 3.6)**. However, inhibition of Bcl-2, with the Bcl-2 specific inhibitor ABT-199, did not radiosensitize p53 mutant, PIK3CA/PTEN intact basal-like breast cancer nor did it increase the percent of apoptotic cells in combination with RT **(Figure 3.7)**. Pharmacologic inhibition of Bcl-2 family proteins led to an increase in Mcl-1 protein, while treatment with RT led to a decrease in Mcl-1 protein, again in a PIK3CA/PTEN – dependent manner. Overexpression of Mcl-1 rescued this radiosensitizing phenotype and led to resistance of Bcl-xL inhibition mediated radiosensitivity. **(Figure 3.8)**. Finally, we show that both Bcl-2 family and Bcl-xL specific inhibition significantly radiosensitizes p53 mutant, PIK3CA/PTEN wild-type basal-like

breast cancer cell lines *in vivo*, with Bcl-xL inhibition leading to more durable and dramatic response with radiation **(Figure 3.9)**. Together, these results demonstrate that Bcl-xL inhibition radiosensitizes p53 mutant breast cancers in a PIK3CA/PTEN dependent manner through the regulation of Mcl-1 protein.

While our nomination of the apoptotic pathway for radiosensitization of aggressive breast cancers was successful, radioresistance is likely explained many factors apart from p53 mutation status. For example, previous studies have found genes including CDKN2A and Keap1 to participate in radioresistance, while mutations in genes such as Rb and EGFR have been found to increase radiosensitivity (38-42). These mutations, as well as others yet to be identified, add complexity in characterizing the radiation response. Furthermore, many studies have shown mutations in p53 can have differential effects (43). Both nonsense mutations and missense mutations can lead to p53 inactivation or gain of function (44-47). Moreover, overexpression of MDM2 can lead to p53 loss, which would not be apparent from solely examining p53 mutation status (48-50). Interestingly, previous studies have developed a p53 inactivation signature that may be more effective at determining p53 inactivation (51). A signature similar to this may be more useful in predicting proteins associated with radioresistance in breast cancer.

After confirming that pan Bcl-2 family inhibition induces radiosensitization in p53 mutant, PIK3CA/PTEN wild-type cell lines we showed that inhibition of Bcl-xL was responsible for radiosensitization. Previous studies have shown that inhibition of Bcl-2, using ABT-737, radiosensitizes multiple breast cancer subtypes (31); however, ABT-737 also inhibits Bcl-xL and this more likely explains the radiosensitization phenotype (52). Previous studies have also shown

that dual targeting of Bcl-xL and PIKC3A in PIK3CA mutant breast cancers blocks tumor growth *in vivo* (28). This growth inhibitory effect is mediated through PIK3CA inhibition which leads to decreased mTOR regulated Mcl-1 translation, thus decreasing Mcl-1 protein expression while inhibiting Bcl-xL. While we also show decreased Mcl-1 expression in our studies, we believe that Mcl-1 protein is being rapidly degraded after RT in PIK3CA/PTEN wild-type cell lines. We hypothesize that RT is leading to increased activation of an E3-ubiquitin ligase or decreased activity of a deubiquitinating protein. Many E3-ubiquitin ligases and deubiquitinating proteins have been identified for Mcl-1, however we have not determined which is leading to decreased Mcl-1 protein expression after RT and this is the subject of ongoing investigation in our group **(Figure 3.10)** (53-56).

While inhibition of Bcl-xL in combination with RT leads to profound radiosensitization in an orthotopic MDA-MB-231 *in vivo* model, we plan to perform additional *in vivo* models using patient derived xenografts (PDXs), which may more accurately reflect tumor heterogeneity in patients. Within these studies we also plan to examine platelet counts as inhibition of Bcl-xL has been shown to acutely decreased platelets (22). These pending studies, coupled with the results reported here, provide the preclinical rational for combination treatment with Bcl-xL inhibitors and RT and suggest this could be a tractable treatment strategy for p53 mutant, PIK3CA/PTEN wild-type breast cancer patients.

Methods

Cell Culture

Triple-negative breast cancer cell lines MDA-MB-231, CAL-120, HCC-38, BT-549, and MDA-MB-453 were grown from frozen samples (ATCC). SUM-159 cells were received from Steve Ethier, from the University of Michigan. MDA-MB-231, CAL-120, MDA-MB-453 cell lines were grown in DMEM (Invitrogen) supplemented with 10% FBS (Invitrogen). BT-549 and HCC-38 cell lines were grown in RPMI 1640 (Invitrogen) and supplemented with 10% FBS. All cell lines were supplemented with 1% penicillin/streptomycin (Invitrogen). SUM-159 cells were grown in Ham's F-12 media (Gibco) supplemented with 5% FBS, 5mL of 1M HEPES, 1ug/mL Hydrocortisone, 1x antibiotic-antimycotic (Thermo Fisher) and 6ug/mL insulin (Sigma). All cells lines were grown in a 5% CO_2 incubator, tested for mycoplasma routinely (MycoALert, Lonza), and authenticated at the University of Michigan DNA sequencing core before use.

Compounds

ABT-263, ABT-199, WEHI-539, and A-1331852 were order from MedChemExpress as a 10mM solution in DMSO. Multiple concentrations of each drug were used for various assays.

Irradiation

Irradiations were performed using a Kimtron IC 225 (Kimtron Medical) at a dose rate of approximately 2 Gy/min in the University of Michigan Comprehensive Cancer Center Experimental Irradiation Core (Ann Arbor, MI). Dosimetry is performed semiannually using an ionization chamber connected to an electrometer system that is directly traceable to a National

Institute of Standards and Technology calibration. The beam was collimated with a 0.1 mm Cu inherent filter and a 0.2 mm Cu filter was used for cell line irradiation. A 2 mm Cu filter was used for in vivo xenograft experiments.

Western Blot

Cells were lysed with RIPA buffer (Thermo Fischer) supplemented with cOmplete Mini protease (Signam-Aldrich) and phosSTOP (Roche) inhibitors and western blot was performed as previously described (57). Cleaved PARP and Mcl-1 (Cell Signaling Technology [CST]) antibodies were used at 1:1,000 dilution in 1% milk. GAPDH (CST) antibody was used at 1:10,000 dilution in 1% milk. Actin (CST) antibody was used at 1:50,000 dilution in 1% milk.

IC50 of proliferation

2,000-5,000 cells were plated per well in a 96-well plate and allowed to adhere overnight. Drug was added at various concentrations and after 72 hours AlamarBlue ($1/10^{th}$ volume) was added. Fluorescence was measured 3-8 hours after the addition of AlamarBlue, based on the proliferation rate of the cell line.

Clonogenic survival assays

Exponentially growing cells were plated at clonal density and allowed to adhere overnight. Drug was added 1 hour prior to radiation and allowed to grow for one to two weeks. Cells were fixed with 7 parts methanol and 1 part acetic acid and stained with crystal violet. A colony was deemed 50 cells or large and a linear-quadratic survival curve was fit to each assay as previously described (58).

Annexin V Staining

The Annexin-VFLUOS Staining Kit (Roche Cat. No. 11858 777 001) was used for quantification of apoptosis and differentiation from necrosis by flow cytometry. In brief, cells (0.25×10^5) grown in 6-well plates were treated with Bcl-2 family inhibitors (ABT-263, ABT-199, and WEHI-539) at the indicated doses. Cells were pretreated with drug 1-hour before RT (4 Gy) and harvested for staining 48-hours after RT. Cells were collected, washed with PBS, and incubated in 100µl of binding buffer containing 2µl of Annexin V-FITC and 2 µl of PI for 15 min at room temperature in the dark according to the manufacturer's instructions. Apoptosis was immediately quantified using FCM. Results were presented as percentages of Annexin V-FITC positive cells, or Annexin V-FITC and PI double positive cells. The total apoptosis was summed up from that of early apoptosis (Annexin V+/PI−) and late apoptosis (Annexin V+/PI+).

In vivo studies

Cells or patient derived xenografts (PDXs) were orthotopically implanted into the mammary fat pad of CB-17 SCID female mice. Tumors were allowed to grow to ~80mm^3 and randomized before treatment began. ABT-263 or A-1331852 were given once a day for ten days at 25mg/kg and nine fractions of radiation were given, starting one day after drug was given. Tumor size was measured approximately three times per week using a digital caliper. Tumor volume was calculated using the equation V= (L * W2) * π/6 (V=volume, L=length, W=width). Synergistic effects were calculated using the fraction tumor volume (FTV) method as previously described (59, 60).

Study approval

The procedures listed above were approved by the Institutional Animal Care and Use Committee (IACUC) at the University go Michigan.

Statistics

Statistical analyses were performed using GraphPad Prism 8.0. One-way ANOVA with Dunnett's multiple comparisons test was used for clonogenic survival and Annexin V assays. One-way ANOVA with Dunnett's multiple comparisons test and Log-rank (Mantel-Cox) test were used for *in vivo* analyses. A P value equal to or less than 0.05 was considered significant.

Figures

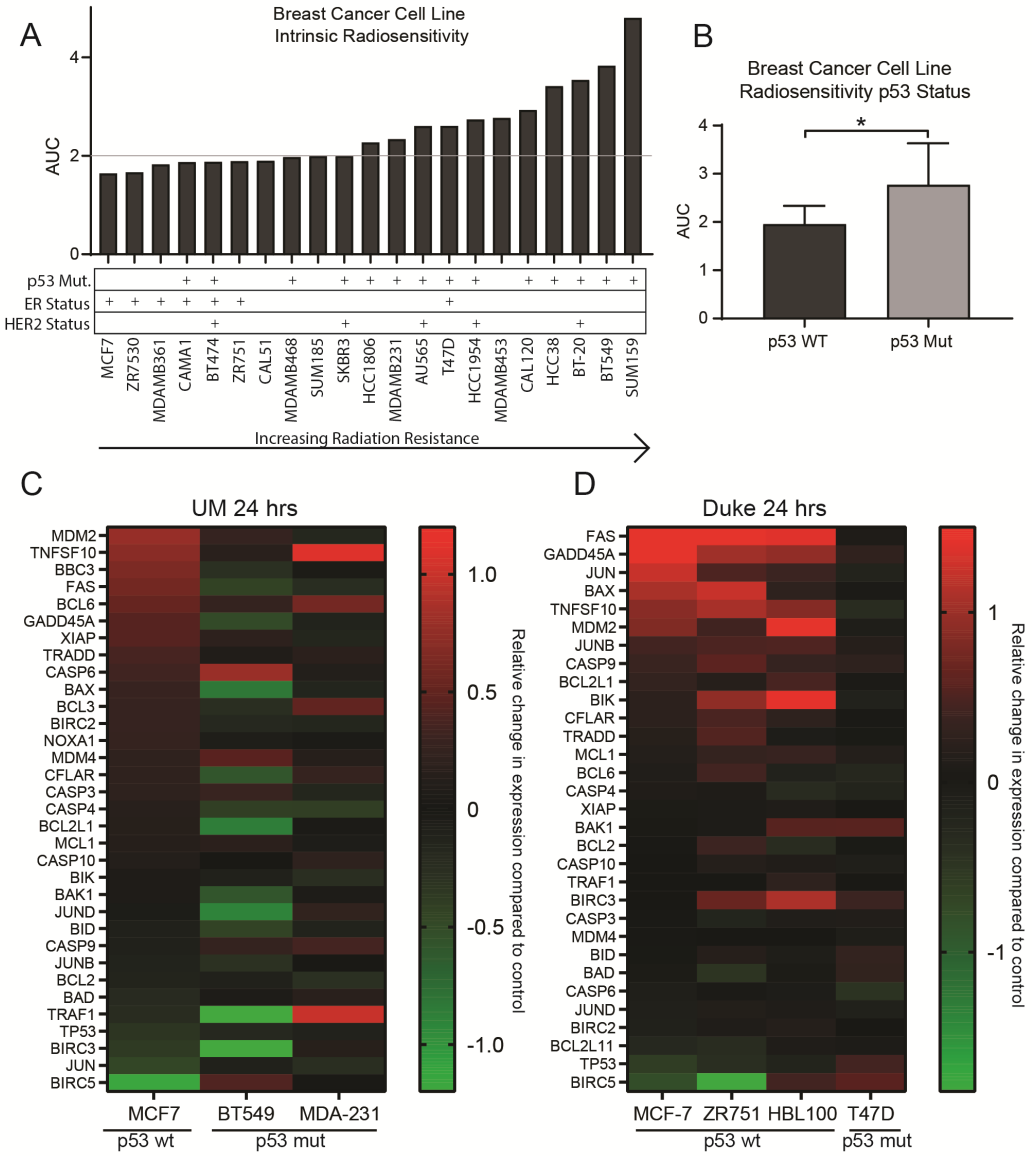

Figure 3.1: p53 mutant breast cancers are more resistant to radiation and do not exhibit an apoptotic response. A) Breast cancer cell lines intrinsic radiosensitivity organized from most radiosensitive to least radiosensitive. ER status, HER2 status, and p53 mutation status depicted. B) p53 wild-type cell lines are more radiosensitive than p53 mutant. C&D) RT induces an apoptosis gene transcriptional response in a p53-dependent manner in both a University of Michigan dataset (C) and a dataset from Duke (D). A two-sided Student's t-test was used for analyses. * $p < 0.05$

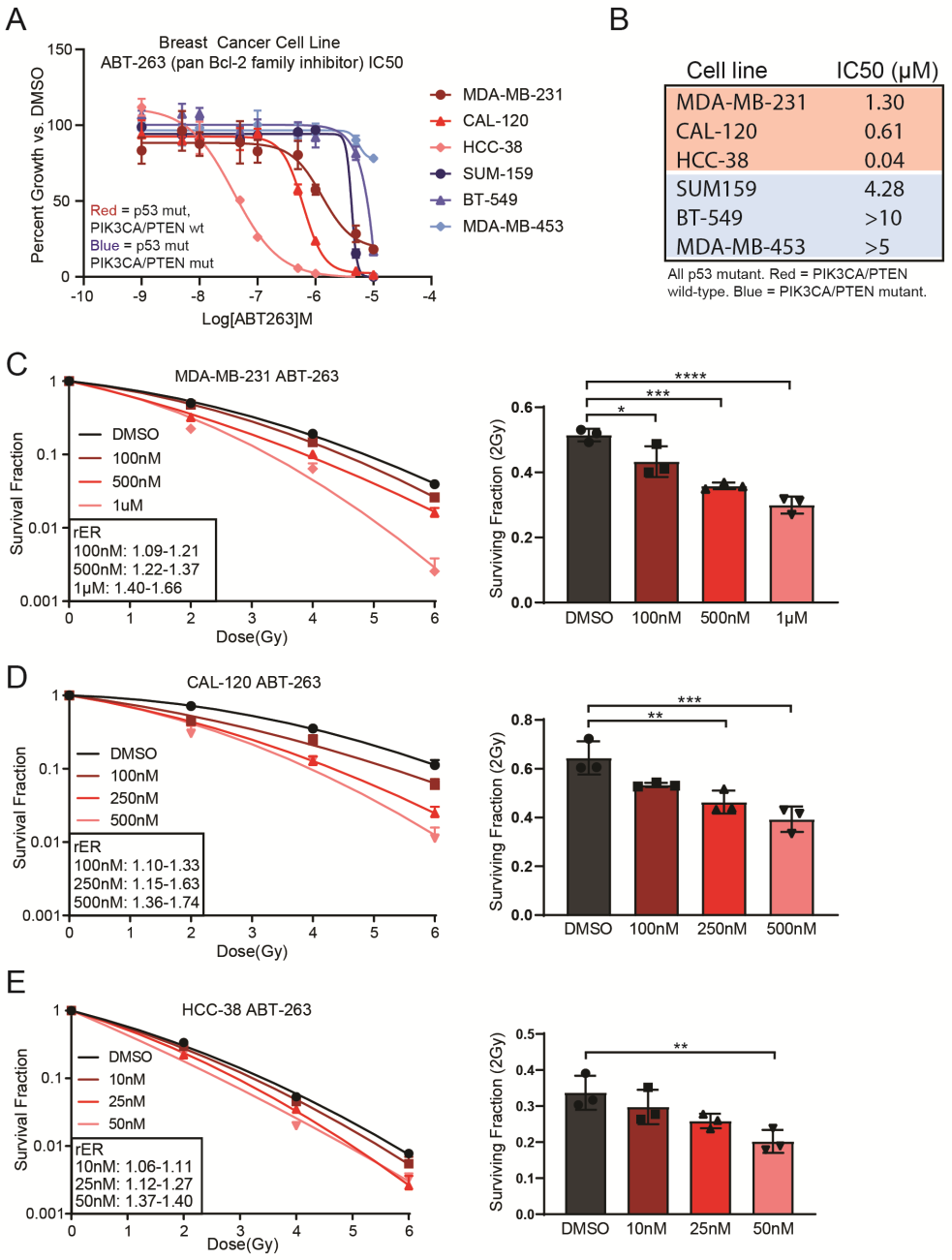

Figure 3.2: Pan Bcl-2 family inhibition radiosensitizes p53 mutant, PIK3CA/PTEN wild-type basal-like breast cancer cell lines. A) ABT-263 (pan Bcl-2, Bcl-xL, and Bcl-w inhibitor) IC50 of proliferation in multiple basal-like breast cancer cell lines. B) Summary of ABT-263 IC50 values. C-E) ABT-263 significantly radiosensitizes MDA-MB-231 (C), CAL-120 (D), and HCC-38 (E) cell lines. One-way

ANOVA with Dunnett's multiple comparisons test was used for analyses. * $p<0.05$, ** $p<0.01$, *** $p<0.001$, **** $p<0.0001$.

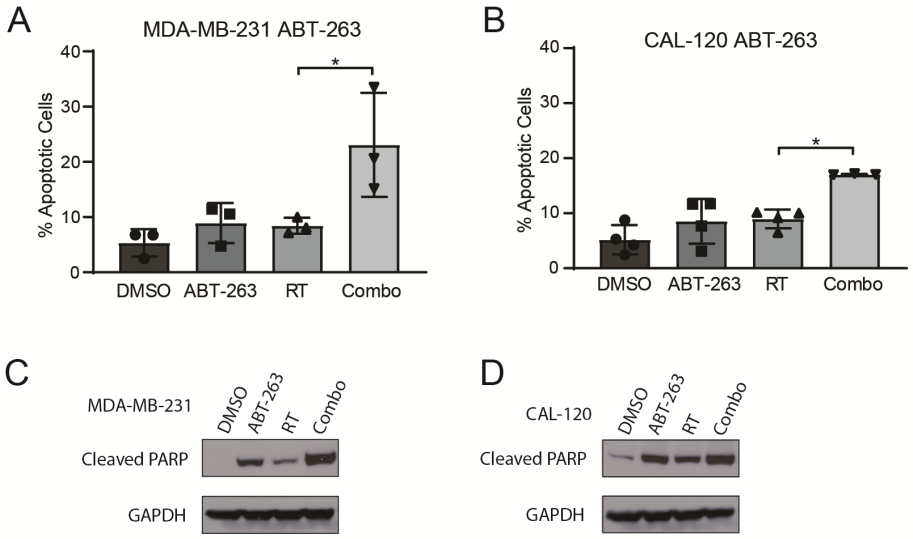

Figure 3.3: Pan Bcl-2 family inhibition in combination with radiation (RT) significantly increases the percent of apoptotic cells in p53 mutant, PIK3CA/PTEN wild-type basal-like breast cancer cell lines. A&B) ABT-263 (pan Bcl-2, Bcl-xL, and Bcl-w inhibitor) in combination with RT significantly increases the percent of apoptotic cells compared to RT alone in MDA-MB-231 (A) and CAL-120 (B) cell lines. C&D) Combination of ABT-263 and RT increases cleaved PARP compared to RT alone in MDA-MB-231 (C) and CAL-120 (D) cell lines. Cells were pretreated with ABT-263 for 1-hour before RT (4 Gy) and harvested either 48-hours after drug or 48-hours after RT. A two-sided Student's t-test was used for analyses. * $p<0.05$

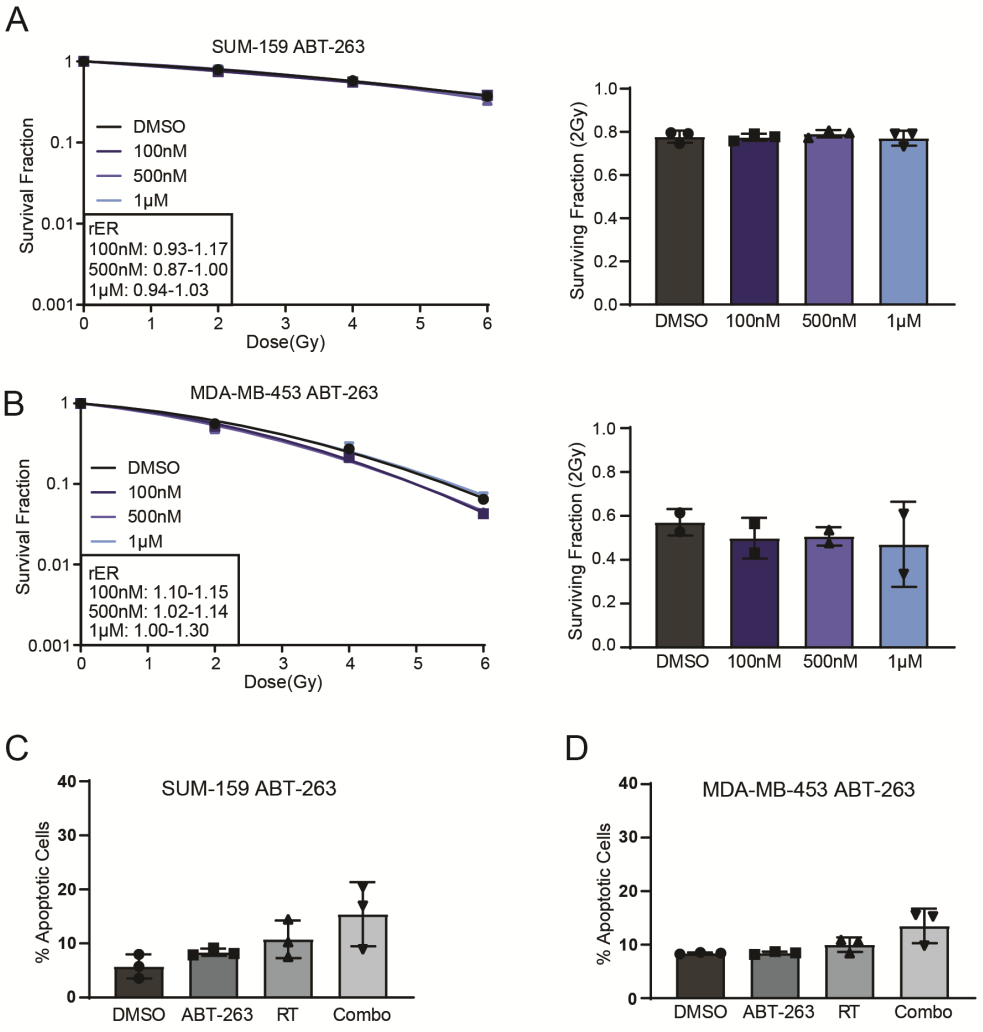

Figure 3.4: Pan Bcl-2 family inhibition does not radiosensitize p53 mutant, PIK3CA/PTEN mutant basal-like breast cancer cell lines and does not increase the percent of apoptotic cells. A&B) ABT-263

(pan Bcl-2, Bcl-xL, and Bcl-w inhibitor) does not radiosensitize SUM-159 (A) and MDA-MB-453 (B) cell lines. C&D) Combination of ABT-263 and RT does not increase the percent of apoptotic cells compared to RT in SUM-159 (C) and MDA-MB-453 (D) cell lines. Cells were pretreated with ABT-263 for 1-hour before RT (4 Gy) and harvested either 48-hours after drug or 48-hours after RT. One-way ANOVA with Dunnett's multiple comparisons test and a two-sided Student's t-test were used for analyses.

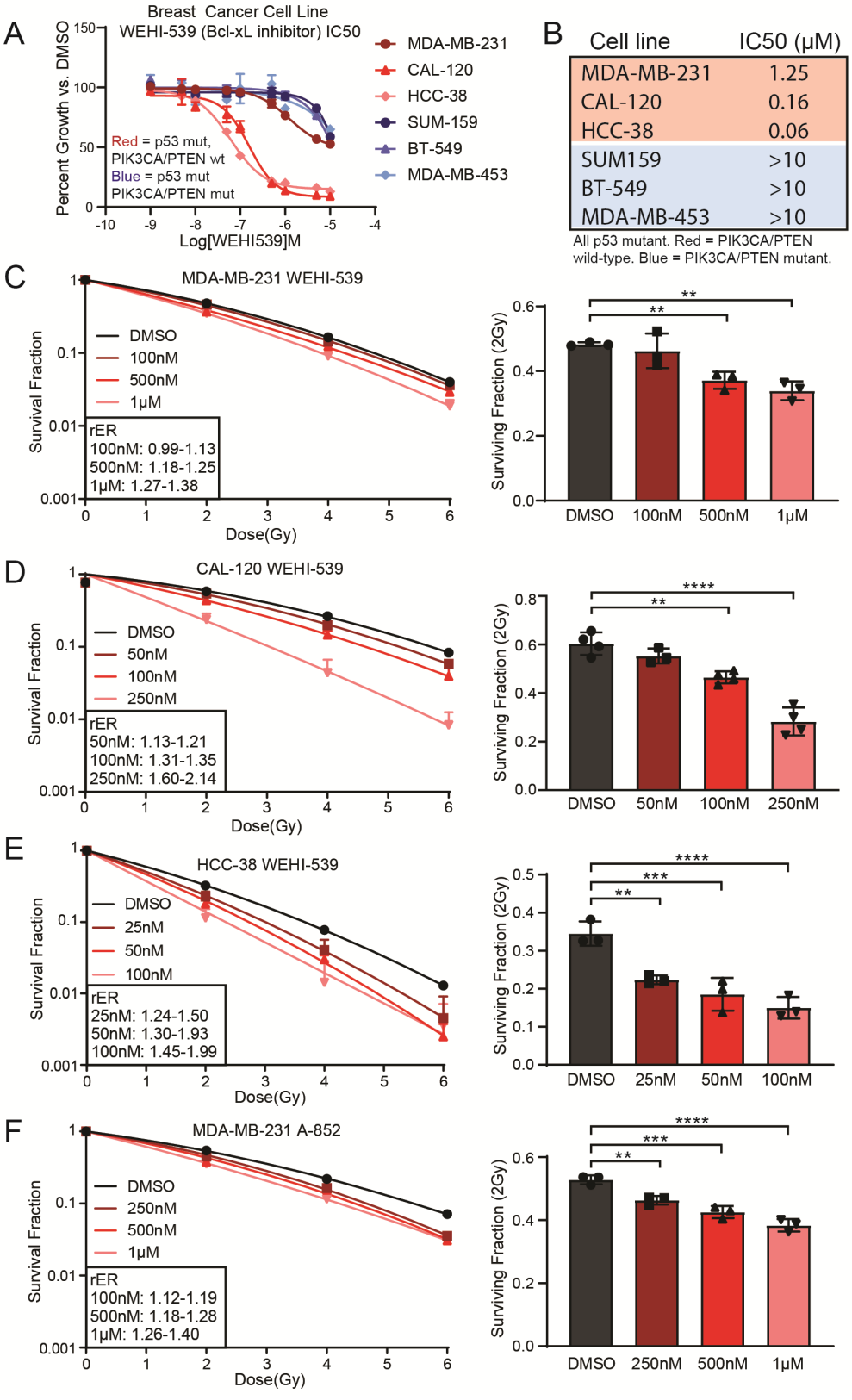
A
Breast Cancer Cell Line
WEHI-539 (Bcl-xL inhibitor) IC50
Percent Growth vs. DMSO
Log[WEHI539]M
Red = p53 mut, PIK3CA/PTEN wt
Blue = p53 mut PIK3CA/PTEN mut
MDA-MB-231
CAL-120
HCC-38
SUM-159
BT-549
MDA-MB-453
B
Cell line IC50 (μM)
MDA-MB-231 1.25
CAL-120 0.16
HCC-38 0.06
SUM159 >10
BT-549 >10
MDA-MB-453 >10
All p53 mutant. Red = PIK3CA/PTEN wild-type. Blue = PIK3CA/PTEN mutant.
C
MDA-MB-231 WEHI-539
Survival Fraction
Dose(Gy)
DMSO
100nM
500nM
1μM
rER
100nM: 0.99-1.13
500nM: 1.18-1.25
1μM: 1.27-1.38
Surviving Fraction (2Gy)
D
CAL-120 WEHI-539
DMSO
50nM
100nM
250nM
rER
50nM: 1.13-1.21
100nM: 1.31-1.35
250nM: 1.60-2.14
E
HCC-38 WEHI-539
DMSO
25nM
50nM
100nM
rER
25nM: 1.24-1.50
50nM: 1.30-1.93
100nM: 1.45-1.99
F
MDA-MB-231 A-852
DMSO
250nM
500nM
1μM
rER
100nM: 1.12-1.19
500nM: 1.18-1.28
1μM: 1.26-1.40

Figure 3.5: The Bcl-xL inhibitor, WEHI-539, radiosensitizes p53 mutant, PIK3CA/PTEN wild-type basal-like breast cancer cell lines. A) WEHI-539 IC50 of proliferation in multiple basal-like breast cancer cell lines. B) Summary of WEHI-539 IC50 values. C-E) WEHI-539 significantly radiosensitizes MDA-MB-231 (C), CAL-120 (D), and HCC-38 (E) cell lines. F) A-1331852, a Bcl-xL inhibitor significantly radiosensitizes MDA-MB-231 cells. One-way ANOVA with Dunnett's multiple comparisons test was used for analyses. **$p<0.01$, ***$p<0.001$, ****$p<0.0001$.

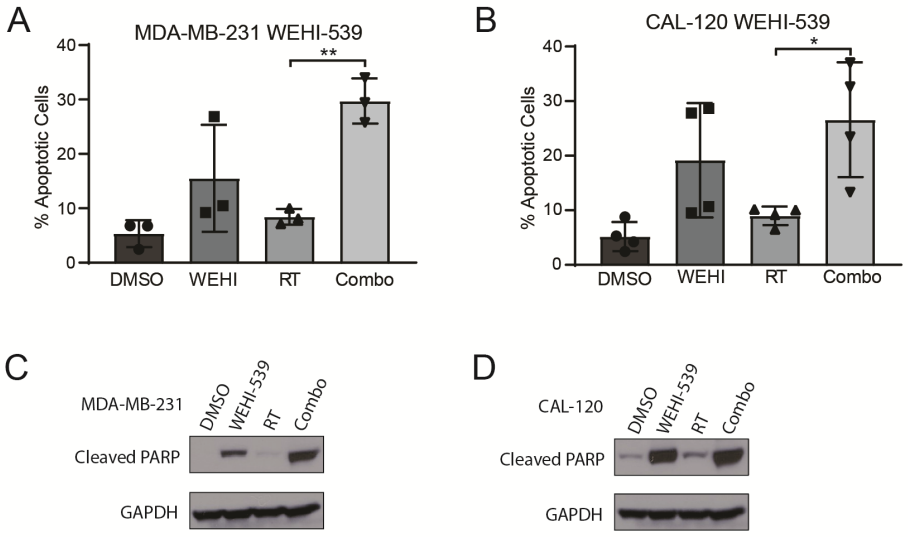

Figure 3.6: Inhibition of Bcl-xL in combination with radiation (RT) significantly increases the percent of apoptotic cells in p53 mutant, PIK3CA/PTEN wild-type basal-like breast cancer cell lines. A&B) WEHI-539 (Bcl-xL inhibitor) in combination with RT significantly increases the percent of apoptotic cells compared to RT alone in MDA-MB-231 (A) and CAL-120 (B) cell lines. C&D) Combination of WEHI-539 and RT increases cleaved PARP compared to RT alone in MDA-MB-231 (C) and CAL-120 (D) cell lines. Cells were pretreated with WEHI-539 for 1-hour before RT (4 Gy) and harvested either 48-hours after drug or 48-hours after RT. A two-sided Student's t-test was used for analyses. * $p<0.05$, ** $p<0.01$

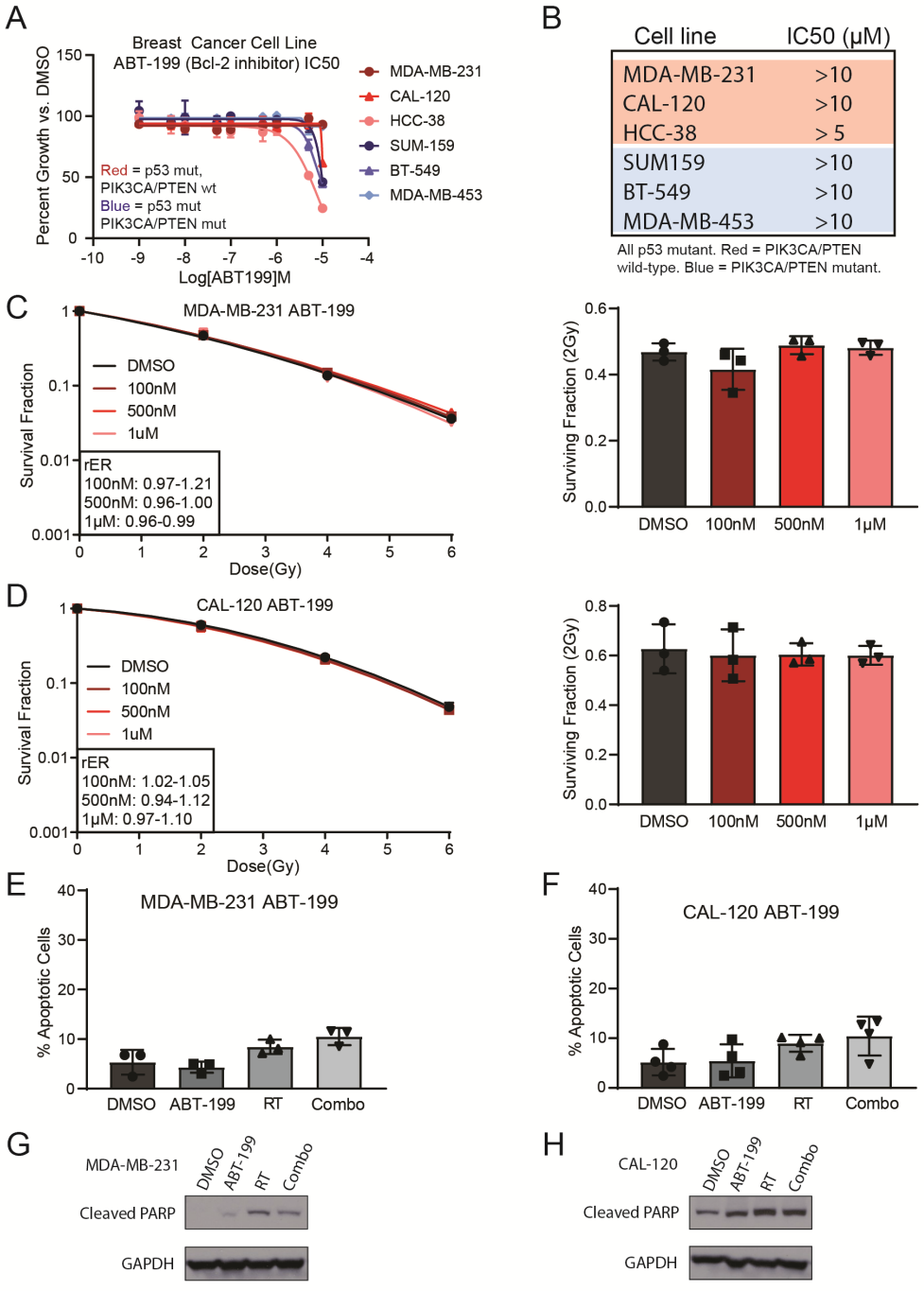

Figure 3.7: Bcl-2 inhibition does not radiosensitize p53 mutant, PIK3CA/PTEN wild-type basal-like breast cancer cell lines. A) ABT-199 (Bcl-2 inhibitor) IC50 of proliferation in multiple basal-like breast cancer cell lines. B) Summary of ABT-199 IC50 values. C&D) ABT-199 does not radiosensitize the p53

mutant, PIK3CA/PTEN wild-type cell lines MDA-MB-231 (C) and CAL-120 (D). E&F) Combination of Bcl-2 inhibition and RT does not increase the percentage of apoptotic cells compared to RT alone. G&H) Combination of Bcl-2 inhibition (ABT-199) and RT does not increase cleaved PARP compared to RT alone. Cells were pretreated with ABT-199 for 1-hour before RT (4 Gy) and harvested either 48-hours after drug or 48-hours after RT. One-way ANOVA with Dunnett's multiple comparisons test and a two-sided Student's t-test were used for analyses.

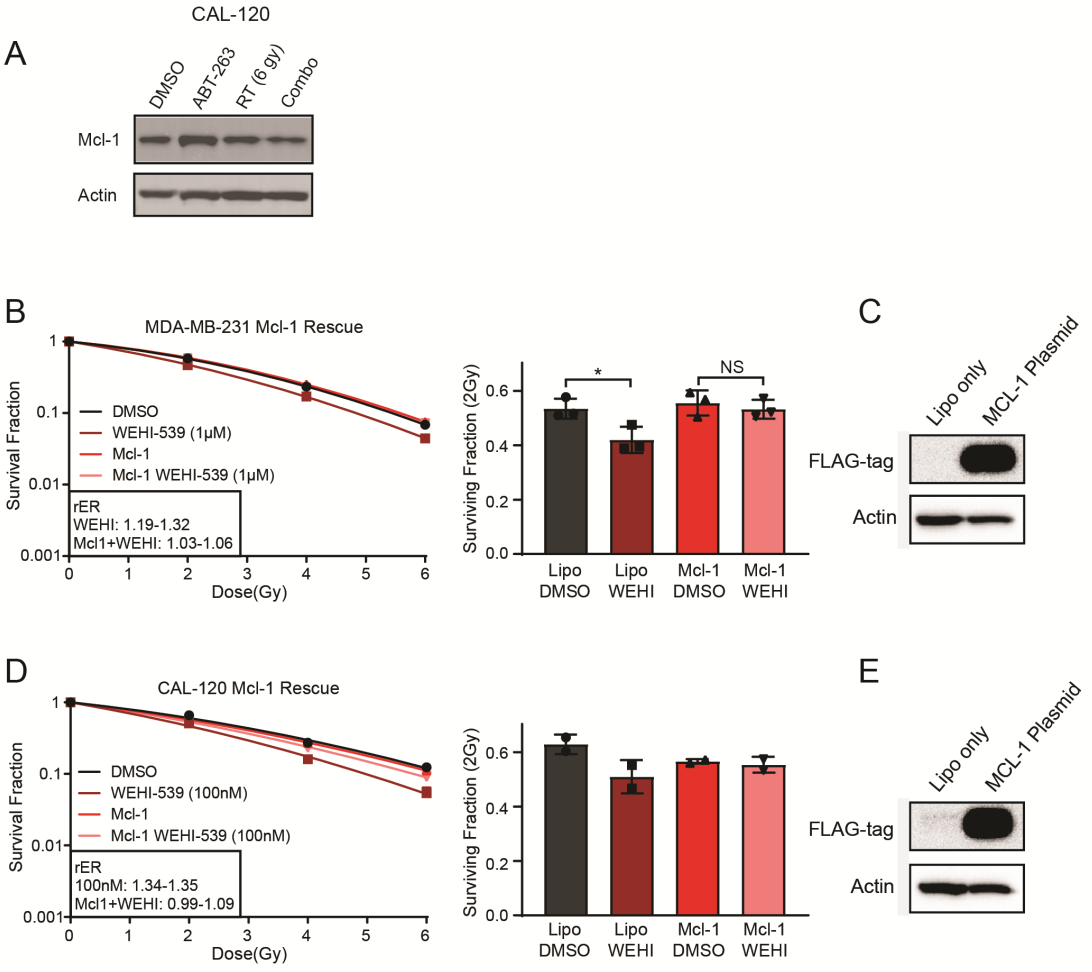

Figure 3.8: Overexpression of Mcl-1 rescues resistance to Bcl-xL inhibition induced radiosensitization in p53 mutant, PIK3CA/PTEN wild-type basal-like breast cancer cell lines. A) Bcl-2 family inhibition (ABT-263 [1μM]) leads to increased Mcl-1 protein after 24 hours. However, RT (6 Gy) reduces Mcl-1 expression after Bcl-2 family inhibition in the CAL-120 cell line. B&D) Overexpression of Mcl-1 rescues resistance to Bcl-xL inhibition in the p53 mutant, PIK3CA/PTEN wild-type cell lines MDA-MB-231 (B) and CAL-120 (D). C&E) Western blot depicting overexpression of Flag-tagged Mcl-1 in MDA-MB-231 (C) and CAL-120 (E) cell lines. Two-sided Student's t-test were used for analyses. *p<0.05

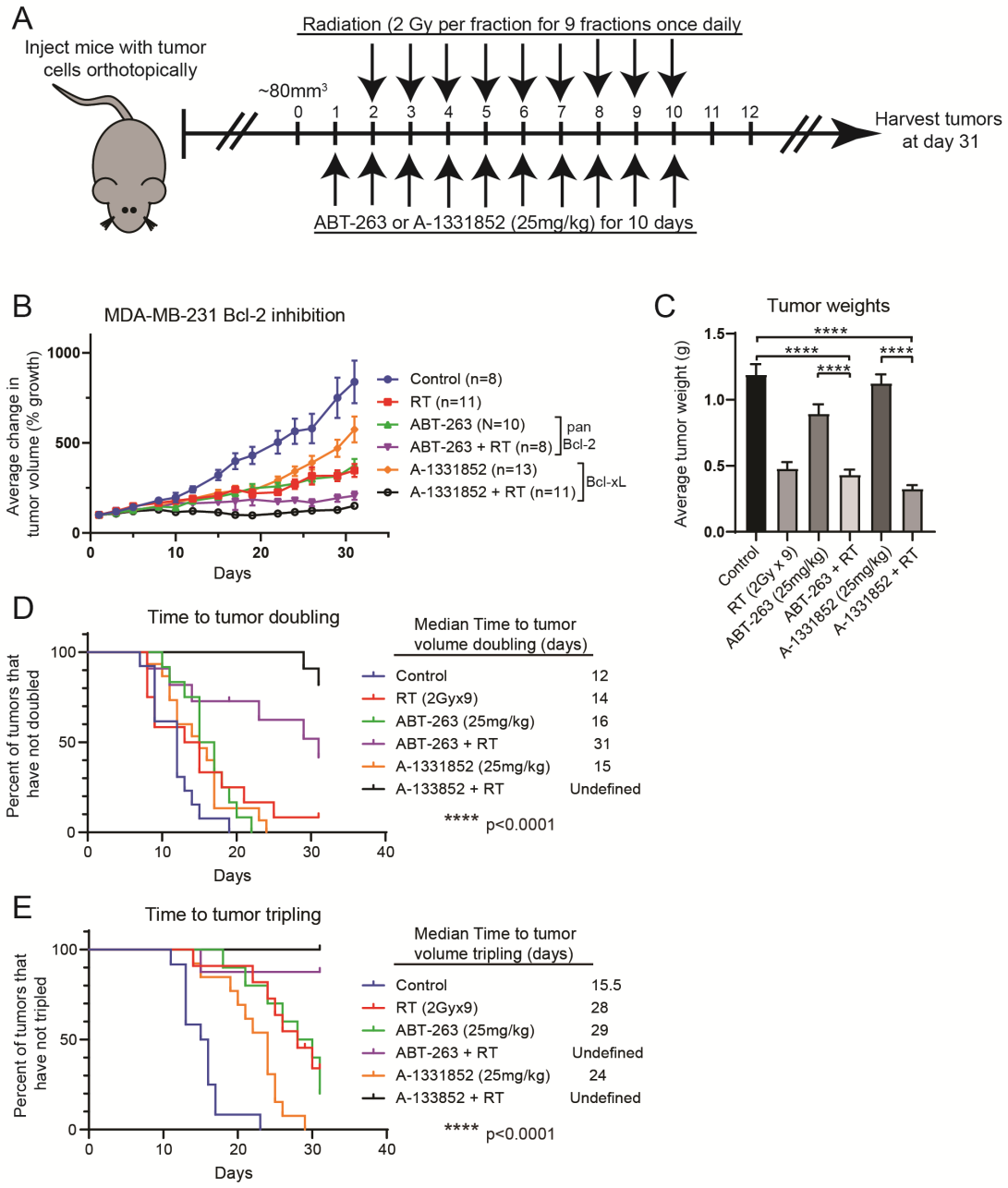

Figure 3.9: In an orthotopic in vivo model, inhibition of Bcl-xL in combination with radiation (RT) significantly radiosensitizes MDA-MB-231 cell. A) Outline of in vivo drug and radiation dosing B) Combination treatment of ABT-263 (pan Bcl-2 family inhibitor) or A-1331852 (Bcl-xL inhibitor) significantly delays tumor growth compared to RT or drug alone. C) Combination of ABT-263 or A-1331852 with RT significantly reduces tumor size. D&E) Combination of either ABT-263 or A-1331852 with RT significantly delays time to tumor doubling (D) or tripling (E) in p53 mutant, PIK3CA/PTEN wild-

type cell line MDA-MB-231. One-way ANOVA with Tukey's multiple comparisons test and Log-rank (Mantel-Cox) test were used for analyses. ****p<0.0001

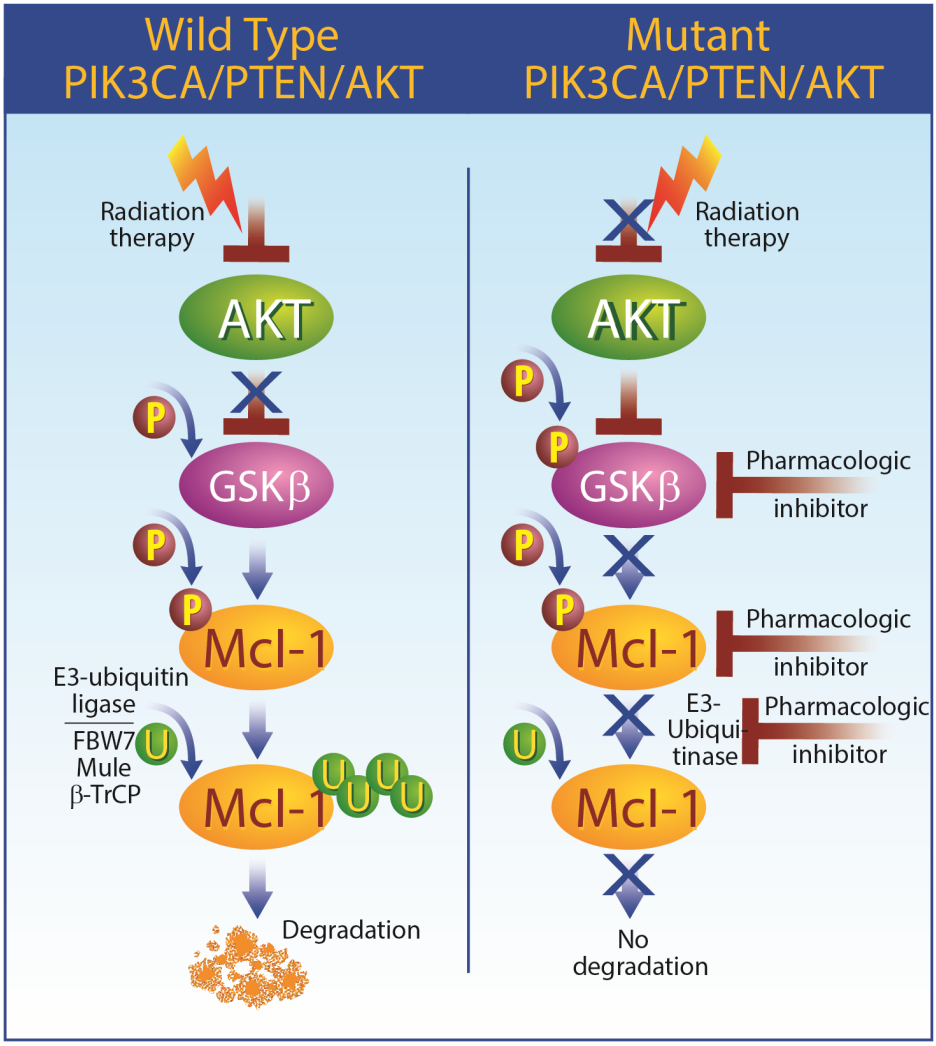

Figure 3.10: Hypothesis for Mcl-1 degradation in PIK3CA/PTEN wild-type and mutant settings. In p53 mutant, PIK3CA/PTEN wild-type basal-like breast cancer cell lines radiation therapy (RT) inhibits AKT related signaling, which decreases AKT phosphorylation of GSK-3β thus stabilizing GSK-3β. GSK-3β phosphorylates Mcl-1 signaling for its proteasome mediated degradation. In a PIK3CA/PTEN mutant setting RT does not decrease AKT related signaling due to activation mutations. This leads to inhibition of GSK-3β through phosphorylation and stabilization of Mcl-1, thus reducing apoptosis.

References

1. Early Breast Cancer Trialists' Collaborative G, Darby S, McGale P, Correa C, Taylor C, Arriagada R, Clarke M, Cutter D, Davies C, Ewertz M, et al. Effect of radiotherapy after breast-conserving surgery on 10-year recurrence and 15-year breast cancer death: meta-analysis of individual patient data for 10,801 women in 17 randomised trials. *Lancet.* 2011;378(9804):1707-16.
2. Sjöström M, Lundstedt D, Hartman L, Holmberg E, Killander F, Kovács A, Malmström P, Niméus E, Werner Rönnerman E, Fernö M, et al. Response to Radiotherapy After Breast-Conserving Surgery in Different Breast Cancer Subtypes in the Swedish Breast Cancer Group 91 Radiotherapy Randomized Clinical Trial. *Journal of Clinical Oncology.* 2017;35(28):3222-9.
3. Kyndi M, Sørensen FB, Knudsen H, Overgaard M, Nielsen HM, and Overgaard J. Estrogen Receptor, Progesterone Receptor, HER-2, and Response to Postmastectomy Radiotherapy in High-Risk Breast Cancer: The Danish Breast Cancer Cooperative Group. *Journal of Clinical Oncology.* 2008;26(9):1419-26.
4. Arvold ND, Taghian AG, Niemierko A, Abi Raad RF, Sreedhara M, Nguyen PL, Bellon JR, Wong JS, Smith BL, and Harris JR. Age, breast cancer subtype approximation, and local recurrence after breast-conserving therapy. *J Clin Oncol.* 2011;29(29):3885-91.
5. Horton JK, Siamakpour-Reihani S, Lee C-T, Zhou Y, Chen W, Geradts J, Fels DR, Hoang P, Ashcraft KA, Groth J, et al. FAS Death Receptor: A Breast Cancer Subtype-Specific Radiation Response Biomarker and Potential Therapeutic Target. *Radiat Res.* 2015;184(5):456-69.
6. Pauwels B, Korst AEC, Lardon F, and Vermorken JB. Combined Modality Therapy of Gemcitabine and Radiation. *The Oncologist.* 2005;10(1):34-51.
7. de Haan R, van Werkhoven E, van den Heuvel MM, Peulen HMU, Sonke GS, Elkhuizen P, van den Brekel MWM, Tesselaar MET, Vens C, Schellens JHM, et al. Study protocols of three parallel phase 1 trials combining radical radiotherapy with the PARP inhibitor olaparib. *BMC Cancer.* 2019;19(1):901.
8. Jagsi R, Griffith KA, Bellon JR, Woodward WA, Horton JK, Ho A, Feng FY, Speers C, Overmoyer B, Sabel M, et al. Concurrent Veliparib With Chest Wall and Nodal Radiotherapy in Patients With Inflammatory or Locoregionally Recurrent Breast Cancer: The TBCRC 024 Phase I Multicenter Study. *J Clin Oncol.* 2018;36(13):1317-22.

9. Ellis HM, and Horvitz HR. Genetic control of programmed cell death in the nematode C. elegans. *Cell.* 1986;44(6):817-29.
10. Oltval ZN, Milliman CL, and Korsmeyer SJ. Bcl-2 heterodimerizes in vivo with a conserved homolog, Bax, that accelerates programed cell death. *Cell.* 1993;74(4):609-19.
11. Kozopas KM, Yang T, Buchan HL, Zhou P, and Craig RW. MCL1, a gene expressed in programmed myeloid cell differentiation, has sequence similarity to BCL2. *Proceedings of the National Academy of Sciences.* 1993;90(8):3516.
12. O'Connor L, Strasser A, O'Reilly LA, Hausmann G, Adams JM, Cory S, and Huang DC. Bim: a novel member of the Bcl-2 family that promotes apoptosis. *EMBO J.* 1998;17(2):384-95.
13. Vogler M. BCL2A1: the underdog in the BCL2 family. *Cell Death & Differentiation.* 2012;19(1):67-74.
14. Montero J, and Letai A. Why do BCL-2 inhibitors work and where should we use them in the clinic? *Cell Death & Differentiation.* 2018;25(1):56-64.
15. Youle RJ, and Strasser A. The BCL-2 protein family: opposing activities that mediate cell death. *Nature Reviews Molecular Cell Biology.* 2008;9(1):47-59.
16. Yang J, Liu X, Bhalla K, Kim CN, Ibrado AM, Cai J, Peng T-I, Jones DP, and Wang X. Prevention of Apoptosis by Bcl-2: Release of Cytochrome c from Mitochondria Blocked. *Science.* 1997;275(5303):1129.
17. Kluck RM, Bossy-Wetzel E, Green DR, and Newmeyer DD. The Release of Cytochrome c from Mitochondria: A Primary Site for Bcl-2 Regulation of Apoptosis. *Science.* 1997;275(5303):1132.
18. Chipuk JE, and Green DR. Dissecting p53-dependent apoptosis. *Cell Death & Differentiation.* 2006;13(6):994-1002.
19. Lanni JS, Lowe SW, Licitra EJ, Liu JO, and Jacks T. p53-independent apoptosis induced by paclitaxel through an indirect mechanism. *Proceedings of the National Academy of Sciences.* 1997;94(18):9679-83.
20. Wei MC, Lindsten T, Mootha VK, Weiler S, Gross A, Ashiya M, Thompson CB, and Korsmeyer SJ. tBID, a membrane-targeted death ligand, oligomerizes BAK to release cytochrome c. *Genes Dev.* 2000;14(16):2060-71.
21. Gross A, Jockel J, Wei MC, and Korsmeyer SJ. Enforced dimerization of BAX results in its translocation, mitochondrial dysfunction and apoptosis. *EMBO J.* 1998;17(14):3878-85.
22. Souers AJ, Leverson JD, Boghaert ER, Ackler SL, Catron ND, Chen J, Dayton BD, Ding H, Enschede SH, Fairbrother WJ, et al. ABT-199, a potent and selective BCL-2 inhibitor, achieves antitumor activity while sparing platelets. *Nature Medicine.* 2013;19(2):202-8.
23. Oltersdorf T, Elmore SW, Shoemaker AR, Armstrong RC, Augeri DJ, Belli BA, Bruncko M, Deckwerth TL, Dinges J, Hajduk PJ, et al. An inhibitor of Bcl-2 family proteins induces regression of solid tumours. *Nature.* 2005;435(7042):677-81.
24. Park C-M, Bruncko M, Adickes J, Bauch J, Ding H, Kunzer A, Marsh KC, Nimmer P, Shoemaker AR, Song X, et al. Discovery of an Orally Bioavailable Small Molecule Inhibitor of Prosurvival B-Cell Lymphoma 2 Proteins. *Journal of Medicinal Chemistry.* 2008;51(21):6902-15.
25. Wilson WH, O'Connor OA, Czuczman MS, LaCasce AS, Gerecitano JF, Leonard JP, Tulpule A, Dunleavy K, Xiong H, Chiu Y-L, et al. Navitoclax, a targeted high-affinity inhibitor of BCL-2, in lymphoid malignancies: a phase 1 dose-escalation study of safety, pharmacokinetics, pharmacodynamics, and antitumour activity. *The Lancet Oncology.* 2010;11(12):1149-59.

26. Gandhi L, Camidge DR, Ribeiro de Oliveira M, Bonomi P, Gandara D, Khaira D, Hann CL, McKeegan EM, Litvinovich E, Hemken PM, et al. Phase I Study of Navitoclax (ABT-263), a Novel Bcl-2 Family Inhibitor, in Patients With Small-Cell Lung Cancer and Other Solid Tumors. *Journal of Clinical Oncology.* 2011;29(7):909-16.
27. Merino D, Whittle JR, Vaillant F, Serrano A, Gong J-N, Giner G, Maragno AL, Chanrion M, Schneider E, Pal B, et al. Synergistic action of the MCL-1 inhibitor S63845 with current therapies in preclinical models of triple-negative and HER2-amplified breast cancer. *Science Translational Medicine.* 2017;9(401):eaam7049.
28. Anderson GR, Wardell SE, Cakir M, Crawford L, Leeds JC, Nussbaum DP, Shankar PS, Soderquist RS, Stein EM, Tingley JP, et al. PIK3CA mutations enable targeting of a breast tumor dependency through mTOR-mediated MCL-1 translation. *Science translational medicine.* 2016;8(369):369ra175-369ra175.
29. Oakes SR, Vaillant F, Lim E, Lee L, Breslin K, Feleppa F, Deb S, Ritchie ME, Takano E, Ward T, et al. Sensitization of BCL-2–expressing breast tumors to chemotherapy by the BH3 mimetic ABT-737. *Proceedings of the National Academy of Sciences.* 2012;109(8):2766.
30. Vaillant F, Merino D, Lee L, Breslin K, Pal B, Ritchie Matthew E, Smyth Gordon K, Christie M, Phillipson Louisa J, Burns Christopher J, et al. Targeting BCL-2 with the BH3 Mimetic ABT-199 in Estrogen Receptor-Positive Breast Cancer. *Cancer Cell.* 2013;24(1):120-9.
31. Wu H, Schiff DS, Lin Y, Neboori HJR, Goyal S, Feng Z, and Haffty BG. Ionizing radiation sensitizes breast cancer cells to Bcl-2 inhibitor, ABT-737, through regulating Mcl-1. *Radiat Res.* 2014;182(6):618-25.
32. Tse C, Shoemaker AR, Adickes J, Anderson MG, Chen J, Jin S, Johnson EF, Marsh KC, Mitten MJ, Nimmer P, et al. ABT-263: A Potent and Orally Bioavailable Bcl-2 Family Inhibitor. *Cancer Research.* 2008;68(9):3421.
33. Boulares AH, Yakovlev AG, Ivanova V, Stoica BA, Wang G, Iyer S, and Smulson M. Role of Poly(ADP-ribose) Polymerase (PARP) Cleavage in Apoptosis: CASPASE 3-RESISTANT PARP MUTANT INCREASES RATES OF APOPTOSIS IN TRANSFECTED CELLS. *Journal of Biological Chemistry.* 1999;274(33):22932-40.
34. Lessene G, Czabotar PE, Sleebs BE, Zobel K, Lowes KN, Adams JM, Baell JB, Colman PM, Deshayes K, Fairbrother WJ, et al. Structure-guided design of a selective BCL-XL inhibitor. *Nature Chemical Biology.* 2013;9(6):390-7.
35. Leverson JD, Phillips DC, Mitten MJ, Boghaert ER, Diaz D, Tahir SK, Belmont LD, Nimmer P, Xiao Y, Ma XM, et al. Exploiting selective BCL-2 family inhibitors to dissect cell survival dependencies and define improved strategies for cancer therapy. *Science Translational Medicine.* 2015;7(279):279ra40.
36. Lee EF, Harris TJ, Tran S, Evangelista M, Arulananda S, John T, Ramnac C, Hobbs C, Zhu H, Gunasingh G, et al. BCL-XL and MCL-1 are the key BCL-2 family proteins in melanoma cell survival. *Cell Death & Disease.* 2019;10(5):342.
37. Weeden CE, Ah-Cann C, Holik AZ, Pasquet J, Garnier J-M, Merino D, Lessene G, and Asselin-Labat M-L. Dual inhibition of BCL-XL and MCL-1 is required to induce tumour regression in lung squamous cell carcinomas sensitive to FGFR inhibition. *Oncogene.* 2018;37(32):4475-88.
38. Robinson TJW, Liu JC, Vizeacoumar F, Sun T, Maclean N, Egan SE, Schimmer AD, Datti A, and Zacksenhaus E. RB1 status in triple negative breast cancer cells dictates response to radiation treatment and selective therapeutic drugs. *PLoS One.* 2013;8(11):e78641-e.

39. Jeong Y, Hoang NT, Lovejoy A, Stehr H, Newman AM, Gentles AJ, Kong W, Truong D, Martin S, Chaudhuri A, et al. Role of KEAP1/NRF2 and TP53 Mutations in Lung Squamous Cell Carcinoma Development and Radiation Resistance. *Cancer Discovery.* 2016:CD-16-0127.
40. Saki M, Makino H, Javvadi P, Tomimatsu N, Ding L-H, Clark JE, Gavin E, Takeda K, Andrews J, Saha D, et al. EGFR Mutations Compromise Hypoxia-Associated Radiation Resistance through Impaired Replication Fork-Associated DNA Damage Repair. *Mol Cancer Res.* 2017;15(11):1503-16.
41. Anakura M, Nachankar A, Kobayashi D, Amornwichet N, Hirota Y, Shibata A, Oike T, and Nakano T. Radiosensitivity Differences between EGFR Mutant and Wild-Type Lung Cancer Cells are Larger at Lower Doses. *Int J Mol Sci.* 2019;20(15):3635.
42. Fu XY, Zhang SW, Ran RQ, Shen ZH, Gu JX, and Cao SL. Restoration of the p16 gene is related to increased radiosensitivity of p16-deficient lung adenocarcinoma cell lines. *Journal of Cancer Research and Clinical Oncology.* 1998;124(11):621-6.
43. Kastenhuber ER, and Lowe SW. Putting p53 in Context. *Cell.* 2017;170(6):1062-78.
44. Dittmer D, Pati S, Zambetti G, Chu S, Teresky AK, Moore M, Finlay C, and Levine AJ. Gain of function mutations in p53. *Nature Genetics.* 1993;4(1):42-6.
45. Chène P. In vitro analysis of the dominant negative effect of p53 mutants11Edited by A. R. Fersht. *Journal of Molecular Biology.* 1998;281(2):205-9.
46. Sigal A, and Rotter V. Oncogenic Mutations of the p53 Tumor Suppressor: The Demons of the Guardian of the Genome. *Cancer Research.* 2000;60(24):6788.
47. Liu DP, Song H, and Xu Y. A common gain of function of p53 cancer mutants in inducing genetic instability. *Oncogene.* 2010;29(7):949-56.
48. Momand J, Zambetti GP, Olson DC, George D, and Levine AJ. The mdm-2 oncogene product forms a complex with the p53 protein and inhibits p53-mediated transactivation. *Cell.* 1992;69(7):1237-45.
49. Patterson H, Barnes D, Gill S, Spicer J, Fisher C, Thomas M, Grimer R, Fletcher C, Gusterson B, and Cooper C. Amplification and Over-Expression of the MDM2 Gene in Human Soft Tissue Tumours. *Sarcoma.* 1997;1(1):17-22.
50. Hou H, Sun D, and Zhang X. The role of MDM2 amplification and overexpression in therapeutic resistance of malignant tumors. *Cancer Cell International.* 2019;19(1):216.
51. Miller LD, Smeds J, George J, Vega VB, Vergara L, Ploner A, Pawitan Y, Hall P, Klaar S, Liu ET, et al. An expression signature for p53 status in human breast cancer predicts mutation status, transcriptional effects, and patient survival. *Proc Natl Acad Sci U S A.* 2005;102(38):13550-5.
52. Kline MP, Rajkumar SV, Timm MM, Kimlinger TK, Haug JL, Lust JA, Greipp PR, and Kumar S. ABT-737, an inhibitor of Bcl-2 family proteins, is a potent inducer of apoptosis in multiple myeloma cells. *Leukemia.* 2007;21(7):1549-60.
53. Zhang S, Zhang M, Jing Y, Yin X, Ma P, Zhang Z, Wang X, Di W, and Zhuang G. Deubiquitinase USP13 dictates MCL1 stability and sensitivity to BH3 mimetic inhibitors. *Nat Commun.* 2018;9(1):215-.
54. Schwickart M, Huang X, Lill JR, Liu J, Ferrando R, French DM, Maecker H, O'Rourke K, Bazan F, Eastham-Anderson J, et al. Deubiquitinase USP9X stabilizes MCL1 and promotes tumour cell survival. *Nature.* 2010;463(7277):103-7.
55. Zhong Q, Gao W, Du F, and Wang X. Mule/ARF-BP1, a BH3-Only E3 Ubiquitin Ligase, Catalyzes the Polyubiquitination of Mcl-1 and Regulates Apoptosis. *Cell.* 2005;121(7):1085-95.

56. Gasca J, Flores ML, Giráldez S, Ruiz-Borrego M, Tortolero M, Romero F, Japón MA, and Sáez C. Loss of FBXW7 and accumulation of MCL1 and PLK1 promote paclitaxel resistance in breast cancer. *Oncotarget.* 2016;7(33):52751-65.
57. Lu C, Speers C, Zhang Y, Xu X, Hill J, Steinbis E, Celestino J, Shen Q, Kim H, Hilsenbeck S, et al. Effect of epidermal growth factor receptor inhibitor on development of estrogen receptor-negative mammary tumors. *J Natl Cancer Inst.* 2003;95(24):1825-33.
58. Gill S, Loprinzi C, Kennecke H, Grothey A, Nelson G, Woods R, Speers C, Alberts SR, Bardia A, O'Connell MJ, et al. Prognostic web-based models for stage II and III colon cancer: A population and clinical trials-based validation of numeracy and adjuvant! online. *Cancer.* 2011;117(18):4155-65.
59. Yokoyama Y, Dhanabal M, Griffioen AW, Sukhatme VP, and Ramakrishnan S. Synergy between Angiostatin and Endostatin: Inhibition of Ovarian Cancer Growth. *Cancer Research.* 2000;60(8):2190.
60. Matar P, Rojo F, Cassia R, Moreno-Bueno G, Di Cosimo S, Tabernero J, Guzmán M, Rodriguez S, Arribas J, Palacios J, et al. Combined Epidermal Growth Factor Receptor Targeting with the Tyrosine Kinase Inhibitor Gefitinib (ZD1839) and the Monoclonal Antibody Cetuximab (IMC-C225). *Clinical Cancer Research.* 2004;10(6487-501.

Chapter 4

TTK Inhibition Radiosensitizes Basal-like Breast Cancer through Impaired Homologous Recombination

Summary

Increased rates of locoregional recurrence are observed in patients with basal-like breast cancer (BC) despite the use of radiation therapy (RT); therefore, approaches that result in radiosensitization of basal-like BC are critically needed. Using patient tumor gene expression data from four independent datasets, we correlated gene expression with recurrence to find genes significantly correlated with early recurrence after RT. The highest ranked gene, TTK, was most highly expressed in basal-like BC across multiple datasets. Inhibition of TTK, using both genetic and pharmacologic methods, enhanced radiosensitivity in multiple basal-like cell lines. Radiosensitivity was mediated, at least in part, through persistent DNA damage after treatment with TTK inhibition and RT. Inhibition of TTK impaired homologous recombination (HR), but not non-homologous end joining, repair efficiency and decreased Rad51 foci formation. Re-introduction of wild-type TTK rescued both radioresistance and HR repair efficiency after TTK knockdown, however, re-introduction of kinase-dead TTK did not. *In vivo*, TTK inhibition combined with RT, led to a significant decrease in tumor growth in both heterotopic and orthotopic, including patient derived xenograft, BC models. These data support the rationale for clinical development of TTK inhibition as a radiosensitizing strategy for basal-like BC patients and these efforts are currently underway.

Introduction

Breast cancer (BC) is the most commonly diagnosed invasive cancer for women in the United States and the second leading cause of cancer related deaths (1). Radiation therapy (RT) remains a mainstay therapy for BC patients and has been shown to not only reduce local recurrence, but improve overall survival for BC patients (2). While RT is effective for many BC patients, a significant proportion of patients, especially those with basal-like BC, continue to have high rates of local recurrence and poor overall survival, suggesting RT is not as effective in those patient populations (3-7).

While effective targeted treatment options are available for estrogen receptor-positive (ER+) and HER2-positive (Her2+) BCs, fewer targeted treatment options exist for women with basal-like BCs. Recent advancements in BC subtyping have allowed for more advanced clinical risk stratification and treatment recommendations for patients; however, recommendations for radiation dose and treatment scheduling remain similar for all BC subtypes (8, 9). In an era of precision medicine and molecularly targeted therapy, understanding the molecular drivers of radiation resistance in basal-like BC remains a critical unmet clinical need.

To that end, previous studies have attempted to identify and characterize targets for the radiosensitization of BC, including basal-like BC. These studies have identified cell cycle and DNA damage response proteins that may be implicated in RT resistance (10). As expected, targeting DNA damage response related proteins is a promising strategy for radiosensitization (11).

Recently, cell cycle proteins have also been shown as possible radiosensitization targets, often through modulating the effectiveness of DNA damage repair genes (12, 13). To date, however, few therapies targeting these proteins have been clinically implemented owing, in part, to the dose limiting toxicities and off-target effects of these agents.

Here we sought to identify novel radiosensitizing targets in aggressive basal-like BC. In this study, we use clinical datasets to correlate gene expression to recurrence-free survival after radiation in women with BC and nominate TTK as a potential mediator of radioresistance in aggressive subtypes of BC. Using clinical and preclinical data we demonstrate that TTK is overexpressed in locally recurrent and basal-like BC. Preclinical studies show that inhibition of TTK, both genetically and pharmacologically, leads to increased radiosensitivity of basal-like BC cell line and PDX models. Radiosensitization is kinase function dependent and mediated, at least in part, through impaired homologous recombination repair efficiency. Finally, we validate TTK inhibition mediated radiosensitivity *in vivo* using a clinical grade pharmacologic inhibitor.

Results

TTK is the top gene correlated to recurrence after radiation in breast cancer across four independent datasets

In an effort to identify genes that play a role in radioresistance and thus increase rates of local recurrence (LR) in BC, we correlated gene expression to early (defined as 3 years or earlier) recurrence, including LR, across four independent datasets that included women treated with

radiation as per standard of care. We restricted our results to genes with an odds ratio of greater than or equal to 2.0 and multiple-testing corrected p-value < 1.0 x 10e-6. Within these constraints, ten genes were found to significantly correlate with early recurrence across all four breast cancer datasets **(Figure 4.1A)**. These genes were ranked based on their average differential log2 fold change across all four datasets, between patients with early (≤3 years) recurrence and those who did not have evidence of recurrence at 3 years. This nomination identified TTK, also known as Monopolar spindle 1 (Mps1), as the top ranked gene with an average log2 fold change of 1.73 across the four independent datasets. To further refine our nomination, we focused on genes with a clinical grade inhibitor currently in development. TTK was one of only three genes found to currently have a pharmacological agent in clinical trial according to clinicaltrials.gov **(Table 1)**. To confirm our findings, we performed Kaplan-Meier analyses in two independent datasets (Servant and Vande Vijver), as well as with one of the original four datasets (Wang).These datasets all had more carefully annotated local recurrence-specific information and included women treated with RT. In all three datasets, TTK expression above the median correlated to decreased local recurrence-free survival (LRFS) **(Figure 4.1B-D**; Servant: HR=1.70 p-value=0.004, Vande Vijver: HR=2.42 p-value=0.005, Wang: HR=2.23 p-value<0.0001). Furthermore, when divided into quartile expression, TTK expression is associated with a stepwise decrease in LRFS in these datasets **(Figure 4.2A-C)**. Univariate analysis shows TTK expression is significantly correlated with LRFS in all three datasets **(Table 2)**. In multivariate analysis (MVA), using a stepwise logistic regression model, TTK remained the strongest predictor of LR (HR 1.29-11.29) independent of all other clinicopathologic features **(Table 2)**.

We then evaluated TTK expression in multiple independent datasets to see if it was associated with any intrinsic subtype of BC. In each dataset evaluated, TTK expression is significantly elevated in patients with estrogen receptor-negative (ER-) tumors compared to patients with estrogen receptor-positive (ER+) tumors **(Figure 4.2D-F**; p-value<0.001). Moreover, using the METABRIC dataset (14) (n=1,986 patients) to evaluate TTK expression by breast cancer intrinsic subtype we found TTK expression was highest in the basal-like subtype and is significantly overexpressed in BC versus normal tissue (p-value<0.0001, **Figure 4.1E)**. Furthermore, in an institutionally assembled dataset of BC metastatic tumors (MET500 patients (15)), we found that TTK is significantly overexpressed in basal-like BC compared to other subtypes **(Figure 4.1F)**. This association was also seen in the TCGA BC dataset (n=945 patients) **(Figure 4.2G)**. Using RNA sequencing data of BC cell lines from the Cancer Cell Line Encyclopedia (CCLE), we found TTK is overexpressed in ER- BC cell lines compared to ER+ BC cell lines, and is more highly expressed in basal-like cell lines compared to Her2+ or luminal cell lines **(Figure 4.2H&I**; p-value<0.001). TTK protein expression was measured in a panel of BC cell lines confirming higher expression of TTK protein in basal-like BC cell lines, with MDA-MB-231 and BT-549 having the highest TTK protein expression **(Figure 4.2J&K)**. Finally, we compiled the mutational landscapes of cell lines used for further studies **(Figure 4.2L)** (16).

TTK inhibition radiosensitizes basal-like breast cancer cell lines

The correlation between TTK and early recurrence suggests TTK may be involved in the RT response of BC. To further examine this, we performed Gene Set Enrichment Analysis

(GSEA). Here, TTK expression was correlated with the expression of all other genes in the TCGA dataset and rank ordered by correlation coefficient. That gene list was then inputted into GSEA to identify pathways and networks associated with TTK expression. We found cell cycle genes in ionizing radiation (IR) response at 6 and 24 hours were significantly enriched concepts at the top of the list (Enrichment Score > 3.5 and p-value < 0.00001) **(Figure 4.4A)**. Negatively correlated concepts were related to ER+ and luminal BC, further validating our original nomination of TTK as being associated with basal-like BC **(Figure 4.4B)**. Together these results indicate that TTK may be involved in the radiation response of BC and may function as a mediator of radiosensitivity.

To measure the effect of TTK perturbation on radiosensitivity *in vitro*, we used previously characterized radioresistant BC cell lines with high TTK expression (MDA-MB-231 and BT-549) **(Figure 4.2J&K)** (17). We performed clonogenic survival assays on stable, basal-like BC cell lines, expressing doxycycline (dox) inducible shRNA, for TTK knockdown. Dox-induced TTK knockdown increased radiosensitivity in multiple shTTK stable clones in both MDA-MB-231 **(Figure 4.3A**, rER: shTTK#1 1.42-1.63, shTTK#2 1.21-1.25) and BT-549 **(Figure 4.3C**, rER: shTTK#1 1.21-1.25, shTTK#2 1.21-1.26) cell lines.). We also observed a significant decrease in the percent of surviving cells after 2 Gy radiation (SF-2 Gy) in shTTK dox+ compared to shTTK dox-. Knockdown of TTK protein was confirmed with varying degrees of cytotoxicity in both cell lines **(Figure 4.3B&D, and Figure 4.4C&D)**. Additionally, dox treatment had no effect on radiosensitivity in shControl stable MDA-MB-231 and BT-549 cell lines **(Figure 4.3A-D)**.

To confirm that TTK kinase function, and not just protein structural or scaffolding function, is important in mediating the response to RT in basal-like BC models, we performed clonogenic

assays with the ATP-competitive TTK inhibitor, Bayer 1161909 - Empesertib (hereafter referred to as B909), currently in clinical development (18). This drug was chosen as it is currently the only TTK-inhibitor in phase I/II clinical trials and because the target specificity, pharmacodynamics, and pharmacokinetics have already been well established (18). Drug doses used for radiosensitization studies were approximately half of the IC50 of proliferation in order to evaluate radiosensitization, and not single agent antiproliferative effects **(Figure 4.4E-G)**. TTK inhibition was confirmed using western blot analysis of phospho-Histone 3 (Ser10), a reported marker of functional TTK **(Figure 4.4H&I)** (19). As with TTK knockdown, we observed a dose-dependent increase in radiosensitization in MDA-MB-231 (rER: 1.15-1.39), BT-549 (rER: 1.10-1.39), and SUM159 (rER: 1.11-2.27) cell lines treated with B909 **(Figure 4.3E-G)**. A dose-dependent decrease in SF-2 Gy was also observed in all cell lines and B909 caused varying degrees of cytotoxicity in both cell lines **(Figure 4.4K-M)**. However, combination treatment of B909 and RT did not significantly decrease growth compared to B909 alone **(Figure 4.4J)**.

As a final, independent confirmation of radiosensitization, clonogenic survival assays were performed using an additional TTK inhibitor, NMS-P715 (19). TTK inhibition with NMS-P715 also increased radiosensitivity and significantly decreased the SF-2 Gy, further indicating TTK kinase function is important for radioresistance **(Figure 4.4N)**. Cytotoxicity and rER with NMS-P715 are summarized in **Figure 4.4O**.

TTK inhibition leads to persistent DNA damage after radiation

While radiosensitization can be induced through a number of mechanisms, we hypothesized TTK-mediated radiosensitization may be due, in part, to decreased double-strand DNA (dsDNA) damage repair efficiency. To evaluate the effect of TTK inhibition on dsDNA break repair, we measured γH2AX foci (greater than 15 foci per cell), a marker for unresolved dsDNA damage, in cells treated with TTK inhibition, RT, or combination treatment over time (20). Using the MDA-MB-231 shTTK and BT-549 shTTK models, we measured γH2AX foci at various time points after treatment with DMSO, dox (2μg/mL) alone, RT (2 Gy) alone, or a combination of dox and RT. 30 minutes after RT there were equivalent levels of γH2AX positive cells in RT alone and combination treated cells (~70% in MDA-MB-231 shTTK and ~80% in BT-549 shTTK), while the non-irradiated cells had few γH2AX positive cells. Over time, the cells treated with RT alone repaired the RT-induced dsDNA damage more efficiently than the combination treated group at 4, 16, and 24 hours in MDA-MB-231 shTTK cells **(Figure 4.5A)** and at 4, 12, and 16 hours in BT-549 shTTK cells **(Figure 4.5B)**, suggesting TTK knockdown delayed dsDNA break repair efficiency. Representative images of γH2AX are shown 24 hours after RT in MDA-MB-231 shTTK cells **(Figure 4.6A)** and 16 hours after RT in BT-549 shTTK cells **(Figure 4.5C)**.

To assess the contribution of TTK kinase function in dsDNA break repair, unresolved dsDNA damage was also measured after treatment with B909 (75nM) in MDA-MB-231 and BT-549 cell lines. Approximately 75% of cells treated with 2 Gy were positive for γH2AX foci 30 minutes after radiation **(Figure 4.5D&E)**. As seen in the shTTK cell lines, combination treatment of B909 and RT resulted in persistent γH2AX foci positive cells over time in MDA-MB-231 cells

(16 and 24 hours) **(Figure 4.5D)** and BT-549 (12 and 16 hours) **(Figure 4.5E)**. Representative images of γH2AX foci staining are shown 24 hours after RT in MDA-MB-231 **(Figure 4.5F)** and 16 hours after RT in BT-549 cells **(Figure 4.6B)**.

Finally, we assessed dsDNA break repair using a second inhibitor, NMS-P715, in MDA-MB-231 cells. As previously seen, TTK inhibition in combination with RT led to persistent γH2AX foci at 16 and 24 hours **(Figure 4.6C)**. Representative images of γH2AX foci at the 24 hour time point can be found in **Figure 4.6D**. These results indicate that TTK inhibition may lead to radiosensitization of basal-like BC cell lines, at least in part, due to impaired dsDNA damage repair.

TTK inhibition decreases homologous recombination mediated DNA damage repair

Homologous recombination (HR) and non-homologous end joining (NHEJ) are the two prominent mechanisms for dsDNA repair. Although either may be involved in dsDNA break repair, previous reports suggested a potential correlation between TTK expression and HR (21). To further investigate these possible mechanisms of radiosensitization we again performed GSEA by correlating gene expression with TTK expression. Here, we used the Kyoto Encyclopedia of Genes and Genomes (KEGG) to nominate cellular pathways related to TTK expression. In both the METABRIC and TCGA datasets HR was significantly correlated to TTK gene expression and was listed in the top eight positively correlated concepts **(Figure 4.7A&B)**. However, NHEJ was not significantly correlated to TTK expression in either dataset. Thus, we hypothesized that TTK-mediated radiosensitization and persistent unresolved dsDNA breaks are due, at least in part, to

decreased HR repair efficiency. Using stable cell lines, with a well-characterized and validated HR specific GFP reporter system, we tested the efficiency of HR after TTK knockdown (22-24). In both MDA-MB-231 and BT-549 cell lines, siRNA-mediated TTK knockdown significantly decreased HR efficiency compared to siNT **(Figure 4.7C&D)**. As controls, knockdown of Rad51, a key protein in the HR pathway, significantly decreased HR efficiency using this reporter system, while knockdown of XRCC6 (Ku70), a key protein in NHEJ, had no effect on HR efficiency **(Figure 4.7C&D)** (25). To evaluate the dependence of this TTK-mediated HR repair on TTK kinase function, we used pharmacological TTK inhibition, via B909 (50nM and 75nM). As with TTK knockdown, treatment with B909 significantly decreased HR efficiency in MDA-MB-231 and BT-549 cells **(Figure 4.7E&F)**. Chk1/2, critical proteins in the HR response, and DNAPK, which is required for effective NHEJ repair, served as model-system controls. As expected, pharmacologic inhibition of Chk1/2, by AZD7762 (150nM), an equipotent Chk1/2 inhibitor, decreased HR efficiency while the DNAPK inhibitor, NU7441 (1.5μM), which is not known to affect HR, had no effect on HR proficiency **(Figure 4.7E&F)** (26-28). All experiments were repeated in a second clone to reduce clone-specific effects and confirm TTK knockdown/inhibition decreases HR efficiency **(Figure 4.8A-D)**.

To further corroborate our findings that TTK knockdown and inhibition decreased HR proficiency, we performed Rad51 foci formation assays after RT (4 Gy) in MDA-MB-231 shTTK and BT-549 shTTK stable cell lines. Rad51 foci formation is a marker for active HR repair; therefore, inhibition of Rad51 foci formation is indicative of impaired HR proficiency (25). In both cell lines, combination treatment of dox (TTK knockdown) and RT resulted in a significant

decrease in Rad51 foci formation at both early and late time points (MDA-MB-231: 6 and 24 hours, BT-549: 4 and 16 hours) compared to RT alone. Few Rad51 foci were seen at either time point in cells treated with DMSO or dox alone **(Figure 4.7G&I)**. Representative images at 24 (MDA-MB-231) and 16 (BT-549) hours are shown and western blot analyses depict Rad51 protein expression is equal across all treatment groups, indicating that the decrease in Rad51 foci cannot be attributed to a more general decrease in Rad51 protein after TTK knockdown **(Figure 4.7H&J)**. These results indicate RT induces Rad51 foci formation, while TTK knockdown inhibits this formation, likely leading to decreased HR efficiency.

Finally, we treated BT-549 cell lines with B909 alone, RT alone, or a combination of B909 and RT and found a decrease in both phospho-BRCA1 and phospho-CHK1 after a combination of B909 and RT compared to RT alone **(Figure 4.8E)**. Decreased phosphorylation of BRCA1 and CHK1 are canonical markers of impaired HR efficiency. Additionally, combination treatment of B909 with RT decreases phospho-RPA, indicating disruption of the HR pathway and possibly the lack of Rad51 foci formation after TTK knockdown **(Figure 4.8F)** (29). This further indicates that TTK inhibition via B909 disrupts HR, likely leading to increased radiosensitivity of basal-like breast cancer cell lines.

TTK inhibition has no effect on non-homologous end joining repair

While TTK inhibition decreased HR efficiency, we also tested the effect of TTK inhibition on NHEJ efficiency using a well-characterized and validated NHEJ-specific reporter plasmid system (30, 31). Dox induced TTK knockdown in MDA-MB-231 and BT-549 shTTK cells did

not decrease NHEJ efficiency, while treatment with the known DNAPK inhibitor NU7441 (1.5 μM) significantly decreased efficiency of NHEJ in both cell lines **(Figure 4.9A&B)**. To evaluate the effect of TTK kinase function on NHEJ efficiency, we also treated MDA-MB-231 and BT-549 cells with B909 (50nM and 75nM). Neither B909 nor AZD7762 (Chk1/2 inhibitor) affected NHEJ efficiency, while NU7441 (DNAPK inhibitor) significantly decreased the efficiency of NHEJ **(Figure 4.9C&D)**.

Additionally, we treated MDA-MB-231 and BT-549 cells with B909 alone, RT alone, or a combination of B909 and RT to determine if canonical NHEJ phospho-proteins were affected. No difference in pKu80 (Thr714) was found between combination treatment of B909 and RT compared to RT alone in both MDA-MB-231 and BT-549 cells **(Figure 4.9E&F)**. Together, these results confirm that TTK inhibition has no effect on NHEJ repair efficiency.

Kinase-dead TTK does not rescue radiosensitivity phenotype

To validate that inhibition of TTK kinase function is responsible for the radiosensitization phenotype previously observed, we performed clonogenic survival assays using siRNAs to deplete endogenous TTK expression while re-introducing siRNA resistant wild-type (WT) or kinase-dead (KD) TTK. As previously demonstrated, knockdown of TTK using siRNA significantly increased radiosensitivity in both MDA-MB-231 and SUM-159 cell lines. Re-expression of WT TTK restored radioresistance in both cell lines; however, re-expression of KD TTK did not restore radioresistance in either cell line **(Figure 4.10A&B)**. Western blot analyses showed siRNA dramatically reduced endogenous TTK expression. It also confirmed robust expression of WT and

KD TTK upon reintroduction using siRNA resistant constructs **(Figure 4.11A)**. A summary of cytotoxicity and rER can be found in **Figures 4.11B&C**. Together, these results confirm that the kinase function of TTK is essential for the radioresistance phenotype observed in basal-like breast cancers models.

We also wanted to confirm that inhibition of TTK kinase function was responsible for impaired HR phenotype. Using the stable HR GFP reporter cell lines previously described, we measured the impact of TTK knockdown using siRNA as well as the reintroduction of WT and KD TTK. In both MDA-MB-231 and BT-549 cell lines we found that re-expression of WT TTK rescued HR efficiency, while expression of KD TTK was not able to rescue HR competency after siRNA-mediated TTK knockdown of TTK **(Figure 4.10C&D)**. To further confirm, the role of TTK's kinase function on HR we conducted Rad51 foci formation experiments. BT-549 cells were pretreated with either lipofectamine alone, siRNA targeting TTK, siRNA + WT TTK, or siRNA + KD TTK 48 hours before RT (4 Gy). TTK knockdown resulted in a significant decrease in Rad51 foci. However, re-expression of WT TTK after knockdown rescued Rad51 foci formation, whereas re-expression of KD TTK was unable to rescue appropriate Rad51 foci formation **(Figure 4.10E)**. Representative images of Rad51 foci 4 hours after RT are shown in **Figure 4.10F**.

TTK knockdown or inhibition reduces tumor growth *in vivo*

Once we established that TTK knockdown or inhibition leads to radiosensitization of basal-like BC *in vitro* and that this effect is mediated, at least in part, by decreased dsDNA break repair efficiency through HR, we wanted to determine whether inhibition of TTK *in vivo* similarly led to

radiosensitization. We initially utilized the MDA-MB-231 shTTK knockdown model in heterotopic xenograft studies, injecting cells subcutaneously into the flanks of female mice. After the tumors were established and grew to ~100mm^3, mice received either no treatment, TTK knockdown with dox, RT alone, or a combination of TTK knockdown with dox and RT. RT was given in six doses of 2 Gy over six days, beginning 72 hours after initial dox treatment to knockdown TTK **(Figure 4.12A)**. Combination treatment significantly reduced relative tumor growth compared to no treatment, TTK knockdown with dox, and RT alone **(Figure 4.12B)**. Time to tumor tripling significantly increased for combination treatment (undefined) compared to no treatment (14 days), TTK knockdown with dox (19 days), and RT (17.5 days) **(Figure 4.12C)**. Mouse weights were not significantly different between treatment groups in this study **(Figure 4.13A)**. To confirm that the addition of dox reduced TTK expression, we performed immunohistochemistry on tumor samples. Dox induced TTK knockdown significantly reduced TTK expression in the shTTK dox+ tumors compared to shTTK Dox- tumors **(Figure 4.12D&E)**. Finally, using the fraction tumor volume (FTV) method to measure synergy between treatments, we found that a combination of TTK knockdown and RT led to at least an additive, if not superadditive, effect (Ratio [R] <1) **(Figure 4.13B)**.

To establish that dox has no effect on tumor growth as well as to determine that the decrease in tumor growth previously seen was not an artifact of a single shTTK clone, we performed a second study with four independent stable MDA-MB-231 shRNA groups (shControl dox-, shControl dox+, shTTK#2 dox+, and shTTK#2 dox+ plus RT). No difference in tumor growth was observed between shControl +/- dox, indicating dox alone has no effect on tumor growth **(Figure**

4.13C&D). As seen in our previous xenograft study, a combination of TTK knockdown and RT decreased tumor growth and increased time to tumor tripling (34 days) compared to shControl dox- (10.5 days), shControl dox+ (13 days), and shTTK#2 dox+ (15 days) **(Figure 4.13C&D)**. Again mouse weights were similar in all groups **(Figure 4.13E)**.

To assess the role of TTK kinase function, and not just protein expression, on radiosensitization *in vivo*, we performed a xenograft study using the clinical grade TTK inhibitor B909 to test whether TTK kinase inhibition would also decrease tumor growth and increase time to tumor tripling. Using a similar design scheme, mice received either placebo treatment (CMC-Tween80), RT alone, B909 (1mg/kg) alone, or combination therapy (RT + B909). Combination treatment significantly decreased relative tumor growth and significantly increased time to tumor tripling (undefined days) compared to placebo (11 days), RT alone (22 days), and B909 alone (15 days) **(Figure 4.12F&G)**. Interestingly, 19% of tumors in the combination treatment group remained stable in size and were not growing even at the time of study completion (38 days), suggesting sustained durable response even weeks after the completion of therapy. As with TTK knockdown, combination treatment of B909 and RT had little effect on mouse weights **(Figure 4.13F)**. Furthermore, using the FTV method to measure synergy between treatments, we found that inhibition of TTK kinase function had a synergistic effect with RT (R>1) **(Figure 4.13G)**.

To confirm these findings independently, we utilized an orthotopic PDX model to test the efficacy of B909 plus RT. In this model we implanted basal-like BC PDX (PDX mutations listed in Figure 4.2L) tumors in the mammary fat pad of mice and allowed them to grow to ~100mm^3. Mice received either placebo treatment (CMC-Tween80), RT alone, B909 (2.5mg/kg) alone, or

combination therapy (RT + B909). In agreement with the previous animal studies, combination treatment led to a significant decrease in tumor growth and increased time to tumor tripling (undefined days) compared to placebo (9 days), RT alone (22 days), and B909 alone (13 days) **(Figure 4.12H&I)**. Combination treatment of B909 and RT did not cause weight loss in mice. However, mice that received either placebo or B909 alone gained weight throughout the study which can be attributed to the growth of the PDX tumors **(Figure 4.13H)**. As seen in our previous study, combination treatment of B909 and RT was synergistic (R>1) and led to tumor regression in many mice **(Figure 4.13I)**. These results indicate that TTK inhibition, using B909, in combination with RT inhibits tumor growth and delays time to tumor tripling. Together, our findings in multiple non-overlapping models suggest the combination treatment of B909 and RT may be a feasible strategy for the treatment of patients with basal-like BC with high risk of local recurrence.

Discussion

In this study we unbiasedly nominated TTK as the gene most strongly correlated with BC recurrence after radiation in four independent patient datasets **(Figure 4.1&4.2)**. TTK expression is strongly associated with TNBC/basal-like BC subtypes. Using both genetic (shRNA/siRNA) and pharmacologic (NMS-P715 and Bayer 1161909 – Empesertib) TTK inhibition we induced radiosensitization in multiple basal-like BC cell lines **(Figure 4.3&4.4)**. We found that TTK inhibition led to persistent unresolved dsDNA damage over time **(Figure 4.5&4.6)**. TTK knockdown or inhibition led to impaired HR with no effect on NHEJ, and impaired HR is

responsible, at least in part, for increased radiosensitivity of basal-like BC cell lines **(Figure 4.7-4.9)**. We also show inhibition of TTK kinase function is responsible for increased radiosensitivity and loss of HR efficiency through the use of wild-type and kinase-dead TTK re-expression after endogenous TTK knockdown **(Figure 4.10&4.11)**. *In vivo*, both genetic and pharmacologic TTK inhibition decreased tumor growth and increased time to tumor tripling in both cell line and orthotopic PDX models **(Figure 4.12&4.13)**. Together, these results demonstrate that TTK inhibition, in combination with RT, is a potentially effective strategy for the radiosensitization of basal-like BC that may ultimately lead to decreased rates of recurrence for patients.

In our nomination of novel targets for the radiosensitization of BC, we found TTK, also known as Monopolar Spindle 1 (Mps1), as the top target for radiosensitization of basal-like BC. TTK is overexpressed in various cancers and has previously been studied as a target for treatment of BC, glioblastoma, ovarian cancer, colon cancer, and others (18, 19, 32-35). TTK has been well characterized for its role in the spindle assembly checkpoint (SAC) complex, which prevents progression from metaphase to anaphase in mitosis when problems occur in metaphase (36-40). Previously, TTK inhibition has been shown to cause irregular mitosis as well as increased aneuploidy, lagging chromosomes, and mitotic catastrophe (41, 42). Given these findings, previous groups have focused on TTK inhibition as a monotherapy, in combination with conventional chemotherapies, or in combination with anti-PD-1 antibodies (18, 33, 41, 43). To date, however, few studies have characterized the role of TTK in the radiation response and as a possible combination therapy with RT (32). Additionally, previous studies have implicated TTK in HR- and NHEJ-mediated dsDNA break repair, though these studies suggest TTK may be more

strongly linked to HR pathway than NHEJ (21, 32). Our results add to this growing body of literature and are the first to suggest TTK inhibition is a viable strategy for the radiosensitization of basal-like BC. We also demonstrate for the first time that this radiosensitivity in BC is mediated, at least in part, through impaired HR repair.

Our nomination process, in four distinct BC datasets, identified ten genes correlated with recurrence in patients treated with radiation. In addition to the top nominated gene (TTK), multiple other identified genes (including EZH2 and KPNA2) have previously been associated with recurrence and radioresistance in various cancers (44, 45). This suggests our unbiased approach to nominate novel mediators of recurrence was rational and effective. While we only studied the effect of TTK inhibition on radiosensitization in this study, these additional genes may also be strong targets for the radiosensitization of BC and warrant further investigation.

Here we show TTK kinase function mediates HR competency; however, there are likely additional mechanisms for radiosensitization influenced by TTK. Increases in mitotic catastrophe, aneuploidy, and cell cycle defects have previously been linked to TTK inhibition and are likely to contribute to the observed radiosensitization (32, 33, 40, 42, 46). In our study, we used three basal-like breast cancer cell lines and a PDX model that are all BRCA1 wild-type in ordered to asses HR competency. We hypothesize that TTK inhibition may also have utility in BRCA1 mutant breast cancer cell lines through its role in the spindle assembly checkpoint complex and not through impaired HR. However, further studies are necessary to validate this hypothesis.

We have demonstrated that TTK inhibition had no effect on non-homologous end joining (NHEJ) efficiency **(Figure 5)**, despite other groups reporting reduced NHEJ efficiency after TTK

inhibition (32). This discrepancy may be explained by the different model systems and different pharmacological inhibitors used. For example, previous studies reporting TTK inhibition led to impaired NHEJ used the TTK inhibitor NMS-P715 (32). However, at higher doses NMS-P715 also inhibits maternal embryonic leucine zipper kinase (MELK), a kinase that our lab has shown to be critical to the NHEJ pathway (19). These off-target effects may have caused the decreased NHEJ efficiency seen in their study. However, further research needs to be performed, in multiple non-overlapping models, to reasonably address this concern. Furthermore, while we demonstrate that TTK inhibition leads to a decrease in HR repair efficiency, we have not yet identified the mechanism by which this occurs. Additional studies are currently underway to understand how TTK interacts with proteins in the HR pathway and how TTK inhibition leads to decreased HR efficiency.

Local recurrences after radiation remain a significant issue for women with basal-like BC, as the molecular drivers of these radioresistant recurrences are currently unclear. This study identifies TTK as a potential molecular mediator of radioresistance in basal-like BC. These data suggest that utilizing TTK inhibitors in combination with radiation may lead to improved rates of local control and disease cure for women with basal-like BC with high TTK expression. Future studies by our group and others will test this hypothesis in clinical trials with the goal of improving local control and survival in women with these aggressive forms of BC.

Methods

Gene Nomination

Four independent datasets of primary tumor samples from women with breast cancer with associated, curated recurrence data and gene expression were utilized for nomination (Wang (47), Desmedt (48), van't Veer (49), and Schmidt (50)). Using Oncomine.org for analysis and "Invasive Ductal Breast Carcinoma - Recurrence at 3 Years - Top 1% over-expressed" as a primary concept filter, we identified the genes whose expression was significantly correlated with recurrence event within 3 years of diagnosis with an odds ratio of >2 and a multiple testing corrected p-value <0.000001 in each data set as originally reported (51). The identified genes from each dataset were then compared for overlap in all four datasets to generate the final list of genes for further investigation.

Gene Set Enrichment Analysis (GSEA)

Gene expression was correlated to TTK expression in the TCGA breast cancer datasets and ranked by correlation coefficient. The settings used in GSEA were c2.all.v6.symbols.gmt [curated] as the gene sets database, 1000 permutations, and the minimum size was 15. For GSEA KEGG analysis both METABRIC and TCGA were used with c2.cp.kegg.v7.0.symbols.gmt, 1000 permutations, and a minimum size of 10 (52, 53).

Cell Culture

Basal-like BC cell lines MDA-MB-231 and BT-549 were grown from frozen samples (ATCC). MDA-MB-231 cells were grown in DMEM (Invitrogen) supplemented with 10% FBS (Invitrogen)

and penicillin/streptomycin (Invitrogen). BT-549 cells were grown in RPMI 1640 (Invitrogen) with 10% FBS (Invitrogen). SUM-159 were originally sourced from Steve P. Ethier at the University of Michigan and were obtained internally from Dr. Sofia Merajver. SUM-159 cells were grown in HAMS F-12 media (Thermo Fisher) supplemented with 5% FBS (Invitrogen), 5 mg/ml human insulin (Sigma), 10mmol/L HEPES (Thermo Fisher), 1 mg/kg Hydrocortisone (Sigma), and antibiotic-antimycotic. All cell lines were grown in 5% CO2 incubator. Cells were passaged at ~70% confluence. Cell lines were authenticated at the University of Michigan DNA Sequencing core facility before use and tested for mycoplasma routinely (MycoAlert®, Lonza).

Clonogenic Survival Assays

Exponentially growing cells were plated in 6-well plates overnight before treatment with doxycycline, drug, siRNA, or TTK plasmids. Cells were pretreated with, doxycycline (2µg/ml) for 36 hours, drug for 2 hours, siRNA for ~8-24 hours, and TTK plasmids for 24 hours before radiation treatment. Cells were allowed to grow for 7-14 days before being fixed (7:1, methanol: acetic acid) and stained (crystal violet). Colonies were counted as ≥50 cells. A linear-quadratic survival curve was fit to each assay, as previously described (54).

Western Blot Analysis

Cells were washed twice with ice cold PBS and lysed with RIPA buffer (Thermo Fisher) supplemented with phosSTOP (Roche) and cOmplete Mini protease inhibitors (Sigma-Aldrich). Western blot analysis was performed as previously described (55). Specific antibody information and dilutions can be found in Table 4.3.

Transfections, siRNAs, shRNAs, plasmids

siRNAs and shRNAs were ordered from Dharmacon and are listed in Table 4.3. siRNAs were transfected using Lipofectamine RNAiMax (Invitrogen) and Opti-MEM media (Invitrogen). Wild-type and kinase-dead TTK plasmids were generously given by the Yu lab and contain a 6x Myc tag (56). Specific information of siRNAs, shRNAs, and plasmids can be found in Table 4.3.

Irradiation

Irradiations were performed using a Kimtron IC 225 (Kimtron Medical) at a dose rate of approximately 2 Gy/min in the University of Michigan Comprehensive Cancer Center Experimental Irradiation Core (Ann Arbor, MI). Dosimetry is performed semiannually using an ionization chamber connected to an electrometer system that is directly traceable to a National Institute of Standards and Technology calibration. The beam was collimated with a 0.1 mm Cu inherent filter and a 0.2 mm Cu filter was used for cell line irradiation. A 2 mm Cu filter was used for in vivo xenograft experiments.

IC_{50} Analysis

2,000 cells per well were plated in a 96 well plate and allowed to adhere overnight. Drug was added at varying concentrations (1nM-10μM) and the cells were incubated for an additional 72 hours. After 72 hours, AlamarBlue (Thermo-Fisher) was added at 1/10 the volume of media and incubated for 3 hours at 37˚C. The plate was read using a BioTek™ Cytation™ 3 Cell Imaging Multi-Mode Reader. A dose-response curved was made using GraphPad Prism 7 software.

Proliferation Assay

Cells were plated in 96 well plates (1,500 cells/well) and allowed to sit overnight. The following day cells were pretreated with DMSO or B909 for 1 hour before radiation (2 Gy). Cells were then placed in an IncuCyte® Machine which measured the confluence of the plate every 4 hours for ~4 days.

Gamma H2AX and Rad51 foci formation assay

γH2AX and Rad51 foci were analyzed as previously described (57). Cells with >15 γH2AX foci or >10 Rad51 foci were scored as positive. Blinded analysis was performed when counting cells positive for foci. Antibody information can be found in Table 4.3.

Homologous recombination reporter assay

Cells were transfected with the HR reporter DR-GFP plasmid using Lipofectamine 2000 (Invitrogen) following the manufacturer's recommendations, with geneticin (ThermoFisher) selection, and validated using flow cytometry by GFP after SceI treatment (58). Validated clones were plated in a 6-well plate, pretreated with the indicated siRNA for 24 hours, drug for 1 hour, or TTK plasmids for 48 hours. SceI adenovirus was added to the cells for 48 hours; cells were harvested and sorted via flow cytometry for GFP+ cells, which indicated successful HR.

Non-homologous end joining reporter assay

The pEYFP plasmid (gift from Canman Lab) was completely digested with 20U of NheI-HF and purified using QIAquick PCR purification kit (CAT# 28104). Cells ($1.0x10^5$ per well) were plated in six well plates. The following day, 1µg of the digested pEYFP plasmid was transfected per well.

One hour before transfection, the cells were treated with either TTK inhibitor or DMSO. Cells were harvested at indicated time points, and the DNA plasmids were isolated with QIAprep Spin Miniprep Kit (Cat#27106). SYBR green real time qPCR was conducted in triplicate in 384-well PCR system, using DNAas template. Specific primers used are listed in Table 4.3. Relative DNA repair efficiency was calculated by comparative method normalized to the CT value of internal control.

Mouse Xenograft Experiments

Cells were injected subcutaneously on the bilateral flanks or orthotopically in the mammary fat pads of CB-17 SCID female mice originally sourced from Charles River Laboratories in Wilmington, Massachusetts and maintained in a breeding colony at the University of Michigan. Tumors were allowed to grow to ~100mm^3 and randomized before treatment began. Doxycycline (1µg/ml) was given through drinking water to induce shTTK cells 72 hours prior to the beginning of radiation therapy (RT). Bayer 1161909 (B909) was administered at a dose of 1mg/kg twice a day for 2 days over 4 weeks, one day prior to the start of RT. RT was given as 6 doses of 2 Gy. Tumor size was measured 3 times a week using a digital caliper and tumor volume was calculated using the equation $V= (L * W^2) * \pi/6$. Additive/synergistic effects were calculated using the fraction tumor volume (FTV) method as previously described (59, 60).

Study Approval

The procedures listed above were approved by the Institutional Animal Care and Use Committee (IACUC) at the University of Michigan.

Statistics

Statistical analyses were performed using GraphPad Prism 7.0. A log-rank (Mantel-Cox) test was used for analyses of survival curves. One-way ANOVA was performed for breast cancer subtype analysis. Two-sided Student's *t*-test and one-way ANOVA with Dunnett's multiple comparisons test were used for *in vitro* statistical analysis. One-way ANOVA with Dunnett's multiple comparisons test and Log-rank (Mantel-Cox) test were used for *in vivo* analyses. A P value less than or equal to 0.05 was considered significant.

Figures

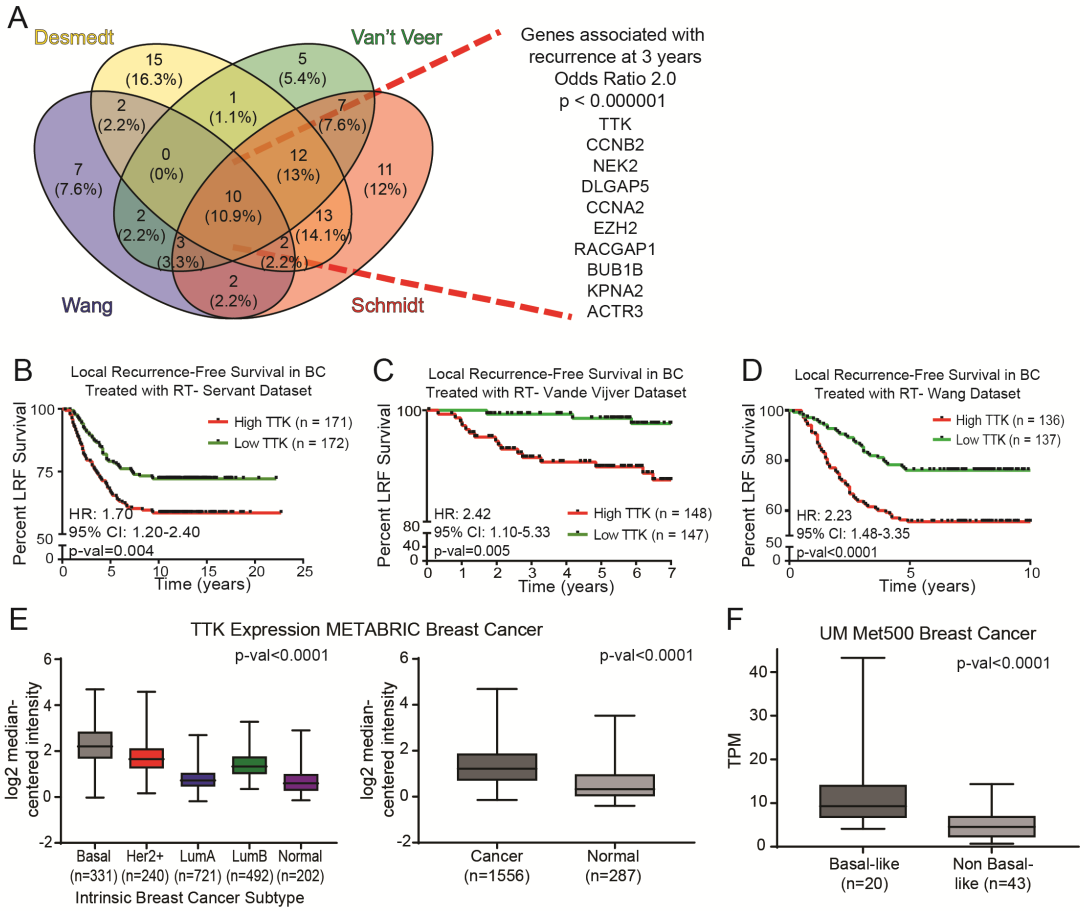

Figure 4.1 TTK expression correlates with breast cancer (BC) recurrence and independently predicts local recurrence-free survival (LRFS). A) Four BC datasets (Desmedt, van't Veer, Wang, and Schmidt) were used to identify genes associated with early recurrence (within 3 years) (Odds Ratio > 2.0 and p-value < 1.0E-6). B-D) Kaplan Meier local recurrence-free survival analysis in three independent datasets: Servant (B), Vande Vijver (C), and Wang (D) demonstrates that patients with higher than median expression of TTK have significantly higher rates of local recurrence after radiation compared to patients with lower than median TTK expression. E) TTK is overexpressed in basal-like BC compared to other subtypes (p<0.0001) and is overexpressed in BC compared to normal tissue (p<0.0001) in the METABRIC dataset. F) TTK is overexpressed in basal-like BC compared to non basal-like BC, using transcripts per million (TPM), in the

University of Michigan institutional dataset (Met500) ($p<0.0001$). Two-sided Student's *t*-test and ANOVA were used for analyses. Error bars represent standard deviation.

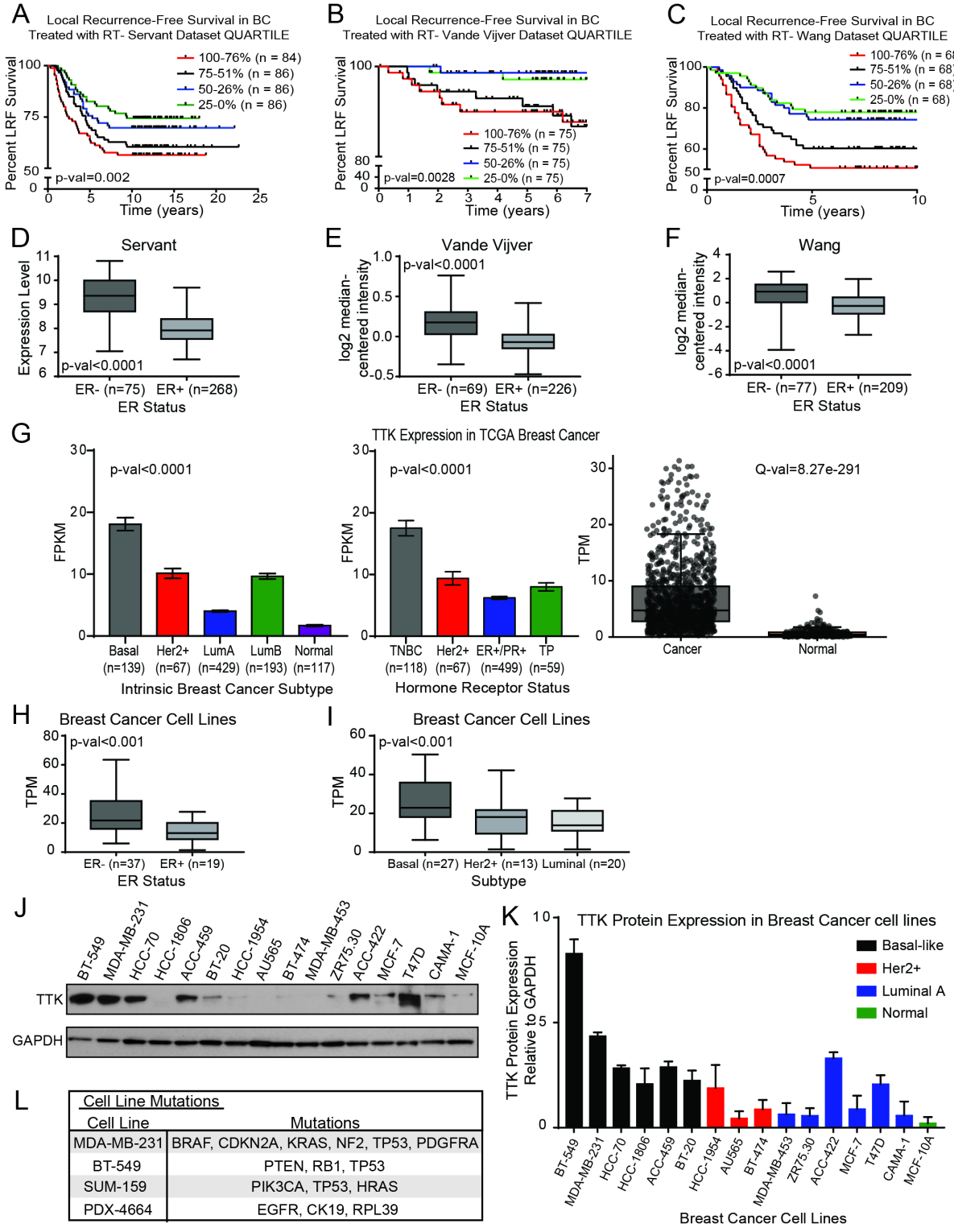

L

Cell Line Mutations	
Cell Line	Mutations
MDA-MB-231	BRAF, CDKN2A, KRAS, NF2, TP53, PDGFRA
BT-549	PTEN, RB1, TP53
SUM-159	PIK3CA, TP53, HRAS
PDX-4664	EGFR, CK19, RPL39

Figure 4.2: TTK expression correlates with local recurrence-free survival (LRFS) in breast cancer (BC) and is overexpressed in estrogen receptor-negative (ER-) BC compared to estrogen receptor-positive (ER+) breast cancer. A-C) Kaplan Meier analysis by quartile expression demonstrates higher TTK expression correlates with decreased LRFS in the Servant (A), Vande Vijver (B), and Wang (C) datasets. D-F) TTK is overexpressed in ER- BC compared to ER+ BC in the Servant (D), Vande Vijver (E), and Wang (F) datasets. Log-rank (Mantel-Cox) test was used for analyses of survival curves. G) TTK is overexpressed in patients with TNBC/basal-like BC compared to other subtypes in the TCGA BC dataset. Additionally, TTK is overexpressed in BC compared to normal tissue. H&I) TTK is overexpressed in ER- BC cell lines compared to ER+ BC cell lines and TTK has highest expression in basal-like BC cell lines compared to other subtypes using CCLE data measured in transcripts per million (TPM). J&K) TTK protein expression is highest in MDA-MB-231 and BT-549 BC cell lines and TTK protein expression is highest in basal-like BC compared to other subtypes. L) Mutational landscapes of cell lines and PDX models used for *in vitro* and *in vivo* studies. Two-sided Student's *t*-test and one-way ANOVA were used for analyses. Error bars represent standard deviation.

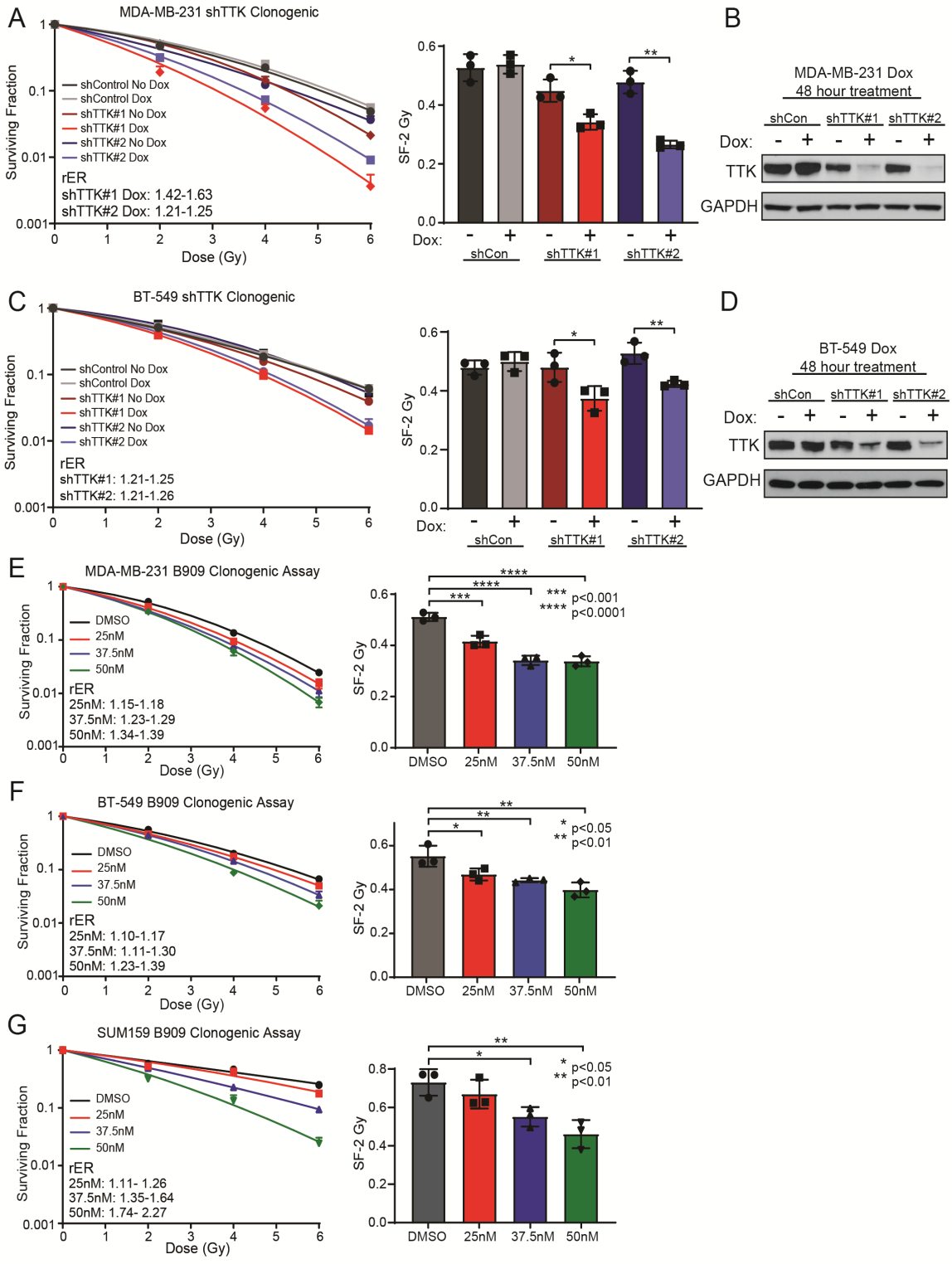
A
MDA-MB-231 shTTK Clonogenic
Surviving Fraction
Dose (Gy)
shControl No Dox
shControl Dox
shTTK#1 No Dox
shTTK#1 Dox
shTTK#2 No Dox
shTTK#2 Dox
rER
shTTK#1 Dox: 1.42-1.63
shTTK#2 Dox: 1.21-1.25
SF-2 Gy
Dox:
shCon
shTTK#1
shTTK#2
B
MDA-MB-231 Dox
48 hour treatment
TTK
GAPDH
C
BT-549 shTTK Clonogenic
shTTK#1: 1.21-1.25
shTTK#2: 1.21-1.26
D
BT-549 Dox
48 hour treatment
E
MDA-MB-231 B909 Clonogenic Assay
DMSO
25nM
37.5nM
50nM
25nM: 1.15-1.18
37.5nM: 1.23-1.29
50nM: 1.34-1.39
p<0.001
p<0.0001
F
BT-549 B909 Clonogenic Assay
25nM: 1.10-1.17
37.5nM: 1.11-1.30
50nM: 1.23-1.39
p<0.05
p<0.01
G
SUM159 B909 Clonogenic Assay
25nM: 1.11- 1.26
37.5nM: 1.35-1.64
50nM: 1.74- 2.27

Figure 4.3: Inhibition of TTK confers radiosensitivity in multiple basal-like breast cancer cell lines with high baseline TTK expression. A&C) shRNA induced TTK knockdown increases radiosensitivity in MDA-MB-231 (rER: 1.21-1.63) and BT-549 (rER: 1.21-1.26) cell lines. B&D) The addition of doxycycline leads to TTK knockdown in multiple stable clones in MDA-MB-231 and BT-549 cell lines. E-G) Pharmacological inhibition of TTK induces radiosensitivity of MDA-MB-231 cells (rER: 25nM 1.15-1.18, 37.5nM 1.23-1.29, 50nM 1.34-1.39) and BT-549 (rER: 25nM 1.10-1.17, 37.5nM 1.11-1.30, 50nM 1.23-1.39), and SUM-159 cells (rER: 25nM 1.11-1.26, 37.5nM 1.35-1.64, 50nM 1.74-2.27) in a dose-dependent fashion Data represent the mean of three independent experiments and error bars represent SEM for clonogenic assays and SD for SF-2 Gy. Two-sided Student's *t*-test was used for comparison of shRNA clonogenic assays and one-way ANOVA with Dunnett's multiple comparisons test was used for comparison of B909 clonogenic assays. * $p<0.05$, ** $p<0.01$, *** $p<0.001$, **** $p<0.0001$.

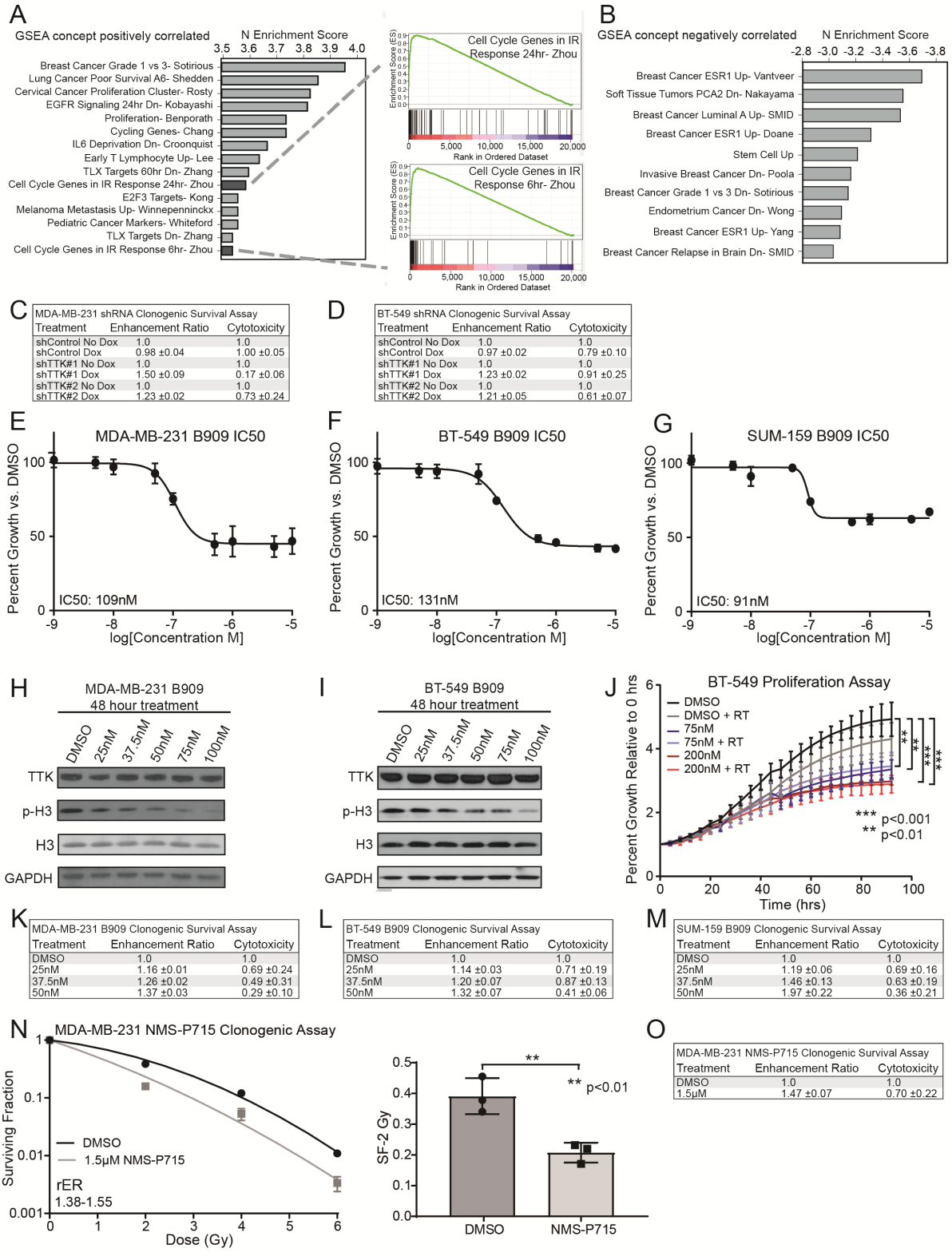
A
GSEA concept positively correlated
N Enrichment Score
Breast Cancer Grade 1 vs 3- Sotirious
Lung Cancer Poor Survival A6- Shedden
Cervical Cancer Proliferation Cluster- Rosty
EGFR Signaling 24hr Dn- Kobayashi
Proliferation- Benporath
Cycling Genes- Chang
IL6 Deprivation Dn- Croonquist
Early T Lymphocyte Up- Lee
TLX Targets 60hr Dn- Zhang
Cell Cycle Genes in IR Response 24hr- Zhou
E2F3 Targets- Kong
Melanoma Metastasis Up- Winnepenninckx
Pediatric Cancer Markers- Whiteford
TLX Targets Dn- Zhang
Cell Cycle Genes in IR Response 6hr- Zhou
Cell Cycle Genes in IR Response 24hr- Zhou
Cell Cycle Genes in IR Response 6hr- Zhou
Rank in Ordered Dataset
B
GSEA concept negatively correlated
N Enrichment Score
Breast Cancer ESR1 Up- Vantveer
Soft Tissue Tumors PCA2 Dn- Nakayama
Breast Cancer Luminal A Up- SMID
Breast Cancer ESR1 Up- Doane
Stem Cell Up
Invasive Breast Cancer Dn- Poola
Breast Cancer Grade 1 vs 3 Dn- Sotirious
Endometrium Cancer Dn- Wong
Breast Cancer ESR1 Up- Yang
Breast Cancer Relapse in Brain Dn- SMID
C
MDA-MB-231 shRNA Clonogenic Survival Assay
Treatment | Enhancement Ratio | Cytotoxicity
shControl No Dox | 1.0 | 1.0
shControl Dox | 0.98 ±0.04 | 1.00 ±0.05
shTTK#1 No Dox | 1.0 | 1.0
shTTK#1 Dox | 1.50 ±0.09 | 0.17 ±0.06
shTTK#2 No Dox | 1.0 | 1.0
shTTK#2 Dox | 1.23 ±0.02 | 0.73 ±0.24
D
BT-549 shRNA Clonogenic Survival Assay
Treatment | Enhancement Ratio | Cytotoxicity
shControl No Dox | 1.0 | 1.0
shControl Dox | 0.97 ±0.02 | 0.79 ±0.10
shTTK#1 No Dox | 1.0 | 1.0
shTTK#1 Dox | 1.23 ±0.02 | 0.91 ±0.25
shTTK#2 No Dox | 1.0 | 1.0
shTTK#2 Dox | 1.21 ±0.05 | 0.61 ±0.07
E
MDA-MB-231 B909 IC50
Percent Growth vs. DMSO
IC50: 109nM
log[Concentration M]
F
BT-549 B909 IC50
Percent Growth vs. DMSO
IC50: 131nM
log[Concentration M]
G
SUM-159 B909 IC50
Percent Growth vs. DMSO
IC50: 91nM
log[Concentration M]
H
MDA-MB-231 B909
48 hour treatment
DMSO
25nM
37.5nM
50nM
75nM
100nM
TTK
p-H3
H3
GAPDH
I
BT-549 B909
48 hour treatment
DMSO
25nM
37.5nM
50nM
75nM
100nM
TTK
p-H3
H3
GAPDH
J
BT-549 Proliferation Assay
DMSO
DMSO + RT
75nM
75nM + RT
200nM
200nM + RT
Percent Growth Relative to 0 hrs
Time (hrs)
*** p<0.001
** p<0.01
K
MDA-MB-231 B909 Clonogenic Survival Assay
Treatment | Enhancement Ratio | Cytotoxicity
DMSO | 1.0 | 1.0
25nM | 1.16 ±0.01 | 0.69 ±0.24
37.5nM | 1.26 ±0.02 | 0.49 ±0.31
50nM | 1.37 ±0.03 | 0.29 ±0.10
L
BT-549 B909 Clonogenic Survival Assay
Treatment | Enhancement Ratio | Cytotoxicity
DMSO | 1.0 | 1.0
25nM | 1.14 ±0.03 | 0.71 ±0.19
37.5nM | 1.20 ±0.07 | 0.87 ±0.13
50nM | 1.32 ±0.07 | 0.41 ±0.06
M
SUM-159 B909 Clonogenic Survival Assay
Treatment | Enhancement Ratio | Cytotoxicity
DMSO | 1.0 | 1.0
25nM | 1.19 ±0.06 | 0.69 ±0.16
37.5nM | 1.46 ±0.13 | 0.63 ±0.19
50nM | 1.97 ±0.22 | 0.36 ±0.21
N
MDA-MB-231 NMS-P715 Clonogenic Assay
Surviving Fraction
DMSO
1.5μM NMS-P715
rER
1.38-1.55
Dose (Gy)
SF-2 Gy
** p<0.01
DMSO
NMS-P715
O
MDA-MB-231 NMS-P715 Clonogenic Survival Assay
Treatment | Enhancement Ratio | Cytotoxicity
DMSO | 1.0 | 1.0
1.5μM | 1.47 ±0.07 | 0.70 ±0.22

Figure 4.4: Gene set enrichment analysis (GSEA) correlates TTK with radiation response and TTK inhibition radiosensitizes multiple basal-like breast cancer (BC) cell lines. A) GSEA identifies cell cycle genes at 6 and 24 hours as the top positively correlated concepts with TTK expression in TCGA BC dataset. B) GSEA concepts negatively correlated with TTK expression in the TCGA BC dataset. C&D) Summary of radiation enhancement ratios (rER) and cytotoxicity caused by TTK knockdown in MDA-MB-231 (C) and BT-549 (D) cells. E-G) IC50 of proliferation analyses of B909 in MDA-MB-231 (E) (109nM), BT-549 (F) (131nM), and SUM-159 (G) (91nM) cell lines. Error bars represent SEM. H&I) B909 reduces pH3 (Ser10) expression dose dependently in MDA-MB-231 (H) and BT-549 (I) cell lines. J) Proliferation assays of BT-549 cells treated with RT alone, B909 alone, or a combination treatment. Two-way ANOVA with Dunnett's Multiple Comparisons test was used to compare treatment groups. Data are a representation of 2-3 replicates. K-M) Radiation enhancement ratio (rER) and cytotoxicity of B909 clonogenic survival assays in MDA-MB-231 (J), BT-549 (K), and SUM-159 (L) cell lines. N) Clonogenic survival assay and SF-2 Gy in MDA-MB-231 cells using the TTK inhibitor NMS-P715 (1.5μM). O) Summary of radiation enhancement ratios (rER) and cytotoxicity caused by NMS-P715. Unless otherwise stated, data represent the mean of three independent experiments. Error bars represent SEM for clonogenic survival assays and proliferation assays and standard deviation for SF-2 Gy. A Two-sided Student's *t*-test was used for comparison. **$p<0.01$, ***$p<0.001$

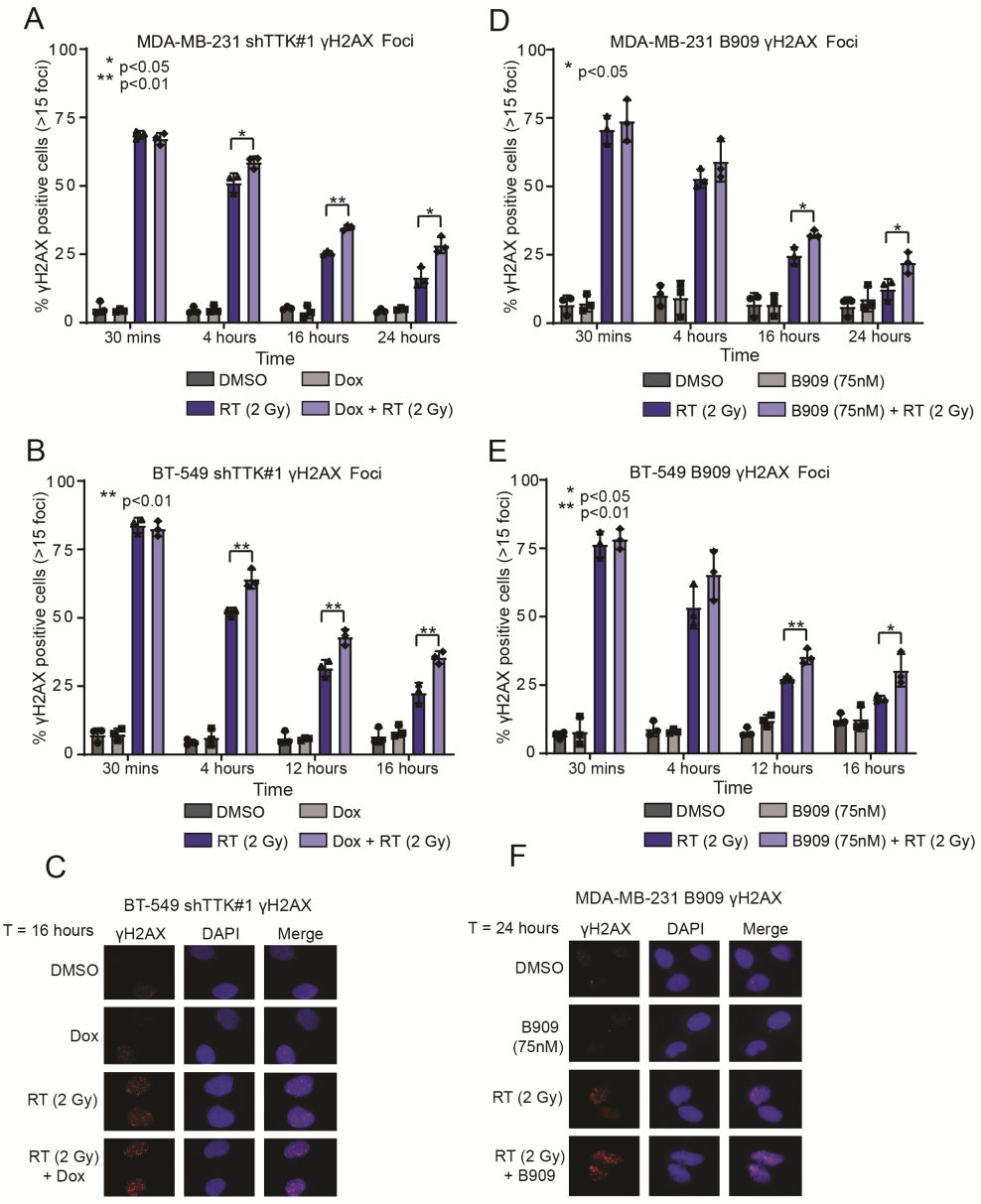

Figure 4.5: TTK inhibition in combination with RT leads to persistent double-strand DNA (dsDNA) damage over time. A&B) Combination treatment of dox inducible shRNA and RT leads to persistent dsDNA damage over time in two basal-like breast cancer cell lines: MDA-MB-231 (A) and BT-549 (B). C) Representative images of BT-549 γH2AX foci at 16 hours. D&E) Pharmacological inhibition of TTK kinase function, using B909, in combination with RT leads to persistent dsDNA damage over time in two basal-like breast cancer cell lines, MDA-MB-231 (D) and BT-549 (E). F) Representative images of MDA-MB-231 γH2AX foci at 24 hours. Data represent the mean of three independent experiments repeated in

triplicate, with ~100 cells counted for each experiment, and error bars represent standard deviation. Two-sided Student's *t*-test was used for comparison. * $p<0.05$, ** $p<0.01$

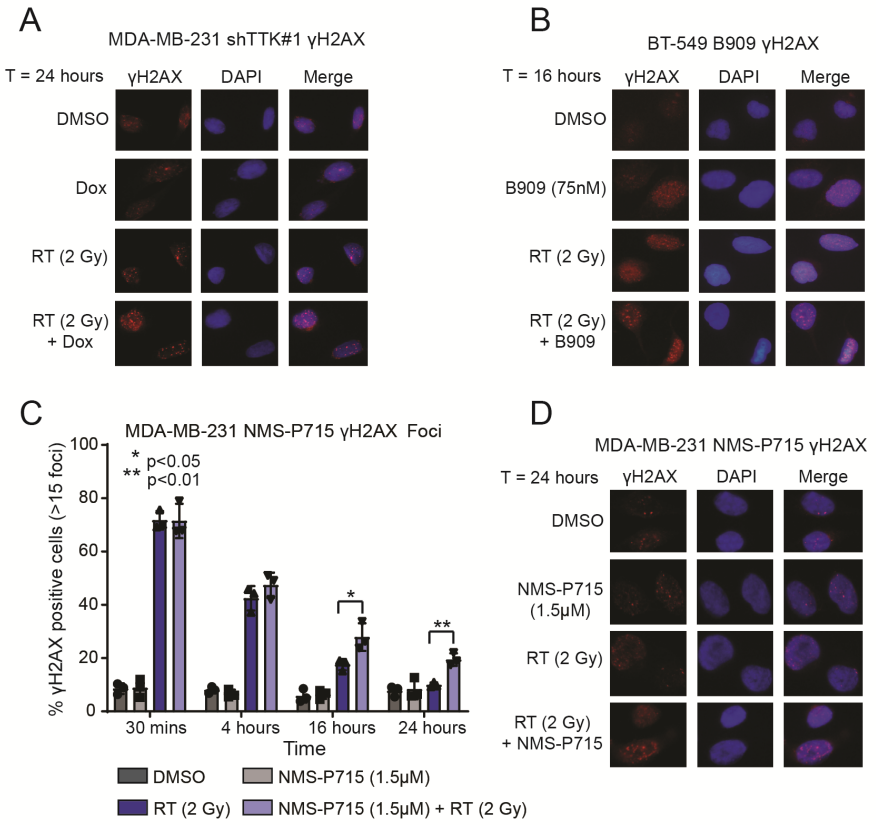

Figure 4.6: Representative images of γH2AX foci. A) Representative images of γH2AX foci in MDA-MB-231 shTTK#1 cells 24 hours after radiation. B) Representative images of γH2AX foci in BT-549 cells treated with Bayer 1161909 at 16 hours after radiation. C) Combination treatment of TTK inhibition (NMS-P715) and RT lead to persistent double strand DNA damage over time. D) Representative images of γH2AX foci at 24 hours in MDA-MB-231 cells treated with NMS-P715. Data represent the mean of three independent experiments repeated in triplicate, with ~100 cells counted for each experiment, and error bars represent standard deviation. Two-sided Student's *t*-test was used for comparison. * $p < 0.05$, ** $p < 0.01$

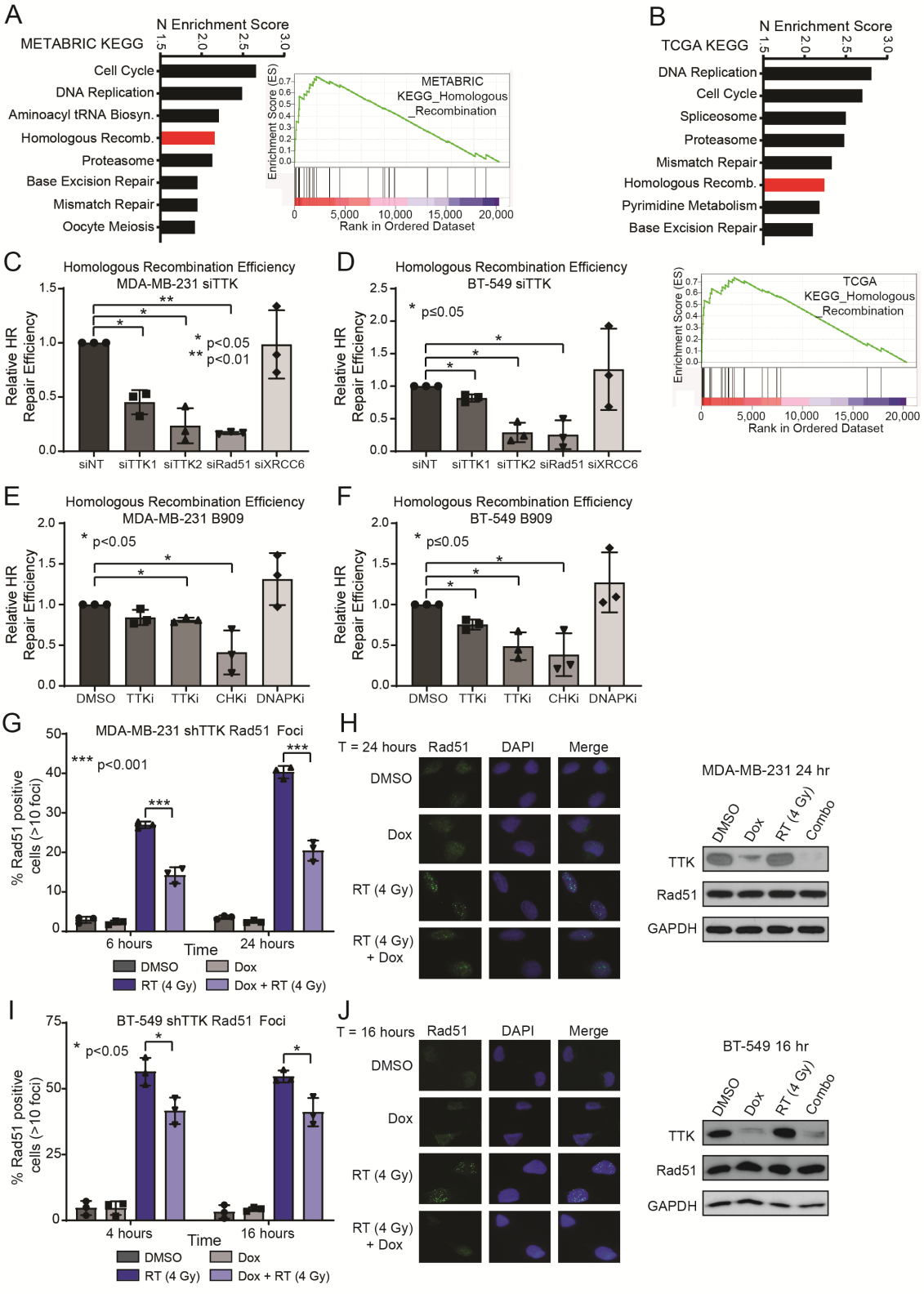
A
METABRIC KEGG
N Enrichment Score
Cell Cycle
DNA Replication
Aminoacyl tRNA Biosyn.
Homologous Recomb.
Proteasome
Base Excision Repair
Mismatch Repair
Oocyte Meiosis
METABRIC KEGG_Homologous _Recombination
Enrichment Score (ES)
Rank in Ordered Dataset
B
TCGA KEGG
N Enrichment Score
DNA Replication
Cell Cycle
Spliceosome
Proteasome
Mismatch Repair
Homologous Recomb.
Pyrimidine Metabolism
Base Excision Repair
TCGA KEGG_Homologous Recombination
C
Homologous Recombination Efficiency
MDA-MB-231 siTTK
Relative HR Repair Efficiency
* p<0.05
** p<0.01
siNT
siTTK1
siTTK2
siRad51
siXRCC6
D
Homologous Recombination Efficiency
BT-549 siTTK
* p≤0.05
E
Homologous Recombination Efficiency
MDA-MB-231 B909
* p<0.05
DMSO
TTKi
CHKi
DNAPKi
F
Homologous Recombination Efficiency
BT-549 B909
* p≤0.05
G
MDA-MB-231 shTTK Rad51 Foci
% Rad51 positive cells (>10 foci)
*** p<0.001
6 hours
24 hours
Time
DMSO
Dox
RT (4 Gy)
Dox + RT (4 Gy)
H
T = 24 hours
Rad51
DAPI
Merge
DMSO
Dox
RT (4 Gy)
RT (4 Gy) + Dox
MDA-MB-231 24 hr
DMSO
Dox
RT (4 Gy)
Combo
TTK
Rad51
GAPDH
I
BT-549 shTTK Rad51 Foci
% Rad51 positive cells (>10 foci)
* p<0.05
4 hours
16 hours
Time
J
T = 16 hours
BT-549 16 hr

Figure 4.7: TTK inhibition reduces homologous recombination repair (HR) efficiency. A&B) KEGG analysis through GSEA correlates the HR pathway with TTK expression in the METBRIC (A) and TCGA (B) datasets. C&D) TTK knockdown, by siRNA, reduces HR efficiency in an HR specific report system in MDA-MB-231 (C) and BT-549 (D) cells. E&F) Inhibition of TTK kinase function, by B909 at 50nM and 75nM, reduces HR efficiency in MDA-MB-231 (E) and BT-549 (F) cells. G&I) TTK knockdown, via a dox inducible shRNA, reduces RAD51 foci formation after 4 Gy radiation in MDA-MB-231 (G) and BT-549 (I) cell lines. H&J) Representative images of MDA-MB-231 (H) and BT-549 (J) RAD51 foci and western blots showing no change in total RAD51 levels after dox or RT treatment. Data represent the mean of three independent experiments and error bars represent standard deviation. One-sided *t*-tests corrected for multiple comparisons were used for comparison of HR efficiency assays and Two-sided Student's *t*-test was used for comparison of RAD51 foci experiments. * $p<0.05$, ** $p<0.01$, *** $p<0.001$

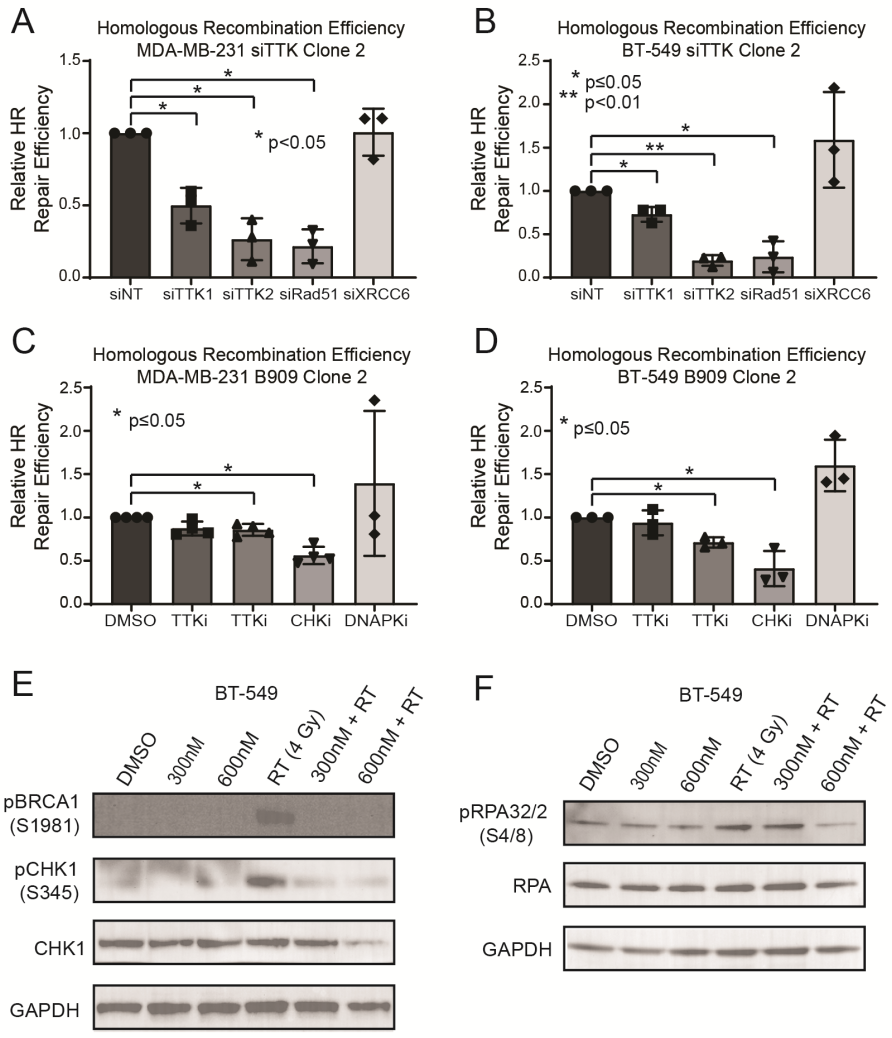

Figure 4.8: Homologous recombination (HR) efficiency is reduced by TTK inhibition in a second stable HR specific reporter clone and through western blot analysis. A&B) Knockdown of TTK by siRNA significantly reduces HR efficiency in MDA-MB-231 (A) and BT-549 (B) cells. C&D) TTK inhibition by Bayer 1161909 reduces HR efficiency in MDA-MB-231 (C) and BT-549 (D) cells. Data represent the mean of 3-4 independent experiments and error bars represent standard deviation. E) TTK inhibition reduces phospho-BRCA1 and phospho-CHK1 after RT compared to RT alone in BT-549 cells. Western blots represent two independent experiments. F) TTK inhibition reduces phospho-RPA after RT compared to RT alone in and BT-549 cells. Western blots represent two independent experiments. One-way ANOVA with Dunnett's multiple comparisons test was used for comparison. *p≤0.05, **p<0.01.

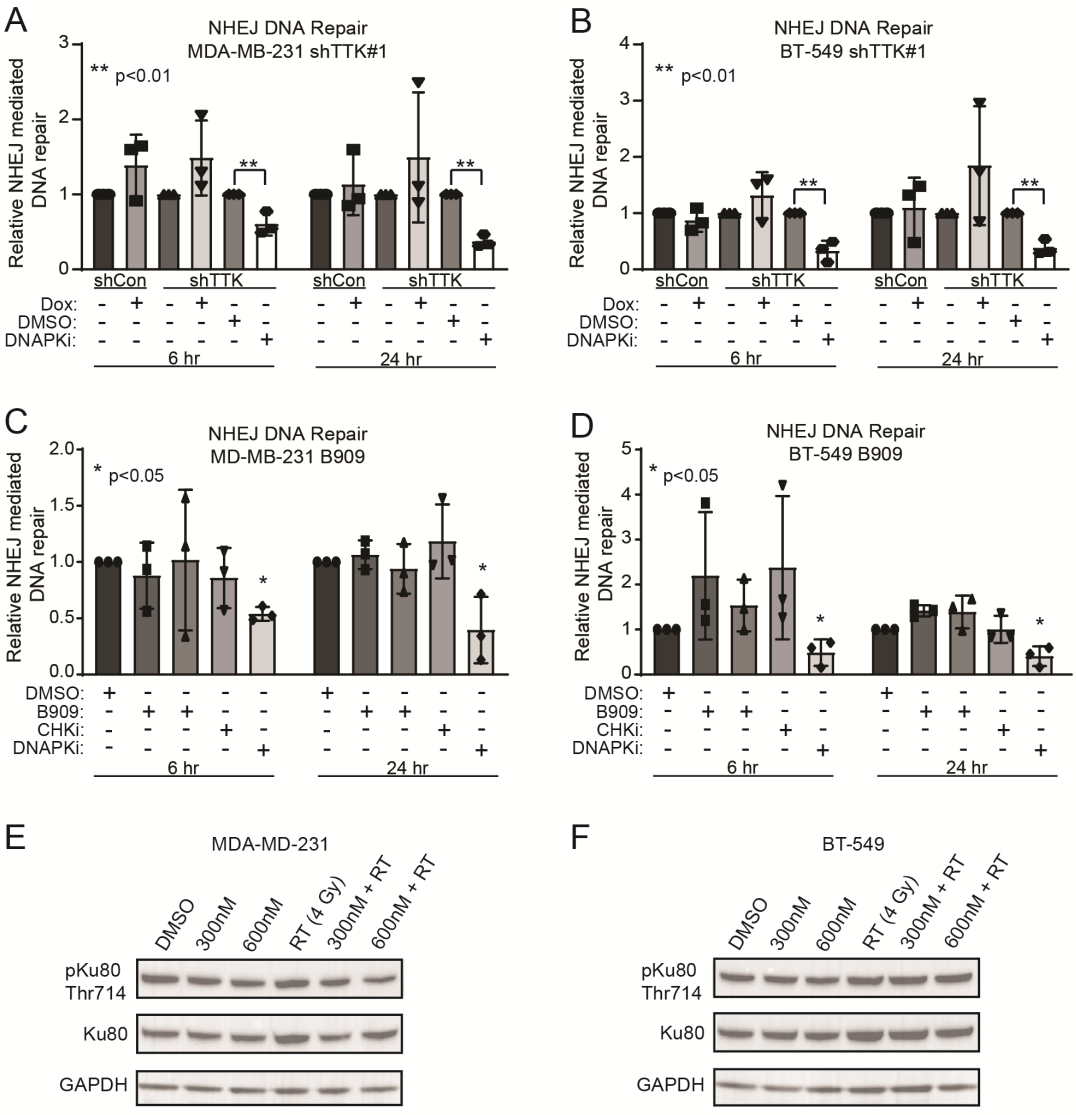

Figure 4.9: TTK knockdown has no effect on non-homologous end joining repair efficiency. A&B) TTK knockdown, via dox inducible shRNA has no effect on NHEJ efficiency in MDA-MB-231 (A) nor BT-549 (B) cells, while DNAPK inhibition significantly reduces NHEJ efficiency. C&D) Pharmacologic inhibition of TTK kinase, using B909, at 50nM and 75nM, has no effect on NHEJ, while DNAPK inhibition significantly reduces NHEJ efficiency in MDA-MB-231 (C) and BT-549 (D) cell lines. E&F) Inhibition of

TTK with B909 has no effect on pKu80 (Thr714). Data represent the mean of three independent experiments and error bars represent standard deviation. Two-sided Student's *t*-test was used for comparison of shTTK NHEJ assays and one-way ANOVA with Dunnett's multiple comparisons test was used for comparison of B909 NHEJ assays. * $p<0.05$, ** $p<0.01$

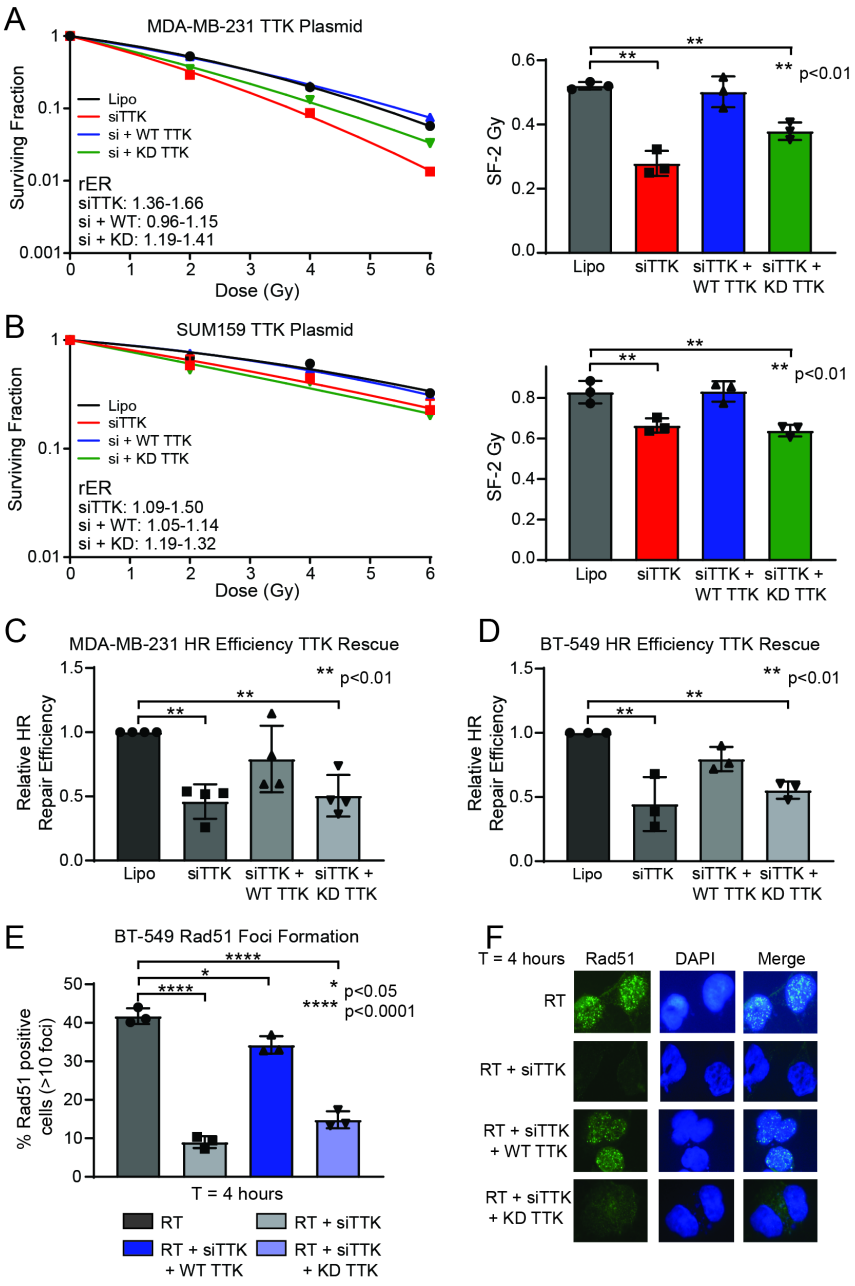

Figure 4.10: After knockdown of TTK, wild-type (WT) TTK rescues the radiosensitization phenotype, while kinase-dead (KD) TTK does not. A&B) TTK knockdown, with siRNA, leads to radiosensitization of MDA-MB-231 (A) and SUM-159 (B) cell lines. The addition of WT TTK rescues this phenotype, while KD TTK does not. C&D) Knockdown of TTK using siRNA decreases homologous recombination (HR) efficiency, while the reintroduction of wild-type TTK rescues HR efficiency. However, reintroduction of KD TTK does not rescue HR efficiency in both MDA-MB-231 (C) and BT-549 (D) cell lines. E) TTK knockdown, by siRNA, decreases RAD51 foci formation, however, reintroduction of WT

TTK rescues RAD51 foci formation. Introduction of KD TTK is unable to rescue RAD51 foci formation. F) Representative images of RAD51 foci at 4 hours. Data represent the mean of three to four independent experiments and error bars represent standard deviation. One-way ANOVA with Dunnett's multiple comparisons test was used for comparison. * $p<0.05$, ** $p<0.01$, **** $p<0.0001$

A

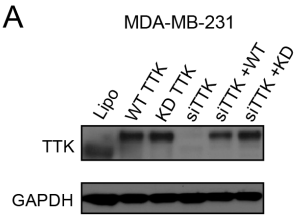

B

MDA-MB-231 TTK Rescue Clonogenic Survival Assay

Treatment	Enhancement Ratio	Cytotoxicity
Lipo	1.0	1.0
siTTK	1.19 ±0.06	0.69 ±0.16
siTTK + WT TTK	1.46 ±0.13	0.63 ±0.19
siTTK + KD TTK	1.97 ±0.22	0.36 ±0.21

C

SUM-159 TTK Rescue Clonogenic Survival Assay

Treatment	Enhancement Ratio	Cytotoxicity
Lipo	1.0	1.0
siTTK	1.48 ±0.15	0.15 ±0.11
siTTK + WT TTK	1.03 ±0.09	0.45 ±0.18
siTTK + KD TTK	1.29 ±0.09	0.41 ±0.15

D

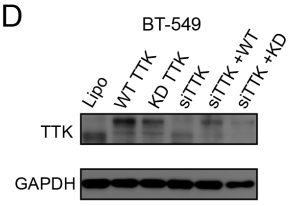

Figure 4.11: TTK rescue representative western blots and clonogenic assay cytotoxicity information. A) Representative western blot of TTK knockdown by siRNA and overexpression of wild-type (WT) or kinase dead (KD) TTK. B&C) Cytotoxicity and radiation enhancement ratio information for MDA-MB-231 (B) and SUM-159 (C) clonogenic assays. D) Representative western blot of TTK knockdown by siRNA and overexpression of WT or KD TTK in the BT-549 cell line. Western blots are representative of duplicate experiments**.**

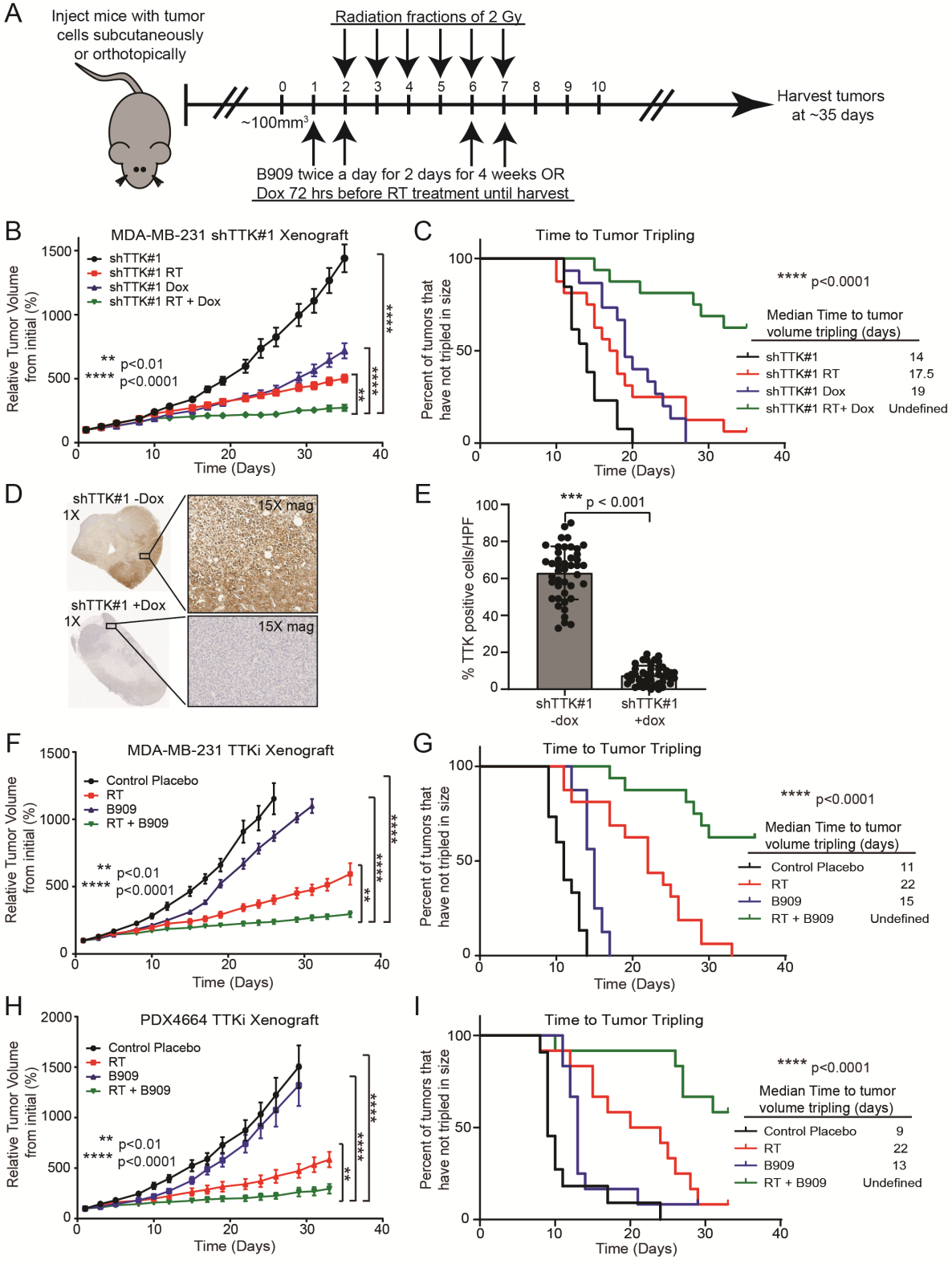
A
Inject mice with tumor cells subcutaneously or orthotopically
Radiation fractions of 2 Gy
0 1 2 3 4 5 6 7 8 9 10
~100mm3
Harvest tumors at ~35 days
B909 twice a day for 2 days for 4 weeks OR
Dox 72 hrs before RT treatment until harvest
B
MDA-MB-231 shTTK#1 Xenograft
shTTK#1
shTTK#1 RT
shTTK#1 Dox
shTTK#1 RT + Dox
** p<0.01
**** p<0.0001
Relative Tumor Volume from initial (%)
Time (Days)
C
Time to Tumor Tripling
**** p<0.0001
Median Time to tumor volume tripling (days)
shTTK#1 14
shTTK#1 RT 17.5
shTTK#1 Dox 19
shTTK#1 RT+ Dox Undefined
Percent of tumors that have not tripled in size
Time (Days)
D
shTTK#1 -Dox
1X
15X mag
shTTK#1 +Dox
1X
15X mag
E
*** p < 0.001
% TTK positive cells/HPF
shTTK#1 -dox
shTTK#1 +dox
F
MDA-MB-231 TTKi Xenograft
Control Placebo
RT
B909
RT + B909
** p<0.01
**** p<0.0001
Relative Tumor Volume from initial (%)
Time (Days)
G
Time to Tumor Tripling
**** p<0.0001
Median Time to tumor volume tripling (days)
Control Placebo 11
RT 22
B909 15
RT + B909 Undefined
Percent of tumors that have not tripled in size
Time (Days)
H
PDX4664 TTKi Xenograft
Control Placebo
RT
B909
RT + B909
** p<0.01
**** p<0.0001
Relative Tumor Volume from initial (%)
Time (Days)
I
Time to Tumor Tripling
**** p<0.0001
Median Time to tumor volume tripling (days)
Control Placebo 9
RT 22
B909 13
RT + B909 Undefined
Percent of tumors that have not tripled in size
Time (Days)

Figure 4.12: Combination treatment of TTK inhibition and RT reduces basal-like breast cancer tumor growth *in vivo*. A) Model of treatment schedule for *in vivo* studies. B) Doxycycline (dox) inducible MDA-MB-231 shTTK cells have decreased tumor growth with a combination of dox and RT (n=16) compared to TTK knockdown (n=15) or RT alone (n=16). C) Combination treatment (RT + dox) leads to increased time to tumor tripling *in vivo*. D) Immunohistochemistry from shTTK *in vivo* model depicts success knockdown of TTK after the addition of dox. E) Average percent of TTK positive cells across four tumors from the shTTK *in vivo* model plus or minus dox. F) TTK inhibition, by B909 (1mg/kg), in combination with RT leads to decreased tumor growth and G) increased time to tumor tripling in MDA-MB-231 breast cancer cells (n=16 tumors per group). H) In an orthotopic PDX model, combination treatment of B909 (2.5mg/kg) and RT decreases tumor growth compared to placebo, B909 only, and RT only. I) Combination treatment of B909 and RT leads to increased time of tumor tripling. One-way ANOVA with Dunnett's multiple comparisons test and Log-rank (Mantel-Cox) test were used for analyses. Error bars represent standard error of the mean. ** $p<0.01$, *** $p<0.001$, **** $p<0.0001$.

A

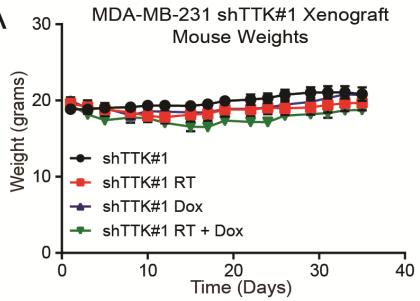

B

MDA-MB-231 shTTK#1 Xenograft
Fractional Tumor Volume (FTV)

			Combination		
Day	Dox	RT	Expected	Observed	Ratio
10	0.79	0.95	0.75	0.79	0.96
22	0.60	0.58	0.34	0.37	0.94
31	0.51	0.40	0.21	0.23	0.89
33	0.51	0.38	0.19	0.21	0.91
35	0.50	0.35	0.17	0.20	0.92

C

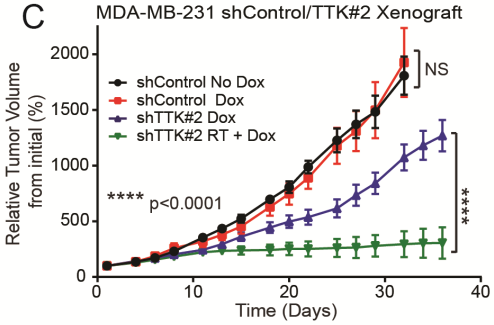

D

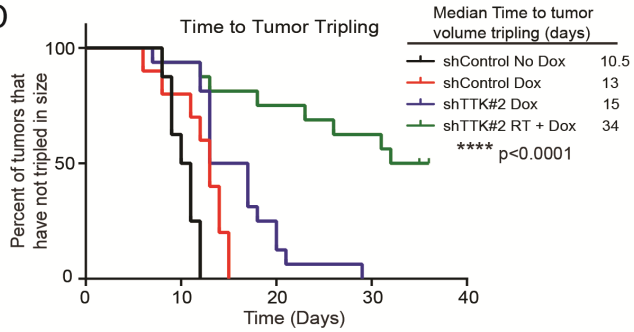

E

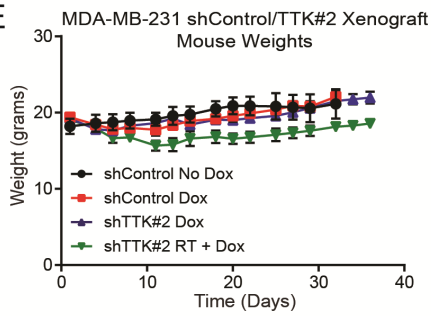

F

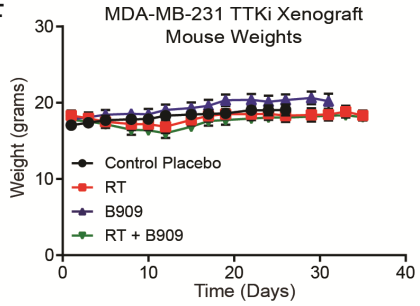

G

MDA-MB-231 B909 Xenograft
Fractional Tumor Volume (FTV)

			Combination		
Day	RT	B909	Expected	Observed	Ratio
8	0.77	0.80	0.62	0.69	0.90
15	0.52	0.67	0.35	0.42	0.83
22	0.38	0.74	0.28	0.25	1.12
24	0.37	0.78	0.29	0.23	1.24
26	0.35	0.76	0.27	0.21	1.28

H

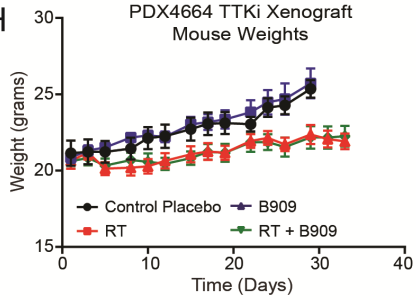

I

PDX4664 B909 Xenograft
Fractional Tumor Volume (FTV)

			Combination		
Day	RT	B909	Expected	Observed	Ratio
8	0.73	0.74	0.54	0.59	0.92
15	0.50	0.72	0.36	0.34	1.07
22	0.39	0.85	0.33	0.23	1.43
24	0.36	0.89	0.32	0.21	1.52
26	0.34	0.88	0.30	0.19	1.63

Figure 4.13: *In vivo* studies additional information. A) MDA-MB-231 shTTK#1 mouse weights from *in vivo* study. B) Additive/synergistic analysis for MDA-MB-231 shTTK#1 *in vivo* study using fractional tumor volume (FTV) method. C) In a second dox inducible MDA-MB-231 shTTK cell line (shTTK#2), tumor growth is inhibited by a combination of dox and RT compared to dox alone, while dox has no effect on shControl cells. Two-sided Student's *t*-test was used for analyses. Error bars represent standard error of the mean. D) Combination treatment (dox + RT) leads to increased time to tumor tripling, while dox alone has no effect on shControl cells (n=16 tumors per group). Log-rank (Mantel-Cox) tests were used for analyses. E) Mouse weights from MDA-MB-231 shControl/shTTK#2 *in vivo* study. F) Mouse weights from MDA-MB-231 Bayer 1161909 (B909) *in vivo* study. G) Additive/synergistic analysis for MDA-MB-231 B909 *in vivo* study using the FTV method. H) Mouse weights from the PDX4664 orthotopic study. I) Additive/synergistic analysis for PDX4664 B909 *in vivo* study using the FTV method. ****$p<0.0001$.

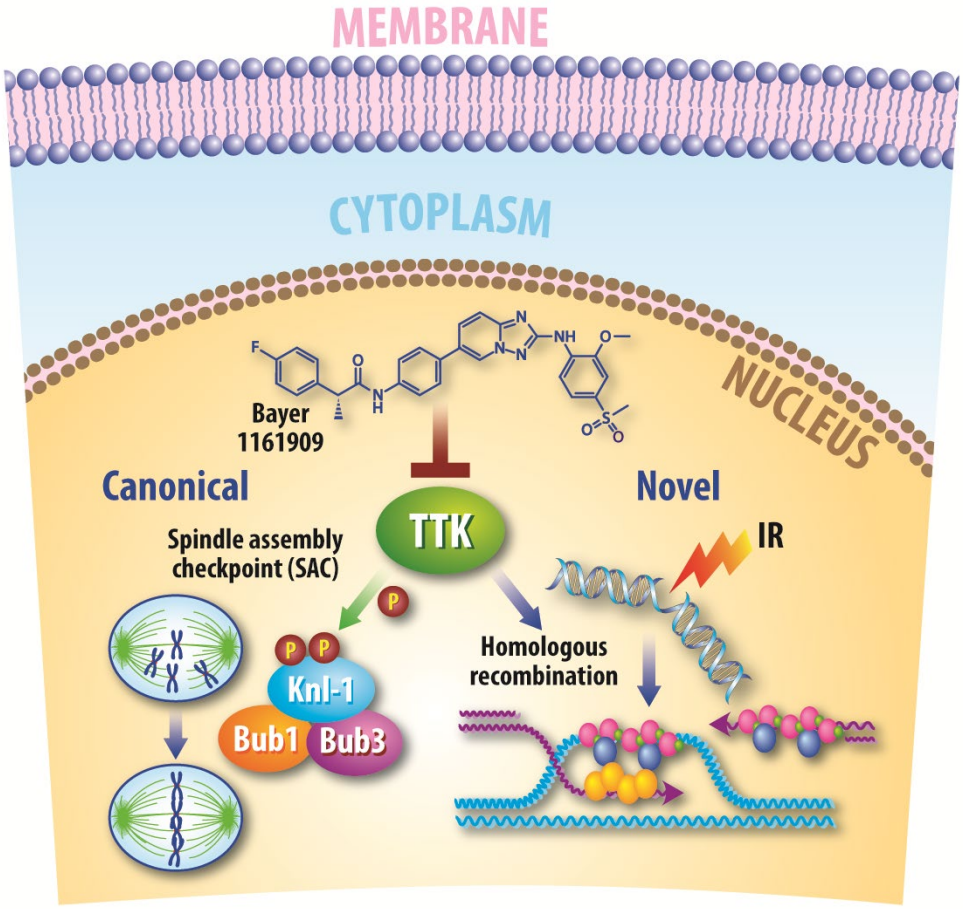

Figure 4.14: TTK interacts with the spindle assembly checkpoint (SAC) complex to ensure accurate chromosomal alignment and regulates homologous recombination to ensure accurate double strand DNA repair. Inhibition of TTK leads to an increase in aneuploidy, lagging chromosomes, and mitotic catastrophe through its canonical role in the SAC complex. Our findings demonstrate a novel role for TTK in the homologous recombination pathway. Inhibition of TTK with knockdown, kinase-dead constructs,

and a clinical grade inhibitor, Bayer 1161909, decreases in the efficiency of homologous recombination but has no effect on non-homologous end joining.

Tables

Dataset	Desmedt	Van't Veer	Wang	Schmidt	Log2(FC)	Clinical
Gene	Log2(FC)	Log2(FC)	Log2(FC)	Log2(FC)	(average)	Development
TTK	1.70	1.35	1.66	2.22	1.73	X
CCNB2	1.54	1.20	1.60	2.39	1.68	
NEK2	1.30	1.15	1.79	2.10	1.58	
DLGAP5	1.52	1.12	1.48	2.19	1.58	
CCNA2	1.35	1.12	1.55	2.11	1.53	X
EZH2	1.28	1.15	1.55	1.78	1.44	X
RACGAP1	1.32	1.10	1.47	1.79	1.42	
BUB1B	1.22	1.09	1.39	1.70	1.35	
KPNA2	1.19	1.13	1.49	1.51	1.33	
ACTR3	1.19	1.08	1.23	1.53	1.26	

Table 1: Genes associated with locoregional recurrence after radiation. List of ten overlapping genes across four datasets (Desmedt, Van't Veer, Wang, and Schmidt) associated with locoregional recurrence after radiation. Fold change between recurrent and non-recurrent genes listed under each dataset. List of genes under clinical development noted.

Servant Dataset

Univariate Analysis- Servant		
Covariate	Hazard Ratio (HR)	P-value
TTK	1.34 (95% CI 1.07-1.71)	0.01
ER-status	0.80 (95% CI 0.47-1.36)	0.41
Age	0.94 (95% CI 0.90-0.98)	0.008
T-stage	1.13 (95% CI 0.71-1.79)	0.02
Nodes	1.13 (95% CI 0.71-1.80)	0.62
Chemotherapy	0.98 (95% CI 0.62-1.55)	0.95
Surgical margin +	1.55 (95% CI 0.77-3.10)	0.73
Grade 1	Reference	
Grade 2	0.99 (95% CI 0.50-1.96)	0.98
Grade 3	1.83 (95% CI 1.12-2.98)	0.02
Luminal A subtype	Reference	
Basal subtype	1.48 (95% CI 0.80-2.86)	0.24
HER2 subtype	3.75 (95% CI 1.22-11.50)	0.02
Luminal B subtype	1.99 (95% CI 1.13-3.50)	0.02

Multivariate Analysis- Servant		
Covariate	Hazard Ratio (HR)	P-value
TTK	1.29 (95% CI 1.04-1.65)	0.03
HER2 subtype	2.09 (95% CI 1.10-3.90)	0.02

All other covariates NS on MVA including ER-status, age, T-stage, nodes, chemotherapy, surgical margin positivity, grade, other other intrinsic subtypes

Vande Vijver Dataset

Univariate Analysis- Vande Vijver		
Covariate	Hazard Ratio (HR)	P-value
TTK	4.05 (95% CI 1.33-38.85)	0.01
ER-status	0.92 (95% CI 0.29-2.99)	0.89
Age	0.91 (95% CI 0.83-0.99)	0.02
T-stage	0.96 (95% CI 0.90-1.03)	0.25
Nodes	1.13 (95% CI 0.71-1.80)	0.62
Chemotherapy	1.76 (95% CI 0.63-4.89)	0.28
Mastectomy	0.69 (95% CI 0.24-1.98)	0.49
Grade	1.25 (95% CI 0.65-2.42)	0.51
Hormonal therapy	0.65 (95% CI 0.14-3.02)	0.59

Multivariate Analysis- Vande Vijver		
Covariate	Hazard Ratio (HR)	P-value
TTK	11.29 (95% CI 1.49-28.06)	0.04
Age	0.90 (95% CI 0.83-0.99)	0.02

All other covariates NS on MVA including ER-status, T-stage, nodes, chemotherapy, hormonal therapy, type of surgery, and grade

Wang Dataset

Univariate Analysis- Wang		
Covariate	Hazard Ratio (HR)	P-value
TTK	1.44 (95% CI 1.15-1.80)	<0.001
ER-status	0.87 (95% CI 0.50-1.50)	0.62
Age	0.99 (95% CI 0.97-1.01)	0.20
T-stage	0.97 (95% CI 0.63-1.48)	0.88
PR-status	1.43 (95% CI 0.87-2.36)	0.16
Grade	2.77 (95% CI 1.35-5.69)	0.002
Menopausal status	0.92 (95% CI 0.56-1.50)	0.73

Multivariate Analysis- Wang		
Covariate	Hazard Ratio (HR)	P-value
TTK	1.32 (95% CI 1.15-1.87)	0.03
Grade	2.63 (95% CI 1.16-5.98)	0.02

All other covariates NS on MVA including ER-status, age, T-stage, PR status, and menopausal status

Table 2: Univariate and multivariate analysis of Servant, Vande Vijver, and Wang datasets. Univariate and multivariate analyses were performed for the Servant, Vande Vijver, and Wang datasets independently. In multivariate cox proportional hazards regression analysis of all patients, only TTK expression (continuous variable) remained significantly associated with worse local RFS in all three datasets. Log-rank (Mantel-Cox) test was used for analyses of survival curves.

References

1. Siegel RL, Miller KD, and Jemal A. Cancer statistics, 2018. *CA Cancer J Clin.* 2018;68(1):7-30.
2. Early Breast Cancer Trialists' Collaborative G, Darby S, McGale P, Correa C, Taylor C, Arriagada R, Clarke M, Cutter D, Davies C, Ewertz M, et al. Effect of radiotherapy after breast-conserving surgery on 10-year recurrence and 15-year breast cancer death: meta-analysis of individual patient data for 10,801 women in 17 randomised trials. *Lancet (London, England).* 2011;378(9804):1707-16.
3. Caan BJ, Sweeney C, Habel LA, Kwan ML, Kroenke CH, Weltzien EK, Quesenberry CP, Castillo A, Factor RE, Kushi LH, et al. Intrinsic Subtypes from the PAM50 Gene Expression Assay in a Population-Based Breast Cancer Survivor Cohort: Prognostication of Short- and Long-term Outcomes. *Cancer Epidemiology Biomarkers & Prevention.* 2014;23(5):725.
4. Horton JK, Jagsi R, Woodward WA, and Ho A. Breast Cancer Biology: Clinical Implications for Breast Radiation Therapy. *International Journal of Radiation Oncology*Biology*Physics.* 2018;100(1):23-37.
5. Lowery AJ, Kell MR, Glynn RW, Kerin MJ, and Sweeney KJ. Locoregional recurrence after breast cancer surgery: a systematic review by receptor phenotype. *Breast Cancer Research and Treatment.* 2012;133(3):831-41.
6. Kyndi M, Sørensen FB, Knudsen H, Overgaard M, Nielsen HM, and Overgaard J. Estrogen Receptor, Progesterone Receptor, HER-2, and Response to Postmastectomy Radiotherapy in High-Risk Breast Cancer: The Danish Breast Cancer Cooperative Group. *Journal of Clinical Oncology.* 2008;26(9):1419-26.
7. Sjöström M, Lundstedt D, Hartman L, Holmberg E, Killander F, Kovács A, Malmström P, Niméus E, Werner Rönnerman E, Fernö M, et al. Response to Radiotherapy After Breast-Conserving Surgery in Different Breast Cancer Subtypes in the Swedish Breast Cancer Group 91 Radiotherapy Randomized Clinical Trial. *Journal of Clinical Oncology.* 2017;35(28):3222-9.
8. Perou CM, Sørlie T, Eisen MB, van de Rijn M, Jeffrey SS, Rees CA, Pollack JR, Ross DT, Johnsen H, Akslen LA, et al. Molecular portraits of human breast tumours. *Nature.* 2000;406(747.
9. Prat A, Parker JS, Fan C, and Perou CM. PAM50 assay and the three-gene model for identifying the major and clinically relevant molecular subtypes of breast cancer. *Breast Cancer Research and Treatment.* 2012;135(1):301-6.
10. Speers C, Tsimelzon A, Sexton K, Herrick AM, Gutierrez C, Culhane A, Quackenbush J, Hilsenbeck S, Chang J, and Brown P. Identification of novel kinase targets for the treatment of estrogen receptor-negative breast cancer. *Clinical cancer research : an official journal of the American Association for Cancer Research.* 2009;15(20):6327-40.
11. Balbous A, Cortes U, Guilloteau K, Rivet P, Pinel B, Duchesne M, Godet J, Boissonnade O, Wager M, Bensadoun RJ, et al. A radiosensitizing effect of RAD51 inhibition in glioblastoma stem-like cells. *BMC cancer.* 2016;16(604-.
12. Speers C, Zhao SG, Kothari V, Santola A, Liu M, Wilder-Romans K, Evans J, Batra N, Bartelink H, Hayes DF, et al. Maternal Embryonic Leucine Zipper Kinase (MELK) as a Novel Mediator and Biomarker of Radioresistance in Human Breast Cancer. *Clinical cancer research : an official journal of the American Association for Cancer Research.* 2016;22(23):5864-75.
13. Wei D, Parsels LA, Karnak D, Davis MA, Parsels JD, Marsh AC, Zhao L, Maybaum J, Lawrence TS, Sun Y, et al. Inhibition of protein phosphatase 2A radiosensitizes pancreatic cancers by

modulating CDC25C/CDK1 and homologous recombination repair. *Clinical cancer research : an official journal of the American Association for Cancer Research.* 2013;19(16):4422-32.
14. Curtis C, Shah SP, Chin SF, Turashvili G, Rueda OM, Dunning MJ, Speed D, Lynch AG, Samarajiwa S, Yuan Y, et al. The genomic and transcriptomic architecture of 2,000 breast tumours reveals novel subgroups. *Nature.* 2012;486(7403):346-52.
15. Robinson DR, Wu Y-M, Lonigro RJ, Vats P, Cobain E, Everett J, Cao X, Rabban E, Kumar-Sinha C, Raymond V, et al. Integrative clinical genomics of metastatic cancer. *Nature.* 2017;548(7667):297-303.
16. Lehmann BD, Bauer JA, Chen X, Sanders ME, Chakravarthy AB, Shyr Y, and Pietenpol JA. Identification of human triple-negative breast cancer subtypes and preclinical models for selection of targeted therapies. *J Clin Invest.* 2011;121(7):2750-67.
17. Speers C, Zhao S, Liu M, Bartelink H, Pierce LJ, and Feng FY. Development and Validation of a Novel Radiosensitivity Signature in Human Breast Cancer. *Clinical cancer research : an official journal of the American Association for Cancer Research.* 2015;21(16):3667-77.
18. Wengner AM, Siemeister G, Koppitz M, Schulze V, Kosemund D, Klar U, Stoeckigt D, Neuhaus R, Lienau P, Bader B, et al. Novel Mps1 Kinase Inhibitors with Potent Antitumor Activity. *Molecular cancer therapeutics.* 2016;15(4):583-92.
19. Colombo R, Caldarelli M, Mennecozzi M, Giorgini ML, Sola F, Cappella P, Perrera C, Depaolini SR, Rusconi L, Cucchi U, et al. Targeting the Mitotic Checkpoint for Cancer Therapy with NMS-P715, an Inhibitor of MPS1 Kinase. *Cancer Research.* 2010;70(24):10255.
20. Rogakou EP, Pilch DR, Orr AH, Ivanova VS, and Bonner WM. DNA double-stranded breaks induce histone H2AX phosphorylation on serine 139. *The Journal of biological chemistry.* 1998;273(10):5858-68.
21. Peng G, Chun-Jen Lin C, Mo W, Dai H, Park YY, Kim SM, Peng Y, Mo Q, Siwko S, Hu R, et al. Genome-wide transcriptome profiling of homologous recombination DNA repair. *Nature communications.* 2014;5(3361.
22. Pierce AJ, Johnson RD, Thompson LH, and Jasin M. XRCC3 promotes homology-directed repair of DNA damage in mammalian cells. *Genes Dev.* 1999;13(20):2633-8.
23. Rouet P, Smih F, and Jasin M. Expression of a site-specific endonuclease stimulates homologous recombination in mammalian cells. *Proceedings of the National Academy of Sciences of the United States of America.* 1994;91(13):6064-8.
24. Weinstock DM, Nakanishi K, Helgadottir HR, and Jasin M. Assaying double-strand break repair pathway choice in mammalian cells using a targeted endonuclease or the RAG recombinase. *Methods Enzymol.* 2006;409(524-40.
25. Cruz C, Castroviejo-Bermejo M, Gutiérrez-Enríquez S, Llop-Guevara A, Ibrahim YH, Gris-Oliver A, Bonache S, Morancho B, Bruna A, Rueda OM, et al. RAD51 foci as a functional biomarker of homologous recombination repair and PARP inhibitor resistance in germline BRCA-mutated breast cancer. *Annals of oncology : official journal of the European Society for Medical Oncology.* 2018;29(5):1203-10.
26. Zabludoff SD, Deng C, Grondine MR, Sheehy AM, Ashwell S, Caleb BL, Green S, Haye HR, Horn CL, Janetka JW, et al. AZD7762, a novel checkpoint kinase inhibitor, drives checkpoint abrogation and potentiates DNA-targeted therapies. *Molecular cancer therapeutics.* 2008;7(9):2955.
27. Leahy JJJ, Golding BT, Griffin RJ, Hardcastle IR, Richardson C, Rigoreau L, and Smith GCM. Identification of a highly potent and selective DNA-dependent protein kinase (DNA-PK)

inhibitor (NU7441) by screening of chromenone libraries. *Bioorganic & Medicinal Chemistry Letters.* 2004;14(24):6083-7.
28. Zhao Y, Thomas HD, Batey MA, Cowell IG, Richardson CJ, Griffin RJ, Calvert AH, Newell DR, Smith GCM, and Curtin NJ. Preclinical Evaluation of a Potent Novel DNA-Dependent Protein Kinase Inhibitor NU7441. *Cancer Research.* 2006;66(10):5354.
29. Shi W, Feng Z, Zhang J, Gonzalez-Suarez I, Vanderwaal RP, Wu X, Powell SN, Roti Roti JL, Gonzalo S, and Zhang J. The role of RPA2 phosphorylation in homologous recombination in response to replication arrest. *Carcinogenesis.* 2010;31(6):994-1002.
30. Zhang Q, Karnak D, Tan M, Lawrence TS, Morgan MA, and Sun Y. FBXW7 Facilitates Nonhomologous End-Joining via K63-Linked Polyubiquitylation of XRCC4. *Mol Cell.* 2016;61(3):419-33.
31. Deans AJ, Khanna KK, McNees CJ, Mercurio C, Heierhorst J, and McArthur GA. Cyclin-Dependent Kinase 2 Functions in Normal DNA Repair and Is a Therapeutic Target in BRCA1-Deficient Cancers. *Cancer Research.* 2006;66(16):8219.
32. Maachani UB, Kramp T, Hanson R, Zhao S, Celiku O, Shankavaram U, Colombo R, Caplen NJ, Camphausen K, and Tandle A. Targeting MPS1 Enhances Radiosensitization of Human Glioblastoma by Modulating DNA Repair Proteins. *Molecular cancer research : MCR.* 2015;13(5):852-62.
33. Faisal A, Mak GWY, Gurden MD, Xavier CPR, Anderhub SJ, Innocenti P, Westwood IM, Naud S, Hayes A, Box G, et al. Characterisation of CCT271850, a selective, oral and potent MPS1 inhibitor, used to directly measure in vivo MPS1 inhibition vs therapeutic efficacy. *British journal of cancer.* 2017;116(9):1166-76.
34. Ling Y, Zhang X, Bai Y, Li P, Wei C, Song T, Zheng Z, Guan K, Zhang Y, Zhang B, et al. Overexpression of Mps1 in colon cancer cells attenuates the spindle assembly checkpoint and increases aneuploidy. *Biochemical and Biophysical Research Communications.* 2014;450(4):1690-5.
35. Xie Y, Wang A, Lin J, Wu L, Zhang H, Yang X, Wan X, Miao R, Sang X, and Zhao H. Mps1/TTK: a novel target and biomarker for cancer. *Journal of drug targeting.* 2017;25(2):112-8.
36. Lim G, and Huh W-K. Rad52 phosphorylation by Ipl1 and Mps1 contributes to Mps1 kinetochore localization and spindle assembly checkpoint regulation. *Proceedings of the National Academy of Sciences of the United States of America.* 2017;114(44):E9261-E70.
37. Isokane M, Walter T, Mahen R, Nijmeijer B, Hériché J-K, Miura K, Maffini S, Ivanov MP, Kitajima TS, Peters J-M, et al. ARHGEF17 is an essential spindle assembly checkpoint factor that targets Mps1 to kinetochores. *The Journal of cell biology.* 2016;212(6):647-59.
38. Moura M, Osswald M, Leça N, Barbosa J, Pereira AJ, Maiato H, Sunkel CE, and Conde C. Protein Phosphatase 1 inactivates Mps1 to ensure efficient Spindle Assembly Checkpoint silencing. *eLife.* 2017;6(e25366.
39. Espert A, Uluocak P, Bastos RN, Mangat D, Graab P, and Gruneberg U. PP2A-B56 opposes Mps1 phosphorylation of Knl1 and thereby promotes spindle assembly checkpoint silencing. *The Journal of cell biology.* 2014;206(7):833-42.
40. Dou Z, Liu X, Wang W, Zhu T, Wang X, Xu L, Abrieu A, Fu C, Hill DL, and Yao X. Dynamic localization of Mps1 kinase to kinetochores is essential for accurate spindle microtubule attachment. *Proceedings of the National Academy of Sciences of the United States of America.* 2015;112(33):E4546-E55.

41. Mason JM, Wei X, Fletcher GC, Kiarash R, Brokx R, Hodgson R, Beletskaya I, Bray MR, and Mak TW. Functional characterization of CFI-402257, a potent and selective Mps1/TTK kinase inhibitor, for the treatment of cancer. *Proceedings of the National Academy of Sciences of the United States of America.* 2017;114(12):3127-32.
42. Daniel J, Coulter J, Woo J-H, Wilsbach K, and Gabrielson E. High levels of the Mps1 checkpoint protein are protective of aneuploidy in breast cancer cells. *Proceedings of the National Academy of Sciences of the United States of America.* 2011;108(13):5384-9.
43. Maia ARR, de Man J, Boon U, Janssen A, Song JY, Omerzu M, Sterrenburg JG, Prinsen MBW, Willemsen-Seegers N, de Roos JADM, et al. Inhibition of the spindle assembly checkpoint kinase TTK enhances the efficacy of docetaxel in a triple-negative breast cancer model. *Annals of Oncology.* 2015;26(10):2180-92.
44. Debeb BG, Gong Y, Atkinson RL, Sneige N, Huo L, Gonzalez-Angulo AM, Hung M-C, Valero V, Ueno NT, and Woodward WA. EZH2 expression correlates with locoregional recurrence after radiation in inflammatory breast cancer. *Journal of experimental & clinical cancer research : CR.* 2014;33(1):58-.
45. Dahl E, Kristiansen G, Gottlob K, Klaman I, Ebner E, Hinzmann B, Hermann K, Pilarsky C, Dürst M, Klinkhammer-Schalke M, et al. Molecular Profiling of Laser-Microdissected Matched Tumor and Normal Breast Tissue Identifies Karyopherin α2 as a Potential Novel Prognostic Marker in Breast Cancer. *Clinical Cancer Research.* 2006;12(13):3950-60.
46. Choi M, Min YH, Pyo J, Lee C-W, Jang C-Y, and Kim J-E. TC Mps1 12, a novel Mps1 inhibitor, suppresses the growth of hepatocellular carcinoma cells via the accumulation of chromosomal instability. *British journal of pharmacology.* 2017;174(12):1810-25.
47. Wang Y, Klijn JG, Zhang Y, Sieuwerts AM, Look MP, Yang F, Talantov D, Timmermans M, Meijer-van Gelder ME, Yu J, et al. Gene-expression profiles to predict distant metastasis of lymph-node-negative primary breast cancer. *Lancet (London, England).* 2005;365(9460):671-9.
48. Desmedt C, Piette F, Loi S, Wang Y, Lallemand F, Haibe-Kains B, Viale G, Delorenzi M, Zhang Y, d'Assignies MS, et al. Strong time dependence of the 76-gene prognostic signature for node-negative breast cancer patients in the TRANSBIG multicenter independent validation series. *Clinical cancer research : an official journal of the American Association for Cancer Research.* 2007;13(11):3207-14.
49. van 't Veer LJ, Dai H, van de Vijver MJ, He YD, Hart AA, Mao M, Peterse HL, van der Kooy K, Marton MJ, Witteveen AT, et al. Gene expression profiling predicts clinical outcome of breast cancer. *Nature.* 2002;415(6871):530-6.
50. Schmidt M, Bohm D, von Torne C, Steiner E, Puhl A, Pilch H, Lehr HA, Hengstler JG, Kolbl H, and Gehrmann M. The humoral immune system has a key prognostic impact in node-negative breast cancer. *Cancer Res.* 2008;68(13):5405-13.
51. Rhodes DR, Kalyana-Sundaram S, Mahavisno V, Varambally R, Yu J, Briggs BB, Barrette TR, Anstet MJ, Kincead-Beal C, Kulkarni P, et al. Oncomine 3.0: genes, pathways, and networks in a collection of 18,000 cancer gene expression profiles. *Neoplasia.* 2007;9(2):166-80.
52. Mootha VK, Lindgren CM, Eriksson K-F, Subramanian A, Sihag S, Lehar J, Puigserver P, Carlsson E, Ridderstråle M, Laurila E, et al. PGC-1α-responsive genes involved in oxidative phosphorylation are coordinately downregulated in human diabetes. *Nature Genetics.* 2003;34(267.
53. Subramanian A, Tamayo P, Mootha VK, Mukherjee S, Ebert BL, Gillette MA, Paulovich A, Pomeroy SL, Golub TR, Lander ES, et al. Gene set enrichment analysis: A knowledge-based

approach for interpreting genome-wide expression profiles. *Proceedings of the National Academy of Sciences.* 2005;102(43):15545.
54. Gill S, Loprinzi C, Kennecke H, Grothey A, Nelson G, Woods R, Speers C, Alberts SR, Bardia A, O'Connell MJ, et al. Prognostic web-based models for stage II and III colon cancer: A population and clinical trials-based validation of numeracy and adjuvant! online. *Cancer.* 2011;117(18):4155-65.
55. Lu C, Speers C, Zhang Y, Xu X, Hill J, Steinbis E, Celestino J, Shen Q, Kim H, Hilsenbeck S, et al. Effect of epidermal growth factor receptor inhibitor on development of estrogen receptor-negative mammary tumors. *J Natl Cancer Inst.* 2003;95(24):1825-33.
56. Kang J, Chen Y, Zhao Y, and Yu H. Autophosphorylation-dependent activation of human Mps1 is required for the spindle checkpoint. *Proceedings of the National Academy of Sciences of the United States of America.* 2007;104(51):20232-7.
57. Wei D, Li H, Yu J, Sebolt JT, Zhao L, Lawrence TS, Smith PG, Morgan MA, and Sun Y. Radiosensitization of Human Pancreatic Cancer Cells by MLN4924, an Investigational NEDD8-Activating Enzyme Inhibitor. *Cancer Research.* 2012;72(282-93.
58. Mao Z, Seluanov A, Jiang Y, and Gorbunova V. TRF2 is required for repair of nontelomeric DNA double-strand breaks by homologous recombination. *Proceedings of the National Academy of Sciences.* 2007;104(32):13068.
59. Matar P, Rojo F, Cassia R, Moreno-Bueno G, Di Cosimo S, Tabernero J, Guzmán M, Rodriguez S, Arribas J, Palacios J, et al. Combined Epidermal Growth Factor Receptor Targeting with the Tyrosine Kinase Inhibitor Gefitinib (ZD1839) and the Monoclonal Antibody Cetuximab (IMC-C225). *Clinical Cancer Research.* 2004;10(6487-501.
60. Yokoyama Y, Dhanabal M, Griffioen AW, Sukhatme VP, and Ramakrishnan S. Synergy between Angiostatin and Endostatin: Inhibition of Ovarian Cancer Growth. *Cancer Research.* 2000;60(8):2190.

Chapter 5

Discussion

Summary

While the 5- and 10-year survival rates of breast cancer continue to rise, patients with basal-like breast cancer continue to have the worst outcomes (1). The lack of targeted therapies as well as resistance to radiation therapy (RT) in basal-like breast cancer contribute to their lower survival rates (2, 3). Although there have been extensive efforts to increase the effectiveness of RT in breast cancer patients, few to date, have provided clinical benefit to patients without substantial toxicities (4, 5).

Our studies aimed to characterize the RT response in breast cancer cell lines to help unearth novel targets for radiosensitization of basal-like breast cancer. We hypothesized that comparing gene and protein expression differences induced by RT across multiple breast cancer cell lines and subtypes would provide novel insights into what may be causing radioresistance in basal-like breast cancers. We describe, for the first time, changes in genes related to cell cycle, DNA damage, p53, and apoptosis that may contribute to radioresistance **(Figure 2.7-2.15)**. We use this data to highlight important differences between luminal and basal-like breast cancer cell lines that could be leveraged for radiosensitization of basal-like breast cancers.

After RT many breast cancer cell lines are dependent on p53 signaling to drive apoptosis related transcriptional changes (6, 7). In the context of tumors with mutations in p53, this activation of the apoptotic pathway is silenced at the transcriptional and translational level. When this

pathway is intact, cells are markedly more sensitive to ionizing radiation than when the pathway is silenced, and our multi-level –omics approaches nominate this pathway as a key mediator of radiation resistance in p53 mutant tumors **(Figure 3.1)**. We therefore nominate anti-apoptosis genes as potential radiosensitization targets. *In vitro*, we test whether activation of the apoptosis pathway, through inhibition of anti-apoptosis proteins, could radiosensitize basal-like breast cancer cell lines. Interesting, we see that inhibition of Bcl-2 family proteins (Bcl-2, Bcl-xL, Bcl-w) specifically radiosensitizes p53 mutant, PIK3CA/PTEN wild-type cell lines but not p53 mutant, PIK3CA/PTEN mutant cell lines **(Figure 3.2)**. We demonstrate that radiosensitization of p53 mutant, PIK3CA/PTEN wild-type cell lines is caused by inhibition of specifically Bcl-xL and not Bcl-2 **(Figure 3.5-3.7)**. Radiosensitization is mediated, at least in part, through RT induced Mcl-1 degradation in p53 mutant, PIK3CA/PTEN wild-type cell lines. Overexpression of Mcl-1 in p53 mutant, PIK3CA/PTEN wild-type cell lines rescues resistance to Bcl-xL inhibition induced radiosensitization **(Figure 3.8-3.9)**. Finally, we show that inhibition of Bcl-2 family proteins (ABT-263) or Bcl-xL alone (A-1331852) radiosensitizes basal-like breast cancer cell lines *in vivo* and extends time to tumor doubling and tripling compared to treatment with drug or RT alone **(Figure 3.10)**.

Next, we leverage open source clinical outcomes data from women with breast cancer treated with RT to nominate genes associated with early (<3 years) locoregional recurrence. We identify ten genes to be significantly associated with early locoregional recurrence across four independent datasets. The most differentially expressed gene associated with early locoregional recurrence was TTK, also known as monopolar spindle 1 (Mps1). TTK is significantly

overexpressed in breast cancer compared to normal tissue and most overexpressed in the basal-like breast cancer subtype **(figure 4.1)**. Using gene set enrichment analysis (GSEA) we correlate TTK expression with cell cycle genes in the radiation response at both 6- and 24-hours **(Figure 4.4)**. *In vitro*, inhibition of TTK, through either genetic knockdown (shRNA/siRNA) or pharmacologic inhibition of kinase function (Bayer 1161909 [B909]), significantly radiosensitizes multiple basal-like breast cancer cell lines **(Figure 4.3)**. Reintroduction of wild-type TTK, after endogenous TTK knockdown, rescues radioresistance but reintroduction of a kinase-dead mutant of TTK was unable to rescue this radioresistance **(Figure 4.10)**. Radiosensitization is mediated, at least in part, through impaired double stranded DNA (dsDNA) repair and TTK inhibition (both genetic and pharmacologic) decreases homologous recombination (HR) repair but had no effect on non-homologous end-joining (NHEJ) **(Figure 4.5-4.9)**. Reintroduction of wild-type TTK rescues HR efficiency but reintroduction of kinase dead TTK mutant was unable to do so **(Figure 4.10)**. Finally, we show *in vivo* that TTK inhibition (both genetic and pharmacologic) in combination with RT significantly decreases tumor growth and increases time to tumor tripling. Furthermore, pharmacologic inhibition of TTK synergistically radiosensitizes both basal-like breast cancer cell line and patient derived xenograft (PDX) models *in vivo* **(Figure 4.12-13)** (8).

Together, we are able to demonstrate that more complete characterization of the RT response leads to the nomination of multiple novel radiosensitization targets. Additionally, our work highlights the utility of multi-omic "big data" in the nomination of modulators of radioresistance. Perturbation of these nominated protein suggests novel functions of these proteins

in the context of basal-like breast cancer function. Finally, the use of clinical grade inhibitors and clinically relevant model systems minimizes the barriers to clinical translation.

Future Directions

While we characterize the RT response in multiple breast cancer cell lines across multiple time points, both transcriptionally and proteomically, additional work remains to gain a comprehensive understanding of how breast cancer cells respond to RT. First, additional cell lines need to be characterized transcriptionally and proteomically after RT to more completely understand how RT effects different breast cancer subtypes and how different mutations contribute to the RT response. While we discuss and provide data on how p53 mutations may contribute to the RT response, breast cancers have additional common mutations in PIK3CA, PTEN, Rb, and BRCA1/2 (9). Each of these mutations, as well as others, likely contribute to the RT response, meaning radiosensitization efforts across different breast cancer mutational landscapes will likely be different. Providing additional data from cell line models and creating new models to modulate mutational status of genes will allow us to understand how each gene contributes to the RT response. This information could then be used clinically to identify patients for whom radiation is likely to be more (or less) effective.

Reverse phase protein array (RPPA) is a powerful tool to quantitate protein and phosphoprotein changes after RT (10). However, we used a limited number of antibodies in our study of the RT response. Adding additional validated antibodies would provide more detail into how pathways change at the protein and phosphoprotein level after RT. In addition, creating a tool

to combine microarray/RNA-sequencing data with RPPA data would provide new insights into understanding how changes in RNA, protein, and phosphoprotein expression work together to modulate cellular pathways after RT. Furthermore, layering additional data types, such as chromatin immunoprecipitation followed by sequencing (ChIP-Seq) of genes enriched in breast cancer, such as estrogen receptor (ER), androgen receptor (AR), or E2F1, would aid in understanding how transcription factor (TF) binding changes in response to RT (9, 11-14). Furthermore, transposase-accessible chromatin with high-throughput sequencing (ATAC-seq) could be used to identify changes in chromatin accessibility after RT. Together, these data would give a more 'complete' understanding of how breast cancer cell lines respond to RT. Understanding chromatin accessibility, TF binding, transcriptional, and proteomic changes after RT would allow us to further understand differences in the RT response between radiosensitive and radioresistant breast cancers. This data would be used to nominate novel targets for radiosensitization within breast cancer subtypes as well as within specific mutational profiles.

These studies would further aid in understanding how cellular machineries work together to govern the RT response in breast cancer and would greatly aid in uncovering the complexity of this response. However, combining unique datasets will require the creation of novel bioinformatic tools to fully utilize all the information provided by these platforms. While analyzing each dataset alone is much more feasible with the methods currently available, combining datatypes at a "systems-wide" level is more challenging. These analyses require unique and currently under-developed techniques for the datasets we used. Although tools are available for specific combinations of data types (i.e. – RNA-sequencing and ChIP-sequencing), nothing currently exists

to combine RPPA with additional unique types of data (15, 16). The complexity of the data types and lack of necessary tools needed to address the union of these datasets underscores the difficulty in fully understanding how specific treatments impact diverse cancer types and subtypes.

Our studies examining inhibition of Bcl-2 family proteins, and specific inhibition of Bcl-xL, as a radiosensitization strategy demonstrate, for the first time, the importance of Bcl-xL, and not Bcl-2, in avoiding apoptosis in p53 mutant, PIK3CA/PTEN wild-type breast cancer. However, while we show that inhibition of Bcl-xL has no impact on p53 mutant, PIK3CA/PTEN mutant basal-like breast cancer cell lines, we have not identified why mutations in the PIK3CA/PTEN pathway blunts Bcl-xL inhibition mediated radiosensitization. Previous studies have found that PIK3CA/PTEN mutant breast cancers depend on both Bcl-xL and Mcl-1 for survival and that Mcl-1 expression is controlled by mTOR/4E-Bp in PIK3CA mutant breast cancers, which may stabilize Mcl-1 expression (17). Interestingly, some studies have found that mutations and amplifications in PIK3CA do not increase mTOR activity (18-20). Mutations in the PIK3CA/PTEN pathway also affect downstream targets such as GSK-3β, which has been shown to regulate Mcl-1 stability through phosphorylation of Mcl-1 (21-24). Alternatively, other groups have reported that E3 ubiquitin ligases (FBW7, Mule, β-TrCP) and deubiquitinases (USP13, OTUD1, DUB3) may regulate Mcl-1 stability, both dependently and independently of GSK-3β or mTOR, which may also lead to stable expression of Mcl-1 in PIK3CA/PTEN mutant basal-like breast cancers (17, 22, 24-29). To date, the E3 ubiquitin ligase and deubiquitinase responsible for regulating Mcl-1 stability in basal-like breast cancer has yet to be identified. Furthermore, in prostate cancer, inhibition of epidermal growth factor receptor (EGFR) increases Mcl-1 degradation through

mechanisms independent of GSK-3β and ubiquitination, though it is unknown whether this process occurs in breast cancer (30). Identifying the mechanism through which Mcl-1 stability is determined would allow us to more completely understand why RT reduces Mcl-1 expression in p53 mutant, PIK3CA/PTEN wild-type basal-like breast cancer cell lines but has no effect in PIK3CA/PTEN mutant cell lines.

We demonstrate that inhibition of Bcl-2 family proteins or Bcl-xL alone significantly radiosensitizes the p53 mutant, PIK3CA/PTEN wild-type cell line *in vivo*; however, additional *in vivo* studies are needed to confirm our results. For example, we plan to perform similar studies using orthotopic patient derived xenograft (PDX) models that are both PIK3CA/PTEN wild-type as well as mutant. These studies will provide further evidence that PIK3CA/PTEN mutations cause resistance to Bcl-xL inhibition mediated radiosensitization in additional models of basal-like breast cancer. Results showing significant radiosensitization in PIK3CA/PTEN wild-type basal-like models will further confirm our *in vitro* and *in vivo* findings, strengthening the case for translatability to the clinic.

Our research adds to the growing body of literature that links cell cycle proteins to DNA damage repair mechanisms (8, 31, 32). Through multiple experimental modalities we show TTK inhibition decreases homologous recombination (HR) repair efficiency but has no impact on non-homologous end joining (NHEJ) repair efficiency. While previous groups have correlated TTK to HR or demonstrated a loose connection to the HR pathway, we provide the most robust evidence to date that TTK directly impacts HR efficiency (8, 33, 34). Despite this novel association, we have not yet identified exactly how TTK interacts with the HR pathway. Previous studies have

suggested TTK may directly interact with p53 and/or Chk2, which may explain why TTK inhibition reduces HR efficiency (35, 36). p53 has previously been linked to HR through both transcriptional means and through direct interaction with Rad51 (37, 38). However, p53 is often mutated in basal-like breast cancer, potentially changing its role within HR (9, 39-41). Furthermore, previous studies have also shown that p53 can directly regulate NHEJ repair, complicating how TTK could interact with p53 to impair HR but not NHEJ (42, 43). Chk2 has been linked to HR through interactions with both BRCA1 and BRCA2, core proteins of the HR pathway, therefore TTK inhibition could reduce the ability of Chk2 to interact with BRCA protein, limiting the efficiency of the HR repair pathway (44-46). Alternatively, TTK may interact with other proteins related to the HR pathway. Further experiments are needed to identify and characterize the relationship between TTK and proteins in the HR repair pathway. To that end, our group has connected MELK, a cell cycle protein, as a mediator of NHEJ repair efficiency through interactions with both Ku70 and Ku80 (data not published), by performing immunoprecipitation (IP) mass spectrometry experiments. This same technique could be used to identify the protein(s) that interact with TTK in the HR pathway. This method would provide non-biased data depicting binding partners of TTK and potentially provide novel links between TTK and proteins in the HR repair pathway.

TTK is well established as the apical signaling protein of the spindle assembly checkpoint (SAC) complex, which is responsible for ensuring appropriate alignment of chromosomes in metaphase of mitosis (47-49). Previous studies have shown that inhibition of TTK increases mitotic errors, lagging chromosomes, and aneuploidy leading to increased cell death (50-52).

However, few studies have examined the cell death pathway that is activated by inhibition of TTK (53). While apoptosis and/or mitotic catastrophe may be the most likely or most prominent cell death pathway, ferroptosis, necrosis, or autophagy may also contribute to cell death after TTK inhibition (54-57). Furthermore, combination treatment of TTK inhibition and RT may activate different cell death pathways compared to TTK inhibition or RT alone, an area of continued interest by our group (58).

Final Remarks

In conclusion, our studies provide the most complete view of the RT response in breast cancer to date. We use this data from cell line models as well as patient tumor microarray data to nominate multiple radiosensitization targets in basal-like breast cancer. Our characterization of TTK and Bcl-xL as radiosensitization targets in basal-like breast cancer provides a first indication for a role in radiation response for these proteins in the radioresistant phenotype common to basal-like breast cancer. Furthermore, the use clinical grade inhibitors in both *in vitro* and *in vivo* experiments increases the translatability of our studies. While additional experiments need to be performed to further understand the mechanism of radiosensitization in both studies, we demonstrate the efficacy of both treatment strategies in basal-like breast cancer cell lines and patient derived xenograft (PDX) models. These data also provide the preclinical rationale for the development of Bcl-xL and TTK inhibitors for the radiosensitization of basal-like breast cancers in women at high risk for locoregional recurrence after treatment.

References

1. DeSantis CE, Ma J, Gaudet MM, Newman LA, Miller KD, Goding Sauer A, Jemal A, and Siegel RL. Breast cancer statistics, 2019. *CA: A Cancer Journal for Clinicians.* 2019;69(6):438-51.
2. Kyndi M, Sørensen FB, Knudsen H, Overgaard M, Nielsen HM, and Overgaard J. Estrogen Receptor, Progesterone Receptor, HER-2, and Response to Postmastectomy Radiotherapy in High-Risk Breast Cancer: The Danish Breast Cancer Cooperative Group. *Journal of Clinical Oncology.* 2008;26(9):1419-26.
3. Sjöström M, Lundstedt D, Hartman L, Holmberg E, Killander F, Kovács A, Malmström P, Niméus E, Werner Rönnerman E, Fernö M, et al. Response to Radiotherapy After Breast-Conserving Surgery in Different Breast Cancer Subtypes in the Swedish Breast Cancer Group 91 Radiotherapy Randomized Clinical Trial. *Journal of Clinical Oncology.* 2017;35(28):3222-9.
4. Zhou Z-R, Yang Z-Z, Yu X-L, and Guo X-M. Highlights on molecular targets for radiosensitization of breast cancer cells: Current research status and prospects. *Cancer Med.* 2018;7(7):3110-7.
5. Jagsi R, Griffith KA, Bellon JR, Woodward WA, Horton JK, Ho A, Feng FY, Speers C, Overmoyer B, Sabel M, et al. Concurrent Veliparib With Chest Wall and Nodal Radiotherapy in Patients With Inflammatory or Locoregionally Recurrent Breast Cancer: The TBCRC 024 Phase I Multicenter Study. *J Clin Oncol.* 2018;36(13):1317-22.
6. Fridman JS, and Lowe SW. Control of apoptosis by p53. *Oncogene.* 2003;22(56):9030-40.
7. Gasco M, Shami S, and Crook T. The p53 pathway in breast cancer. *Breast Cancer Research.* 2002;4(2):70.
8. Chandler BC, Moubadder L, Ritter CL, Liu M, Cameron M, Wilder-Romans K, Zhang A, Pesch AM, Michmerhuizen AR, Hirsh N, et al. TTK inhibition radiosensitizes basal-like breast cancer through impaired homologous recombination. *The Journal of Clinical Investigation.* 2020;130(2):958-73.
9. Lehmann BD, Bauer JA, Chen X, Sanders ME, Chakravarthy AB, Shyr Y, and Pietenpol JA. Identification of human triple-negative breast cancer subtypes and preclinical models for selection of targeted therapies. *The Journal of Clinical Investigation.* 2011;121(7):2750-67.
10. Paweletz CP, Charboneau L, Bichsel VE, Simone NL, Chen T, Gillespie JW, Emmert-Buck MR, Roth MJ, Petricoin Iii EF, and Liotta LA. Reverse phase protein microarrays which capture disease progression show activation of pro-survival pathways at the cancer invasion front. *Oncogene.* 2001;20(16):1981-9.
11. Vidula N, Yau C, Wolf D, and Rugo HS. Androgen receptor gene expression in primary breast cancer. *npj Breast Cancer.* 2019;5(1):47.
12. Hollern DP, Swiatnicki MR, Rennhack JP, Misek SA, Matson BC, McAuliff A, Gallo KA, Caron KM, and Andrechek ER. E2F1 Drives Breast Cancer Metastasis by Regulating the Target Gene FGF13 and Altering Cell Migration. *Scientific Reports.* 2019;9(1):10718.
13. Field SJ, Tsai F-Y, Kuo F, Zubiaga AM, Kaelin WG, Livingston DM, Orkin SH, and Greenberg ME. E2F-1 Functions in Mice to Promote Apoptosis and Suppress Proliferation. *Cell.* 1996;85(4):549-61.
14. Qin G, Kishore R, Dolan CM, Silver M, Wecker A, Luedemann CN, Thorne T, Hanley A, Curry C, Heyd L, et al. Cell cycle regulator E2F1 modulates angiogenesis via p53-dependent transcriptional control of VEGF. *Proceedings of the National Academy of Sciences.* 2006;103(29):11015.

15. Ramazzotti D, Lal A, Wang B, Batzoglou S, and Sidow A. Multi-omic tumor data reveal diversity of molecular mechanisms that correlate with survival. *Nat Commun.* 2018;9(1):4453-.
16. Forsberg EM, Huan T, Rinehart D, Benton HP, Warth B, Hilmers B, and Siuzdak G. Data processing, multi-omic pathway mapping, and metabolite activity analysis using XCMS Online. *Nat Protoc.* 2018;13(4):633-51.
17. Anderson GR, Wardell SE, Cakir M, Crawford L, Leeds JC, Nussbaum DP, Shankar PS, Soderquist RS, Stein EM, Tingley JP, et al. PIK3CA mutations enable targeting of a breast tumor dependency through mTOR-mediated MCL-1 translation. *Sci Transl Med.* 2016;8(369):369ra175-369ra175.
18. Holst F, Werner HMJ, Mjøs S, Hoivik EA, Kusonmano K, Wik E, Berg A, Birkeland E, Gibson WJ, Halle MK, et al. PIK3CA Amplification Associates with Aggressive Phenotype but Not Markers of AKT-MTOR Signaling in Endometrial Carcinoma. *Clin Cancer Res.* 2019;25(1):334-45.
19. Stemke-Hale K, Gonzalez-Angulo AM, Lluch A, Neve RM, Kuo W-L, Davies M, Carey M, Hu Z, Guan Y, Sahin A, et al. An integrative genomic and proteomic analysis of PIK3CA, PTEN, and AKT mutations in breast cancer. *Cancer Res.* 2008;68(15):6084-91.
20. Vasudevan KM, Barbie DA, Davies MA, Rabinovsky R, McNear CJ, Kim JJ, Hennessy BT, Tseng H, Pochanard P, Kim SY, et al. AKT-independent signaling downstream of oncogenic PIK3CA mutations in human cancer. *Cancer Cell.* 2009;16(1):21-32.
21. Wang R, Xia L, Gabrilove J, Waxman S, and Jing Y. Downregulation of Mcl-1 through GSK-3β activation contributes to arsenic trioxide-induced apoptosis in acute myeloid leukemia cells. *Leukemia.* 2013;27(2):315-24.
22. Ding Q, He X, Hsu J-M, Xia W, Chen C-T, Li L-Y, Lee D-F, Liu J-C, Zhong Q, Wang X, et al. Degradation of Mcl-1 by β-TrCP Mediates Glycogen Synthase Kinase 3-Induced Tumor Suppression and Chemosensitization. *Molecular and Cellular Biology.* 2007;27(11):4006-17.
23. Hermida MA, Dinesh Kumar J, and Leslie NR. GSK3 and its interactions with the PI3K/AKT/mTOR signalling network. *Advances in Biological Regulation.* 2017;65(5-15.
24. Ren H, Koo J, Guan B, Yue P, Deng X, Chen M, Khuri FR, and Sun S-Y. The E3 ubiquitin ligases β-TrCP and FBXW7 cooperatively mediates GSK3-dependent Mcl-1 degradation induced by the Akt inhibitor API-1, resulting in apoptosis. *Molecular Cancer.* 2013;12(1):146.
25. Tong J, Wang P, Tan S, Chen D, Nikolovska-Coleska Z, Zou F, Yu J, and Zhang L. Mcl-1 Degradation Is Required for Targeted Therapeutics to Eradicate Colon Cancer Cells. *Cancer Res.* 2017;77(9):2512-21.
26. Zhang S, Zhang M, Jing Y, Yin X, Ma P, Zhang Z, Wang X, Di W, and Zhuang G. Deubiquitinase USP13 dictates MCL1 stability and sensitivity to BH3 mimetic inhibitors. *Nat Commun.* 2018;9(1):215.
27. Wu X, Luo Q, Zhao P, Chang W, Wang Y, Shu T, Ding F, Li B, and Liu Z. MGMT-activated DUB3 stabilizes MCL1 and drives chemoresistance in ovarian cancer. *Proceedings of the National Academy of Sciences.* 2019;116(8):2961.
28. Wu L, Lin Y, Feng J, Qi Y, Wang X, Lin Q, Shi W, Zheng E, Wang W, Hou Z, et al. The deubiquitinating enzyme OTUD1 antagonizes BH3-mimetic inhibitor induced cell death through regulating the stability of the MCL1 protein. *Cancer Cell International.* 2019;19(1):222.
29. Zhong Q, Gao W, Du F, and Wang X. Mule/ARF-BP1, a BH3-Only E3 Ubiquitin Ligase, Catalyzes the Polyubiquitination of Mcl-1 and Regulates Apoptosis. *Cell.* 2005;121(7):1085-95.

30. Arai S, Jonas O, Whitman MA, Corey E, Balk SP, and Chen S. Tyrosine Kinase Inhibitors Increase MCL1 Degradation and in Combination with BCLXL/BCL2 Inhibitors Drive Prostate Cancer Apoptosis. *Clinical Cancer Research.* 2018;24(21):5458.
31. Speers C, Zhao SG, Kothari V, Santola A, Liu M, Wilder-Romans K, Evans J, Batra N, Bartelink H, Hayes DF, et al. Maternal Embryonic Leucine Zipper Kinase (MELK) as a Novel Mediator and Biomarker of Radioresistance in Human Breast Cancer. *Clinical Cancer Research.* 2016;22(23):5864.
32. Lazzaro F, Giannattasio M, Puddu F, Granata M, Pellicioli A, Plevani P, and Muzi-Falconi M. Checkpoint mechanisms at the intersection between DNA damage and repair. *DNA Repair.* 2009;8(9):1055-67.
33. Peng G, Chun-Jen Lin C, Mo W, Dai H, Park Y-Y, Kim SM, Peng Y, Mo Q, Siwko S, Hu R, et al. Genome-wide transcriptome profiling of homologous recombination DNA repair. *Nat Commun.* 2014;5(3361-.
34. Maachani UB, Kramp T, Hanson R, Zhao S, Celiku O, Shankavaram U, Colombo R, Caplen NJ, Camphausen K, and Tandle A. Targeting MPS1 Enhances Radiosensitization of Human Glioblastoma by Modulating DNA Repair Proteins. *Mol Cancer Res.* 2015;13(5):852-62.
35. Huang Y-F, Chang MD-T, and Shieh S-Y. TTK/hMps1 Mediates the p53-Dependent Postmitotic Checkpoint by Phosphorylating p53 at Thr18. *Molecular and Cellular Biology.* 2009;29(11):2935.
36. Yeh YH, Huang YF, Lin TY, and Shieh SY. The cell cycle checkpoint kinase CHK2 mediates DNA damage-induced stabilization of TTK/hMps1. *Oncogene.* 2009;28(10):1366-78.
37. Arias-Lopez C, Lazaro-Trueba I, Kerr P, Lord CJ, Dexter T, Iravani M, Ashworth A, and Silva A. p53 modulates homologous recombination by transcriptional regulation of the RAD51 gene. *EMBO Rep.* 2006;7(2):219-24.
38. Stürzbecher HW, Donzelmann B, Henning W, Knippschild U, and Buchhop S. p53 is linked directly to homologous recombination processes via RAD51/RecA protein interaction. *EMBO J.* 1996;15(8):1992-2002.
39. Saintigny Y, and Lopez BS. Homologous recombination induced by replication inhibition, is stimulated by expression of mutant p53. *Oncogene.* 2002;21(3):488-92.
40. Saintigny Y, Rouillard D, Chaput B, Soussi T, and Lopez BS. Mutant p53 proteins stimulate spontaneous and radiation-induced intrachromosomal homologous recombination independently of the alteration of the transactivation activity and of the G1 checkpoint. *Oncogene.* 1999;18(24):3553-63.
41. Boehden GS, Akyüz N, Roemer K, and Wiesmüller L. p53 mutated in the transactivation domain retains regulatory functions in homology-directed double-strand break repair. *Oncogene.* 2003;22(26):4111-7.
42. Gao Y, Ferguson DO, Xie W, Manis JP, Sekiguchi J, Frank KM, Chaudhuri J, Horner J, DePinho RA, and Alt FW. Interplay of p53 and DNA-repair protein XRCC4 in tumorigenesis, genomic stability and development. *Nature.* 2000;404(6780):897-900.
43. Tang W, Willers H, and Powell SN. p53 Directly Enhances Rejoining of DNA Double-Strand Breaks with Cohesive Ends in γ-Irradiated Mouse Fibroblasts. *Cancer Res.* 1999;59(11):2562-5.
44. Zhang J, Willers H, Feng Z, Ghosh JC, Kim S, Weaver DT, Chung JH, Powell SN, and Xia F. Chk2 Phosphorylation of BRCA1 Regulates DNA Double-Strand Break Repair. *Molecular and Cellular Biology.* 2004;24(2):708.

45. Bahassi EM, Ovesen JL, Riesenberg AL, Bernstein WZ, Hasty PE, and Stambrook PJ. The checkpoint kinases Chk1 and Chk2 regulate the functional associations between hBRCA2 and Rad51 in response to DNA damage. *Oncogene.* 2008;27(28):3977-85.
46. Lee J-S, Collins KM, Brown AL, Lee C-H, and Chung JH. hCds1-mediated phosphorylation of BRCA1 regulates the DNA damage response. *Nature.* 2000;404(6774):201-4.
47. Yang C-H, Kasbek C, Majumder S, Yusof AM, and Fisk HA. Mps1 Phosphorylation Sites Regulate the Function of Centrin 2 in Centriole Assembly. *Molecular Biology of the Cell.* 2010;21(24):4361-72.
48. Hardwick KG, Weiss E, Luca FC, Winey M, and Murray AW. Activation of the Budding Yeast Spindle Assembly Checkpoint Without Mitotic Spindle Disruption. *Science.* 1996;273(5277):953.
49. Weiss E, and Winey M. The Saccharomyces cerevisiae spindle pole body duplication gene MPS1 is part of a mitotic checkpoint. *The Journal of Cell Biology.* 1996;132(1):111-23.
50. Mason JM, Wei X, Fletcher GC, Kiarash R, Brokx R, Hodgson R, Beletskaya I, Bray MR, and Mak TW. Functional characterization of CFI-402257, a potent and selective Mps1/TTK kinase inhibitor, for the treatment of cancer. *Proc Natl Acad Sci U S A.* 2017;114(12):3127-32.
51. Maia ARR, Linder S, Song J-Y, Vaarting C, Boon U, Pritchard CEJ, Velds A, Huijbers IJ, van Tellingen O, Jonkers J, et al. Mps1 inhibitors synergise with low doses of taxanes in promoting tumour cell death by enhancement of errors in cell division. *British Journal of Cancer.* 2018;118(12):1586-95.
52. Choi M, Min YH, Pyo J, Lee C-W, Jang C-Y, and Kim J-E. TC Mps1 12, a novel Mps1 inhibitor, suppresses the growth of hepatocellular carcinoma cells via the accumulation of chromosomal instability. *Br J Pharmacol.* 2017;174(12):1810-25.
53. Jemaà M, Galluzzi L, Kepp O, Senovilla L, Brands M, Boemer U, Koppitz M, Lienau P, Prechtl S, Schulze V, et al. Characterization of novel MPS1 inhibitors with preclinical anticancer activity. *Cell Death & Differentiation.* 2013;20(11):1532-45.
54. Denton D, and Kumar S. Autophagy-dependent cell death. *Cell Death & Differentiation.* 2019;26(4):605-16.
55. Xie Y, Hou W, Song X, Yu Y, Huang J, Sun X, Kang R, and Tang D. Ferroptosis: process and function. *Cell Death & Differentiation.* 2016;23(3):369-79.
56. Elmore S. Apoptosis: a review of programmed cell death. *Toxicol Pathol.* 2007;35(4):495-516.
57. Berghe TV, Linkermann A, Jouan-Lanhouet S, Walczak H, and Vandenabeele P. Regulated necrosis: the expanding network of non-apoptotic cell death pathways. *Nature Reviews Molecular Cell Biology.* 2014;15(2):135-47.
58. Eriksson D, and Stigbrand T. Radiation-induced cell death mechanisms. *Tumor Biology.* 2010;31(4):363-72.

Appendices

Appendix I: Author's Contributions

Chapter 2

Benjamin C. Chandler[1,2,3], Cassandra L. Ritter[1], Andrea M. Pesch[1], Anna R. Michmerhuizen[1], Kari Wilder-Romans[1], Meilan Liu[1], Shyam Nyati[1,2], Corey Speers[1,2,3]

[1]Department of Radiation Oncology, University of Michigan, Ann Arbor, MI,
[2]Rogel Cancer Center, Michigan Medicine, University of Michigan,
[3]Cancer Biology Program, University of Michigan,

Chapter 3

Benjamin C. Chandler[1,2,3], Andrea M. Pesch[1], Meilan Liu[1], Kari Wilder-Romans[1], Cassandra L. Ritter[1], Amanda Zhang[1], Anna R. Michmerhuizen[1], Nicole Hirsh[1], Theodore S. Lawrence[1,2], Shyam Nyati[1,2], Lori J. Pierce[1,2], Corey Speers[1,2,3]

[1]Department of Radiation Oncology, University of Michigan, Ann Arbor, MI,
[2]Rogel Cancer Center, Michigan Medicine, University of Michigan,
[3]Cancer Biology Program, University of Michigan,

Chapter 4

Benjamin C. Chandler[1,2,3], Leah Moubadder[1], Cassandra L. Ritter[1], Meilan Liu[1], Meleah Cameron[1], Kari Wilder-Romans[1], Amanda Zhang[1], Andrea M. Pesch[1], Anna R. Michmerhuizen[1], Nicole Hirsh[1], Marlie Androsiglio[1] Tanner Ward[1], Eric Olsen[1], Yashar S. Niknafs[2,4], Sofia Merajver[2,5], Dafydd G. Thomas[2,6], Powel Brown[7], Theodore S. Lawrence[1,2], Shyam Nyati[1,2], Lori J. Pierce[1,2], Arul Chinnaiyan[2,4,8], Corey Speers[1,2,3]

[1]Department of Radiation Oncology, University of Michigan, Ann Arbor, MI,
[2]Rogel Cancer Center, Michigan Medicine, University of Michigan,
[3]Cancer Biology Program, University of Michigan,
[4]Michigan Center for Translation Pathology, [5]Department of Internal Medicine, University of Michigan,
[6]Department of Pathology, University of Michigan,
[7]Department of Radiation Oncology, University of Texas MD Anderson Cancer Center, Houston, TX,
[8]Howard Hughes Medical Institute, University of Michigan, Ann Arbor, MI USA